Functional Imaging of the Locus Coeruleus and Its Indirect Modulation by Short Bursts of Transcutaneous Auricular Vagus Nerve Stimulation

Thesis for the degree of

doctor rerum naturalium (Dr. rer. nat.)

approved by the Faculty of Natural Sciences of

Otto von Guericke University Magdeburg

by **M.Sc. Mareike Ludwig**

born on 23.11.1993 in Ilmenau

Examiner: Prof. Dr. Dorothea Hämmerer

Prof. Dr. Mathias Weymar

Submitted on 17.02.2025

Defended on 16.09.2025

For

the loved ones

and the beloved lost ones

For

inner peace

in the circle of life

May there be a touch more peace and safety in every heart and every place.

Table of Contents

Summary

The aim of this dissertation is to advance our knowledge of the role of the noradrenergic system of the locus coeruleus (LC-NE system) in memory and age-related differences in LC function. Additionally, the dissertation will provide a better understanding of the mechanism of action of transcutaneous auricular vagus nerve stimulation (taVNS) in humans, enabling a more precise and targeted application of taVNS in an individually altered LC-NE system.

In the high-resolution imaging study of the LC, I show age-related differences in the functional involvement of the LC during a cognitive task known to rely on noradrenergic function. Furthermore, I show that functional activation of the LC increased during emotional and task-salient events, aligning with animal studies of LC function. While there is growing evidence for structural degeneration of the LC with age, my findings indicated higher functional activation of the LC among older adults. This may suggest compensatory overactivation of the LC in older adults, as younger and older adults showed comparable performance in completing the experimental task.

In a second study involving younger adults, I investigate the potential effects of short bursts of taVNS on the noradrenergic system of the LC. I systematically investigated how different stimulation parameters during short bursts of taVNS affect changes in pupil size, which is discussed as an indirect measure of LC activation. Additionally, I investigated the effects of taVNS on memory performance. The results I report regarding increased pupil dilation following short bursts of taVNS align with animal and human studies of short bursts of invasive or taVNS, which, in contrast to longer-lasting taVNS impulses, consistently indicated modulation of the LC-NE system. Furthermore, the influence of intensity on pupil dilation appeared to be stronger than the influence of frequency. However, when considering the sensory perception of the stimulation, I show that potential changes in pupil dilation induced by taVNS could no longer be explained solely by the stimulation itself. I also show that memory performance was better with both real and sham stimulation, even when controlling for subjective perception of stimulation. Specifically, real taVNS improved the encoding of negative events compared to neutral events, which is consistent with animal studies reporting the involvement of ascending vagal fibers in emotional memory. Therefore, my findings on short bursts of taVNS may indicate arousal and/or attention-related processes during the stimulation process.

The taVNS results of this dissertation emphasize the importance of carefully controlling and evaluating the sensory effects of various stimulation conditions and locations while also considering the potential cognition-enhancing effects related to the subjective sensation of the

stimulation itself. Furthermore, the functional activations of the LC demonstrate that age-related differences in LC function can be visualized using high-resolution functional MRI and appropriate post-processing methods for small structures in the brainstem. Therefore, future research can build on the findings of my dissertation: For instance, it could conduct combined fMRI-taVNS studies that consider the influence of the subjective sensation of stimulation to investigate the mechanisms of taVNS, the involvement of the LC and other neuronal structures, and the effects of external modulation of NE release in a more targeted manner.

German Summary (Zusammenfassung)

Das Ziel der vorliegenden Dissertation besteht darin, unser Wissen über die Rolle des noradrenergen Systems des Locus Coeruleus (LC-NE System) beim Gedächtnis sowie für die altersbedingten Unterschiede in der LC-Funktion zu vertiefen. Zudem soll ein verbessertes Verständnis für den Wirkmechanismus von taVNS beim Menschen erlangt werden, um eine präzisere und zielgerichtetere Anwendung von taVNS in einem individuell veränderten LC-NE-System zu ermöglichen.

In der hochauflösenden Bildgebungsstudie des LC zeige ich altersbedingte Unterschiede in der funktionellen Aktivierung des LC während einer kognitiven Aufgabe, von der bekannt ist, dass sie auf die noradrenerge Funktion angewiesen ist. Außerdem zeige ich, dass die funktionelle Aktivierung des LC während emotionaler und aufgabenbezogener Ereignisse erhöht war, was mit Tierstudien zur LC-Funktion übereinstimmt. Obwohl es immer mehr Befunde für eine strukturelle Degeneration des LC mit steigendem Alter gibt, zeigten meine Ergebnisse höhere funktionelle Aktivierung des LC bei älteren Erwachsenen. Dies könnte auf eine kompensatorische Überaktivierung des LC bei älteren Erwachsenen hindeuten, da jüngere und ältere Erwachsene vergleichbare Leistungen beim Absolvieren der experimentellen Aufgabe zeigten.

In einer zweiten Studie mit jüngeren Erwachsenen untersuche ich die möglichen Auswirkungen einer transkutanen aurikulären Vagusnervstimulation (taVNS) mit kurzen Stimulationsimpulsen auf das noradrenerge System des LC. Dabei untersuchte ich systematisch, wie sich verschiedene Stimulationsparameter während kurzer Stimulationsimpulse von taVNS auf Veränderungen der Pupillengröße auswirken, was als indirektes Maß für die Aktivierung des LC diskutiert wird. Außerdem untersuchte ich die Auswirkungen von taVNS auf die Gedächtnisleistung. Die von mir berichteten Ergebnisse hinsichtlich einer verstärkten Pupillenerweiterung nach kurzen Stimulationsimpulsen von taVNS stimmen mit Tier- und Humanstudien zu kurzen Stimulationsimpulsen von invasivem oder taVNS überein, die im Gegensatz zu länger anhaltenden taVNS-Impulsen durchweg auf eine Modulation des LC-NE-Systems hinwiesen. Darüber hinaus schien der Einfluss der Intensität auf die Pupillenerweiterung stärker zu sein als der Einfluss der Frequenz. Unter Berücksichtigung der subjektiven Empfindung der Stimulation zeige ich jedoch, dass die möglichen taVNS-induzierten Veränderungen der Pupillenerweiterung nicht mehr allein durch die Stimulation selbst erklärt werden konnten. Zudem berichte ich, dass die Gedächtnisleistung sowohl bei echter als auch bei Placebo-Stimulation besser war, selbst wenn für die subjektive Empfindung der Stimulation kontrolliert wurde. Insbesondere verbesserte echte taVNS die

Kodierung negativer Ereignisse im Vergleich zu neutralen Ereignissen, was mit Tierstudien übereinstimmt, die die Beteiligung aufsteigender vagaler Fasern am emotionalen Gedächtnis berichten. Somit könnten meine Ergebnisse zu kurzen Stimulationsimpulsen der taVNS auf erregungs- und/oder aufmerksamkeitsbezogene Prozesse während des Stimulationsprozesses hinweisen.

Die taVNS-Ergebnisse dieser Dissertation veranschaulichen damit die Wichtigkeit, nicht nur die sensorischen Wirkungen der verschiedenen Stimulationsbedingungen und -orte sorgfältig zu kontrollieren und zu bewerten, sondern auch die möglichen kognitionsfördernde Wirkungen im Zusammenhang mit der subjektiven Empfindung der Stimulationen an sich zu berücksichtigen. Zudem verdeutlichen die Ergebnisse zur funktionellen Aktivierung des LC, dass mit hochauflösendem funktionellen MRT und speziellen Nachbearbeitungsmethoden für kleine Strukturen im Hirnstamm altersbedingte Unterschiede in der LC-Funktion visualisiert werden können. Zukünftige Forschungsarbeiten können somit auf den Erkenntnissen meiner Dissertation aufbauen: Beispielsweise durch kombinierte fMRI-taVNS-Studien unter Berücksichtigung des Einflusses der subjektiven Empfindung der Stimulation, um die Mechanismen der taVNS, die Beteiligung vom LC und weiteren neuronalen Strukturen, sowie die Effekte der externen Modulation der NE-Freisetzung gezielter untersuchen zu können.

List of Original Papers

Parts of this dissertation have been published in the following peer-reviewed articles, to which I have made the contributions described below. Throughout the dissertation, I indicate the parts that belong to the respective publications.

Ludwig, M., Betts, M. J., & Hämmerer, D. (2025). Stimulate to Remember? The Effects of Short Burst of Transcutaneous Vagus Nerve Stimulation (TAVNS) on Memory Performance and Pupil Dilation. *Psychophysiology*, *62*(1), e14753. https://doi.org/10.1111/psyp.14753

- *As a first author, I contributed substantially to conceptualization, data curation, formal analysis, investigation, methodology, project administration, validation, visualization, writing original draft, and review and editing of the publication.*

Ludwig, M., Pereira, C., Keute, M., Düzel, E., Betts, M. J., & Hämmerer, D. (2024a). Evaluating phasic transcutaneous vagus nerve stimulation (taVNS) with pupil dilation: The importance of stimulation intensity and sensory perception. *Scientific Reports*, *14*(1), 24391. https://doi.org/10.1038/s41598-024-72179-4

- *As a first author, I contributed substantially to conceptualization, data curation, formal analysis, investigation, methodology, project administration, validation, visualization, writing original draft, and review and editing of the publication.*

Ludwig, M.*, Wienke, C.*, Betts, M. J., Zaehle, T., & Hämmerer, D. (2021). Current challenges in reliably targeting the noradrenergic locus coeruleus using transcutaneous auricular vagus nerve stimulation (taVNS). *Autonomic Neuroscience*, *236*, 102900. https://doi.org/10.1016/j.autneu.2021.102900

- *As a *shared first author, I contributed substantially to conceptualization, visualization, writing original draft, and review and editing of the publication.*

Ludwig, M., Yi, Y.-J., Lüsebrink, F., Callaghan, M. F., Betts, M. J., Yakupov, R., Weiskopf, N., Dolan, R. J., Düzel, E., & Hämmerer, D. (2024b). Functional locus coeruleus imaging to investigate an ageing noradrenergic system. *Communications Biology*, *7*(1), 1–13. https://doi.org/10.1038/s42003-024-06446-5

- *As a first author, I contributed substantially to conceptualization, formal analysis, methodology, validation, visualization, writing original draft, and review and editing of the publication.*

List of Tables

List of Figures

List of Abbreviations

5-HT	5-hydroxytryptamine
ACh	acetylcholine
ABVN	auricular branch of the vagus nerve
A, B, C-fibers	different types of nerve fibers
ACC	anterior cingulate cortex
AD	alzheimer's disease
AADC	aromatic amino acid decarboxylase
Aß plaque	aß plaque
α1, α2-, β-adrenoreceptors	different types of adrenoreceptors
Alpha2 agonists	alpha2 agonists
ANOVA	analysis of variance
App	application
β-amyloid	β-amyloid deposition
BLA	basolateral amygdala
BLE	bluetooth low energy
BDNF	brain-derived neurotrophic factor
cVNS	cervical vagus nerve
CE	conformité européenne certification
CG	ciliary ganglion
CI	confidence interval
CNS	central nervous system
COMT	catechol-o-methyltransferase
CSF	cerebrospinal fluid
CTT	central tegmental tract
DA	dopamine
DMV	dorsal motor nucleus of the vagus
DOPAC	dihydroxyphenylacetic acid
DOPEG	dihydroxyphenylethanol
DNV	dorsalis nervi vagi
EPI	echo-planar imaging
ERP	event related potential
EWN	edinger-westphal nucleus
FDA	food and drug administration
FLASH	fast low angle shot
FOV	field of view
(f)MRI	(functional) magnetic resonance imaging
FSE	fast spin echo
GABA	gamma-aminobutyric acid
GANE	glutamate enhances noradrenergic effects
GLM	general linear model
HPC	hippocampus
HRV	heart rate variability
Hz	hertz
Hz/Px	hertz per pixel
IML	intermediolateral cell column
iVNS	invasive vagus nerve stimulation
κ2	inhibitory receptors
L-DOPA	levodopa
LC	locus coeruleus
LDP	long-term depression

LMM	linear mixed model
LTP	long-term potentiation
MAO-A	monoamine oxidase A
MCI	mild cognitive impairment
MHGP	metabolite 3-methoxy-4-hydroxyphenylglycol
MHPG	metabolite 3-methoxy-4-hydroxyphenyl glycol
MNI	montreal neurological institute
MT-TFL	transfer-weighted turbo flash
NA	nucleus ambiguous
ND	neurodegenerative diseases
NE	norepinephrine / noradrenaline
NET	norepinephrine transporter
NM	neuromelanin
NTS	nucleus tractus solitarius
PAH	phenylalanine hydroxylase
PCUN	precuneus
PD	parkinson disease
pFDR	false discovery rate
pFWE	family-wise error
PFC	prefrontal cortex
PN	pretectal nucleus
RAVANS	respiratory auricular vagal afferent nerve stimulation
r	right
ROI	region of interest
RT	reaction time
SNR	signal-to-noise ratio
sNRIs	selective norepinephrine reuptake inhibitors
SI	supplementary Information
SN	substantia nigra
SpV N	nucleus spinalis nervi trigemini
T1-weighted (T1w)	mRI imaging based on T1 relaxation time
T2*-weighted (T2*w)	mRI imaging based on T2* relaxation time
taVNS	transcutaneous auricular vagus nerve stimulation
TSE	turbo spin echo
taVNS	transcutaneous auricular vagus nerve stimulation
tcVNS	transcutaneous cervical vagus nerve stimulation
TH	tyrosine hydroxylase
Tyr	tyrosine
tVNS	transcutaneous vagus nerve stimulation
VNS	vagus nerve stimulation
VTA	ventral tegmental area
VAS	visual analog scale
VMAT2	Vesicular Monoamine Transporter

1 Chapter 1: General Introduction

1.1 Introducing the Noradrenergic System of the Locus Coeruleus

The noradrenergic system of the locus coeruleus (LC-NE) plays a critical role in regulating arousal, attention, and cognitive function by modulating neural plasticity and stress responses through widespread norepinephrine (NE) release in the brain (Sara & Bouret, 2012). Aging is associated with structural and functional decline in the LC, including neuronal loss and reduced NE levels (Manaye et al., 1995; Van Egroo et al., 2023; Zucca et al., 2006), which contribute to impaired cognitive flexibility and increased vulnerability to neurodegenerative diseases (ND) (Mather & Harley, 2016). Post-mortem data indicate that tau pathology, a hallmark of ND like Alzheimer's disease (AD), emerges in the LC during early stages, before cortical spread, and prior to the onset of clinically noticeable cognitive symptoms (Braak et al., 2011; Mather & Harley, 2016; Theofilas et al., 2017). Concurrently, non-pathological aging-related decline in LC signal intensity reduces noradrenergic signaling in the brain (Liu et al., 2019; Mather & Harley, 2016), contributing to impaired cognition, attention, and memory in older adults (Berridge & Waterhouse, 2003). Therefore, researchers are investigating improved methods to visualize and validate the structure and function of the LC, underscoring its integrity and functionality as essential biomarkers for healthy aging and the early onset of ND (Betts et al., 2019; Engels-Domínguez et al., 2023).

1.1.1 Locus Coeruleus: Anatomy, Physiology, and Function

The Locus Coeruleus (LC, lat. "blue spot") is a small, symmetrical, thin, elongated nucleus hyperpigmented with neuromelanin (NM), located in the brainstem and is the primary source of norepinephrine (NE) (Sasaki et al., 2006; Zucca et al., 2006). Specifically, the LC is predominantly (90%) composed of noradrenergic tyrosine hydroxylase-positive neurons, with the remainder comprised of serotonergic and gamma-aminobutyric acid (GABA)-ergic neurons (Iijima, 1989). At the same time, animal studies also reported LC neurons' corelease of dopamine (DA) (Devoto et al., 2001; Kempadoo et al., 2016; Lemon & Manahan-Vaughan, 2012; Smith & Greene, 2012; Takeuchi et al., 2016). The human LC (on average 14.5 mm long and 2-2.5 mm thick) is located 1 mm below the fourth ventricle, 3 mm from the midline, and centered 14-21 mm above the pontomedullary junction (Fernandes et al., 2012). The LC contains an average of 48,900 neurons per hemisphere in the human brain (~ 3.000 neurons in the rodent brain) (Beardmore et al., 2021; German et al., 1988; Poe et al., 2020). The LC's lower middle portion is the most densely populated with cells, which results in a thinner appearance due to the neurons' more compact cylindrical shape (Baker et al., 1989; Fernandes et al., 2012;

German et al., 1988). Moreover, the LC synthesizes several significant peptides (e.g., vasopressin, somatostatin, neuropeptide Y), enhancing the LC system's intricacy and its projection regions (Olpe & Steinmann, 1991). The LC's non-myelinated projections can communicate monosynaptically (neuron to neuron) and by volume transmission (neurotransmitter release from varicosities along the axon), with NE diffusing into the surrounding space to act on many neurons, glial cells, and circulating blood (Feinstein et al., 2016). Notably, the LC exhibits spatial differentiation along its rostral-caudal axis, with rostral LC cell clusters primarily targeting frontal and limbic regions (e.g., amygdala, medial temporal lobe), while caudal LC cell clusters project to posterior cortical areas, cerebellum, and spinal cord (Dahl et al., 2019; Dutt et al., 2024; Veréb et al., 2023). Animal studies indicate that the rostral and middle portions of the LC regulate attention and circadian cycles, whereas the caudal regions of the LC influence respiratory, cardiovascular, and gastrointestinal functions (for review, see Beardmore et al., 2021).

1.1.1.1 More than just Norepinephrine? Catecholamine Synthesis and LC-NE Function

NE belongs to the catecholamine group and is the most important neurotransmitter that modulates the activity of the sympathetic nervous system, while most NE in the brain comes from the LC (Breton-Provencher et al., 2021; Eschenko et al., 2012). In particular, NE exerts its effects on neuronal cells (including LC neurons, microglia, astrocytes, and blood vessel endothelial cells) via G-protein-coupled α1-, α2-, and β-adrenoreceptors, with α1- and β-adrenoreceptors having excitatory effects, while α2-adrenoreceptors have an inhibitory effect on the neuron (Samuels & Szabadi, 2008; Szabadi, 2013). In a multi-stage process, NE is produced in vesicles at the axon terminal via the catecholamine synthesis pathway: Phenylalanine is converted to tyrosine (Tyr) by phenylalanine hydroxylase (PAH). Tyr is then converted into the precursor L-3,4-dihydroxyphenylalanine (L-DOPA) by the enzyme tyrosine hydroxylase (TH), which is then converted into DA by aromatic amino acid decarboxylase (AADC) (Eisenhofer et al., 2004; Molinoff & Axelrod, 1971). DA is encapsulated within storage vesicles, a subset of which harbor DA-β-hydroxylase, an enzyme responsible for converting DA into NE. Finally, NE is methylated to epinephrine by phenylethanolamine N-methyltransferase. After the release of NE, it is transported back into the presynaptic neuron via the norepinephrine transporter (NET), which is expressed on the dendrites and axon terminals of the LC and also facilitates DA uptake. In the cytoplasm, NE is either repackaged into synaptic vesicles by VMAT2 or degraded to metabolite 3-methoxy-4-hydroxyphenylglycol (MHPG) by monoamine oxidase A (MAO-A) and catechol-O-methyltransferase (COMT), a process that is important for neuronal health, as free catecholamine metabolites are highly

reactive and can potentially lead to oxidative stress and toxicity (Beardmore et al., 2021; Daubner et al., 2011; Eisenhofer et al., 2004; Goldstein, 2021; Kang et al., 2020; Molinoff & Axelrod, 1971). Importantly, DA has been proposed as a precursor of NE and a co-transmitter of NE (Devoto & Flore, 2006). In fact, lesion and optogenetic stimulation studies in animals demonstrated DA release from the LC (noradrenergic neurons store DA and co-release it together with NE) into the hippocampus (Devoto & Flore, 2006; Duszkiewicz et al., 2019; Kempadoo et al., 2016; Takeuchi et al., 2016; Uematsu et al., 2015; Wagatsuma et al., 2018), which underpins the important role of the LC in memory acquisition and consolidation. Indeed, animal studies showed that increased NE levels improved cognitive function (Luo et al., 2015). Furthermore, NE has the potential to reduce neuroinflammatory processes throughout the CNS through suppression of, e.g., IL-1, TNFα among other pro-inflammatory cytokines in astrocytes and microglia (Feinstein et al., 2002; Heneka et al., 2015; Mercan & Heneka, 2022) and increases the production of brain-derived neurotrophic factor (BDNF), which is crucial for neuronal survival, neuroplasticity, and neurogenesis (Liu et al., 2015). Therefore, the targeted modulation of NE levels represents a promising therapeutic approach for treating neurological and psychiatric disorders.

1.1.1.2 Neuromelanin: Unveiling the "blue spot"

The LC contains large amounts of the pigmented polymer NM, a by-product of NE synthesis (Zucca et al., 2006), but which is also present in the dopaminergic substantia nigra pars compacta (SNpc) (Zecca et al., 2004b). Names like "blue spot" and "black substance" are derived from the intense pigmentation of catecholamine neurons in the LC and SNpc, respectively (Fedorow et al., 2005, 2006; Vicq-d'Azyr, 1786), which affects its color in post-mortem brains. Importantly, this neuronal pigmentation is predominantly present in the brains of humans and non-human primates, whereas in rodents, there is little to no pigmentation (DeMattei et al., 1986; Marsden, 1961). The oxidation of NE or DA by iron and/or copper, abundantly found in SN or LC neurons, initiates the NM synthesis process (Monzani et al., 2019; Zecca et al., 2004b). Specifically, iron catalysts facilitate the oxidation of surplus cytosolic NE and DA, resulting in the formation of dopaquinones, with NE and DA quinones being converted into pheomelanin and eumelanin via different pathways (Bush et al., 2006; Krainc et al., 2023; Nagatsu et al., 2023). These quinones are then converted into NM and stored in autophagic organelles (Sulzer et al., 2000; Zucca et al., 2017). It is assumed that neuronal pigmentation is auto-oxidative (Sulzer et al., 2000). Importantly, NM granules also bind metal cations such as iron, zinc, and copper (Bridelli et al., 1999; Zecca et al., 2004a, 2008; Zucca et al., 2017) and catecholamine metabolites such as 3,4-Dihydroxyphenylacetic (DOPAC) and

3,4-Dihydroxyphenylethylene glycol (DOPEG) (Wakamatsu et al., 2015). Additionally, a substantial proportion of the isolated pigment's mass comprises NM's lipid component, particularly dolichols (Zucca et al., 2018). NM increases in the LC during aging, starting at about 3 years of age (Cowen, 1986; Zecca et al., 2004b), and may have a neuroprotective or neurotoxic role (Zucca et al., 2006, 2017). Specifically, NM's presence can confer cell-protective features, such as its ability to bind metal ions to reduce toxicity. Still, an overabundance of NM might harm cells and perhaps lead to cell death by impeding the synthesis of proteins within the cells, while accumulated NM is released into the extracellular space, causing chronic inflammation processes (Vila, 2019; Zucca et al., 2017). Thus, the NM content in the LC can serve as a potential biomarker for aging processes and ND. Furthermore, NM in the LC is thought to act as an endogenous magnetic resonance contrast agent, with its relaxivity significantly enhanced by the binding of metal ions like iron and copper, which leads to improved visibility of the LC region (Enochs et al., 1989, 1997; Trujillo et al., 2017; Zucca et al., 2006). Therefore, this has led to the development of the so-called neuromelanin-sensitive MRI technique to visualize the LC in the human brain in vivo (Betts et al., 2019; Sasaki et al., 2006). However, the exact signal source is debated (see section 1.1.4.1).

1.1.2 Mapping the Locus Coeruleus: Efferent and Afferent Pathways

Understanding the efferent and afferent pathways of the LC is essential for comprehending its functionality, as the unique projection patterns of individual LC neurons may modulate a wide range of behavioral and cognitive processes. Research to optimize the methods for the precise specification of the different pathways of LC is ongoing, and only the main pathways are presented here (for a comprehensive review, see Poe et al., 2020; Szabadi, 2013).

The **efferent** pathway can be subdivided into three pathways: (1) the ascending, (2) the cerebellar, and (3) the descending pathway (Szabadi, 2013). The **(1) ascending pathway** provides innervation to many structures within the midbrain (e.g., ventral tegmental area, substantia nigra) (Mejias-Aponte, 2016; Rommelfanger & Weinshenker, 2007) and the limbic system (e.g., amygdala, hippocampus, cingulate and parahippocampal gyri), which represents important brain structures for formation, consolidation and retrieval of emotional memories (Sara & Devauges, 1988; Takeuchi et al., 2016). Furthermore, the presence of excitatory noradrenergic receptors (α1 and β) on excitatory neurons and inhibitory receptors (κ2) on GABAergic neurons enable the LC to regulate cortical arousal and cognitive processes via the neocortex and forebrain (Berridge & Abercrombie, 1999; McBurney-Lin et al., 2019; Schwarz et al., 2015; Szabadi, 2013). Additionally, LC-efferent projections, bundled in a fiber tract that

anatomically corresponds to the central tegmental tract (CTT) (Langley et al., 2022), also innervate the thalamus and modulate sensory processing, wakefulness, stress, and pain (Beas et al., 2018; Langley et al., 2022; Rodenkirch et al., 2019; Szabadi, 2013). The **(2) cerebellar pathway** supplies innervation to the cerebellar nuclei and cerebellar cortex through the superior cerebellar peduncle (Dietrichs, 1988), and it has been observed that a lack of NE in the cerebellum led to motor impairments (Watson & McElligott, 1984). At present, LC cerebellar pathways have not yet been thoroughly investigated. The **(3) descending pathway** sends collaterals to the motor nuclei in the lower brainstem, such as the Edinger-Westphal-nucleus (EWN), which is involved in pupil dilation, and the dorsal vagus nucleus (VN) (Szabadi, 2013). Regarding VN, the LC has connections to the dorsal motor nucleus of the vagus (DMV) and the nucleus ambiguus, which are both involved in controlling the vagus nerve (Jones & Yang, 1985; Ter Horst et al., 1991; Westlund & Coulter, 1980). In particular, NE released from the LC can activate α2-adrenoceptors in the DMV (Robertson & Leslie, 1985). These receptors have an inhibitory effect on the DMV, which in turn can reduce the activity of the vagus nerve. In addition, LC and the vagal nuclei are involved in cardiac control (Szabadi, 2013). Subsequently, the LC descends into the spinal cord through the coeruleo-spinal pathway, providing innervation to all three neuron populations of the spinal cord: sensory neurons in the dorsal horn, motor neurons in the ventral horn, and preganglionic sympathetic neurons in the intermediolateral cell column (IML), which are involved in sensory processing, maintenance of muscle tone and control of pelvic reflexes, respectively (Szabadi, 2013).

The **afferent** pathway is characterized by the observation that most structures to which the LC projects also send outputs to the LC (Aston-Jones et al., 1991; Schwarz et al., 2015; Uematsu et al., 2017). The LC receives, for example, afferent connections from the neocortex, including the prefrontal cortex (PFC) (Arnsten & Goldman-Rakic, 1985; Jodo & Aston-Jones, 1997), the fear and anxiety processing amygdala (Cedarbaum & Aghajanian, 1978; Charney et al., 1998), from the wakefulness-promoting ventral tegmental area (VTA) (Deutch et al., 1986), and the arousal-modulating hypothalamus (Sara & Bouret, 2012), among other structures. Furthermore, the vagus nerve transmits information to LC via the nucleus tractus solitarius (NTS), which projects directly into the LC's dendritic region (Van Bockstaele et al., 1993). The illustration of the efferent and afferent pathways to and from the LC highlights its complexity and importance for the entire brain.

1.1.3 Various Firing Patterns of the Locus Coeruleus: Phasic vs. Tonic LC Mode

The activation of the LC can be either in a "tonic" (continuous activity) or "phasic" mode (rapid bursts), which is linked to distinct levels of NE release (Aston-Jones & Bloom,

1981; Aston-Jones & Cohen, 2005; Berridge & Waterhouse, 2003; Clayton et al., 2004; Florin-Lechner et al., 1996; Joshi et al., 2016). While the global increase in NE transmission in tonic mode is related to exploratory and novelty-seeking behavior, the upregulation of NE transmission in phasic mode increases task engagement and exploitative behavior (Aston-Jones & Cohen, 2005; Usher et al., 1999).

Tonic discharge of the LC neurons is characterized by relatively slow discharge rates (~ 0.1-5.0 Hz) to maintain arousal and attention (Berridge & Waterhouse, 2003; Bouret & Sara, 2004). Increased tonic activity is associated with arousal levels during the sleep-wake cycle (Aston-Jones & Bloom, 1981; Berridge & Waterhouse, 2003; Foote et al., 1980), while during wakefulness, it is more associated with goal-directed flexibility in tasks (Aston-Jones et al., 1997; Aston-Jones & Cohen, 2005).

Phasic discharge of the LC neurons is characterized by brief discharge rates (~2-4 spikes at ~10–20 Hz) and associated brief changes in attention and arousal, often followed by prolonged inhibition of spontaneous activity lasting 200-500 ms (Akaike, 1982; Aston-Jones & Bloom, 1981; Clayton et al., 2004). Phasic LC responses occur due to salient or novel stimuli and also by top-down decision and response signals from prefrontal regions (Aston-Jones & Bloom, 1981; Berridge & Waterhouse, 2003; Bouret & Sara, 2004; Foote et al., 1980; Sara & Bouret, 2012). Optogenetic stimulation of the phasic activity of the LC using low-intensity sensory inputs can enhance its salience and encoding, hence reproducing the effects of the LC on salient stimuli (Vazey et al., 2018). Importantly, it has been shown that phasic stimulation leads to a higher NE release than tonic stimulation (Berridge & Abercrombie, 1999; Devoto et al., 2005; Florin-Lechner et al., 1996) and enables a more fine-grained coding of sensory information (Devilbiss & Waterhouse, 2011). Therefore, phasic stimulation seems to be a promising approach to investigate the potential modulation of the LC-NE system. Consequently, the shift and balance between phasic and tonic modes of LC activity are important for the modulation of arousal (Aston-Jones & Cohen, 2005; Chen & Sara, 2007) and different forms of learning, such as memory encoding (Aston-Jones & Cohen, 2005; Mather et al., 2016b; Sara, 2009).

1.1.4 Methods of Assessing Locus Coeruleus in Humans

In recent years, there have been a growing focus on developing and enhancing in vivo measurement methods for longitudinal assessment of the structural and functional decline of the neuromodulatory nucleus of the LC in the human brainstem, to gain a deeper understanding of its specific susceptibility to aging. There are various methods, whereby the dissertation focuses only on structural, functional MRI with a high spatial resolution (typically 1-2 mm),

which is necessary to capture the structure of the LC accurately, and indirect methods, such as pupillometry.

1.1.4.1 Structural Magnetic Resonance Imaging (sMRI) of the Locus Coeruleus

In vivo, structural MRI assessment in humans has improved in recent years, while studies using T1-weighted Turbo Spin Echo (TSE)/Fast Spin Echo (FSE) imaging (García-Lorenzo et al., 2013; Keren et al., 2009; Sasaki et al., 2006; Takahashi et al., 2015), improved protocols such as 3D high-resolution T1-weighted Fast Low Angle Shot (FLASH) MRI for 3T (Betts et al., 2017) or 3D transfer-weighted Turbo Flash (MT-TFL) for 3 and 7T (Priovoulos et al., 2018) have been developed for better localization and visualization of the LC. The LC contrast serves as a proxy measure of LC integrity and shows up as local hyperintensity on those specialized structural MRI sequences (Berger et al., 2023; Keren et al., 2015). It is discussed as an indicator of cell density; however, the exact source of LC contrast extracted with specific MRI sequences remains controversial (Betts et al., 2019; Galgani et al., 2021). The possibilities include the density of neuromelanin-containing noradrenergic neurons within the LC (Betts et al., 2019; Liu et al., 2019; Sasaki et al., 2006) and the high water content and large cell bodies of LC neurons (Priovoulos et al., 2020; Trujillo et al., 2017; Watanabe et al., 2019), and seems to be influenced by lipid accumulation and inflammation (Priovoulos et al., 2020). To ensure that NM-MRI is a suitable measurement of LC integrity, Iannitelli & Weinshenker (Iannitelli & Weinshenker, 2023) suggested that the presence of NM should be associated with living neurons since previous research is predominantly based on post-mortem samples and imaging. It is unclear whether and how long NM persists in the extracellular space after the disappearance of its host cells (Iannitelli & Weinshenker, 2023). The LC contrast may be an early marker of LC-NE dysfunction in neurodegenerative disorders (Betts et al., 2019; Engels-Domínguez et al., 2023). Consistent with previous post-mortem studies, a decrease in LC contrast has been found in AD and Parkinson's disease (PD) (Betts et al., 2019; Keren et al., 2015; Sasaki et al., 2006), whereas higher LC contrast is associated with better memory and cognition (Clewett et al., 2016; Dahl et al., 2019).

1.1.4.2 Functional Magnetic Resonance Imaging (fMRI) of the Locus Coeruleus

Functional magnetic resonance imaging (fMRI) measures changes in blood flow in the region of the LC, which serves as a proxy for LC activation. Advancements in high-resolution recording and processing techniques enable better quantification of functional activations in the brainstem using MRI (Sclocco et al., 2018). FMRI studies in humans at 3 and 7T showed that the LC has both negative and positive functional connections to the cingulate cortex, thalamus, cerebellum, frontal, parietal, and temporal regions in healthy individuals at rest (Jacobs et al.,

2018; Liebe et al., 2020), which emphasizes the significant impact of the LC. Recently, enhanced LC responses to emotionally salient events have been reported in humans (Ludwig et al., 2024b), which is in line with animal studies showing its preferential firing to negative events such as foot shocks (Bouret & Sara, 2004; Sara, 2009) and in vivo findings linking increased LC integrity and better memory performance for negative events in older adults (Clewett et al., 2018; Hämmerer et al., 2018; Liu et al., 2020), However, the variety of s/fMRI methods investigating the small brain structure of the LC poses challenges when comparing results from different studies (Liu et al., 2017a). Therefore, standardization and quality control, particularly concerning spatial precision in the analysis of functional brainstem data, are essential (Yi et al., 2023).

1.1.4.3 Pupillometry: Indirect Measurement of the Locus Coeruleus Activity

Pupillometry is measured with an infrared eye-tracking camera that can capture variations in pupil dilation with millisecond-level precision. Briefly, changes in pupil size are controlled by a parasympathetic constriction pathway via the iris sphincter muscle and a sympathetic dilation pathway via the iris dilator muscle (Mathot, 2018). For the pupil to contract, information from the pretectal nucleus (PN) is transmitted to the EWN through the oculomotor nerve (III) to the ciliary ganglion (CG), which is located directly behind the eye and transmits information to the sphincter muscle of the iris. For the pupil to dilate, information is transmitted via subcortical pathways to the hypothalamus and LC, reaching the iris dilator muscle. In addition, the activity of the EWN can be inhibited by the activation of α2-adrenoceptors, which occurs through the release of NE from the LC, reducing the parasympathetic constriction of the pupil. This inhibition favors activating the sympathetically innervated dilator muscle, which can lead to pupil dilation even when light conditions remain constant (Hall & Chilcott, 2018; Samuels & Szabadi, 2008). Recently, it was outlined that the LC may modulate pupil size not only through its inhibition of the parasympathetic limb via the EWN but also by sending excitatory signals to the sympathetic limb through the intermediolateral cell column (Huang & Clewett, 2024; Joshi & Gold, 2020; Liu et al., 2017b). Importantly, changes in pupil dilation are non-exclusively related to LC activity, as other brain structures (e.g., hypothalamus, superior colliculus), neurotransmitters such as acetylcholine (ACh) and DA in rats (Collins et al., 2021; Manta et al., 2013, p. 201; Mridha et al., 2021) and noradrenergic and cholinergic axons (Hall & Chilcott, 2018; Reimer et al., 2016; Samuels & Szabadi, 2008) can also cause pupil dilation (Joshi et al., 2016; Mathot, 2018).

The potential of changes in pupil dilation as an indirect measure of LC-NE activity was motivated by animal studies showing that the firing rate of LC neurons is closely linked to

fluctuations in pupil diameter (Aston-Jones & Cohen, 2005; Rajkowski et al., 1994) and that phasic LC stimulation resulted in an increase in pupil dilation (Aston-Jones & Cohen, 2005; Joshi et al., 2016; Murphy et al., 2014; Reimer et al., 2016). Additionally, animal and human studies have shown that pupil dilation was associated with both spontaneous LC activity and temporary increases in LC activity, such as those related to task-relevant or salient factors (Breton-Provencher & Sur, 2019; de Gee et al., 2017; Gilzenrat et al., 2010; Varazzani et al., 2015). Furthermore, larger pupil diameters were observed during emotionally negative events (Hämmerer et al., 2017, 2018), consistent with the involvement of the LC-NE system in animals and humans during emotionally negative events (Bouret & Sara, 2004; Hämmerer et al., 2018; Ludwig et al., 2024b; Luo et al., 2015; Sara, 2009). Thus, pupil dilation may serve as a proxy for LC activation.

1.1.5 Theories of the LC-NE System in Behavior and Cognition

Several leading theories explain the LC-NE system's broader role in behavior and cognition, which are provided here as a synopsis.

The **adaptive gain theory** states that the LC regulates neural reinforcement to maximize benefit in a given context by alternating between tonic and phasic activity. The phasic mode promotes exploitative behavior by facilitating the processing of relevant information and filtering out irrelevant stimuli, keeping the focus on the task at hand. The tonic mode, on the other hand, promotes distraction and exploration, which facilitates the search for new behaviors. Therefore, changes in LC activity mode adapt behavior to environmental demands to optimize benefits (Aston-Jones & Cohen, 2005; Usher et al., 1999).

The **network reset theory** states that the LC-NE system resets the brain's neural networks to optimize processing in response to environmental changes, such as new or unexpected events. The idea emphasizes the LC's function in cognitive flexibility and new stimulus responsiveness. This "reset" function may help the brain avoid getting "stuck" in irrelevant patterns and maintain cognitive efficiency (Bouret & Sara, 2005; Sara, 2009; Sara & Bouret, 2012).

The **unexpected uncertainty theory** states that the LC-NE system processes unpredictable or uncertain events, especially those that differ from expectations. The LC releases NE in response to unexpected events, which may improve attention and memory encoding, facilitating faster learning from unexpected events. This theory supports the idea that the LC-NE system is crucial to adapting to uncertainty (Yu & Dayan, 2005).

The "**glutamate enhances noradrenergic effects**" (**GANE**) **model** proposed by Mather et al. (2016a) explains the mechanism in the brain of how arousal itself enhances and

simultaneously impairs the processing of stimuli depending on different factors like saliency and priority. GANE predicts that situations accompanied by arousal and prioritizing our attention for a certain moment for any stimuli will activate local glutamate-NE interaction (Mather et al., 2016a). Under arousal, glutamate, the brain's main excitatory neurotransmitter, increases with high-priority or salient stimuli followed by greater NE release, which in turn stimulates further glutamate via ß-adrenergic receptors (Mather et al., 2016a; Sakaki et al., 2019). The resulting increased GABAergic activation leads to suppression of *low-priority or inconspicuous* stimuli. Moreover, long-term potentiation (LTP) results from high NE levels near high-priority stimuli associated with ß-adrenergic receptor activation, whereas low NE levels elsewhere facilitate long-term depression (LDP) due to alpha one adrenergic receptor activation (Sakaki et al., 2019).

These theories extend the theory of adaptive gain theory and are primarily complementary. They concur that the LC-NE system facilitates behavioral adaptation to the environment, although they emphasize distinct processes by which NE regulates these behavioral adjustments.

1.1.6 The Impact of the LC-NE System with a Focus on Emotional Memory

In addition to the functions of the LC-NE system explained above, based on its anatomy and physiology description, I will now summarize the most important LC-NE functions and give an overview of how the LC-NE system is involved in emotional memory. In general, noradrenergic neuromodulation of the LC is associated with various cognitive processes such as episodic and working memory (Bouret & Sara, 2005; Corbetta et al., 2008; Hämmerer et al., 2018; Sara, 2009; Uematsu et al., 2015) and attention (Berridge & Waterhouse, 2003; Eldar et al., 2013) and has a complex role in regulating arousal (Aston-Jones & Cohen, 2005; Samuels & Szabadi, 2008), which is also linked to the sleep-wake cycle (Osorio-Forero et al., 2022). Regarding emotional memory, electrophysiological studies in rodents and monkeys and physiological studies in humans indicate that the LC-NE system is involved in processing and encoding salient events such as emotionally negative events (Chen & Sara, 2007; Hämmerer et al., 2018; Manaye et al., 1995) or the identification of change points in reward association learning (Hämmerer et al., 2018; Sara & Segal, 1991; Wittmann et al., 2011). In animals, arousal-related NE release from the LC during such tasks has been shown to facilitate memory encoding in the hippocampus (HPC) through ß-adrenoceptors (Luo et al., 2015), which regulate LTP and LTD (Hansen & Manahan-Vaughan, 2015; Mather et al., 2016b). Higher levels of NE release can be achieved by phasic stimulation of the LC (Florin-Lechner et al., 1996). Consistent with this, human studies have demonstrated higher activation in the LC during the

encoding of emotionally salient events (Sterpenich et al., 2006) as well as a better memory for emotionally salient events in individuals with higher LC integrity (Clewett et al., 2018; Hämmerer et al., 2018; Shibata et al., 2006). Chapter two of this dissertation will focus specifically on age-related differences in functional LC activation during emotionally negative events.

1.1.7 The Changing LC-NE System in Aging and Alzheimer's Disease

The LC-NE system may be particularly vulnerable as post-mortem studies indicate that the LC, along with other brain structures and neuromodulatory nuclei of the brainstem, appears to be notably affected by age-related neurophysiological decline (Manaye et al., 1995; Van Egroo et al., 2023). During aging, changes occur in the LC, such as **NM accumulation**, **neuronal cell loss,** and altered **NE modulation**, which can lead to AD in the case of more severe pathological changes. The precise interaction of the individual factors and which of them serve as driving forces in the development of AD is still under investigation.

NM accumulation is a normal aspect of aging; however, excessive accumulation of NM (see section 1.1.1.2) can lead to increased oxidative stress and neurotoxicity, which can damage neuronal structures and exacerbate neuronal loss (Zucca et al., 2006, 2017) and has been associated with pathological neurodegenerative changes affecting cognition and memory (Vila, 2019; Zucca et al., 2017). A structurally intact LC seems to be a better predictor of a more advantageous cognitive development in aging than more intact serotonergic or dopaminergic nuclei (Wilson et al., 2013). Several studies have shown that aging individuals with more structurally intact LC show less cognitive decline (Clewett et al., 2018; Dahl et al., 2019; Hämmerer et al., 2018; Liu et al., 2019; Sara, 2009). Concurrently with aging, the mean LC signal intensity values (contrast ratios, CRs) decline in the rostral parts (Liu et al., 2019), which leads to decreased noradrenergic signaling in the brain (Mather & Harley, 2016) and has been associated with a decline in cognitive function, attention, and memory in older adults (Berridge & Waterhouse, 2003). Lower signal intensity is correspondingly associated with mild cognitive impairment and AD (Dahl et al., 2022; Jacobs et al., 2021, 2023). However, it is not clear whether there is an age-related LC neuron decline by ~ 20 – 40 (Mather & Harley, 2016), as some of these studies were based on too small sample size and did not exclude pathology at other brain regions (Chan-Palay & Asan, 1989; German et al., 1989), while studies that controlled for this found no age differences (Mouton et al., 1994; Ohm et al., 1997).

In contrast, there is unequivocal evidence that the **LC tau pathology**, which is, besides amyloid pathology, a typical feature of ND like AD, increases with age (Braak et al., 2011). Tau pathology can be detected in the LC during the earliest stages of AD before it spreads to the

cortex and prior to the onset of clinically noticeable cognitive symptoms (Braak et al., 2011; Mather & Harley, 2016; Theofilas et al., 2017). In AD, the extent of LC cell loss in the rostral region is higher compared to the caudal third (German et al., 1992; Theofilas et al., 2017). This is in line with recent ultra-high-field imaging LC data, demonstrating a rostral vulnerability to early phosphorylated tau species (Van Egroo et al., 2023). In particular, the authors discovered that higher $ptau_{231}$ concentrations were linked to lower integrity in bilateral dorso-rostral clusters of the LC (at age ~55), and smaller right dorso-rostral clusters were linked to lower LC integrity when $ptau_{217}$ and $ptau_{181}$ levels were higher (at age 60) (Van Egroo et al., 2023). Additionally, pre-death cognitive deficits are tightly linked to the post-mortem existence of neocortical neurofibrillary tangles (Nelson et al., 2012). Currently, the exact underlying factors of this specific susceptibility of the LC and its role in disease progression remain unknown. Interactions between β-amyloid and NE are pivotal in affecting the advancement of AD via the LC-NE pathway. Impaired NE function diminishes protective mechanisms against β-amyloid deposition, facilitating the production of deleterious oligomers that may contribute to the propagation of neuropathology (Feinstein et al., 2002, 2016; Jagust & Mormino, 2011). This is consistent with the earliest reports of Aß plaque density and an associated decrease in LC neurons, which have also been linked to tau pathology in the LC (Bondareff et al., 1987). Increased Aß or tau depositions with a decrease in functional LC responses resulting in reduced NE levels may be associated with the degeneration of the LC in aging or the early stages of dementia (Braak et al., 2011; Heneka et al., 2010; Mann et al., 1980; Matthews et al., 2002). Consequently, the question arises whether the degeneration of LC neurons is a typical sign of healthy aging or can be regarded as a biomarker for mild cognitive impairment (MCI) and, thus, also for AD (Clewett et al., 2016; Shibata et al., 2006).

There are potential explanations for the selective vulnerability of the LC, in addition to the protective and toxic roles of NM (Zucca et al., 2006, 2017). The activity of LC neurons can be maintained independently of external excitatory or inhibitory inputs, which is associated with increased energy expenditure and oxidative stress (Sanchez-Padilla et al., 2014). Furthermore, LC neurons are characterized by an extended projection pattern, with axon bifurcations allowing both thalamic and cortical sensory areas to be reached simultaneously (Berridge & Waterhouse, 2003). Compared to related species, humans have a significantly less favorable ratio of LC neurons to the size of the supplied cortex, suggesting that the LC of humans is more heavily used (Sharma et al., 2010). Additionally, with a decrease in the blood-brain barrier with age and due to the proximity to the fourth ventricle, neurons of the LC are

increasingly exposed to toxins. Indeed, tau pathologies first appear in the axons of the LC before they are found in the nucleus, which may indicate retrograde spread (Braak et al., 2011).

1.1.8 Intervention Methods for Modulating the LC-NE System

Animal studies suggest that increasing brain NE levels may improve memory performance, while blocking adrenergic receptors impairs it (McGaugh, 2004; McGaugh et al., 1993; Van Stegeren, 2008), indicating the potential of NE modulation intervention. Given the alterations in NE function associated with aging and neurodegenerative disorders, it is pertinent to examine the degree to which interventions can affect NE levels in humans. Alpha2 agonists (e.g., clonidine, guanfacine) or reuptake inhibitors (e.g., reboxetine, atomoxetine) are commonly used to increase NE by pharmaceutical techniques, with the drugs either reducing the release of NE or increasing the concentration of NE in the synaptic cleft, respectively, which may support to regulate and stabilize NE activity (Chamberlain & Robbins, 2013). While some studies indicate enhancements in working memory, emotional memory, and attention (Campbell et al., 2008; Coull et al., 1995; Jäkälä et al., 1999; Oei et al., 2010), others report no improvement in memory performance (Chamberlain et al., 2006; Rammsayer et al., 2001; Wanke et al., 2020). However, an elevation in NE modulation appears beneficial, particularly in tasks demanding additional resources (Chamberlain & Robbins, 2013) and in populations with reduced NE levels (Arnsten & Goldman-Rakic, 1985). Current studies indicate that cognitive enhancements associated with pharmacologically increased NE levels in older adults or those with dementia yield inconsistent outcomes; however, the studies imply that apathy, the severity of tau pathologies, and overall inflammation may be ameliorated through NE modulation (David et al., 2022; Levey et al., 2022). The disadvantage of pharmacological interventions is the lack of anatomical specificity, which increases the likelihood of generating side effects that may have a negative impact on quality of life. Research in rodents demonstrated increased LC firing linked to NE release in the hippocampus and cortical target regions over minutes to hours through iVNS techniques (Follesa et al., 2007; Hulsey et al., 2017; Hulsey, 2019; Manta et al., 2013). For this reason, transcutaneous auricular vagus nerve stimulation (taVNS) in humans has been discussed in recent years as a promising non-invasive method that offers a more anatomically precise and potentially rehabilitative NE therapy compared to pharmacological interventions (Ludwig et al., 2021).

The review of the LC has emphasized its pivotal role in brain function, such as arousal, attention, and memory, attributed to its wide-ranging connections and primary NE release throughout the whole brain (Fig. 1). The LC-NE system is generally involved in processing and encoding of salient events such as emotionally negative events. Phasic stimulation of the LC

can result in higher levels of NE release (Florin-Lechner et al., 1996), which supports cognition and memory. Due to the LC's small size, standardization and quality control, particularly for spatial precision in the analysis of functional brainstem data, are crucial (Yi et al., 2023). A structurally intact LC is a better predictor of more advantageous cognitive development in aging. Post-mortem data indicate that tau pathology, a typical feature of ND like AD, can be detected in the LC during the earliest stages of AD before it spreads to the cortex and prior to the onset of clinically noticeable cognitive symptoms (Braak et al., 2003, 2011). The LC is also connected to the VN via other neuronal brain structures (e.g., DMV, NTS), and interventions targeting the LC-NE system may hold promise for mitigating age-related and AD-related deficits. Therefore, taVNS seems to be a promising non-invasive stimulation approach. Importantly, individual vulnerability and changes in the LC-NE system must be carefully considered in taVNS, along with the appropriate application of stimulation design and parameters. For this reason, the current state of taVNS research is presented in more detail in the next section.

Overview

Noradrenergic System of Locus Coeruleus

1. **Noradrenergic system of locus coeruleus (LC-NE):** The LC is a small, symmetrical, thin, elongated nucleus with neuromelanin (NM) hyperpigmentation, located close to the fourth ventricle in the brainstem (Fernandes et al., 2012). The LC is the primary source of NE in the human brain but also supplies parts of the brain with dopamine (DA) (Theofilas et al., 2017; Takeuchi et al., 2016; Zucca et al., 2006).

2. **Various firing patterns of the Locus Coeruleus**: The activation of the LC can be either in a "tonic" (continuous activity) or "phasic" mode (rapid bursts), which is linked to distinct levels of NE release (Aston-Jones & Bloom, 1981; Aston-Jones & Cohen, 2005). Higher levels of NE release can be achieved by phasic stimulation of the LC (Florin-Lechner et al., 1996).

3. **Role of the LC-NE System in processing salient events**: The LC-NE system is generally involved in the processing and encoding of salient events, such as emotionally negative events or identifying change points in reward association learning (Chen & Sara, 2007; Hämmerer et al., 2018; Ludwig et al., 2024b; Manaye et al., 1995; Sara & Segal, 1991; Wittmann et al., 2011).

4. **Changing LC-NE system in aging and Alzheimer's disease**: Post-mortem data indicate that tau pathology, a typical feature of neurodegenerative diseases (ND) like Alzheimer´s disease (AD), can be detected in the LC during the earliest stages of AD before it spreads to the cortex and prior to the onset of clinically noticeable cognitive symptoms (Braak et al., 2011; Mather & Harley, 2016; Theofilas et al., 2017). Importantly, a structurally intact LC is a better predictor of a more advantageous cognitive development in aging (Clewett et al., 2018; Dahl et al., 2019; Hämmerer et al., 2018; Liu et al., 2019).

5. **Structural and functional LC imaging:** The assessments of the LC are methodologically challenging in humans due to its very small size. Thus, standardization and quality control, particularly regarding spatial precision in analyzing functional brainstem data, are crucial (Yi et al., 2023).

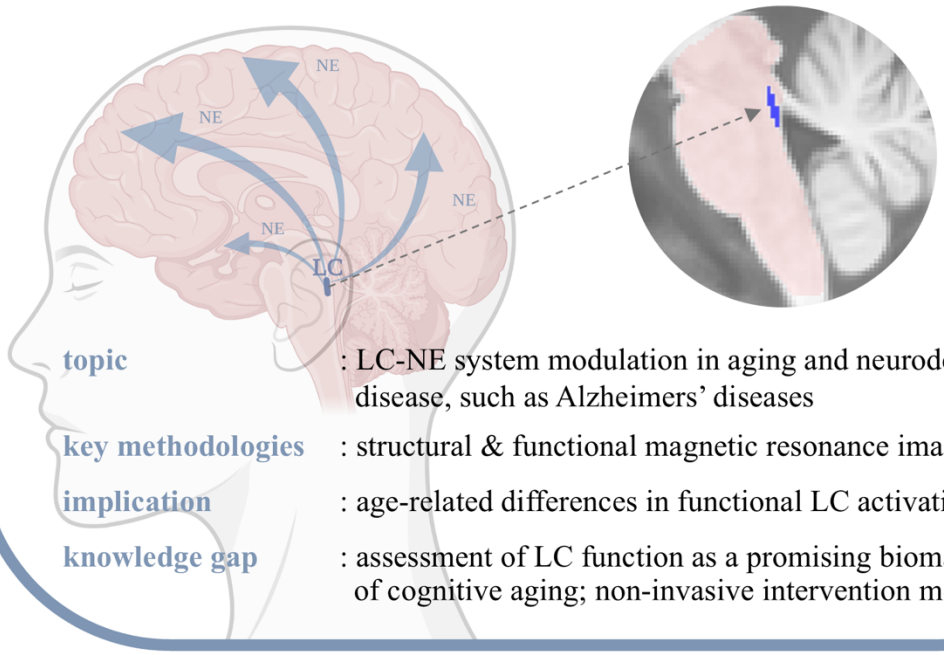

topic	: LC-NE system modulation in aging and neurodegenerative disease, such as Alzheimers' diseases
key methodologies	: structural & functional magnetic resonance imaging (s/fMRI)
implication	: age-related differences in functional LC activation
knowledge gap	: assessment of LC function as a promising biomarker of cognitive aging; non-invasive intervention methods

Figure 1. Overview covering the key aspects of the noradrenergic system of the locus coeruleus (LC-NE system). The blue mask (right) indicates the LC meta mask (Dahl et al., 2022). The image of the head was created with BioRender.com.

1.2 Introducing Transcutaneous Vagus Nerve Stimulation

A version of this section, with minor modifications,
has been published in Autonomic Neuroscience (Ludwig et al., 2021).

Vagus nerve stimulation (VNS) is a neuromodulation therapy that aims to modul function of the autonomic nervous system and neuronal excitability, thereby influen numerous physiological and neurological processes in the human body (Burger et al., 2020; Butt et al., 2020; Farmer et al., 2021; Vonck et al., 2014). Invasive implantable vagus nerve stimulation (iVNS), conceived by Jake Zabara in the 1980s for its antiepileptic properties in animal studies (Zabara, 1985; Zabara, 1992), received approval from the Food and Drug Administration (FDA) in 1997 for the management of pharmacoresistant epilepsy following comprehensive clinical trials (Morris et al., 2013; Penry & Dean, 1990; Uthman et al., 1993) and subsequently for pharmacoresistant depression in 2005 (Cristancho et al., 2011; Desbeaumes Jodoin et al., 2018). Simultaneously, non-invasive transcutaneous vagus nerve stimulation (tVNS) methods have been established as more economical, patient-friendly, and adaptable alternatives (Ventureyra, 2000), with transcutaneous cervical VNS (tcVNS) already receiving FDA approval and being specifically utilized for migraine and cluster headaches (Goadsby et al., 2014; Nesbitt et al., 2015). TaVNS was developed to provide an alternative to iVNS used in humans as an adjunctive therapy for the treatment of refractory epilepsy and depression (Englot et al., 2011; Farmer et al., 2021; Panebianco et al., 2016). TaVNS was first proposed by Ventureya (Ventureyra, 2000) to avoid the surgical procedure required to implant the iVNS devices, which can pose certain risks to patients, such as nerve damage and post-operative infections (Butt et al., 2020). Although taVNS has not yet been approved by the FDA, it is being intensively researched for various clinical applications. It is available in Europe with CE certification, such as the NEMOS® device (Farmer et al., 2021), which has been optimized in recent years for individualized therapy and is now designated as a tVNS® device (tVNS R, tVNS Technologies GmbH).

1.2.1 Anatomical Basis of the Vagus Nerve

The vagus nerve (VN; *10th* cranial nerve) consists of a left (nervus vagus sinister) and right (nervus vagus dexter) branch and is the longest cranial nerve, as it courses from the brainstem to the distal third of the colon (Bonaz et al., 2017; Butt et al., 2020). The VN originates from the medulla oblongata and exits the cranial cavity through the jugular foramen, whereby there are four core regions of the brainstem: the nucleus ambiguus (NA) and nucleus dorsalis nervi vagi (DNV), which are responsible for the parasympathetic and efferent fibers of the vagus nerve, and the NTS and nucleus spinalis nervi trigemini (SpV N), which receive

afferent information (Berthoud & Neuhuber, 2000; Butt et al., 2020)**.**

The VN is a major part of the parasympathetic nervous system and consists mainly of afferent (80%) but also efferent (20%) pathways (Butt et al., 2020). While **efferent** vagus nerve fibers innervate the voluntary muscles of the larynx and pharynx, **afferent** vagus nerve fibers carry visceral information from the lungs, heart, gastrointestinal tract, taste information, and sensory information from the concha of the outer ear through the auricular branch of the vagus nerve (ABVN) (Berthoud & Neuhuber, 2000; Butt et al., 2020). Furthermore, VN consists of different types of fibers (A, B, C) that vary in myelination, size, and conduction velocity (Ruffoli et al., 2011). Approximately 65-80% of the vagal fibers are unmyelinated C-fibers, which are responsible for transmitting visceral information from various organs in the body (Noller et al., 2019; Ruffoli et al., 2011). As the VN is part of a complex neuronal network, VN has a vital role in maintaining homeostasis (Butt et al., 2020).

1.2.2 Transcutaneous Vagus Nerve Stimulation

The anatomical location of the vagus nerve, specifically its trajectory in the cervical and auricular regions, facilitates stimulation that can affect several functions regulated by the parasympathetic nervous system. Unlike iVNS, which involves surgically wrapping a stimulation electrode around the vagus nerve in the neck, and cervical tVNS, which uses external electrodes on the neck (Farmer et al., 2021), taVNS can be applied to various sites in the outer ear controlled by the ABVN (Peuker & Filler, 2002; Yakunina et al., 2017).

Specifically, taVNS is mainly applied to the cymba conchae (depression in the upper part of the auricle), which is solely innervated by ABVN, or to the tragus (rounded protrusion located lateral and rostral to the concha auricularis), which is largely innervated by ABVN but also by the Great Auricular Nerve and the Auricolutemporal Nerve (Peuker & Filler, 2002). Small surface electrodes in taVNS are attached to the cymba concha or the tragus, primarily on the left auricle. Although the left auricle is usually used to avoid potential cardiac side effects, more systematic research is required to ascertain the degree to which cardiac side effects genuinely exist following stimulation of the left or right ear (Farmer et al., 2021). In general, taVNS is modulated by the transmission of excitation from the ABVN through the remaining nerve fiber bundles of the vagus nerve to the brainstem at the nucleus tractus solitarius (NTS), which has prominent projections to the LC-NE system (Butt et al., 2020; Ruffoli et al., 2011).

TaVNS is characterized by the combination of different stimulation parameters (see section 1.2.5.1). As stimulation at the auricular has been shown to potentially activate structures such as NTS and LC along the vagal afferent pathway in humans (Badran et al., 2018; Sclocco, 2020; Yakunina et al., 2017), the efficacy of taVNS as a non-invasive method for modulating

the LC-NE system is increasingly being discussed (D'Agostini et al., 2023; Farmer et al., 2021; Ludwig et al., 2021; Sharon et al., 2021; Yakunina et al., 2017).

1.2.3 Central Nervous Working Mechanism of I/TaVNS

While more direct neurophysiological studies in animals have provided insights into potential mechanisms of VNS, the exact working mechanisms of taVNS in humans are still not completely understood (Farmer et al., 2021). Therefore, animal iVNS studies offer suggestions for possible taVNS-related physiological mechanisms in humans. The underlying working mechanism of VNS is primarily discussed based on the altered release of neurotransmitters such as NE, GABA, and ACh in the central nervous system (for review, see Bonaz et al., 2017; Colzato & Beste, 2020). However, the evidence for the proposed GABAergic and parasympathetic-cholinergic pathways of the iVNS is sparse and indirect. At the same time, there is ample evidence for the role of the LC-NE system in the mechanisms of action of iVNS.

Since the LC containing NE is a downstream projection region of the NTS, which is one of the brain projection regions of the afferent vagus nerve fibers (Aston-Jones & Cohen, 2005; Berthoud & Neuhuber, 2000), the LC-NE system may modulate potential i/taVN-induced effects. Indeed, iVNS in rodents showed increased concentration of extracellular NE in prefrontal areas, hippocampus (Manta et al., 2009, 2013; Roosevelt et al., 2006), in the basolateral amygdala (BLA) (Hassert et al., 2004), and subsequently that of 5-HT neurons (Manta et al., 2009), while there may also be increased extracellular DA levels despite decreased VTA-DA neuron activity due to iVNS (Manta et al., 2013). Similarly, increased levels of NE in combination with increased BDNF in the hippocampus were shown after iVNS in rodents (Follesa et al., 2007). Regarding LC activation, increased LC firing was observed in rats due to dose-dependent iVNS (e.g., higher intensity led to increased LC firing) (Collins et al., 2021; Dorr & Debonnel, 2006; Hulsey et al., 2017). In humans, only one iVNS study directly investigated NE and MHPG in depressed patients but found no effects on NE and MHPG concentrations in CSF from lumbar punctures (Carpenter et al., 2004). Non-invasive indicators of NEergic activity in humans, including the P300 component of the event-related potential and pupil size, have shown contradictory results (D'Agostini et al., 2023; De Taeye et al., 2014; Keute et al., 2019; Schevernels et al., 2016; Sharon et al., 2021). However, promising results from taVNS fMRI studies in humans showed increased LC activation due to short bursts of taVNS (Sclocco, 2020; Yakunina et al., 2017). Additionally, the inhibitory GABA may also be implicated in the mechanism of action of taVNS, as iVNS studies in patients indicated that prolonged use may increase the concentration of GABA in the cerebrospinal fluid (CSF) and increase the density of GABA receptors (Ben-Menachem et al., 1995; Marrosu et al., 2003).

Furthermore, ACh and NE modulate cortical activity and excitability; hence, ACh may be implicated in VNS-induced cortical activity alterations (Collins et al., 2021; Rho et al., 2018), although the evidence for this involvement is currently limited. IVNS studies in rats, for example, showed that shortly after the onset of iVNS, there was an increase in the activity of ACh in the cortical axons (Collins et al., 2021). Comparable findings have been demonstrated in anesthetized rats, wherein VNS disrupts ongoing brain activity via cholinergic muscarinic receptors (Nichols et al., 2011). Moreover, iVNS studies in rats showed the involvement of basal forebrain cholinergic axon activity in the neocortex in pupil dilation, while cholinergic axon activation correlated with VNS stimulation intensity (Mridha et al., 2021). Nevertheless, the specific neural pathway that links the VNS to cortical ACh remains uncertain. The insights gained from iVNS animal studies pave the way for translational research to validate these mechanisms and explore their therapeutic applications in humans.

In sum, there is solid evidence that i/taVNS may increase NE release by activating the LC. However, compared to iVNS in animal models, there is little evidence that the LC is effectively targeted with taVNS in humans. This is also attributable to the fact that the LC is known to release both NE and DA (Takeuchi et al., 2016). Therefore, the technique is not yet suitable as a reliable method for modifying noradrenergic modulation in humans (Ludwig et al., 2021), and further taVNS research in humans with appropriate outcome measurements for the LC-NE system is required (Fig. 2).

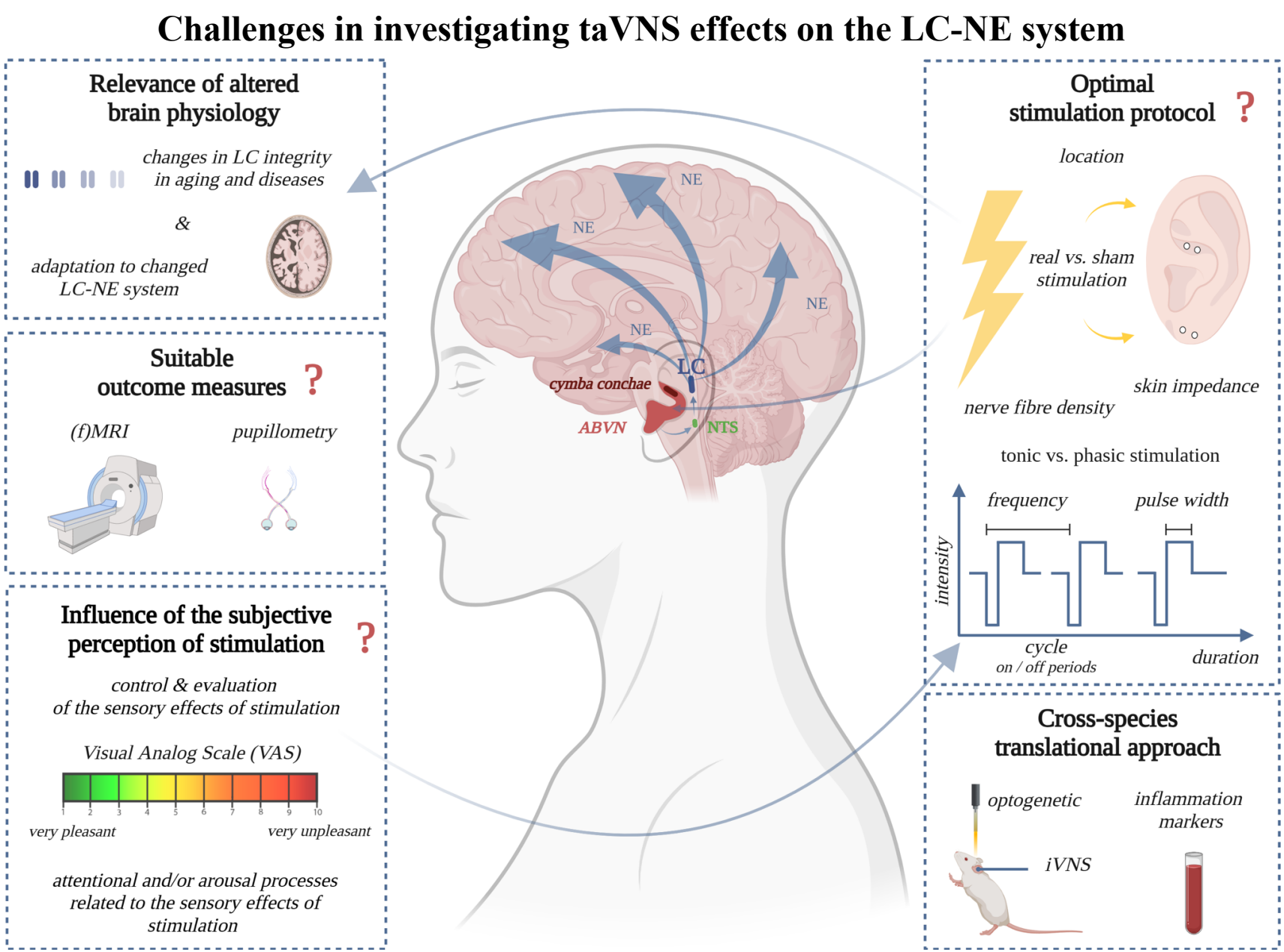

Figure 2. Challenges in investigating taVNS effects on the LC-NE System. Center: TaVNS is applied to regions in the left ear innervated by the Auricular Branch of the Vagus Nerve (ABVN). The stimulation is relayed via the ABVN to the Nucleus tractus solitarius (NTS) which projects to the Locus Coeruleus (LC) from where norepinephrine (NE) is released into various projection areas. Top right: Currently, taVNS in humans is characterized by heterogeneous stimulation protocols. Short burst (phasic) and longer lasting bursts (tonic) of mono- or biphasic stimulation approaches are based on different stimulation parameters (intensity, frequency, pulse width, cycle, duration), which are tested on different stimulation locations. Bottom right: Cross-species translational approaches can be used to investigate new taVNS applications in humans and improve current stimulation methods. Middle left: Suitable outcome measures for taVNS are needed to study taVNS effects on the LC-NE system in an optimal manner. Top left: Alterations in brain physiology, such as the integrity of the LC and adaptation to an altered LC-NE system might account for heterogeneous outcomes and need to be considered especially in clinical populations to adjust the stimulation parameters accordingly. Bottom left: The sensory effects of the different stimulation conditions and locations must be carefully controlled and evaluated to distinguish between pure stimulation effects and attention and/or arousal-related effects of taVNS. The image was created with BioRender.com.

1.2.4 Indirect Outcome Measurements of TaVNS

Most human taVNS studies lack adequately validated physiological and cognitive outcome markers necessary to assess the temporal and spatial precision of taVNS intervention effects on the LC-NE system. This refers to the challenge of measuring LC activation directly in humans, which is why indirect measures of LC activity, such as pupil dilation, P300 event-related potential (ERP), and salivary alpha-amylase, have been proposed in terms of their respective usefulness in indicating potential activation of the LC-NE resulting from taVNS (Burger et al., 2020; Ludwig et al., 2021) (Fig. 2). In addition, taVNS-related improvements in memory performance are being investigated (Jacobs et al., 2015; Ventura-Bort et al., 2021).

Regarding **changes in pupil dilation** due to i/taVNS, it is discussed that vagal afferent projections modulate the LC-NE system via projections from the NTS in the brainstem (Dorr & Debonnel, 2006; Hulsey et al., 2017; Yakunina et al., 2017). As previously outlined in section 1.1.4.3, pupil dilation has been shown to be a promising indirect measure of LC-NE activity, as animal studies indicate that phasic LC stimulation leads to an increase in pupil dilation (Joshi et al., 2016; Reimer et al., 2016), and both animal and human studies revealed that pupil dilation is related to LC activity (Breton-Provencher & Sur, 2019; de Gee et al., 2017; Joshi & Gold, 2020; Murphy et al., 2014; Varazzani et al., 2015). At the same time, VNS in rodents led to increased LC activity (Hulsey et al., 2017) and pupil dilation (Bianca & Komisaruk, 2007; Mridha et al., 2021). Changes in pupil dilation can thus be considered as an indirect outcome measure to investigate the effects of taVNS. However, there is currently no reliable evidence for a potential pupil modulation due to tAVNS (D'Agostini et al., 2023; Keute et al., 2019; Ludwig et al., 2021; Pervaz et al., 2025; Sharon et al., 2021).

FMRI is as a more direct outcome measurement than pupillometry for visualizing LC activation in humans. However, fMRI reflects changes in blood flow in the region of the LC, which serves as a proxy for LC activation (Jacobs et al., 2020; Yi et al., 2023). Combined taVNS fMRI studies in humans showed promising taVNS-induced functional activation of NTS in LC-NE projection areas such as the amygdala and hippocampus (Sclocco et al., 2019; Yakunina et al., 2017). Importantly, several methodological considerations should be considered, especially because target regions such as NTS and LC span only a few millimeters. Consideration should be given to ultra-high-resolution fMRI in the 1-2 mm voxel size range, even at higher field strengths, and customized high-precision spatial post-processing approaches optimized for the LC-NE system (Liu et al., 2017a). Furthermore, combined taVNS fMRI studies should incorporate structural measurements of the LC-NE system, such as LC-sensitive magnetic resonance imaging (MRI), to anatomically identify the LC in vivo (Betts et al., 2017, 2019;

Hämmerer et al., 2018; Liu et al., 2019; Priovoulos et al., 2018; Sasaki et al., 2006; Trujillo et al., 2019; Ye et al., 2021). Lastly, as the brainstem fMRI is more prone to poor signal-to-noise ratio (SNR) and high physiological noise (Sclocco et al., 2018), suitable imaging paradigms and employing denoising or noise control techniques should be incorporated (Brooks et al., 2013; Sclocco et al., 2018).

In addition, **memory performance** is being studied to determine the effectiveness of taVNS in improving cognitive function. While the VN and LC seem to be involved in the processing of emotional memories (Hämmerer et al., 2017, 2018; Sterpenich et al., 2006; Uematsu et al., 2015; Vonck et al., 2014) the underlying mechanism involved in the possible improvement of emotional memory by taVNS appears complex. According to Vonck et al. (2014), VNS may increase hippocampal synaptic plasticity by influencing the trisynaptic circuit through adrenergic signaling mediated by the LC. Indeed, electrophysiological studies in rodents showed that phasic stimulation increased LC-released NE, which could support memory encoding via ß-adrenoceptors in the hippocampus (Dorr & Debonnel, 2006; Florin-Lechner et al., 1996; Luo et al., 2015; Raedt et al., 2011; Roosevelt et al., 2006), thus improving memory storage after avoidance learning (Clark et al., 1998) and increasing NE levels in the amygdala after stimulation (Hassert et al., 2004). The most promising indirect outcome measurements are thus pupillometry and fMRI for taVNS-induced LC-NE modulation (Ludwig et al., 2021) (Fig. 2).

1.2.5 Methodological Challenges and Considerations of TaVNS on LC-NE System

The effectiveness of taVNS studies to date has been characterized by high heterogeneity and low reliability of stimulation effects (Farmer et al., 2021; Ludwig et al., 2021). Furthermore, only a limited number of human studies have investigated the effects of taVNS on the LC-NE system (Sclocco, 2020; Sharon et al., 2021; Yakunina et al., 2017). This is due to inadequately validated stimulation protocols and a deficiency of appropriately validated methods to assess the physiological and cognitive outcomes of an individually altered LC-NE system (Fig. 2).

1.2.5.1 Inadequately verified Stimulation Protocols

Regarding the **stimulation protocols**, the applied stimulation parameters to be set differ greatly between taVNS studies, which makes it difficult to compare the studies with each other and to gain insightful knowledge about potential taVNS-induced effects on the LC-NE system based on certain stimulation parameters. TaVNS is characterized by the combination of the following stimulation parameters: waveform of weak electrical pulses (rectangular, mono- or biphasic pulses), temporal dynamics of stimulation (short bursts (phasic) vs. longer lasting bursts (tonic) stimulation), stimulation intensity (in milliamperes (mA); the amplitude of each

pulse), stimulation frequency (in Hertz (Hz); the number of pulses per second), pulse width (in microseconds (μs); duration between leading and trailing edges of single pulse), duty cycle (time where stimulation is on vs. off) and total duration of stimulation (Farmer et al., 2021). The most commonly applied stimulation frequency is 25 Hz with a duty cycle of 30 s on and 30 s off, while pulse width is between 200 – 300 μs, and stimulation intensity is applied based on individual needs (Ludwig et al., 2021; Yap et al., 2020). This is mainly because many studies in the past used a commercially available taVNS device that did not allow flexible adjustment of stimulation parameters, which limits possible taVNS study designs. Conversely, iVNS studies in rats have already used customized stimulation protocols and tested different stimulation parameters, revealing that, e.g., higher intensities resulted in increased LC firing and NE release (Collins et al., 2021; Hulsey et al., 2017; Mridha et al., 2021).

At present, systematic human research examining the impact of varying stimulation **intensities** for taVNS is absent. Two methodologies are employed: (i) fixed stimulation intensities for all subjects and (ii) personalized intensities that may be either beneath or over the perceptual threshold. The initial method guarantees consistent parameters, but the subsequent one prevents unpleasant or painful stimulation. Both approaches are feasible, provided that the intensity reaches the threshold necessary to activate myelinated A-fibers of the ABVN ($\geq$ 0.75 mA, (Safi et al., 2016)). Using cervical VN, computer models predicted effective intensities ranging from 0.75 to 1.75 mA with 200 – 500 μs pulse widths (Helmers et al., 2012). In real life, electrical stimulation levels are likely higher since skin impedance and subcutaneous tissues affect the current flow (Keller & Kuhn, 2009). Therefore, skin cleaning can diminish impedance and enhance the efficacy of electrical stimulation (Burger et al., 2020).

The predominant **frequency** for taVNS in humans is 25 Hz (Farmer et al., 2021); however, evidence supporting its efficacy is insufficient. Research on rats indicated that elevated frequencies (0, 7.5, 15, 30, 60, 120 Hz) increased short-term discharge rates in the LC without impacting overall activity (Hulsey et al., 2017). In humans, Sclocco et al. (2020) tested a first more systematic stimulation protocol and discovered that perceptual ratings were consistent when higher intensities were paired with lower frequencies (7.18 ± 0.95 mA (2 Hz) > 6.46 ± 1.30 mA (10 Hz) > 5.93 ± 1.21 mA (25 Hz) > 5.57 ± 1.18 mA (100 Hz)). Moreover, respiratory-gated taVNS (RAVANS) at 100 Hz produced more extensive activation patterns in serotonergic and noradrenergic regions compared to 2 Hz (Sclocco, 2020).

Pulse width also influences iVNS effectiveness in a dose-dependent fashion. In rodent iVNS studies, elevated pulse widths resulted in enhanced LC firing rates (0, 30, 100, 500 μs (Hulsey et al., 2017)), pupil dilation (100, 200, 400, or 800 μs (Mridha et al., 2021)), and

increased behavioral as well as cortical arousal states (100, 500, or 800 μs (Collins et al., 2021)). In human taVNS studies, pulse width generally ranges from 200 to 1000 μs (Farmer et al., 2021), while a recently published paper showed increased pupil dilation during higher pulse width paired with lower intensity (D'Agostini et al., 2023).

The total **duration** of taVNS depends on the specific intervention and its application, particularly in therapeutic settings where stimulation occurs over days to weeks, or in experimental settings where stimulation lasts from minutes to hours (Farmer et al., 2021). Consequently, it is essential to carefully investigate and evaluate the appropriate stimulation duration, as the optimal time range for taVNS studies in humans and its potential effects on the LC-NE system remain uncertain.

Another often neglected aspect is the **stimulation side** of the ear, i.e., left vs. right. The right vagus nerve strongly innervates the sinus node (Ardell & Randall, 1986; Guiraud et al., 2016; Kaniusas et al., 2019), and right-sided iVNS in animals led to increased heart rate variability (HRV), while left-sided stimulation yields mixed effects (Lee et al., 2018a; Martlé et al., 2014; Samniang et al., 2016; Yoshida et al., 2018). In humans, only the left side is typically stimulated due to concerns about cardiac side effects (Borges et al., 2021; Burger et al., 2020), which is currently under debate (e.g., stronger HRV indices for right-sided taVNS reported by De Couck et al. (2017)). Accordingly, studies in animals indicate that the right nodose ganglia (NG) have better access to dopaminergic regions such as the SN (Han et al., 2018), while in humans, stimulation of the left ear has a greater impact on invigoration when food reward is included (Neuser et al., 2020). These findings advocate for a more comprehensive investigation in this domain, while according to HRV indicators (Keute et al., 2021) and mood variations (Ferstl et al., 2022), it is likely that the stimulation side does not exert a systematic influence on taVNS effects at the present moment.

One non-trivial open question is the systematic assessment of real vs. sham stimulation **location**. Electrical stimulation over the sensory threshold produces an identifiable somatosensory percept that may explain stimulation effects. Thus, an appropriate sham stimulation is needed to ensure that reported effects are due to LC stimulation, not somatosensory perception. The decision for a specific taVNS stimulation location is mostly based on the results of Peuker & Filler (Peuker & Filler, 2002). In humans, different real stimulation locations using taVNS-fMRI were already tested (Yakunina et al., 2017), but different sham stimulation locations have not been extensively investigated. Since the earlobe is generally regarded as being relatively free of ABVN fibers (Peuker & Filler, 2002), it is commonly used as the location for sham stimulation (Burger et al., 2020; Butt et al., 2020).

However, due to the inhomogeneous density of sympathetic nerves in the human ear, this location has been questioned as a suitable target for sham stimulation (Borges et al., 2021; Cakmak, 2019; Rangon, 2018). As perivascular, sympathetic neurotransmitters are richer in the higher auricular areas close to the cymba concha for real stimulation than in the lower auricular areas, Cakmak et al. (2018) recommended using the upper parts of the ear rather than the earlobe for sham stimulation. Another potential control strategy is using real taVNS locations without stimulation (Garcia et al., 2017) or with a very low stimulation frequency (1 Hz) (Bauer et al., 2016; Garcia et al., 2017; Sclocco, 2020). However, these methods are infrequently utilized and need validation.

These findings indicate that further investigation is required to identify appropriate targets for active sham stimulation. The comparison of real and sham stimulation should also consider placebo or expectancy-related confounding when using stimulation protocols that differ in (subjective) intensity or stimulation patterns between real and sham control (Farmer et al., 2021). Currently, no sham stimulation fulfills the criteria proposed by Butt et al. (2020), i.e., there is no innervation of ABNV fibers, which cannot be distinguished from real taVNS.

1.2.5.2 Leveraging Short Bursts of Stimulation to Elucidate the Link between TaVNS and LC-NE Activation

LC neurons are characterized by two distinct firing modes: phasic and tonic activity (see section 1.1.3), which differ in their discharge patterns and NE releasing properties (Aston-Jones & Bloom, 1981; Berridge & Waterhouse, 2003; Clayton et al., 2004; Florin-Lechner et al., 1996), with phasic stimulation of the LC in rats promoting greater NE release compared to tonic stimulation, which enhances memory and inhibitory control (Aston-Jones & Cohen, 2005; Berridge & Waterhouse, 2003; Florin-Lechner et al., 1996; Luo et al., 2015). Additionally, animal and human research has already demonstrated that an increased pupil dilation is associated with phasic LC activation (Aston-Jones & Cohen, 2005; Eckstein et al., 2017; Gilzenrat et al., 2010; Joshi et al., 2016; Murphy et al., 2014; Samuels & Szabadi, 2008). Therefore, it remains to be determined to what extent short bursts ("phasic") rather than longer-lasting bursts ("tonic") of electrical vagus nerve stimulation may have a beneficial effect on the LC-NE system. Notably, short bursts of externally applied stimuli must be distinguished from the natural phasic activity of the LC, which involves much shorter, rapid bursts of NE release, typically lasting a few tens of milliseconds (Aston-Jones & Cohen, 2005).

The effects of various stimulation settings, particularly phasic stimulation, on the LC-NE system have been more thoroughly investigated in **animal studies**. An iVNS in monkeys revealed that phasic bursts exceeding 30 to 50 Hz produce larger vagus-evoked potentials than

low-frequency bursts of 5 Hz (Rembado et al., 2021). Even at 0.2 mA, it was confirmed that iVNS bursts of 0.5 s generate phasic LC activity and that greater VNS amplitude causes an increase in LC firing (Hulsey et al., 2017). The strongest effects of iVNS in mice on pupil dilation were observed at 0.9 mA, 20 Hz, and 800 μs with brief bursts of 10 s (Mridha et al., 2021). A dose-dependent effect of iVNS on the LC-NE system was confirmed by Collins et al. (Collins et al., 2021), who found that more pupil dilatation was elicited by higher stimulation intensity and longer stimulation duration (0.8 mA and 5 s as opposed to 0.5 s of short bursts). In addition, another iVNS study showed an association between the degree of cholinergic axon activation and the strength of iVNS stimulation (Mridha et al., 2021). The specific timing of cortical activation in response to VNS showed that NE and ACh activation occurred after the onset of VNS, followed by purring and locomotion about 1 s later and pupil dilation about 1.5 s later in awake and anesthetized rats (Collins et al., 2021). Furthermore, Hulsey et al. (2019) demonstrated that the motor cortex was involved in brief bursts of iVNS stimulation (0.8 mA, brief bursts of 0.5 s). Brief bursts of 0.5 s of iVNS at 0.8 mA effectively eliminated previously induced tinnitus pathology in the rat auditory cortex, demonstrating the effects of phasic iVNS on stimulus-specific plasticity (Engineer et al., 2011).

In **human research**, Sharon et al. (2021) showed a robust pupil dilation based on short bursts of 3.4 s taVNS (2.20 ± 0.24 mA), results was also replicated (Lloyd et al., 2023). Likewise, short taVNS bursts (5 s) enhanced the evoked pupil dilation with increased stimulation intensity (0.2 mA, 0.5 mA, calibration intensity) and pulse width (200, 400 μs) as compared to sham stimulation (D'Agostini et al., 2023). Short bursts of 4 s taVNS (2 mA) (Keute et al., 2021) or 1 s taVNS (Sclocco et al., 2019) also affected HR and HRV indices (Keute et al., 2021) and changed HRV indices during the exhalation phase of the respiratory cycle (eRAVANS) (Sclocco et al., 2019). Moreover, increased LC activation was observed during short bursts of 1.5 s taVNS (Sclocco, 2020). However, it should be noted that those studies did not choose an active sham control stimulation location (no current at all) (Keute et al., 2021; Sclocco, 2020; Sclocco et al., 2019). Studies with more prolonged stimulation bursts found no immediate effects of taVNS, neither regarding pupil dilation (e.g., 60 s of taVNS (Keute et al., 2019)) or HRV indices (e.g., 30 s of taVNS (Borges et al., 2019; De Couck et al., 2017). However, a recent study suggested that both short and longer stimulation bursts of taVNS in humans led to an evoked pupil dilation (Skora et al., 2024), while further, more systematic research is needed. Considering those i/taVNS studies, short bursts of stimulation may presently be a promising approach for examining the effects of different stimulation

parameters and may serve as a valuable method for elucidating the impact of i/taVNS on the LC-NE system.

1.2.6 The LC-NE System as a Target for TaVNS: Addressing Interindividual Variability

Interindividual variability in the LC-NE system and the ABVN may contribute to the heterogeneous results of taVNS interventions in humans. The integrity of the LC is particularly crucial when taVNS is contemplated as an additional therapy in clinical populations potentially impacted by diminished NE regulation, such as those with depression or neurodegenerative disorders. Currently, the ABVN has been the subject of only one study conducted by Safi et al. (2016), which quantified the number of myelinated nerve fibers in the ABVN and noted significant variability among subjects (Yap et al., 2020). It is important to acknowledge that the subjects of this study had varying histories of medical conditions. Consequently, healthy populations may exhibit less variability (Safi et al., 2016). Additionally, the density of nerve fibers in the cavum conchae (recess auricle), a component of the ABVN, fluctuates (Bermejo et al., 2017). This variability may already be a significant factor in elucidating why certain individuals experience benefits from taVNS while others do not (Butt et al., 2020).

Furthermore, a decrease or alteration in LC-NE function occurs in various conditions where taVNS may be applied. For example, in AD and PD, changes in LC function occur prior to the onset of clinical symptoms (Braak et al., 2003, 2011). Post-mortem investigations of AD indicate that specific NE metabolites remain unchanged despite a reduction in the number of NE neurons. This served as evidence for compensatory upregulation in NE production in response to the loss of LC-NE neurons, whereby the remaining LC neurons augment their firing rate (Hermann, 1992). In the early phases of LC decline, increased adrenoreceptor density in the hippocampus and amygdala may compensate for decreased LC-NE signaling (Andrés-Benito et al., 2017; Szot et al., 2006). Thus, adaptive brain processes that compensate for altered LC function may improve the response of individual LC neurons or target area sensitivity through receptor levels to impact externally applied stimuli. Likewise, a post-mortem analysis of signaling genes and growth factors found a reduction in LC function in depressed people (Bernard et al., 2011), which may explain the use of selective norepinephrine reuptake inhibitors (sNRIs) to treat depression. A meta-analysis found that i/taVNS therapy for depression had stronger effects in seriously affected patients after controlling for severity (Martin & Martín-Sánchez, 2012). Similarly, Ferstl et al. (2022) found that healthy volunteers with lower baseline positive mood had larger taVNS-induced motivation improvements. The extent to which clinical and cognitive assessments of disease severity are associated with a

greater decline in the LC-NE system is currently unclear. However, current research indicates that cognitively normal groups also exhibit diversity in taVNS effects. Major depression and some clinical populations, including PD and AD, have been shown to have reduced LC integrity (for a comprehensive review, see (Liu et al., 2017a). Thus, improvements in our knowledge of the significance of a changed LC-NE system functionality (Betts et al., 2017; Hämmerer et al., 2018; Liu et al., 2019) can motivate diverse interventional approaches utilizing stimulation strategies that remain inadequately explored. Particularly, high-frequency stimulation may inhibit overcompensated (overactive) LC neurons, which may cause chronic pain (Bernard et al., 2011) and aggressive behavior in conditions of declining LC-NE integrity due to excessive LC activity (Liu et al., 2018). Nevertheless, interactions among brain regions should be considered while examining different stimulation protocols. For instance, high-frequency (100 Hz) optogenetic stimulation of basolateral amygdala (BLA) neurons decreased excitatory activity in the medial prefrontal cortex (Klavir et al., 2017), but excessive activation of the LC-BLA pathway induced pain and anxiety, which were mitigated by pathway inhibition (Llorca-Torralba et al., 2019). Consequently, high-frequency stimulation may have the capacity to suppress hyperactive LC neurons, which are believed to contribute to chronic pain, while excessive LC activity linked to declining LC-NE integrity may underlie aggressive behavior (Liu et al., 2018). Owing to a long-standing lack of appropriate imaging measures for the LC-NE system and a still-developing understanding of its role in higher cognitive functions (Sara & Bouret, 2012), current commercially available taVNS devices may not fully exploit their therapeutic potential. However, some companies are working to tailor these devices to individual needs.

The review of taVNS has emphasized that taVNS may represent a more precise alternative compared to pharmacological approaches (e.g., sNRIs) for a dysregulated LC-NE system in neurodegenerative and psychiatric diseases, such as AD, PD, and depression. Nonetheless, taVNS research in humans encounters challenges in identifying appropriate biomarkers and refining stimulation protocols for addressing an individual-altered LC-NE system. Consequently, short bursts of i/taVNS have demonstrated consistent modulation of LC-NE activity in both animal and human studies (Collins et al., 2021; D'Agostini et al., 2023; Hulsey et al., 2017; Mridha et al., 2021; Sharon et al., 2021), while longer bursts of stimulation have yielded less reliable results. Moreover, the precise impact of the mere sensation of stimulation remains inadequately elucidated (Fig. 3).

Overview

Transcutaneous vagus nerve stimulation

1. **Transcutaneous vagus nerve stimulation (taVNS):** TaVNS is a non-invasive stimulation technique in humans applied at the outer ear, controlled by the auricular branch of the vagus nerve (ABVN) (Peuker and Filler, 2002).

2. **TaVNS targeting the LC-NE system:** TaVNS is modulated by the transmission of excitation from the ABVN through the remaining nerve fiber bundles of the vagus nerve to the brainstem at the nucleus tractus solitarius (NTS), which has prominent projections to the LC-NE system (Butt et al., 2020; Ruffoli et al., 2011).

3. **Need for individualized stimulation parameters**: TaVNS research should integrate individually adjustable stimulation parameters to systematically investigate the effects of various stimulation parameters on the LC-NE system, enhancing study precision and reliability (Ludwig et al., 2021).

4. **Validating taVNS impact on the LC-NE system:** There are still insufficiently established and validated indirect outcome measures that reliably show the effectiveness of taVNS in humans on the LC-NE system (Ludwig et al., 2021). Additionally, the precise impact of subjective perception due to stimulation remains inadequately elucidated.

5. **Phasic stimulation preference**: Findings suggest that phasic or burst-like taVNS may be more effective than tonic stimulation, especially when translating optimal parameters from animal studies to human applications (e.g., Collins et al., 2021; Hulsey et al., 2017; Sclocco et al., 2019; Keute et al., 2019; Sharon et al., 2021).

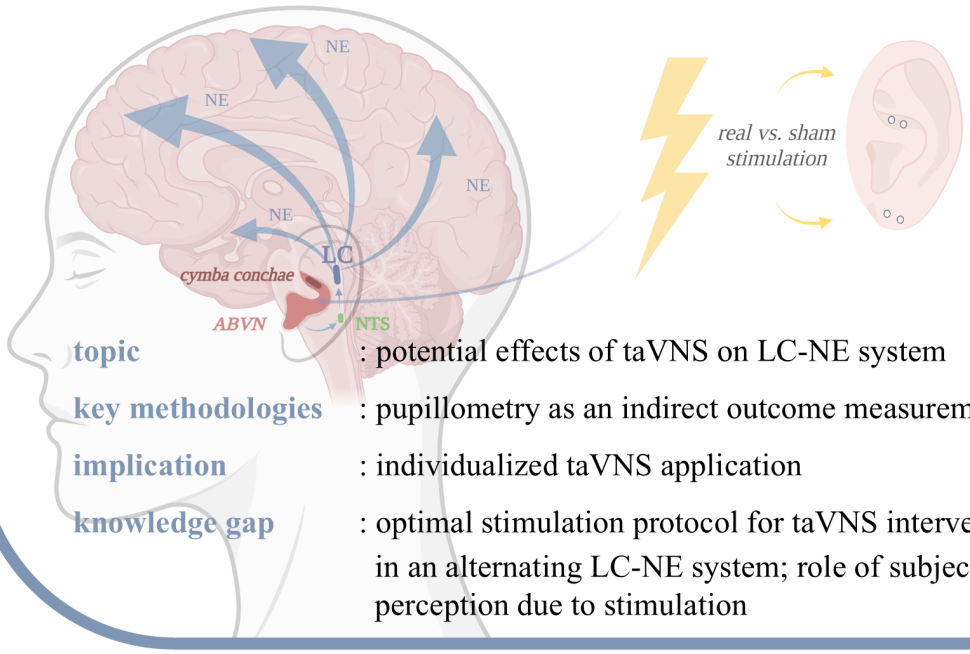

topic : potential effects of taVNS on LC-NE system

key methodologies : pupillometry as an indirect outcome measurement

implication : individualized taVNS application

knowledge gap : optimal stimulation protocol for taVNS intervention in an alternating LC-NE system; role of subjective perception due to stimulation

Figure 3. Overview covering the key aspects of transcutaneous vagus nerve stimulation (taVNS). The image was created with BioRender.com.

1.3 Aims and Outline of the Dissertation

The overall objective of this dissertation is to advance our knowledge of the involvement of the LC-NE system in memory and age-related differences in LC function and gain a better understanding of the mechanism of action of taVNS in humans for a more precise and targeted application in an individually altered LC-NE system. Based on the above literature review, I will address this with two distinct questions:

1. **Can the assessment of LC function serve as a measure of cognitive aging?**
   Although there is growing evidence of in vivo structural LC decline in aging, there is little evidence of age-related changes in LC function. This is especially because of the challenge of reliably imaging the small structure of the LC. In chapter two, I will empirically investigate age-related differences in LC function. I provide new findings from a high-resolution fMRI study using a reversal reinforcement learning task and specific post-processing methods to visualize age differences in LC function (N = 50 (28 younger adults; 22 older adults)). In particular, I assess whether (1) (emotionally) salient events such as negative feedback (loss feedback > gain feedback) are associated with increased LC activation, (2) whether task-related salient events, such as condition reversals (reversal feedback > no reversal feedback), are associated with increased LC activation, and whether (3-4) LC activation during such events contributes to memory performance (remembered > not remembered) for salient events (remembered before loss feedback > not remembered before loss feedback). Moreover, I investigate (5) age differences in LC reactivity in these instances by comparing younger and older adults.
   I hypothesize:
   1. There is higher functional LC activation during (1) emotionally salient, (2) task-related salient events, and (3-4) for memory performance of such salient events.
   2. There is higher functional LC activation for (5) younger adults compared to older adults.

2. **How do short bursts of taVNS affect pupil dilation and memory performance?**
   IVNS animal studies and some taVNS human studies have already shown more reliable effects regarding short bursts of stimulation and modulation of the LC-NE system compared to longer bursts of stimulation. However, as current taVNS studies in humans indicate, the challenges of establishing a suitable stimulation protocol with appropriate outcome measures to investigate potential taVNS effects on an individually altered LC-NE system have not yet been fully addressed. It is still unclear which combination of

stimulation parameters is required and whether higher stimulation parameters are important for the stimulation process in humans. In chapter three, I empirically assess short bursts of event-related taVNS as a potential non-invasive stimulation approach to modulate the LC-NE system. I provide new taVNS findings of an experimental setup that I established to allow systematic testing of different stimulation parameters with a time-synchronous recording of pupil dilation by comparing real (cymba conchae) and sham (earlobe) stimulation within healthy younger adults (N = 24) on a single day. Specifically, I present behavioral and pupillometry-related taVNS results on an emotional memory task with negative events involving the LC-NE system and on a resting-state task, both combined with short bursts of event-related taVNS (3 sec). Importantly, I will also investigate the effects of subjective perception of taVNS on changes in pupil dilation and memory performance.

I hypothesize:

3. Short bursts of taVNS lead to increased pupil dilation and better memory performance.
4. Higher stimulation parameters during short bursts of taVNS lead to increased pupil dilation.
5. The subjective perception of stimulation contributes to the variability of taVNS-induced effects on pupil dilation and memory performance.

In the General Discussion, chapter four, I will discuss the empirical findings regarding age-related differences in functional LC activation and short bursts of tAVNS on pupil dilation and memory performance. I will focus on and advance our current understanding of the LC-NE system and taVNS research, emphasizing the merits of prospective study directions.

2 Chapter 2: High-Resolution Functional Locus Coeruleus Imaging Study

A version of this chapter, with minor modifications,
has been published in Communication Biology (Ludwig et al., 2024b)

.

2.1 Brief Introduction

The LC, our main source of NE in the brain, declines with age and is a potential epicenter of protein pathologies in ND (Braak et al., 2011; Mather & Harley, 2016; Theofilas et al., 2017). Although the LC-NE system may be particularly vulnerable, studies indicate that individuals with more structurally intact LC show less cognitive decline (Clewett et al., 2016; Dahl et al., 2019; Hämmerer et al., 2018; Liu et al., 2019; Sara, 2009). Indeed, there is growing evidence that LC integrity and function serve as important biomarkers of both healthy aging and early development of ND (Engels-Domínguez et al., 2023). Despite the increasing evidence of in vivo structural decrease of LC with age, less evidence indicates age-related changes in LC function, which presumably should be associated with structural decline. Considering that neuronal function loss likely precedes cell death (Giguère et al., 2018), it is essential to evaluate functional indicators of LC decline in aging carefully. However, assessing LC function in humans is a major methodological challenge due to its small size (about 14.5 mm long and 2-2.5 mm thick (Fernandes et al., 2012)), which requires specialized imaging sequences and advanced data analysis techniques.

In chapter two, I present high-resolution fMRI (1.5 mm) in combination with a newly developed MR data analysis pipeline, which facilitates sufficient spatial precision in the analyses of brainstem activations through a rigorous post-processing procedure (Liu et al., 2019; Yi et al., 2023). Specifically, I assess whether (1) emotionally salient events such as negative feedback (loss feedback > gain feedback) are associated with increased LC activation, (2) whether task-related salient events, such as condition reversals (reversal feedback > no reversal feedback), are associated with increased LC activation, and whether (3-4) LC activation during such events contributes to memory performance (remembered > not remembered) for salient events (remembered before loss feedback > not remembered before loss feedback; see Table 1). Moreover, by comparing younger and older adults (N = 50; 28 younger and 22 older adults), I investigate (5) age differences in LC reactivity in these instances.

2.2 Methods

The data reported in this chapter are part of a study that included structural and functional brainstem imaging, pupillometric recording, and a reversal reinforcement learning task (Hämmerer et al., 2018). The present chapter focuses on functional brain imaging and behavioral data during the reversal reinforcement learning task.

2.2.1 Subjects

A total of 50 English speaking people, 28 healthy younger adults (16 females) with a mean age of 23.14 (range: 20 to 31 yrs., SD = 3.18) and 22 healthy older adults (12 females) with a mean age of 67.68 (range: 65 to 84 yrs., SD = 5.68) participated in the study (for sample description see Supplementary Table S1). Suitability for the study was assessed using a telephone questionnaire administered by research assistants during recruitment and again in person by radiographers before the experimental examination. Specifically, subjects who were unsuitable for scanning (e.g., metallic implants, claustrophobia) and subjects with a history of neurological (e.g., neurodegenerative diseases) or psychiatric disorders were excluded. Subjects were right-handed (Oldfield questionnaire lateralization quotient > 80) (Oldfield, 1971). The study was approved by the local ethics committee (University College London ethics reference no. 5506/001), and written informed consent was obtained from each subject prior to participation. All ethical regulations relevant to human research participants were followed. Subjects received a payment of £50 for their participation, including a bonus payment of £6 based on task performance (all subjects performed at a high level and received the bonus payment). An abbreviated version of the Raven's Progressive Matrices (Raven, J. C., & Court, J. H., 1998) was used to examine whether subjects matched known markers of age differences in adult fluid intelligence (Li et al., 2004). Performance was assessed as the number of correctly solved matrices of the 18 given matrices within 20 minutes. Due to changes in the test design, only 19 younger adults completed the fluid intelligence tasks. The younger adults performed better than older adults [$t(39) = 3.45$, $p < 0.001$], indicating that subjects were consistent with the known age differences in fluid intelligence.

2.2.2 Procedure

The study was conducted as a between-subject design (younger vs. older adults) including structural and functional MRI combined with pupillometric recording during reversal reinforcement learning task as well as early and delayed memory tests, which were performed on the same day. At the beginning of the experiment, subjects first completed a practice session to get familiar with the use of the button box. After that, subjects were positioned in the MR scanner and performed the reversal reinforcement learning task while pupillometric recording

and brain imaging acquisition were proceeding simultaneously. After the scanning session, subjects underwent an unannounced immediate (60 min after encoding) and delayed (4 - 6 h after encoding) memory test (each test lasting approximately 35 min) to assess whether memory for scene stimuli before loss vs. gain feedback and reversal vs. no reversal points differed.

2.2.3 Reversal Reinforcement Learning Task

Subjects performed a reversal reinforcement learning task (Fig. 4) to assess the impact of salient events on memory while undergoing fMRI recording (57 – 61 min). Each trial began with a grey fixation cross (jitter between 0.5 - 6.5 s), followed by an image (2.5 s) showing either indoor or outdoor scenes. This was followed by another grey fixation cross (jitter between 0.5 - 6.5 s) and then a positive or negative feedback (2.5 s).

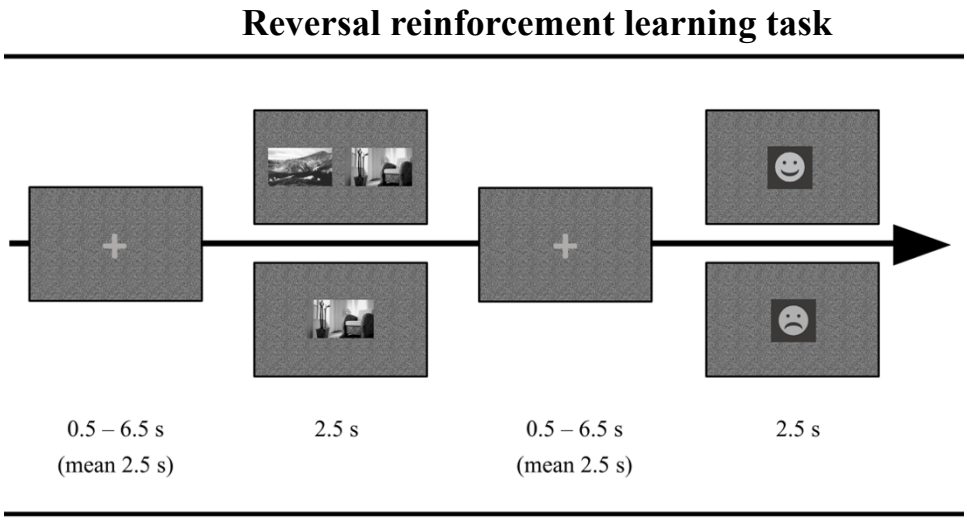

Figure 4. Reversal reinforcement learning task (adapted from Hämmerer et al., 2018). Each trial began with a grey fixation cross (jitter between 0.5 - 6.5 s), followed by an image (2.5 s) showing either indoor or outdoor scenes. This was followed by another grey fixation cross (jitter between 0.5 - 6.5 s) and then a positive or negative feedback (2.5 s).

Specifically, subjects learned through positive (smiling face, two-point gain) and negative (sad face, two-point loss) feedback on both forced (one image) and free choice (two images) trials whether indoor or outdoor scenes were rewarded or not, as well as whether a reversal in the rewarded scene category has occurred (forced trials: 66.26 loss trials and 60.64 gain trials on average; free choice trials: 13.08 loss trials and 120.04 gain trials on average; 303 trials in total; 6 runs × 9.62 min). The rewarded stimulus category changed every ~ 20 trials without warning. Missed responses resulted in a 2-point loss. To incentivize performance, subjects had to score 20 points per scanner run to receive a bonus payment of £6, with feedback on scores given after each run. Crucially, because subjects are typically loss-averse when faced with tasks that involve both gains and losses, rewards were larger than losses (McGraw et al., 2010). Importantly, using forced choice trials, the task design allowed for examining two

different types of saliences in processing choice feedback (loss vs. gain and reversal vs. no reversal) by balancing loss and gain feedback, in particular, on reversal trials. The reversal reinforcement learning task was followed by an unannounced immediate (60 min after encoding) and delayed (4 – 6 h after encoding) memory test to assess whether memory for scene stimuli before loss vs. gain feedback and reversal vs. no reversal points differed, each taking ~35 min. The memory test (either in forced trials or free-choice trials) only comprised stimuli selected by the subjects in the reversal learning task. Subjects were instructed to categorize the stimuli as "old" or "new". For "old" stimuli, the subjects were asked to indicate whether they "remembered" (episodic memory trace accessible) or whether they "knew" (feeling of familiarity) the stimuli, a concept with which they were familiarized in advance. On average, each recognition test consisted of 50 new and 150 familiar stimuli, evenly distributed between indoor and outdoor situations. Additionally, subjects were asked to indicate on a 6-point scale how certain they were in their respective responses. The memory tests had no set time limit for response, although subjects were advised to rely on their initial impression and avoid overthinking of their responses.

2.2.4 Materials and Stimuli

The stimuli for the reversal reinforcement learning task were taken from the International Affective Picture System Datenbank (IAPS (J, 1995)). Stimuli presentation, button press response and pupillometry (EyeLink 1000 Plus; SR Research, 2010) were controlled by custom-made scripts in MATLAB version 2015a (The MathWorks, www.mathworks.com) using the Cogent 2000 toolbox (www.vislab.ucl.ac. uk/cogent.php). Backgrounds and images brightness variations were luminance controlled to prevent interference of luminance changes with pupillometric recordings. Responses were recorded with MR scanner-compatible button boxes (fiber optic response pad HHSC-1X4-CL; Current Designs).

2.2.5 s/fMRI Data Acquisition

MRI data were acquired on a 3T Tim Trio System (Siemens Healthineers, Erlangen, Germany) with a standard 32-channel radiofrequency (RF) coil. Structural and functional imaging sequences were optimised for LC imaging. 3D multi-echo FLASH structural images were acquired as part of a modified multiparameter mapping protocol (Weiskopf et al., 2013). Anisotropic voxel sizes (0.4 × 0.4 x 3 mm^3) aiming to match the stick-like shape of the LC were acquired in a slab oriented parallel to the back of the brainstem aiming to have the longer voxel dimension coincide with that of the LC (Sasaki et al., 2006). In addition, a whole-brain isotropic T1-weighted FLASH image (voxel sizes: 0.75 isotropic, FOV 240 × 240 × 64 3 mm^3) was

acquired as an anatomical scan for image registration. Further details on the structural MRI data acquisition can be found in Hämmerer et al. (2018). Resolution and coverage of the fMRI data were optimized both to measure the small LC (which is only about 14.5 mm long and 2-2.5 mm thick (Fernandes et al., 2012)) with sufficient resolution and to have a field of view (FoV) that allows assessment of the HPC and amygdala along with other brainstem nuclei (Fig. 5). For this purpose, a 6 cm wide angulated 3D T2*-weighted EPI (TE = 37.3 ms, TR = 76 ms, FA 15 ° water-selective excitation, parallel imaging with GRAPPA factor 2 in the phase-encoded EPI direction, Bandwidth 1395 Hz/Px, FOV 192 mm x 192 mm x 48 mm, with a 1.5 mm isotropic voxel size, 32 partitions plus 25% oversampling) was positioned as described above. The volume acquisition time was 3.04 s. During the reversal reinforcement learning task each subject had a total of 1140 measurements spaced across 6 runs of 190 measurements each, resulting in 6 runs of about 9.62 min per subject (first 5 measurements of each run were discarded). The full sample also comprises 5 pilot subjects with a slightly different run separation of a total of 1200 measurements, spaced across 5 runs of 240 measurements each, resulting in 5 runs of about 12.16 min.

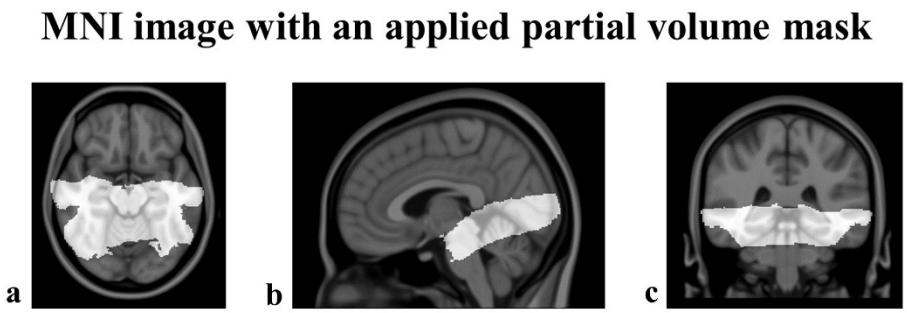

Figure 5. MNI image with an applied partial volume mask. Montreal Neurological Institute (MNI) image with an applied partial volume mask (light grey) in a) axial, b) sagittal, c) coronal view.

2.2.6 LC Segmentation

The left and right LC were each manually segmented by two raters in the anatomical MRI images using ITK-Snap (Yushkevich et al., 2016). LC integrity was assessed as signal intensity within segmentations averaged across left and right LC, normalised with respect to a nearby area in the brainstem. Note that due to poor LC visibility in two subjects (older [right LC] and younger [left LC]), segmentations for only one side of the LC were included (see Hämmerer et al., 2018 including Supplementary Figure 4 for more details on LC segmentations and contrast analyses).

2.2.7 fMRI Data Pre-processing and Dedicated Post-Processing Pipeline for Spatially Precise Brainstem Imaging

FMRI data preprocessing and statistical modelling was done using Statistical Parametric Modelling 12 (SPM12; Wellcome Centre for Human Neuroimaging, University College, London, UK, 2012) as well as Advanced Normalization Tools (ANTs) v.2.1.0 software package (http://stnava.github.io/ANTs/). The raw DICOM data were converted to NIfTI images, while preserving the original image parameters. The pre-processing of the functional data was performed in SPM12 and included realignment, unwarping, and smoothing (2mm FWHM). Without registering or normalising pre-processed data, first level contrasts were calculated in native space (see below for more details). Also, all whole-brain T1w images were used to generate a study-specific template, using the antsMultivariateTemplateConstruction2.sh function in ANTs with default parameters except the rigid-body registration option on.

Registration and normalisation of functional and structural data to MNI space (ICBM 152 nonlinear asymmetric template T1w, 1 mm resolution [mni_icbm152_t1_tal_nlin_asym_09c.nii] (Fonov et al., 2011)) followed a pipeline developed for assuring sufficient spatial transformation precision in the brainstem area (see Yi et al., 2023, Fig. 2 for an overview). Specifically, after correcting for B0 field inhomogeneity of the partial-volume brain T1w images (N4BiasFieldCorrection from ANTs (Tustison et al., 2010), the following steps were carried out: To match the above-mentioned MNI space resolution, neuromelanin-sensitive structural images (FLASH) were re-sampled to 1-mm isotropic voxel size using the mri_convert function in FreeSurfer (Version 7.1; http://surfer.nmr.mgh.harvard.edu/, Martinos Center for Biomedical Imaging, Charlestown, Massachusetts; see Yi et al., 2023, Fig. 2f). Using antsRegistrationSyN.sh, the whole-brain T1w images in the native space were non-linearly registered to the study specific template before being non-linearly registered to the MNI space. Concatenated transformation matrices and deformation fields from these steps, using antsApplyTransforms.sh, the whole-brain T1w images were transformed onto the MNI space. Afterwards, the whole-brain T1w images were rigidly registered to the individual mean EPI images (see Yi et al., 2023, Fig. 2d). Additionally, the structural T1w slab and manually drawn individual LC segmentation in the space of the T1w slab was rigidly registered to the partial volume brain T1w images (using antsRegistrationSyN.sh). To align the individual LC segmentation to the whole-brain T1w images rigidly, the same transformation matrix from this registration step was applied to the LC mask. Finally, combinations of the above-described transformations were applied to the mean EPI images and the first-level statistical contrast images as well as the LC masks in each of their respective native space in a single step and were transformed to the MNI space (see Yi

et al., 2023, Fig. 5-1, 5-2) non-linearly (using antsApplyTransforms.sh). Therefore, group level analyses in MNI space were possible while assuring high precision of spatial transformations and reducing bias due to multiple interpolations. All structural and mean EPI images were transformed using the fourth-order B-Spline interpolation, while the statistical contrast data were transformed using linear interpolation, and individual LC segmentations were transformed by using nearest neighbour interpolation.

2.2.8 Quality Checks for Assuring Sufficient Spatial Transformation Precision of Structural and Functional LC Imaging Data

To evaluate the quality of spatial transformation of structural and functional LC imaging data across subjects, guidelines following Yi et al. (2023) were used. For assessing the precision of functional LC imaging data, eight different landmarks were placed by two independent raters on individual mean functional images in MNI space in the brainstem area (see Yi et al., 2023 for more details) (cf. Fig. 7). To ensure a similar approach to setting the landmarks, raters were first trained together on an independent training dataset. Afterwards, to ensure independent ratings, raters worked separately on the present dataset, while balancing across the two raters which part of the data was rated first to account for possible training effects. Both raters had experience with rating several different datasets. Sørensen–Dice coefficient (DSC) score was calculated to assess the consistency across the two raters (0 indicates no spatial overlap, while 1 indicates a complete overlap). The following DSC scores resulted for the eight landmarks: nucleus ruber (l) = 0.70, nucleus ruber (r) = 0.70, periaqueductal grey = 0.62, perifastigial sulcus = 0.53, outline brainstem (l) = 0.34, outline brainstem (r) = 0.33, 4th ventricle border (l) = 0.72, 4th ventricle border (r) = 0.64, representing a good overlap of the two raters (for age-related differences in 8 brainstem landmarks' mean functional images in MNI space see Supplementary Methods 1.2). Note that overlap in landmarks for the brainstem outline is generally lower as more degrees of freedom exist in the anterior-posterior direction (Yi et al., 2023). As can be seen in Figure 7, quality checks suggest a good spatial precision in transforming functional LC data into MNI space, with deviations as assessed in landmarks not exceeding 2.5 mm in the LC (blue bar graphs in Fig. 7), which is the assumed average width of the LC based on post-mortem data (Fernandes et al., 2012). Segmentations delineating the LC in multi-parameter mapping scans for structural LC imaging were performed by two independent raters in native space (see (Hämmerer et al., 2018) for more details), where the DSC score was 0.72, indicating the overlap between the two raters in identifying voxels belonging to the LC (see (Hämmerer et al., 2018)). An overlay of the binary LC segmentations after transformation to MNI space is shown as a heatmap in Figure 6.

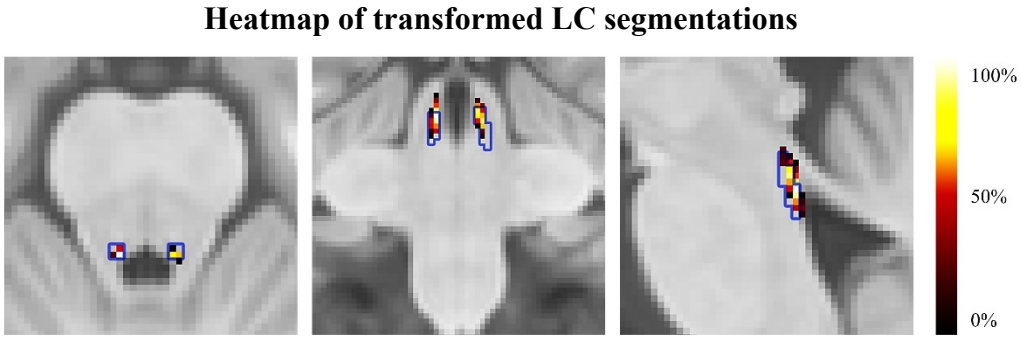

Figure 6. Heatmap of transformed individual LC segmentations. Heatmap of transformed individual LC segmentations in the group space (from left to right: axial, sagittal, coronal view). The blue line indicates the LC meta mask created by Dahl et al. (2022). The maximum overlap across segmentations within the LC meta mask is at 62 % and the minimum overlap at 1.6 %.

In addition, to assess the precision of the alignment of LC segmentations in MNI space across subjects, distances across subjects for the left and right LC centroid voxels were calculated for each slice of the LC segmentation (Fig. 7). Deviations assessed across subjects and averaged across slices within subjects did not exceed 2 mm overall, the median slice-wise distance on the left side was 0.80 mm (Mdn ± MAD: 0.80 ± 0.16) (younger adults: 0.80 mm [Mdn ± MAD: 0.80 ± 0.14], older adults: 0.73 mm [Mdn ± MAD: 0.73 ± 0.19]), and on the right side 0.82 mm (Mdn ± MAD: 0.82 ± 0.21) (younger adults: 0.89 mm [Mdn ± MAD: 0.88 ± 0.26], older adults: 0.76 mm [Mdn ± MAD: 0.76 ± 0.18]). Deviations did not differ between left and right side ($F(1,95) = 0.005$, $p = 0.94$) and only showed a trend for being larger in younger adults ($F(1,95) = 3.4$, $p = 0.07$). Note that deviations in LC positions between subjects likely do not solely stem from imprecisions in spatial transformations, as LC positions in native space also differ between subjects by on average about 1.45 mm (left LC) and 0.96 mm (right LC) (see Yi et al., 2023, Fig. 5), as evident in post-mortem and structural LC imaging data (Fernandes et al., 2012). Spatial deviations across subjects after transformation thus likely represent a mixture of biological variations in LC position and imprecision in spatial transformations.

Quality checks of structural and functional LC imaging data

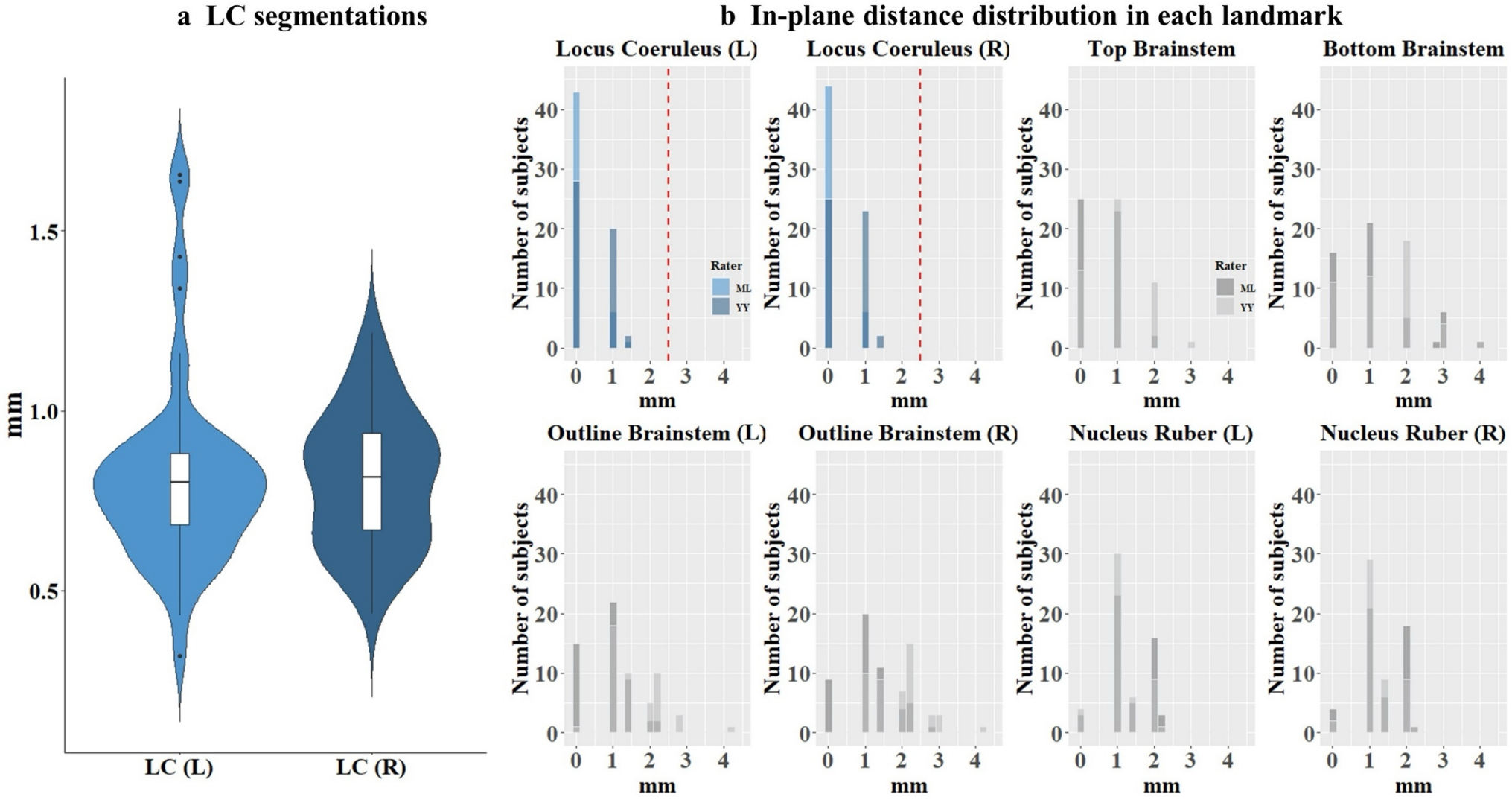

Figure 7. Quality checks of structural and functional LC imaging data. a) The distribution of inter-subject distances for the left and right LC centroid voxels of the aggregated LC meta mask (Dahl et al., 2022) and the MNI-transformed LC segmentations for individual subjects are shown in violin plots. Boxplots within the violin plot show error bars with 95% confidence interval. In-plane distance is calculated separately for the left and right LC, slice by slice, and averaged across slices to obtain a value per subject and left or right **LC segmentation** (**right**: $M \pm SD$: 0.81 ± 0.19, IQR=0.28; **left**: $M \pm SD$: 0.81 ± 0.27, IQR=0.21). **b)** Histograms of in-plane distances between single-subject landmarks and landmarks defined on the MNI template. The dashed red line indicates the typical width of the LC (2.5mm (Fernandes et al., 2012) below which deviations should fall (Yi et al., 2023), in fact median deviations all fell below 1 mm.

2.2.9 Anatomical Masks for Second-Level Analyses

Anatomical masks of study-relevant brain regions (see Supplementary Figure S1) were used in region of interest (ROI) - specific analyses for precise delineations of functional activation patterns with small-volume correction (SVC). For nuclei in the brainstem and midbrain, substantia nigra pars reticulata (SNr, label 9), substantia nigra pars compacta (SNc, label 7), ventral tegmental area (VTA, label 11) and red nucleus (label 8) masks were extracted from a high-resolution probabilistic in vivo atlas by Pauli et al. (2018) (https://identifiers.org/neurovault.collection:3145). Anatomical templates were already in the MNI template space adopted in our study (Fonov et al., 2011) and only needed to be binarized for use of ROI - specific analyses (using mni_binarize). The binarized masks were thresholded at 0.20 to combine the different templates into a mask that matched the anatomical definition of the SN substructures ("SNredVTA mask" - from now on, this nomenclature will refer to these structures: SNr, SNc, VTA, red nucleus) (using SPM image calculator). For the LC, the LC meta mask (https://osf.io/sf2ky/) by Dahl et al. (2022) was used, which is a combination of several already existing individual LC masks (Betts et al., 2017; Keren et al., 2009; Liu et al., 2019; Tona et al., 2017; Ye et al., 2021) and also consistent with LC dimensions reported in post-mortem studies (Fernandes et al., 2012) (for more details see Dahl et al., 2022). The LC meta mask (Dahl et al., 2022) was non-linearly co-registered to the MNI template space adopted in our study (using antsRegistration) with nearest neighbour interpolation (using antsApplyTransforms). As can be seen in Figure 7, the LC meta mask (Dahl et al., 2022) shows good agreement with LC segmentations in our study. In addition, as the study also focuses on salience and memory-related functional activations, a combined bilateral mask including the hippocampus, para-hippocampus and amygdala referred to as "hippocampus-amygdala mask" was created based on the Cerebrum Atlas (CerebrA) by Manera et al. (2020), since it provides non-linear registration of Mindboogle atlas (Klein & Tourville, 2012) to high resolution MNI-ICBM 2009c (Fonov et al., 2011) space of cortical and subcortical regions (Manera et al., 2020). Besides left (label 99) and right (label 48) hippocampus as well as left (label 70) and right (label 19) amygdala, left (label 69) and right (label 18) para hippocampal regions were extracted (using fslmaths). Individual templates were binarized (using mri_binarize) and combined (using SPM image calculator) to create a final bilateral mask. Anatomical templates were already in the MNI template space adopted in our study (Fonov et al., 2011) and only needed to be binarized for use of ROI - specific analyses (using mni_binarize).

Finally, a "grey matter mask" based on the MNI template adopted in our study (Fonov et al., 2011) and a "brainstem mask" based on CerebrA (Manera et al., 2020) were used as an

implicit mask in second-level analyses. The grey matter mask was created by segmenting the MNI template (Fonov et al., 2011) (using SPM segment, Bias FWHM 30 mm cut-off). For creating this brainstem mask, left (label 62) and right (label 11) brainstem as well as left (label 77) and right (label 26) ventral diencephalon were extracted from the CerebrA (Manera et al., 2020) (using fslmaths), were binarized (using mri_binarize) and combined (using SPM image calculator) to one mask representing brainstem and midbrain regions.

2.2.10 Statistical Analyses

2.2.10.1 Behavioral Analyses

Using repeated measures ANOVA and paired-samples t-tests across both age groups, analyses of behavioral data were conducted to compare memory performance and (reaction times) RTs of both age groups for single and double scene stimuli that occurred on trials before and after loss vs. gain feedback, and on trials before and after a reversal. Memory performance was measured as the mean of the hit-FA (false alarms) rate across both recognition tests. These analyses were carried out using Statistical Package for the Social Sciences (SPSS) version 28.0.0.1 (IBM; https://www.ibm.com/analytics/de/de/technology/spss) (*SPSS Software*, 2023) and MATLAB version R2020b (The MathWorks, www.mathworks.com). Correlation analyses between significant LC, MTG activations, LC integrity and memory performance in the elderly were carried out in R version 4.2.2 (R Core Team, 2022, https://www.r-project.org) using RStudio (RStudio Team, 2022) using cor() function for Spearman´s Rank correlation, corr.test() function ({psych} package (Revelle, 2023)) to adjust with Bonferroni correction for multiple comparisons and corrplot() function ({corrplot} package (Wei & Simko, 2010) for visualisation. Graphs were created using the package ggplot2 (Wickham et al., 2023).

2.2.10.2 fMRI Data First-Level and Second-Level Analyses

As the focus of the study was to investigate the processing of salient events in a reinforcement learning task, the main contrasts of interest were (1) loss feedback > gain feedback as an indicator of emotional salience and (2) reversal feedback > no-reversal feedback as an indicator of task-related salience. Furthermore, to investigate memory effects, the contrasts (3) remembered stimuli > not remembered stimuli as an indicator of memory performance and (4) remembered stimuli before loss feedback > not remembered stimuli before loss feedback as an indicator of emotional memory performance were investigated. To address these questions, four event-related General Linear Models (GLMs) were implemented, which allowed investigation of these contrasts in younger adults, older adults, and age group differences in these contrasts. Specifically, GLM 1 assessing emotional salience included loss and gain feedback timepoints while controlling for reversal feedback timepoints. GLM 2 assessing effects of task-related

salience included regressors for reversal and no reversal feedback while controlling for timepoints of loss feedback. GLM 3 assessing memory performance included timepoints of remembered and not remembered stimuli during stimulus presentation, and GLM 4 assessing emotional memory performance included regressors of remembered or not remembered stimuli before gain or loss feedback during stimulus presentations. To account for irrelevant task-related effects, GLMs included regressors indicating where stimuli or feedback (depending on the GLM) were part of a free or forced choice trial (one or two stimuli to choose from), as well as the onset of the fixation cross between stimulus and feedback presentations and left and right response time points. For an overview of all regressors included in the respective GLMS, see Table 1, while the time course of the effect size is shown in Supplementary Figure S2. For an overview of the main fMRI results, see Supplementary Table S2.

Types of event-related GLMs

Types of event-related GLMs	regressors	contrast of interest
(1) emotional salience	forced choice, free choice, reversal, gain, loss, fixation, response left, response right	**loss feedback > gain feedback**
(2) task-related salience	forced choice, free choice, reversal, no reversal, loss, fixation, response left, response right	**reversal feedback > no reversal feedback**
(3) memory performance	forced choice, reversal, gain, loss, response left, response right, remembered, not remembered	**remembered > not remembered**
(4) emotional memory performance	forced choice, reversal, gain, loss, response left, response right, remembered loss, remembered gain, not remembered before loss, not remembered before gain	**remembered before loss feedback > not remembered before loss feedback**

Table 1. Four types of event-related GLMs with corresponding regressors as well as contrasts of interest.

All sets of GLMs also contained regressors of no interest (6 regressors for movement, 14 regressors for physiological data like breathing and pulse). Finally, because high resolution functional images are more susceptible to movement artefacts during recording, individual volumes with movement exceeding a pre-set threshold were excluded from the statistical analyses by modelling them with an individual volume regressor in the first level GLM. Movement artefacts during recording did not differ between healthy younger and older healthy subjects as assessed by mean distance and degree in displacement; $t(47) = 1.17$, $p = 0.25$ (two healthy older adults did not have volumes exceeding exclusion criteria). The first 5 (dummy) volumes were not included in the GLM analyses. First level contrasts effects were then included in second level analyses which assessed contrasts of interest within as well as between age groups using one sample t-tests and two sample t-tests, respectively. Given the small size of our target structures in the brainstem and midbrain, significant activations were assessed using anatomical masks of the LC and a combined mask of SNc, SNr, VTA and red nucleus for small volume corrections. Activations in cortical and subcortical areas were examined using an inclusive grey matter mask. For the confirmatory small volume corrected analyses, significance assessments were corrected for multiple comparisons using family wise error correction (FWE), which is a more conservative measure assessing the ratio of falsely rejected tests to all tests performed. For the more exploratory assessments of significant clusters in cortical and subcortical areas, multiple comparisons were corrected using the false discovery rate correction (FDRc), which is based on the ratio of falsely rejected tests to all rejected tests and more sensitive in detecting clusters of activation. Given the comparatively smaller voxel sizes (1.5 mm isotropic) and the relatively lower SNR per voxel, less conservative voxel cut-offs of $p < 0.005$ were used for cortical and subcortical areas to increase sensitivity. Furthermore, for target structures in the brainstem and midbrain, a more conservative voxel cut-off of $p < 0.003$ in addition to $p < 0.005$ was used to indicate the contribution of more reliably activated areas in the brainstem and midbrain (cf. white lines in Figure 9-11). The analysis procedure described above partially resulted in no suprathreshold clusters for brainstem, midbrain, cortical, and subcortical areas.

2.3 Results

2.3.1 Behavioral Results

Regarding memory effects of (1) emotional salience, a statistically significant interaction between trials before vs. trials after feedback and loss vs. gain feedback was observed, $F(1,48) = 5.82$, $p = 0.02$, partial $\eta^2 = 0.11$. Specifically, higher memory performance was observed for stimuli before loss feedback (M ± SD: 0.21 ± 0.85) as compared to stimuli before gain feedback (M ± SD: 0.18 ± 0.81); $t(49) = 3.55$, $p < 0.001$. The same effect was not observed for memory performance on trials after loss feedback (M ± SD: 0.19 ± 0.89) compared with trials after gain feedback (M ± SD: 0.18 ± 0.07); $t(49) = 0.97$, $p = 0.34$ (Fig. 8). There was no significant main effect of age, $F(1,48) = 0.37$, $p = 0.55$ and no interactions between loss vs. gain feedback and age group ($F(1,48) = 0.013$, $p = 0.911$) and trials before vs. trials after feedback and age group ($F(1,48) = 0.18$, $p = 0.693$) (Supplementary Results 2.1).

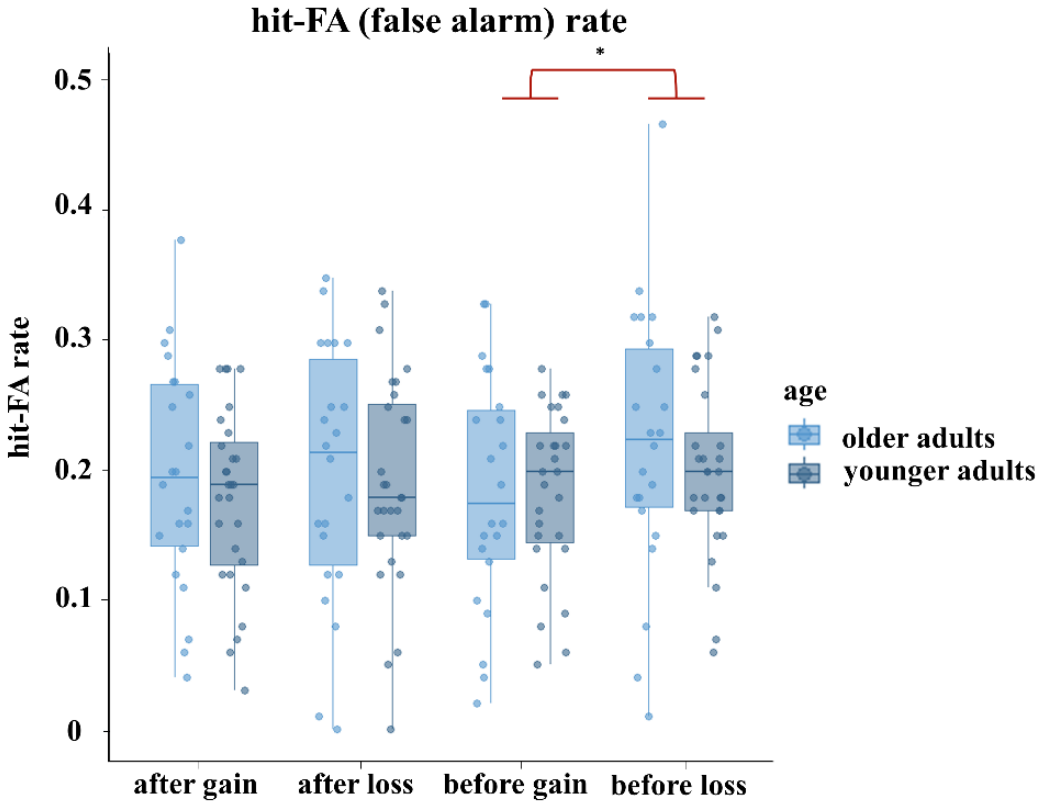

Figure 8. Memory performance (hit-FA (false alarms)) of the reversal reinforcement learning task. Hit-FA (false alarm) rate on trials before loss vs. gain feedback and on trials after loss vs. gain feedback for older (brighter blue) and younger (darker blue) adults. The asterisk highlights the statistically significant difference between higher memory performance for stimuli *before* loss feedback (M ± SD: 0.21 ± 0.85) as compared to stimuli *before* gain feedback (M ± SD: 0.18 ± 0.81) across age groups, $t(49) = 3.55$, $p < 0.001$ (reproduced Hämmerer et al., 2018, Fig. 2a). Boxplots contain the median (horizontal black line), with the lower and upper parts of the boxes indicating the 25th and 75th percentiles of the underlying hit-FA rate, respectively.

RTs related to emotional salience as well as task-related salience were analysed to gain further insight into behavioral adaptations to salient events. Regarding RTs to (1) emotional salience there was a significant interaction between the before vs. after trials with loss vs. gain feedback, $F(1,48) = 19.40$, $p < 0.001$, partial $\eta^2 = .29$: Specifically, RTs slowed down after gain feedback, but sped up after loss feedback (loss feedback: before trials (M ± SD: 1.10 ± 0.03), after trials (M ± SD: 1.07 ± 0.02), gain feedback: before trials (M ± SD: 1.04 ± 0.02), after trials (M ± SD: 1.06 ± 0.02)) (Supplementary Figure S3). Given that, in the current decorrelated design, loss and gain feedback were comparably informative for response correctness, this interaction effect might suggest a behaviorally invigorating effect of emotionally salient events in line with animal work, showing that LC activity is linked to effortful responding (Bouret & Sara, 2004). Effects of (2) task-related saliency on RTs on trials with reversals of the reinforced stimulus category (40 trials in total) were assessed by averaging RTs on three trials before and after reversals, respectively. RTs after reversals were slower (M ± SD: 1.05 ± 0.02) as compared to RTs before the reversal (M ± SD: 1.03 ± 0.03), $F(1,48) = 5.57$, $p = 0.02$, partial $\eta^2 = 0.10$, in both younger as well as older adults, indicating more controlled response behaviour on the first trials of a new reinforced stimulus category. For a complete overview of RT effects related to (1) emotional salience and (2) task-related salience, see Supplementary Results 2.2.

2.3.2 fMRI Results

Since the aim of this chapter is to investigate age differences in functional activations of the LC, only functional brainstem and midbrain activations are reported here. Analyses on fMRI data were conducted to assess the LC and substantia nigra / ventral tegmental area (SN/VTA) response to (1) emotional salience: loss > gain feedback, (2) task-related salience: reversal > no reversal feedback, (3) memory performance: remembered > not remembered and (4) emotional memory performance: remembered before loss feedback > not remembered before loss feedback in younger and older adults, as well as age differences (N = 50) therein (Table 1). Activations in the brainstem and midbrain were investigated using an inclusive brainstem mask (see section 2.2.9).

2.3.2.1 Higher LC Activation in Older Adults during Encoding of Salient and Negative Events

In line with the hypothesis, stronger activations in noradrenergic structures were observed during the processing of salient events, and additionally also in GABAergic (SNr) structures. Unexpectedly, this effect was generally more pronounced in older adults (Fig. 9-11). While younger adults did not show significant activations in the LC, older adults showed a higher activation of the left LC during (1) loss > gain feedback (Fig. 9a, Supplementary Table

S3; T = 4.11, pFWE = 0.04 (voxel cut-off p < 0.005); pFWE = 0.02 (voxel cut-off p < 0.003)). Additionally, older adults also showed higher activation of the right LC (Fig. 9b) and right SNr (Fig. 10) during (2) reversal > no reversal feedback categories (Supplementary Table S6; LC: T = 3.37, pFWE = 0.08 (voxel cut-off p < 0.005); pFWE = 0.05 (voxel cut-off p < 0.003); SNr: T = 4.77, pFWE = 0.02 (voxel cut-off p < 0.005); pFWE = 0.02 (voxel cut-off p < 0.003)). This dovetails findings from electrophysiological recordings in monkeys showing that the LC responds to relevant or unexpected task events (Dayan & Yu, 2005). Age group comparisons confirmed the stronger engagement of LC in older adults, showing more engagement of the bilateral LC during (1) loss > gain feedback for older as compared to younger adults (Fig. 11a, Supplementary Table S4; left LC: T = 3.4, pFWE = 0.06 (voxel cut-off p < 0.005); pFWE = 0.04 (voxel cut-off p < 0.003); right LC: T = 3.14, pFWE = 0.08 (voxel cut-off p < 0.005); pFWE = 0.05 (voxel cut-off p < 0.003)). There was a trend for higher right LC activation during (2) reversal > no reversal feedback for older as compared to younger adults (Fig. 11b, Supplementary Table S7; T = 3.02, pFWE = 0.07 (voxel cut-off p < 0.005); pFWE = 0.06 (voxel cut-off p < 0.003)). No significant emotional and task-related activations in the brainstem were observed in younger adults (Supplementary Table S5 & S8).

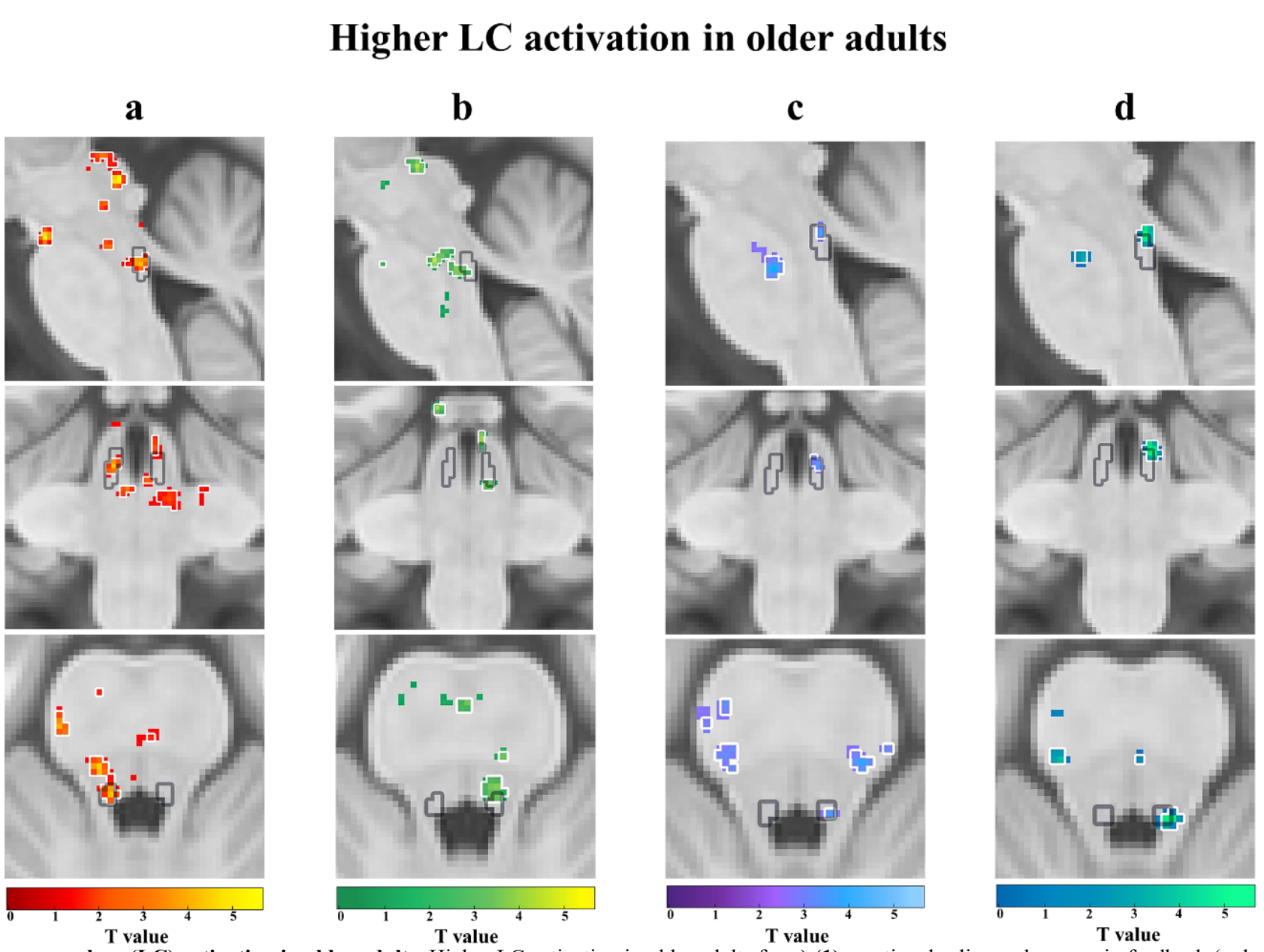

Figure 9. Higher locus coeruleus (LC) activation in older adults. Higher LC activation in older adults for **a) (1)** emotional salience: loss > gain feedback (red-yellow), **b) (2)** task-related salience: reversal > no reversal feedback (green-yellow), **c) (3)** memory performance: remembered > not remembered (purple-blue) and **d) (4)** emotional memory performance: remembered before loss feedback > not remembered before loss feedback (blue-green). Significant activations (a-d) shown in each colour with a threshold of $p < 0.005$ (threshold of $p < 0.003$ outlined in white) are in sagittal (first row), coronal (middle row), and axial (bottom row) views, within the LC meta mask (grey) created by Dahl et al., 2022.

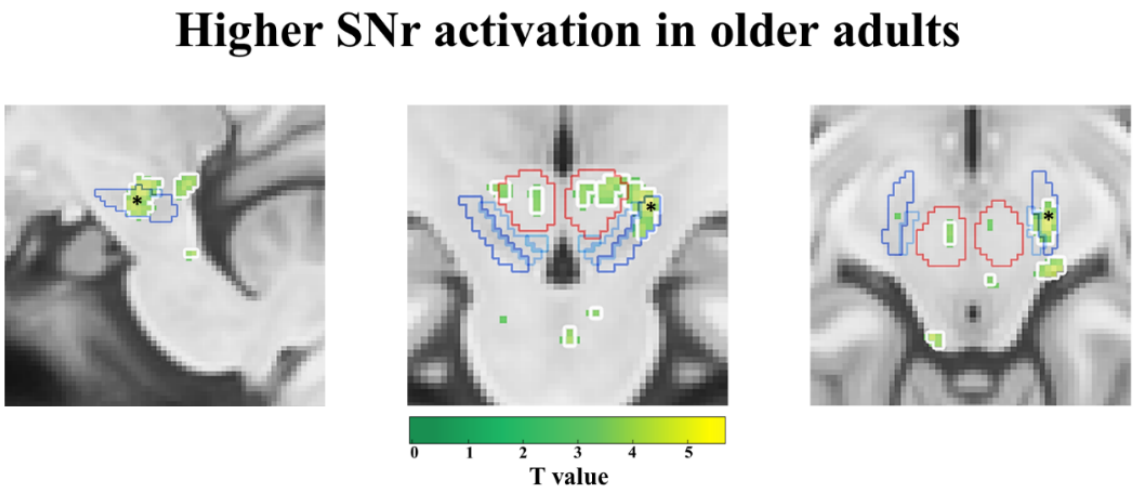

Figure 10. **Higher substantia nigra pars reticulata (SNr) activation in older adults.** Higher SNr activation in older adults for **a) (2)** task-related salience: reversal > no reversal feedback (green-yellow). Activations shown in colour with a threshold of $p < 0.005$ (threshold of $p < 0.003$ outlined in white) are in sagittal (first), coronal (middle), and axial (right) views, within the "SNrSNcVTA mask" (see Supplementary Figure S1: *SNr*: dark blue; *SNc*: middle blue; *VTA*: brighter blue; *red nucleus*: red). The black asterisk indicates the significant activation within SNr.

2.3.2.2 Higher LC Activation in Older Adults for Remembering Negative Events

Older adults additionally exhibited increased LC engagement during later remembered stimuli, particularly if those were associated with negative feedback. Specifically, older adults showed higher activation of the right LC during encoding of later (3) remembered > not remembered stimuli (Fig. 9c, Supplementary Table S9; T = 3.64, pFWE = 0.07 (voxel cut-off $p < 0.005$); pFWE = 0.05 (voxel cut-off $p < 0.003$)) and a trend for higher right LC activation during (4) later remembered stimuli followed by loss as compared to not remembered stimuli followed by loss feedback (Fig. 9d, Supplementary Table S13; T = 4.38, pFWE = 0.07 (voxel cut-off $p < 0.005$); pFWE = 0.06 (voxel cut-off $p < 0.003$)). Age group comparisons confirmed greater engagement of the right LC for (3) remembered > not remembered stimuli (Fig. 11c, Supplementary Table S10; T = 3.42, pFWE = 0.08 ($p < 0.005$); pFWE = 0.05 ($p < 0.003$)), and for (4) later remembered stimuli followed by loss as compared to not remembered stimuli followed by loss feedback (Fig. 11d, Supplementary Table S14; T = 3.46, pFWE = 0.09 ($p < 0.005$); pFWE = 0.05 ($p < 0.003$)) for older adults as compared to younger adults. No significant memory-related activations in the brainstem were observed in younger adults (Supplementary Table S11-S12 & S15-S16). Neither for (1) emotional salience, (3) memory, nor (4) emotional memory performance, a correlation between the behavioral performance indicators and LC activations was observed (Supplementary Figure S7, S9-S10).

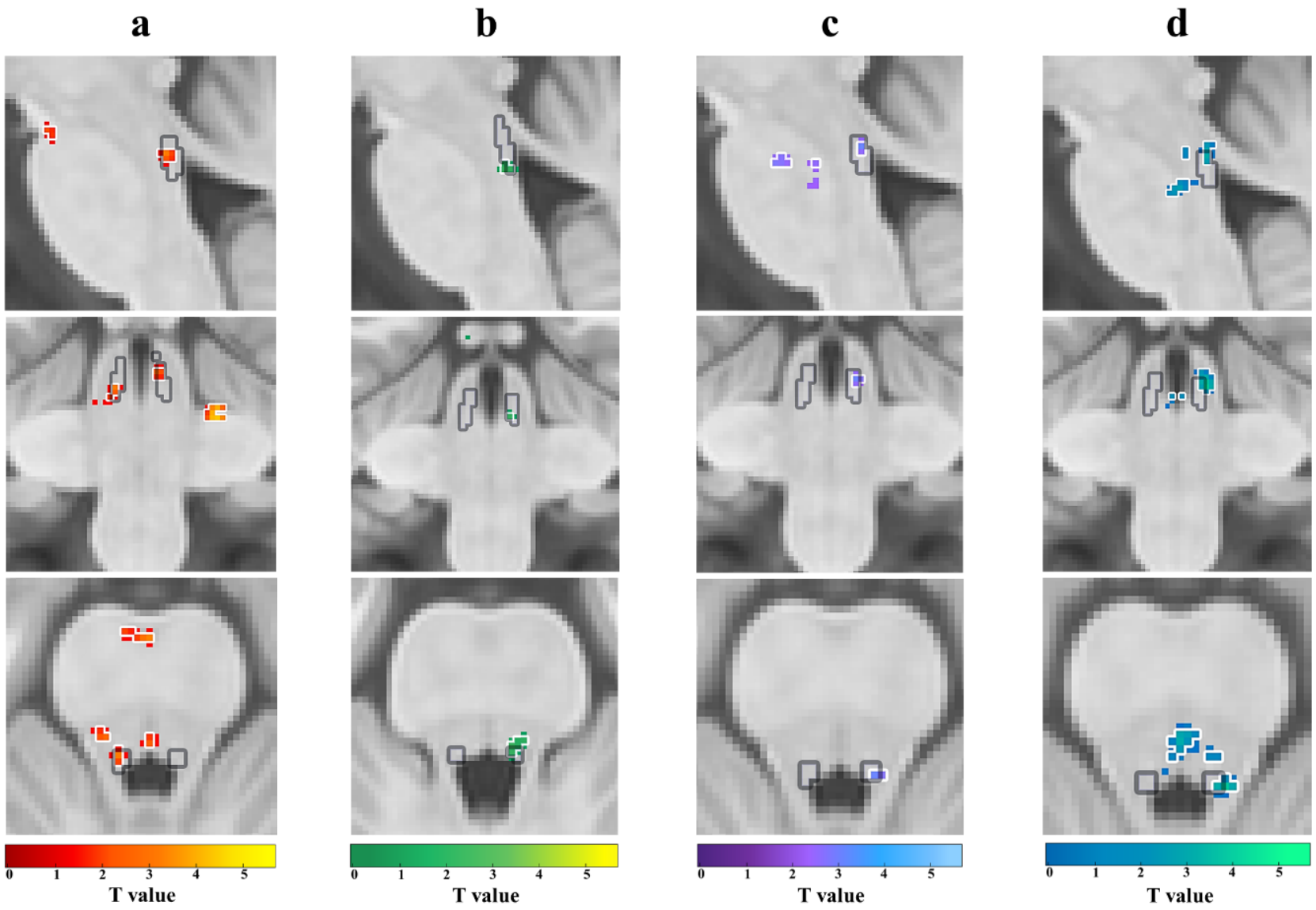

Figure 11. Higher locus coeruleus (LC) activation in older > younger adults. Higher LC activation in older > younger adults for **a) (1)** emotional salience: loss > gain feedback (red-yellow), **b) (2)** task-related salience: reversal > no reversal feedback (green-yellow), **c) (3)** memory performance: remembered > not remembered (purple-blue) and **d) (4)** emotional memory performance: remembered before loss feedback > not remembered before loss feedback (blue-green). Significant activations (a-d) shown in each colour with a threshold of $p < 0.005$ (threshold of $p < 0.003$ outlined in white) are in sagittal (first row), coronal (middle row), and axial (bottom row) views, within the LC meta mask (grey) Dahl et al., 2022.

2.3.2.3 Cortical Area Activations

The focus of the LC fMRI study was to examine the brainstem and adjacent are higher resolution, which allowed me to investigate only cortical and subcortical activations ın limited regions, including parts of the temporal and parietal lobes, amygdala, and HPC, due to the smaller FoV (Fig. 5). Specifically, during (1) loss > gain feedback (see Supplementary Figure S4; Table S17-S19), younger and older adults showed stronger functional activation in the right MTG (younger adults: T = 5.32, pFDR < 0.001; older adults: T = 7.74, pFDR < 0.001). Only older adults showed stronger activation for the left MTG (T = 4.79, pFDR < 0.001). In line with the age group differences in brainstem activations, age group comparisons showed greater engagement of the bilateral MTG (right MTG: T = 4.29, pFDR < 0.04; left MTG: T = 4.54, pFDR < 0.004) for older adults. Similarly, older adults showed a stronger engagement of bilateral MTG (right MTG: T = 8.14, pFDR < 0.001; left MTG: T = 5.70, pFDR = 0.001) during (2) reversal > no reversal feedback category (see Supplementary Figure S5; Table S20-S21) while younger adults also showed higher activation in left MTG (T = 5.28, pFDR = 0.02), as well as bilateral STG (right STG: T = 6.61, pFDR < 0.001; left STG: T = 5.54, pFDR < 0.001). No age group differences in MTG or STG activations during reversal > no reversal feedback were observed. In addition to MTG and STG activations, areas supporting visual processing were more activated during salient events in both age groups, including the calcarine cortex (CAL), fusiform gyrus (FuG) and lingual gyrus (LiG) (see Supplementary Results 2.4). Finally, areas known to support memory consolidation and memory-related stimulus processing were preferentially engaged during (2) reversal > no reversal feedback (see Supplementary Figure S5; Table S20-S22): Younger adults showed higher activation in left entorhinal cortex (EC) (T = 4.58, pFDR = 0.05) and older adults showed higher activation in the right precuneus (PCUN) (T = 6.59, pFDR < 0.001). Age group comparison showed more engagement of the left PCUN (older > younger adults: T = 4.44, pFDR < 0.001) for older adults. For (2) task-related salience, no correlation was found between the behavioral performance indicators and a) LC activation but for b) MTG activation (r (16) = .62, p = 0.009; Supplementary Figure S8).

2.3.2.4 Higher Hippocampus Activation in Older Adults

As salience and memory-related LC activations have been known to modulate HPC (Luo et al., 2015) as well as amygdala function (Cahill et al., 1995), exploratory analyses in these regions using small volume corrections in anatomical masks were added. During (1) loss > gain feedback (Fig. 12; see Supplementary Table S18), older adults showed stronger functional activations in the left HPC (T = 3.94, pFWE = 0.008) as compared to younger adults. This is in line with the observed stronger LC activation in older adults during loss compared to gain feedback and the better memory for stimuli before loss as compared to gain feedback in both age groups.

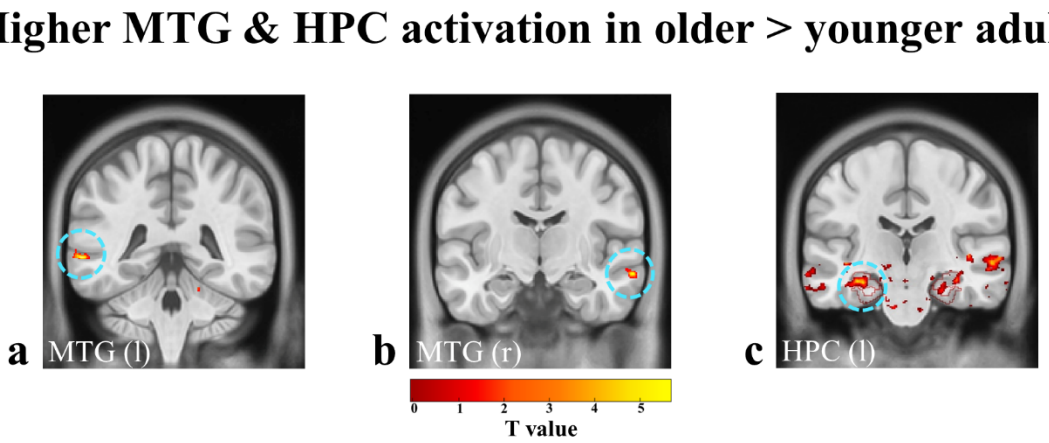

Figure 12. **Higher middle temporal gyrus (MTG) and hippocampus (HPC) activation in older > younger adults**. Higher **(a,b)** MTG (threshold of $p < 0.005$) and **(c)** HPC (threshold of $p < 0.05$) activation in older > younger adults for **(1)** emotional salience: loss > gain feedback (red-yellow). HPC activations shown within "hippocampus-amygdala mask" (see Supplementary Figure S1: amygdalae: rose; hippocampi: middle rose; parahippocampi: dark rose). Turquoise circles highlight the corresponding significant activations.

2.4 Interim Discussion

In vivo measurements of LC integrity and function are potentially important biomarkers for healthy aging and early ND onset. In this chapter, I used high-resolution fMRI, a reversal reinforcement learning task, and dedicated post-processing approaches to visualize age-related differences in LC function (N = 50). The results showed increased LC responses during emotionally and task-related salient events, with subsequent accelerations and decelerations in reaction times, respectively, indicating context-specific adaptive engagement of the LC. This aligns with animal studies indicating preferential LC activation during negative events (e.g., foot shocks) (Bouret & Sara, 2004; Sara, 2009) and in vivo findings linking LC integrity to memory of negative events in older adults (Clewett et al., 2018; Hämmerer et al., 2018; Liu et al., 2020), as further discussed in the General Discussion. Moreover, older adults exhibited increased LC activation compared to younger adults, indicating possible 1) compensatory overactivation of a structurally declining LC in aging. These results (Fig. 13) and their implications are discussed in more detail in the General Discussion, also with respect to 2) that stronger functional responses of the LC might also be related to cell loss in the LC and 3) that age-related differences in task performance might contribute to differences in functional recruitment between age groups. Therefore, the assessment of LC function serves as a promising biomarker of cognitive aging.

Overview

LC fMRI study – main results

N = 50 (28 younger & 22 older adults)

Reversal reinforcement learning task

Behavioral results

- better memory performance for stimuli associated with (1) emotionally salient events
- no age differences in emotional memory

Hypotheses

1. There is higher functional LC activation during (1) emotionally salient, (2) task-related salient events, and (3-4) for memory performance of such salient events.

2. There is higher functional LC activation for (5) younger adults compared to older adults.

fMRI results

Higher LC activation* was unexpectedly observed *in older adults

Types of event-related GLMs	contrast of interest	fMRI results
(1) emotional salience	loss feedback > gain feedback	younger adults: /
		older adults: ▪ left LC
		older > younger: ▪ bilateral LC
(2) task-related salience	reversal feedback > no reversal feedback	younger adults: /
		older adults: ▪ right LC
		older > younger: ▪ right LC
(3) memory performance	remembered > not remembered	younger adults: /
		older adults: ▪ right LC
		older > younger: ▪ right LC
(4) emotional memory performance	remembered before loss feedback > not remembered before loss feedback	younger adults: /
		older adults: ▪ right LC
		older > younger: ▪ right LC

Figure 13. Overview highlighting main results of the LC fMRI study. The image of the head was created with BioRender.com.

3 Chapter 3: Short Bursts of Transcutaneous Auricular Vagus Nerve Stimulation (TaVNS) Study

Versions of this chapter, with minor modifications, have been published in Scientific Reports (Ludwig et al., 2024a) and Psychophysiology (Ludwig et al., 2025).

3.1 Brief Introduction

The decline in noradrenergic LC function in aging is thought to be implicated in episodic memory decline (Ehrenberg et al., 2023; Engels-Domínguez et al., 2023). The efficacy of taVNS as a non-invasive method to modulate physiological markers of noradrenergic activity of LC, such as pupil dilation, and to preserve or improve memory function in aging is increasingly discussed (D'Agostini et al., 2023; Jacobs et al., 2015; Sharon et al., 2021; Ventura-Bort et al., 2021; Vonck et al., 2014). However, taVNS studies show high heterogeneity of stimulation effects, and it is currently unclear which taVNS-induced mechanisms lead to pupil dilation and whether taVNS has an effect on memory (Farmer et al., 2021; Ludwig et al., 2021).

In chapter three, I present the results of a newly established taVNS setup that allows time-synchronized recording of pupil dilation during short bursts of event-related taVNS (3 s) in younger adults (N = 24) to gain insight into the underlying mechanisms of taVNS in a cognitively healthy organism. Subjects performed an emotional memory task with negative events involving the LC-NE system (Hämmerer et al., 2017, 2018) and a resting-state task to investigate different frequencies (10 Hz and 25 Hz) and intensities (3 mA and 5 mA). I will investigate whether short bursts of taVNS lead to increased pupil dilation during encoding (emotional memory task) and resting-state task and whether higher compared to lower stimulation parameters (resting-state task) lead to increased pupil dilation. Furthermore, I will investigate possible taVNS-induced improvements in (emotional) memory performance for early and delayed (24 h) recognition. Importantly, I will also investigate the effects of subjective perception of taVNS on changes in pupil dilation and memory performance.

3.2 Methods

The data reported in this chapter refer to two different tasks, 1) emotional memory task and 2) resting-state task, performed on the same subjects (N = 24, healthy younger adults). The present chapter focuses on possible short bursts of taVNS-induced changes in pupil dilation during the encoding task of the emotional memory task and resting-state task, as well as effects on (emotional) memory performance in the early and delayed (24h) recognition task.

3.2.1 Subjects

Twenty-four younger healthy subjects (12 females; 22.96 ± 2.24 years; see Supplementary Methods 3.1 & 3.2) were recruited through advertisements via the university's mailing list and flyer distributions in Magdeburg. Subjects were included if they were between 20 and 30 years old, German speaking, had a BMI < 27, with low levels of alcohol and cigarette consumption. In addition, subjects were stratified into sporty (more than three times a week sport in the last 4 weeks) vs. non-sporty (less than two times a week sport in the last four weeks) as the whole experiment also included the acquisition of heart-rate variability (HRV) which varies in athletes compared to no athletes (Kiss et al., 2016). Exclusion criteria included cold symptoms, neurological (stroke, epilepsy, traumatic brain injury, syncope) as well as psychiatric (eating disorder, major depressive disorder, schizophrenia, bipolar disorder, any anxiety disorder, posttraumatic stress disorder) and other disorders (e.g., diabetes, alcohol dependence and/or drug use) as well as heart and eye diseases. Telephone screenings were conducted to verify the eligibility of those interested in the study. Subjects were asked to eat a light, healthy breakfast (no industrial sugar), not to drink caffeine, and not to smoke on the day of the experiment, as well as not to drink alcohol on the day of the experiment and the day before. The study was approved by the Ethics Committee of medical faculty at the Otto von Guericke University of Magdeburg (reference no. 107/20) and was carried out in accordance with the ethical standards of Helsinki. A written informed consent was obtained from each subject before participation, and subjects received 90 Euro reimbursement.

3.2.2 Procedure

The study was conducted as a sham-controlled, single-blind, within-subject, counterbalanced, randomized design using a one-day stimulation protocol. At the beginning of each session subjects underwent a HRV baseline measurement, which was repeated halfway through the whole and at the end of the experiment (Fig. 14). Subsequently, the subjects were able to try out the taVNS themselves to become familiar with the device and to adjust the highest stimulation intensity (see section 3.2.3), which was accompanied by a subjective evaluation of the perception using a visual analog scale (VAS) (see section 3.2.7). Regarding the stimulation, it was instructed at the beginning that the stimulation of the ear can be perceived as a harmless tingling sensation in various areas. In addition, the entire ear was cleaned and not just a specific stimulation area and the repositioning of the electrodes was covered up with the story that the cream dries on the electrode after a certain time. This procedure ensured that subjects did not question why the electrodes were being reapplied for real and sham stimulation. The study consisted of two parts: 1) emotional memory task and 2) resting-state task. During the performance of the emotional memory task as well as during the presentation of the fixation-cross during the resting-state task, subjects received real and sham stimulation while changes in pupil dilation were recorded in parallel. Immediately after the encoding sessions of the emotional memory test, an early recognition test was performed on the same day, and 24 hours later, a delayed recognition test was performed, both without stimulation (Fig. 14). Importantly, subjective perceptions of sensations (VAS rating) as well as query of the state of health (potential side effects) were systematically recorded after each stimulation session.

3.2.3 Transcutaneous Auricular Vagus Nerve Stimulation (TaVNS)

TaVNS was delivered using tVNS Technologies nextGen research device (tVNS R, tVNS Technologies GmbH), which is connected via Bluetooth Low Energy (BLE) connection with an android-based application (BOLZIT, Software development and IT Services) to individually set stimulation parameters (tVNS Research App) and check the applied stimulation intensity and duration (tVNS Patient App). Furthermore, BLE connection enables a connection between the stimulator and a “tVNS Manager” (BOLZIT) console application for Windows 10, which allows time-synchronous stimulation with the required design experiment via an HTTP request. Thus, messages about stimulation on and offset were forwarded via the “tVNS Manager”, which were integrated within the MATLAB code of the experiment, so that the stimulation (without ramp-up) was either switched on or off per trial event within a loop. Precise control of all BLE-capable devices was important: In the first step, parameters were set using the tVNS Research app, the BLE connection was then removed so that the BLE connection to the taVNS Manager

could be guaranteed. Successful stimulation throughout the experiment could be guaranteed as the "taVNS Manager" sends messages when the stimulation is on and off according to the set duration, which is additionally accompanied by a continuous light of the tVNS R device while the stimulation is on. The ear electrode "legacy" (tVNS Technologies GmbH) was used, as the size of the electrode holder frame can be adjusted individually. The electrodes were placed on the **left ear** (Fig. 14): At the **cymba conchae** for **real taVNS**, which seems to be innervated exclusively by the auricular branch of the vagus nerve (ABVN) (Peuker & Filler, 2002) and at the **earlobe** for **sham taVNS**, which is not innervated by the ABVN (Burger et al., 2020; Butt et al., 2020; Peuker & Filler, 2002) and seems to not induce functional activation in the target brain areas, like LC and NTS, following taVNS (Yakunina et al., 2017). For real and sham stimulation, the anode was placed more rostrally. Prior to the electrode placement, the ear was cleaned with disinfectant alcohol and afterwards a small amount of EC2+, Grass electrode conductive cream (https://www.cnsac-medshop.com/de/ec2-elektrodenleitcreme/) on the electrodes was used to assure optimal conductance. Subsequently, the subjects were able to test the taVNS themselves with a frequency of 25 Hz, a pulse width of 250 μs and a stimulation cycle of 5 s on vs. off stimulation. The intensity started at 1 mA and subjects were allowed to go as high as possible at a reasonable pace. At the highest level, subjects rated the subjective intensity on a VAS (see section 3.2.7). A priori, it was determined that subjects who did not reach 5 mA as the highest intensity would receive 3 mA as highest and 1.5 mA as lowest intensity, which in the end applied to 7 out of 24 subjects (see Supplementary Methods 3.2).

Regarding the stimulation parameters, a biphasic square-wave pulse with a stimulus phase pulse width of 250 μs and a recovery phase at half the amplitude and double the duration, delivered at a frequency of 25 Hz was applied for short bursts of electrical stimulation of 3 s on and 15 s off stimulation. For 1) **emotional memory task**, intensity of 5 mA (N = 17) or 3 mA (N = 7) and a frequency of 25 Hz were applied and for the **2) resting-state task** low and high intensities (3 mA vs. 5 mA (N = 17) or 1.5 mA vs. 3 mA (N = 7)) as well as frequencies (10 Hz vs. 25 Hz) were systematically tested within subjects.

Study procedure and experimental set-up

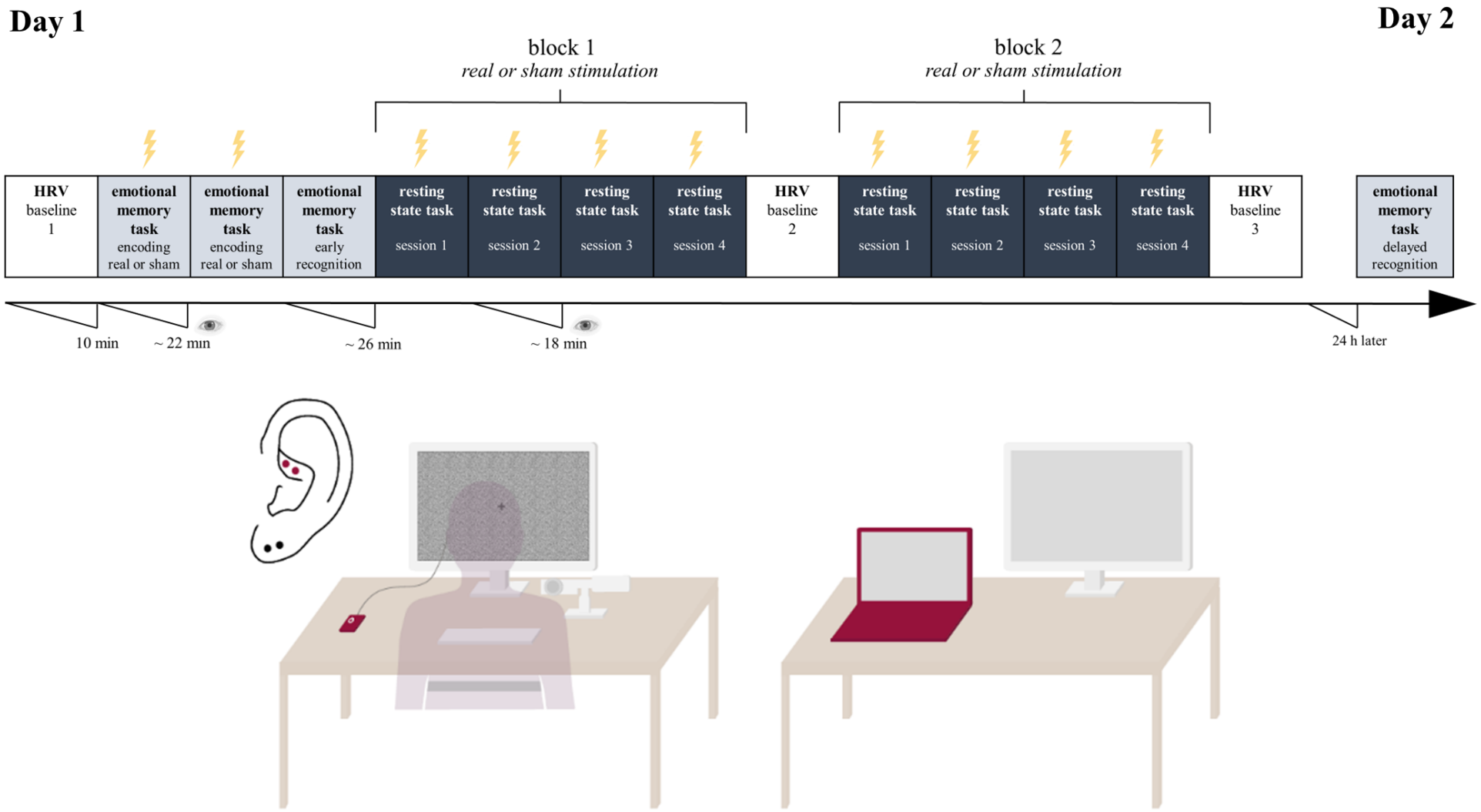

Figure 14. TaVNS study procedure and experimental set-up. The study was conducted as a sham-controlled, single-blind, within-subject, counterbalanced, randomized design with a one-day stimulation protocol (N = 24). The **study procedure** shows (upper panel), that during the emotional memory task real or sham stimulation was applied with highest stimulation parameters (5 mA, 25 Hz), while during the resting-state task 4 different stimulation parameter combinations were systematically tested (3 mA and 5 mA with 10 Hz and 25 Hz) in block 1 compared to block 2 (real or sham stimulation). Additionally, heart-rate variability (HRV; belt, left) and changes in pupil dilation (eyetracker camera, left) during taVNS were recorded. The **experimental set-up** (lower panel) enabled a time-synchronous short bursts stimulation during the resting-state task, while changes in HRV and pupil dilation were recorded in parallel on one computer (red laptop, right). This computer was connected to an extended screen (left) on which the task was presented. Additionally, the computer received stimulation inputs via an HTTP request that turned on or off the taVNS R stimulator (red square, left) in sections programmed for the task. In addition, a second screen (right) facilitated the control of the pupil recordings. The electrodes were placed on the **left** ear: At the **cymba conchae** for **real taVNS** (red dots) and at the **earlobe** for **sham taVNS** (black dots). For all subjects, the same constant ambient light continued to be applied throughout the whole experiment, and background brightness variations were controlled with a greyish background image to prevent interference of luminance changes with pupillometric recordings.

3.2.4 Emotional Memory Task

The emotional memory task consisted of an encoding task during which real and sham stimulation was applied and an early and delayed recognition task without stimulation.

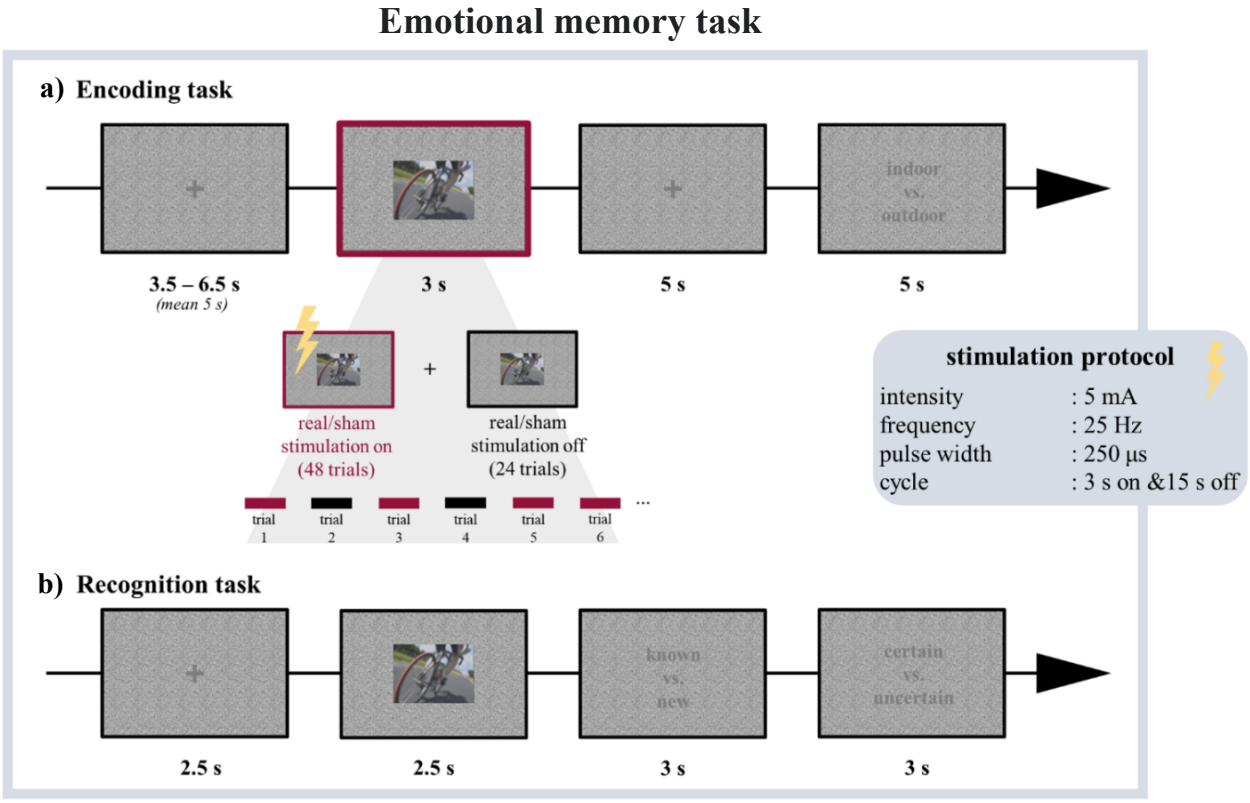

Figure 15. Emotional memory task procedure. In the emotional memory task, each trial of the **a) encoding task** began with a grey fixation cross (jitter between 3.5 - 6.5 s), followed by an image (3 s) showing either indoor or outdoor scene with a negative or neutral valence, while changes in the pupil were recorded in parallel, and stimulation was applied for 2/3 of the images (see section 3.2.4.1). Afterwards a grey fixation cross was presented (5 s) and subsequently subjects were asked to classify the image as outdoor (by pressing key A) or indoor (by pressing key L) as quickly but also as precisely as possible (time limitation of 5 s). The stimulation protocol (blue box) shows the applied stimulation parameters. During the **b) recognition task** (144 trials) no stimulation was applied. Each trial began with a grey fixation cross (2.5 s) followed by an image presentation (2.5 s) with a subsequent question (time limit of 3 s) to classify the image as known (by pressing the A key) or new (by pressing the L key). This was followed by a question (time limit of 3 s) about how certain or uncertain the subjects were in their recognition. For all subjects, the same constant ambient light continued to be applied throughout the whole experiment, and background and image brightness variations were controlled with a greyish background image to prevent interference of luminance changes with pupillometric recordings.

3.2.4.1 Encoding Task

The emotional memory task was based on the task published by Hämmerer et al. (2017) but differed in the following aspects: The encoding task was divided into two sessions for real and sham stimulation, each with 72 trials, and electrodes were repositioned between sessions. As a cover task to ensure attentive processing of stimuli, subjects had to indicate whether the stimuli depicted indoor or outdoor scenes. Each trial began with a grey fixation cross (jitter between 3.5 - 6.5 s), followed by an image (3 s) showing either indoor or outdoor scene with a

negative or neutral valence. During the image presentation, the stimulation was on for 48 trials and off for 24 trials. The number of images for *outdoor* versus *indoor* and *negative* versus *neutral* as well as *real stimulation* and *sham stimulation* condition was balanced for on and off stimulation and resulted in 12 stimulation on trials and 6 stimulation off trials across the four conditions (that is, outdoor neutral, outdoor negative, indoor neutral and indoor negative). After the image a grey fixation cross was presented again (5 s) and subsequently subjects were asked to classify the image as outdoor (by pressing key A) or indoor (by pressing key L) as quickly but also as precise as possible (time limitation of 5 s) as a cover task to ensure attentional processing of the stimuli (Fig. 15a). During the encoding task changes in pupil dilation were measured in parallel. In total, subjects performed 72 trials of 18 s duration, resulting in a total task duration of ~ 22 min per session, with the stimulation lasting a total of 2.4 min (3 s × 48 trials) during each session.

3.2.4.2 Early and Delayed Recognition Task

The recognition tasks consisted of 144 trials each. Each task consisted of 72 old images (from the encoding task) and 72 completely new images balanced for *outdoor*, *indoor*, *negative*, *neutral scenes* and *real stimulation, sham stimulation* as well as *on* and *off stimulation*. The presentation of a grey fixation cross (2.5 s) was followed by an image presentation (2.5 s) with a subsequent question (time limit of 3 s) to classify the image as known (by pressing the A key) or new (by pressing the L key) (Fig. 15b). This was followed by a question (time limit of 3 s) about how certain (1) or uncertain (0) the subjects were in their recognition. Thus, subjects saw images that were either associated with stimulation during encoding or completely new images. Both the question and the certainty had to be completed as quickly but also as precisely as possible. The total task duration per recognition task was 26.40 min (11 s × 144 trials).

3.2.5 Resting-State Task

The resting-state task consisted of two blocks (randomisation and counterbalancing of real and sham stimulation between subjects) of four sessions, each with 60 trials. The subjects were instructed to focus their gaze on a grey fixation cross throughout the task (Fig. 16).

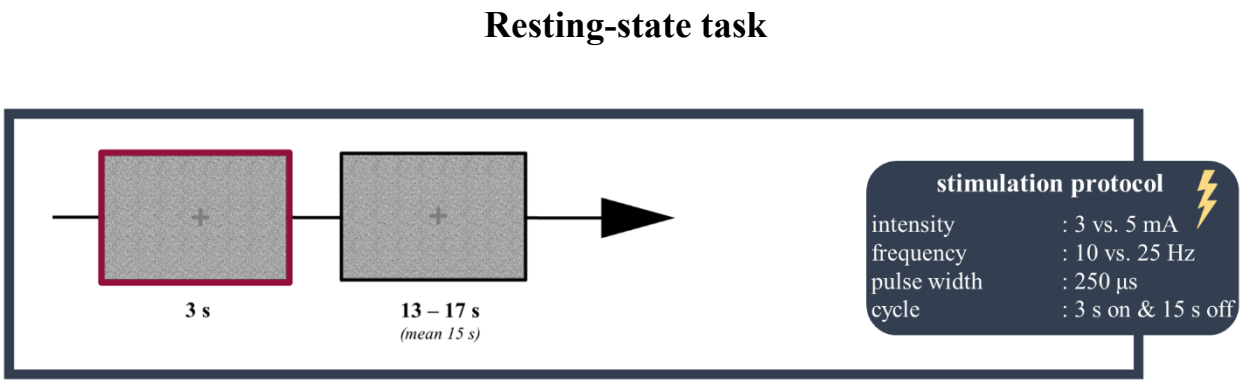

Figure 16. Resting-state task procedure. In the resting-state task, each trial began with a grey fixation cross during which stimulation was turned on for 3 s (red box), followed by another grey fixation cross during which stimulation was turned off for 15 s on average (13 – 17 s). The stimulation protocol (blue box) shows the applied stimulation parameters. For all subjects, the same constant ambient light continued to be applied throughout the whole experiment, and background brightness variations were controlled with a greyish background image to prevent interference of luminance changes with pupillometric recordings.

Each trial began with a grey fixation cross during which stimulation was turned on for 3 s, followed by another grey fixation cross during which stimulation was turned off for 15 s on average (13 – 17 s). To prevent interference with pupillometric recordings, the background's brightness variations were controlled with a greyish background image (Mathot, 2018). Both high and low frequency and intensity were tested in the 4 sessions randomized within and between subjects for real and sham stimulations. Between the single sessions, parameters were adjusted, and subjects were able to take a break (5 – 10 min). Those who needed the longer break were asked to walk around in the hallway outside the lab room to ensure sufficient attentional focus for the next session. Between the two blocks there was a break of 20 min, if necessary up to 30 min. The total task duration was 2 blocks × (18 min + 10 min post HRV measurement × 4 conditions) 4h 10 min, with the stimulation lasting a total of 12 min (60 trials × 4 conditions × 3 s) during each block (3 min per condition).

3.2.6 Materials and Stimuli

The stimuli for the emotional memory task consisted of 288 indoor and outdoor images representing emotionally negative or neutral events taken from the International Affective Picture System database (IAPS (J, 1995)) (272 images) and Geneva affective picture (GAPED (Dan-Glauser & Scherer, 2011)) database (16 images) to allow for categorization of indoor and

outdoor stimuli as a cover task while assessing effects of emotional stimulus materials (neutral indoor (72), neutral outdoor (72), emotional indoor (72), emotional outdoor (72)). Stimulus conditions were furthermore balanced with respect to stimulation conditions and early and delayed recognition. This means that the same proportion of the four stimulus categories was present for real stimulation, sham stimulation and off stimulation trials, as well as for early and delayed memory task (for more details see Supplementary Table S24). This procedure not only ensured that the distribution of images for all conditions was randomized between subjects and balanced within but also allowed analyses to clearly separate memory and pupil effects related to stimulus types (emotional or neutral) and stimulation conditions (real, sham or no stimulation (off)). Importantly, in both tasks, the background's brightness variations were controlled with a greyish background image and stimuli were luminance controlled to prevent interference of luminance changes with pupillometric recordings.

3.2.7 Visual Analog Scale (VAS)

Subjects were asked to rate how pleasant or unpleasant each stimulation session was perceived after stimulation, based on a visual analog scale (VAS) (Yeung & Wong, 2019) ranging from (1) very pleasant to (10) very unpleasant (Fig. 17).

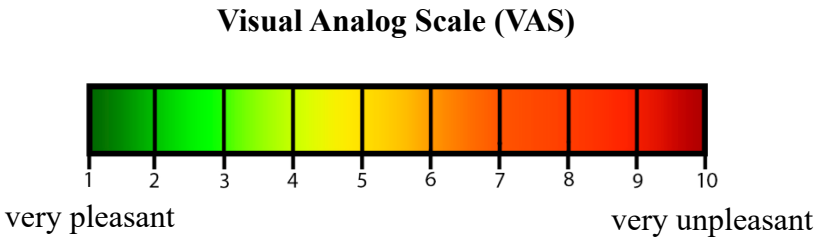

Figure 17. Visual analog scale (VAS). VAS rating (Yeung & Wong, 2019) ranging from (1) very pleasant (dark green) to (10) very unpleasant (dark red).

Since it has been shown that the perception of sensations differs between real and sham stimulation, the VAS rating is often kept constant as a controlling factor in many studies and the individual intensity is allowed to vary for each subject based on e.g., a "tingling" sensation below the pain threshold (Farmer et al., 2021; Ferstl et al., 2022; Müller et al., 2022). However, because I systematically tested a fixed set of different intensities and frequencies, I could not hold VAS rating constant but could document effects of the different parameters on subjective perception of sensations.

For the emotional memory task, the subjective perception of sensations (VAS) was higher for real stimulation (M ± SD: 5.78 ± 0.41) compared to sham stimulation (M ± SD: 4.86 ± 0.35), $F(1,20) = 4.31$, $p = 0.05$) (Fig. 18a). There was no significant effect for either gender

($F(1,20) = 0.03$, $p = 0.87$), sporty ($F(1,20) = 0.14$, $p = 0.71$), or sensitivity ($F(1,20) = 0.05$, $p = 0.83$) and no significant interaction between sensitivity and stimulation ($F(1,20) = 0.19$, $p = 0.66$). For the resting-state task, the subjective perception of sensations (VAS) was not only higher for **(1)** *real stimulation* (M ± SD: 4.40 ± 0.34) compared to sham stimulation (M ± SD: 2.97 ± 0.29) (Fig. 18b), ($F(1,20) = 17.85$, $p < 0.001$), but also for **(2)** *high frequency* (M ± SD: 4.08 ± 0.28) compared to low frequency (M ± SD: 3.29 ± 0.28) (Fig. 18c), ($F(1,20) = 19.57$, $p < 0.001$), and **(3)** *high intensity* (M ± SD: 4.56 ± 0.23) compared to low intensity (M ± SD: 2.81 ± 0.23), ($F(1,20) = 70.90$, $p < 0.001$) (Fig. 18c). There was no significant effect for either gender ($F(1,20) = 0.02$, $p = 0.88$), sporty ($F(1,20) = 0.17$, $p = 0.69$), or sensitivity ($F(1,20) = 0.07$, $p = 0.79$). There was a significant interaction between *sensitivity and stimulation* ($F(1,20) = 4.86$, $p = 0.04$), whereas sensitive subjects perceived higher sensations during real stimulation (M ± SD: 4.71 ± 0.59) than during sham stimulation (M ± SD: 2.51 ± 0.5); $t(20) = 3.78$, $p = 0.006$. Additionally there were trends for interactions between stimulation and frequency ($F(1,20) = 4.06$, $p = 0.06$) as well as between sensitivity and frequency ($F(1,20) = 3.61$, $p = 0.07$). However, there was no significant interaction between in stimulation and intensity ($F(1,20) = 0.20$, $p = 0.66$) (see Supplementary Figure S12).

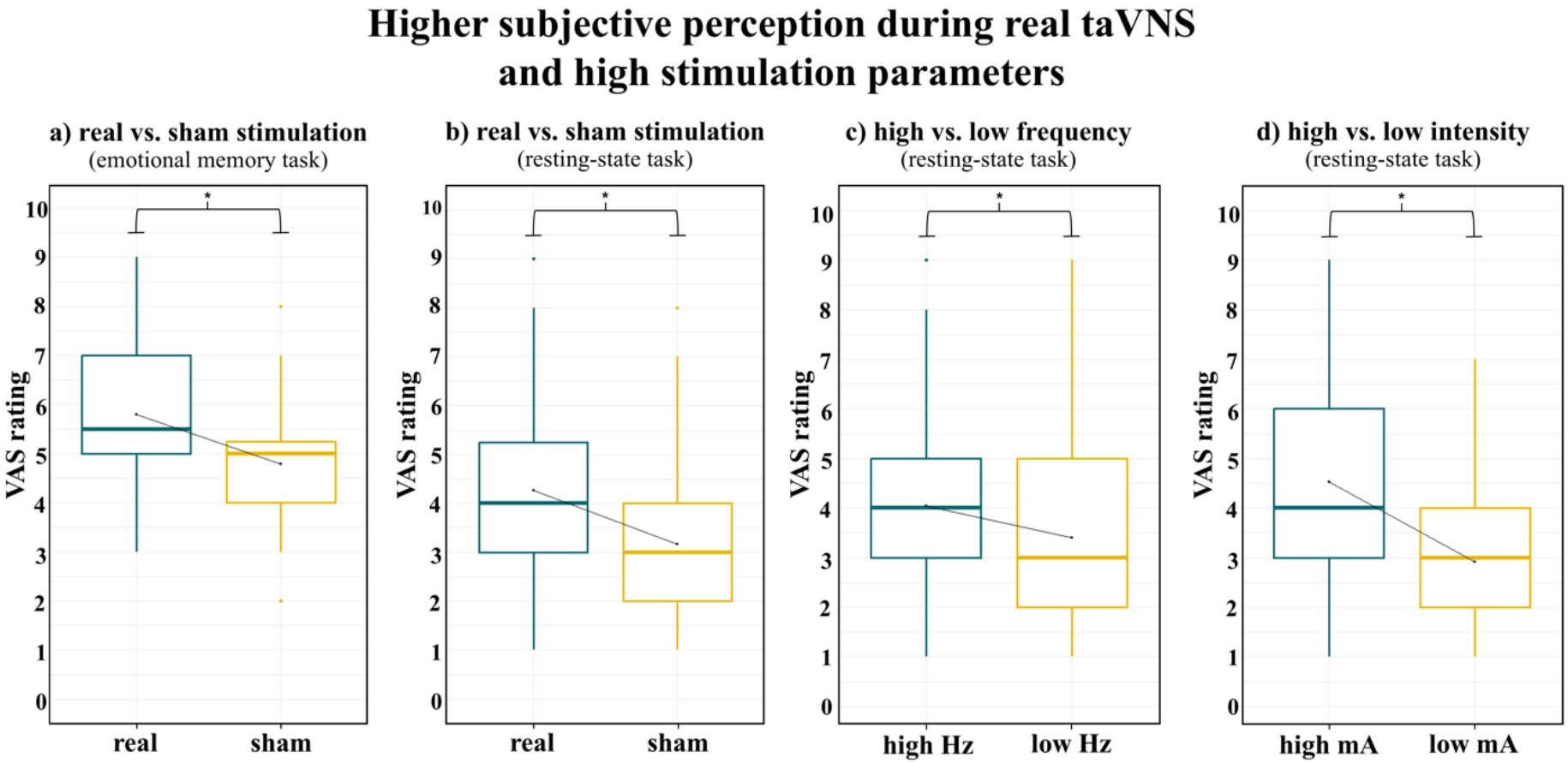

Figure 18. Subjective perception of sensations for the emotional memory and resting-state task. Subjective perception of sensations (VAS rating) for a) emotional memory task and b-d) resting-state task are shown here using boxplots (N = 24). VAS ratings were higher for real (dark turquoise) compared to sham (dark ochre) stimulation in a) emotional memory task ($F(1,20) = 4.31$, $p = 0.05$) and b) resting-state task ($F(1,20) = 17.85$, $p < 0.001$). VAS ratings were also higher for c) high (dark turquoise) compared to low (dark ochre) frequency ($F(1,20) = 19.57$, $p < 0.001$), and for d) high (dark turquoise) compared to low (dark ochre) intensity ($F(1,20) = 70.90$, $p < 0.001$) for the resting-state task. Significant differences are indicated by asterisks.

3.2.8 State of Health

The state of health was queried for each subject after stimulation to control for potential side effects. The following items were asked: (1) headache, (2) nausea, (3) tiredness, (4) dizziness, (5) tingling sensation at the previously stimulated area, (6) feeling of heat at the previously stimulated area, (7) reddening of the skin at the previously stimulated area, (8) skin irritation at the previously stimulated site, (9) impaired concentration, (10) itching at the previously stimulated area. Subjects indicated on a 4-point scale (0 - 3 (not at all – strong)) to what extent they perceived potential side effects.

The reported sensations during **emotional memory task** did not differ between real (M ± SD: 0.20 ± 0.04) and sham (M ± SD: 0.19 ± 0.04) stimulation ($F(1,9) = 0.06$, $p = 0.81$) (see Supplementary Table S26). The reported sensations during **resting-state task** also did not differ between real (M ± SD: 0.21 ± 0.13) and sham (M ± SD: 0.17 ± 0.10) stimulation ($F(1,9) = 3.30$, $p = 0.10$) and between low (M ± SD: 0.18 ± 0.12) and high (M ± SD: 0.18 ± 0.21) frequency ($F(1,9) = 0.13$, $p = 0.72$). There was a significant difference between low (M ± SD: 0.16 ± 0.11) and high (M ± SD: 0.20 ± 0.12) intensity ($F(1,9) = 5.34$, $p = 0.05$) (see Supplementary Table S27). Overall, it can be concluded that there were no side effects due to the stimulation and that the minimal impairments were rather due to the long measurement day and the monotonous resting-state task (e.g., item tiredness (3) and concentration (9)) than to the stimulation itself. Thus, the stimulation can be considered safe, which is in line with previous reports (Farmer et al., 2021).

3.2.9 Pupil Data Acquisition

Changes in pupil diameter were continuously recorded monocularly from the left eye at a sampling rate of 1000 Hz using a desked-mounted infrared EyeLink 1000 eyetracker (SR Research, www.sr-research.com) with a chin rest. The centroid measure of pupil change was chosen to provide more accurate estimates of changes in pupil dilation over time. The recording of pupillometry was controlled by custom-made scripts in MATLAB version 2020b (The Mathworks, www.mathworks.com) using Psychtoolbox 3 (www.psychtoolbox.org) and the Eyelink add-in toolbox for eyetracker control. For all subjects, the same constant ambient light continued to be applied throughout the whole experiment. At the start of the experiment, the camera was calibrated using 5-point calibration.

3.2.10 Pupil Data Analyses

Pupil data were pre-processed and analysed using custom-made scripts in MATLAB version 2020b (The MathWorks, www.mathworks.com). For the pre-processing of the pupil data from the emotional memory task, pupil data were segmented 200 ms before (Hämmerer et

al., 2017; Mathot, 2018; Mathôt & Vilotijević, 2022) and 9 s after stimulus onset. For the pre-processing of the pupil data from the resting-state task, pupil data were segmented 200 ms before and 17.5 s after trial onset. To remove artefacts and blinks from the pupil data, the data was further processed according to Mathot's recommendations (Mathôt, 2013). First, the signal was smoothed using a moving Hanning window (15 ms) average. A velocity profile was then created based on the smoothed signal to detect, using a threshold of mean-standard deviation, to identify the beginning (velocity is below a threshold) and the end of a blink (velocity is above a threshold) as well as closed eyes (velocity is zero). Since the blink period can be underestimated (Mathôt, 2013) 40 ms were additionally subtracted from the beginning time and added to the end time. All defined artefacts and blinks were set to NaN, summarized and then linearly interpolated. For the analyses, only trials whose raw signal was 70% free of blinks and artefacts, allowing 30% for interpolated data were included. Variations in trial numbers per condition were observed following artifact correction. Finally, all trials were also quality controlled by visual inspection. For the both tasks, more trials survived artifact correction in sham stimulation as compared to real stimulation (emotional memory task: sham (M ± SD: 70.92 ± 2.43) vs. real (M ± SD: 66.54 ± 7.52), $F(1,23) = 14.48$, $p < 0.001$; resting-state task: sham (M ± SD: 58.5 ± 1.07) vs. real (M ± SD: 53.8 ± 1.91), $F(1,23) = 15.89$, $p < 0.001$; Supplementary Methods 3.8). Pupil data were baseline-corrected (200 ms before stimulation onset) as well as individually z-scored to allow comparison of task conditions independent of individual differences in pupil dilation size (Hämmerer et al., 2017, 2019). For the **emotional memory task**, the z standardized, and baseline corrected data were analyzed in a time window between 0.8 - 3.8 s (see Fig. 21). For the **resting-state task**, the z standardised, and baseline corrected data were analysed separately in three-time windows (see Fig. 22): (I) the 3 s during on stimulation ("on stimulation"), (II) the first 3 s during off stimulation ("immediate response") and (III) the subsequent last 10 s during off stimulation ("delayed response"). The selection of the three different time windows was based on 3 s of short bursts of stimulation and an also equal length of an immediate response followed by a longer delayed response due to the trial duration.

3.2.11 Statistical Analyses

Statistical analyses were conducted in R version 4.2.2 (R Core Team, 2022, https://www.r-project.org) using the RStudio version (RStudio Team, 2022), and graphs were created using the package ggplot2 (Wickham et al., 2023). The mean value of the respective items for potential side effects (state of health) as well as the perception of sensations (VAS rating) for emotional memory task and for (I) "on stimulation" of the resting-state task were

analysed across all subjects by using aov_ez() function for repeated-measures ANOVA ({afex} package (Singmann et al., 2023) and lsmeans() function ({emmeans} package (Lenth, 2017/2023)). Additionally, Pearson correlation coefficients between VAS and pupil dilation (averaged per subject across trials), memory performance (hit-FA) and pupil dilation (averaged per subject across trials), and reaction times (RTs) and pupil dilation (averaged per subject across trials) were calculated by using color () function ({Hmisc} package (Harrell, 2013/2025) and corrected for outliers based on interquartile range (1.5 × IQR).

In general, changes in pupil dilation were analysed using a linear mixed-effects (LMM) model, implemented with the {lme4} package (Bates et al., 2015) to account for repeated measurements and individual-level variability, including "trials" as a fixed effect to model the overall time-on-task effect across all subjects, following a forward model selection approach, by using the {lme4} package (Bates et al., 2015). Model comparisons were conducted using the ANOVA () function (lme4 package (Bates et al., 2015) with likelihood-ratio chi-squared tests, and models were fit using maximum likelihood (ML) estimation to ensure valid comparisons between models with different fixed effects. AIC (Akaike Information Criterion) values of the best model for statistical modelling and model selection were reported. In general, models with lower AIC values are indicative of a superior trade-off between data explanation and prevention of overfitting, in comparison to alternative assessed models (Vrieze, 2012). To assess the relevant assumptions of LMM, the check_model() function (performance package (Lüdecke et al., 2021)) was used to investigate linearity, homogeneity of variance, influential observations, collinearity, normality of residuals, and random effects (emotional memory task: https://osf.io/xuwsm/; resting-state task: https://osf.io/va64p/). The significance of predictors on the goodness of fit of the model was assessed using the ANOVA () function (car package (Fox et al., 2023)), which computes type-II analysis-of-variance tables for mixed-effects models and provides likelihood-ratio Chi-Square statistics. The significance of the deviance of individual groups from the intercept was assessed using the summary() function (lmerTest package (Kuznetsova et al., 2017)), which calculates the model's coefficients, standard errors, t-values, and p-values associated with each coefficient. Moreover, emmip() and extends () functions (emmeans package (Lenth, 2017/2023) were utilized to analyse interaction effects, such as for emotional memory task interactions of VAS and stimulation conditions and for resting-state task VAS changes along its range with respect to categorical variables (stimulation, frequency, intensity). The function emmip() generates an interaction plot to see how the categorical variable affects the variable over its entire range. The function extends () calculates estimated marginal means for different levels of the categorical variable.

3.2.11.1 Statistical Analyses of the Emotional Memory Task

For the **behavioral analysis**, RTs, hit rate (old images) (hits / (hits + misses)), false alarm (FA) rate (new images) (FA / (FA + correct rejections)), hit-FA rate were calculated for early and delayed recognition task, while RTs were also assessed for the encoding task, by using aov_ez() function for repeated-measures ANOVA ({afex} package (Singmann et al., 2023) and emmeans() function ({emmeans} package (Lenth, 2017/2023)). RTs ± 2 standard deviations from the mean were excluded from RT analyses. RT analyses during the encoding task were based on 4 experimental levels of stimulation (*(real on stimulation (1) vs. real off stimulation (2) vs. sham on stimulation (3) vs. sham off stimulation (4))*. Detailed behavioral and RT analyses for the recognition task were based on 3 levels of stimulation (real (1) vs. sham (2) vs. off (0) stimulation), since there was no significant difference between real off stimulation and sham off stimulation (Supplementary Results 4.1). Specifically, the analyses included two (encoding task) or three (recognition task) within-subject factors: stimulation (with levels indicating real vs. sham vs. off conditions), valence (representing negative and neutral valence), and timepoint (indicating early vs. delayed recognition).

Changes in pupil dilation were analysed based on a LMM model, following a forward model selection approach. The forward model selection approach included dummy coded variables identifying real and sham ***"stimulation"*** *[real (1) vs. sham (2) vs. off stimulation (0)]* and the differences in ***"valence"*** *[negative (1) vs. neutral (0)]* (Supplementary Table S28), after ruling out any significant differences in the off stimulation condition in an initial analysis across real and sham stimulation *[real on stimulation (1) vs. real off stimulation (2) vs. sham on stimulation (3) vs. sham off stimulation (4)]* (Supplementary Methods 3.7). Furthermore, a random intercept "ID" was included to account for inter-individual variations in the mean pupil change, and the variable "trials" was included to capture the impact of "time-on-task" on pupil dilations. Model comparisons were conducted (*anova(m0, m1, m2, m3, m4*) and revealed that the best model was **model m_3** (AIC = 10847 (χ^2 = 5.71, p = 0.02)):

- **StimValence-LMM**

  pupil dilation ~ trials + stimulation + valence + (1|ID)

Second, based on **model m_3** the following factors were added stepwise: ***"VAS"*** ratings as a measure of subjective perception of sensations due to stimulation, ***"sensitivity"*** *[sensitive (1) vs. not sensitive (0)]* differentiating whether subjects received 3 and 5 mA, whether subjects received real stimulation first ***"real_first"*** *[counterbalanced: real (1) before sham (0) stimulation]*, ***"gender"*** *[female (1) vs. male (0)* and ***"sporty"*** *[sporty (1) vs. non-sport (0)]*. Subsequently model comparisons were conducted again based on all models (*anova(m0, m1,*

m2, m3, m3_1, m3_2, m3_3, m3_4, m3_5, m4_6)) and the best fitting model from the second step for was **model m3_3** (AIC = 10839 (χ^2 = 8.01, p = 0.005), see Supplementary Table S28-S29):

- **StimValence-VAS-LMM**

  pupil dilation ~ trials + stimulation + valence + VAS + sensitivity + real_first (1|ID)

Consequently, statistical analyses regarding changes in pupil dilation are based on the **"StimValence-VAS-LMM"** model. Distinct models based on the average pupil dilation per session are also reported using the same criteria, but without the covariate "trial number" (Supplementary Table S34).

Additionally, two theory-driven exploratory analyses were conducted to investigate to what extent a) stimulation had an additional benefit to the effect of stimulus valence on pupil dilation and b) how sensitivity affects the subjective perception of stimulation on pupil dilation. Based on the best model for the pupil analysis, interactions between a) stimulation and valence, and b) valence and sensitivity were incorporated:

- a) Stim*Valence-VAS-LMM

  pupil dilation ~ trials + stimulation × valence + VAS + sensitivity + real_first + (1|ID)
- b) Sensitivity*VAS-LMM

  pupil dilation ~ trials + stimulation + valence + VAS × sensitivity + real_first + (1|ID)

Finally, to explore potential effects of subjective sensory perception caused by stimulation on memory performance a comparable model for the behavioral data based on the average memory performance (averaged per subject across trials) was performed (Supplementary Results 4.8).

3.2.11.2 Statistical Analyses of the Resting-State Task

Changes in pupil dilation were analysed based on a LMM model, following a forward model selection approach. Thereby, a distinct model was fitted for each time window of analysis, that is **(I)** the 3 s during "**on stimulation"** time window, **(II)** the first 3 s during off stimulation "**immediate response**" time window and **(III)** the subsequent last 10 s during off stimulation "**delayed response**" time window using the dummy coded variables (Supplementary Table S30-S33). In addition, to incorporating a random intercept "ID", which accounts for interindividual variations in mean pupil change, and the inclusion of the trial number variable "trials" to capture the impact of "time-on-task" on pupil dilations, the forward model selection approach initially considered variables related to the distinction between real and sham ***"stimulation"*** *[real (1) vs. sham (0)]*, as well as differences in ***"frequency"*** *[high (1) vs. low (0)]* and ***"intensity"*** *[high (1) vs. low (0)]* (Supplementary Table S30). It was furthermore investigated whether incorporating interactions between stimulation, frequency and intensity further improved the model (Supplementary Table S30-33*; anova(m0, m1, m2, m3, m4, m5, m6, m7)*). This did not lead to a significant improvement in the model fit for the time windows (I-III). Hence, it was determined that the best model from the first step (see results) for each distinct model at every given time (**I-III**) point was **model m_4** (StimIntFreq-LMM) with the following lowest AIC values in the model comparison for (I) AIC = 29404 (χ^2 = 102.95, $p < 0.001$), (II) AIC = 37688 (χ^2 = 76.54, $p < 0.001$) and (III) AIC = 39305 (χ^2 = 8.27, $p = 0.004$):

- **StimIntFreq-LMM**

  pupil dilation ~ trials + stimulation + intensity + frequency + (1|ID)*

  **pupil dilation during (I) or (II) or (III)*

Second, based on **model m_4** the following factors were added stepwise: ***"VAS"*** ratings as a measure of subjective perception of sensations due to stimulation, ***"sensitivity"*** *[sensitive (1) vs. not sensitive (0)]* differentiating whether subjects received 3 and 5 mA or 1.5 and 3 mA (Supplementary Figure S11)*,* whether subjects received real stimulation first ***"real_first"*** *[counterbalanced: real (1) before sham (0) stimulation],* in which order the four stimulation combinations were applied ***"position"*** *[randomised: low mA & low Hz (1), high mA & low Hz (2), low mA & high Hz (3), high mA & high Hz (4)],* ***"gender"*** *[female (1) vs. male (0)* and ***"sporty"*** *[sporty (1) vs. non-sport (0)].* The renewed model comparison (*anova(m0, m1, m2, m3, m4, m4_1, m4_2, m4_3, m4_4, m4_5, m4_6*) now showed that the model with VAS (**model m_4_1**: StimIntFreq-VAS-LMM) was the best model at each time window (I-III) with the

following lowest AIC values in the model comparison for (I) AIC = 29367 (χ^2 = 38.76, p < 0.001), (II) AIC = 37659 (χ^2 = 30.81, p < 0.001):

- **StimIntFreq-VAS-LMM**

  pupil dilation ~ trials + stimulation + intensity + frequency + VAS + (1|ID)*

  pupil dilation during **(I) or **(II)** or **(III)***

However, for (III) **"delayed response"** the StimIntFreq-LMM was not significant (AIC = 39304 (χ^2 = 3.32, p = 0.07)), but StimIntFreq-LMM was again the best model (AIC = 39305 (χ^2 = 8.27, p = 0.004)) (Supplementary Table S33).

Additionally, random effects for stimulation, frequency and intensity were added stepwise to the model "StimIntFreq-VAS-LMM", while only the model with intensity as a random effect led to evaluable results (see Supplementary Results 4.11), possibly due to intensity variations yielding strongest stimulation effects. Based on the exploratory analysis for the emotional memory task, which examined how sensitivity to the subjective perception of stimulation affects pupil dilation, interactions between VAS and sensitivity were also exploratively included in the resting-state task based on the best model for pupil analysis (see Supplementary Results 4.12). However, there was no significant interaction between VAS rating and sensitivity (χ^2 = 0.20, p = 0.65), likely due to the strong stimulation effects of intensity variations (see Supplementary Results 4.12).

Furthermore, for the resting-state task a theory-driven exploratory analyses (see Supplementary Results 4.12) were conducted to better explain the potential influence of sensory perception (VAS) due to stimulation on pupil dilation controlled for sensitivity.

- StimIntFreq*VAS-LMM

  pupil dilation ~ trials + stimulation × VAS + intensity × VAS + frequency × VAS + sensitivity + (1|ID)*

  pupil dilation during **(I) or **(II)** or **(III)***

Distinct models based on the average pupil dilation per session are also reported for each time window (**I-III**) using the same criteria, but without the covariate "trial number" (Supplementary Table S35-36).

3.3 Results

The results of this chapter facilitate the investigation of the potential effects of short bursts of event-related taVNS on pupil dilation and memory performance in the emotional memory task. It also explores the effects of short bursts of event-related taVNS at different intensities and frequencies on pupil dilation during the resting-state task. Additionally, the influence of the subjective perception of sensations of stimulation is considered.

3.3.1 Behavioral Results – TaVNS during Encoding Task

During the cover task (indoor-outdoor classification) of the emotional memory task, subjects showed high accuracy ratings on indoor (M ± SD: 0.96 ± 0.18) and outdoor (M ± SD: 0.98 ± 0.14) scenes, indicating that all subjects followed the instructions of the cover task relevant for incidental encoding. With regard to main effects of response times during the **encoding task**, subjects did not show faster reactions times (RTs) when classifying whether an image was "inside or outside" for negative (M ± SD: 0.79 ± 0.47) as compared to neutral (M ± SD: 0.79 ± 0.50) events, $F(1,23) = 0.12$, $p = 0.73$. RTs also did not differ between real (M ± SD: 0.76 ± 0.47) as compared to sham (M ± SD: 0.82 ± 0.49) stimulation sessions (collapsed across on or off stimulation trials within session), $F(1,23) = 2.29$, $p = 0.14$ or during on (M ± SD: 0.81 ± 0.48) as compared to off (M ± SD: 0.77 ± 0.49) stimulation, $F(1,23) = 3.02$, $p = 0.1$. There was no interaction between “real vs. sham” stimulation and valence ($F(1,23) = 2.05$, $p = 0.17$), “real vs. sham” stimulation and “on vs. off” stimulation ($F(1,23) = 0.0003$, $p = 0.1$), valence and “on vs. off” stimulation ($F(1,23) = 0.21$, $p = 0.65$) for RTs during encoding task.

3.3.2 Better Memory Performance (Hit-FA) for Negative Events: more pronounced during Real Stimulation

Consistent with studies showing that **negative events** improve memory performance (Hämmerer et al., 2017, 2018) subjects showed a higher recognition accuracy (hit-FA rate) for negative events (M ± SD: 0.63 ± 0.26) compared to neutral events (M ± SD: 0.55 ± 0.25) (Fig. 19c) in the emotional memory task, which underpins the impact of negative emotionality on memory performance, $F(1,23) = 18.68$, $p < 0.001$. Likewise, as expected, memory performance was decreased on the delayed (M ± SD: 0.53 ± 0.23) as compared to the early (M ± SD: 0.65 ± 0.26) recognition task, $F(1,23) = 54.79$, $p < 0.001$ (Fig. 19e). There was no interaction between timepoint and valence, $F(1,23) = 0.27$, $p = 0.61$ (Supplementary Figure S15).

Importantly, **stimulation** per se, but not the stimulation condition (real vs. sham stimulation), had an influence on memory performance as indicated by hit-FA, $F(2,46) = 509$, $p < 0.001$ (Fig. 19d). Subjects, in particular, showed better memory performance during real (M ± SD: 0.73 ± 0.15) as compared to off (M ± SD: 0.31 ± 0.10) stimulation (off-real: $\beta = -0.42$

(SE = 0.01; t-value = -38.37, p < 0.001)) and during sham (M ± SD: 0.74 ± 0.13) as compared to off (M±SD: 0.31±0.10) stimulation (off-sham: β = -0.42 (SE = 0.02; t-value = -26.30, p < 0.001)); however memory performance was not better during real as compared to sham stimulation (real-sham: β = -0.01 (SE = 0.02; t-value = -0.54, p =1)).

Interestingly, there was a significant ordinal interaction between stimulation and valence, F(2,46) = 6.46, p = 0.003 (Fig. 19a). Specifically, the effect that negative events were better remembered than neutral events was more pronounced during real stimulation than during sham stimulation (emo-neu real-sham: β = 0.07 (SE = 0.03; t-value = 2.64, p = 0.01)) and during off stimulation (emo-neu off-real: β = -0.08 (SE = 0.02; t-value = -3.89, p = 0.007)). There was no interaction between valence and off vs. sham stimulation (emo-neu off-sham: β = -0.02 (SE = 0.03; t-value = -0.59, p = 0.56)). Additionally, there was a significant ordinal interaction between stimulation and timepoint, F(2,46) = 5.54, p = 0.007 (Fig. 19b), indicating that during off stimulation memory performance during early and delayed recognition was worse than during real stimulation (delay-early off-real: β = 0.1 (SE = 0.03; t-value = 3.77, p = 0.001)) and sham stimulation (delay-early off-sham: β = 0.07 (SE = 0.03; t-value = 2.25, p = 0.03)). However, there was no significant interaction between timepoint and real compared to sham stimulation (delay-early real-sham: β = -0.02 (SE = 0.03; t-value = -0.70, p = 0.49)). This suggests that stimulation per se had stronger effects on memory performance than off stimulation. An additional exploratory analysis of memory performance was conducted to investigate individual factors associated with taVNS, such as subjects' sensitivity and gender (Supplementary Results 4.9), which revealed no significant effects. Additionally, there were no correlations between subjective perception of sensation due to stimulation and memory performance (Supplementary Results 4.10). The effects for correct recognition (hit) and false alarms (FA) are reported in Supplementary Results 4.3 and 4.4. The effects for hits were generally consistent with the effects for hit-FAs, suggesting that the memory effects were primarily due to encoding rather than response biases.

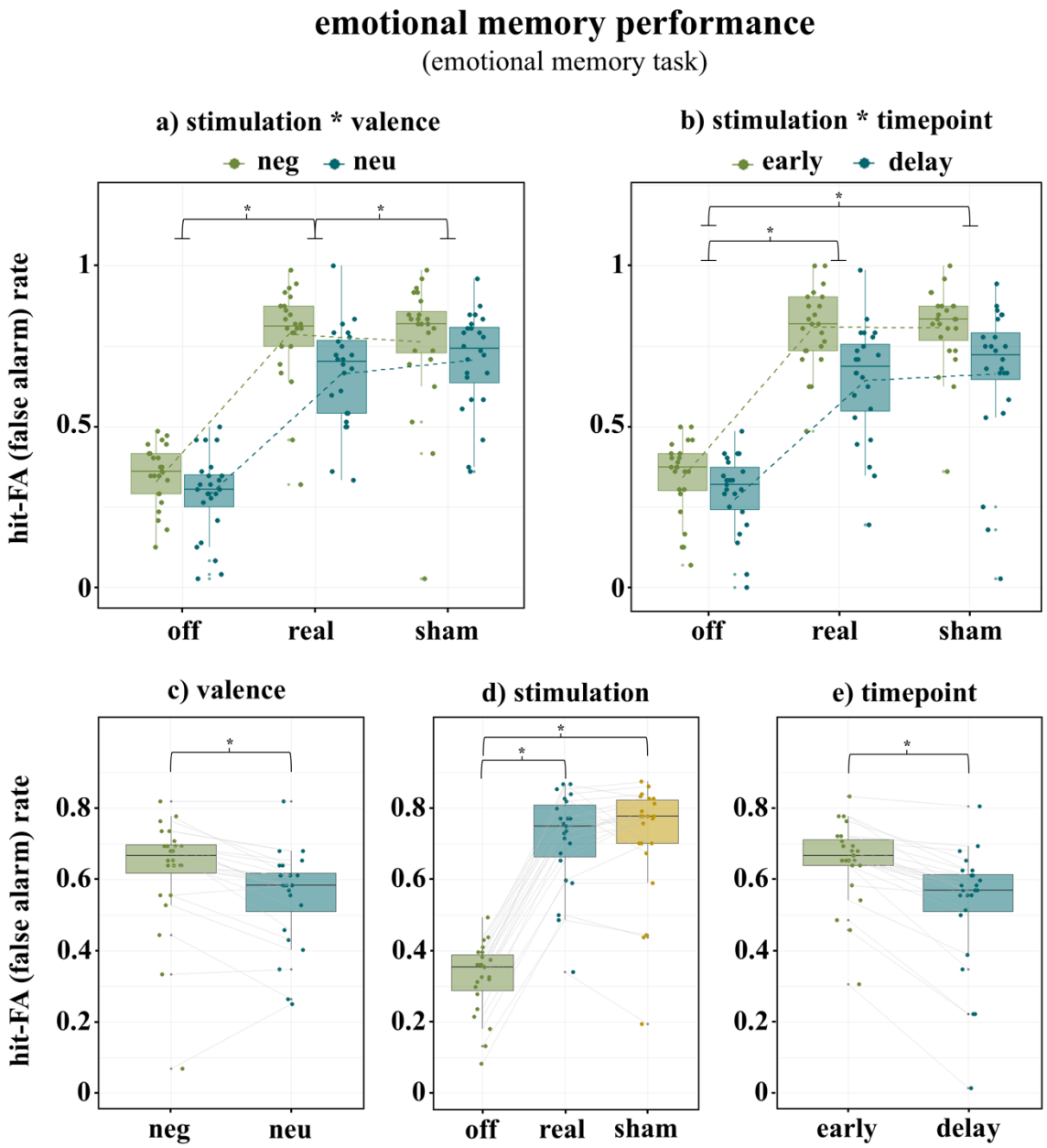

Figure 19. Memory performance (hit-FA (false alarms)) of the emotional memory task. Memory performance (hit-FA (false alarms)) of the emotional memory task is shown here aggregated at the subject level (N=24) using boxplots. Panel a) shows a significant interaction between stimulation (off, real, and sham) and valence (negative (green) and neutral (turquoise)), $F(2,46) = 6.46$, $p = 0.003$, indicating that negative events specifically benefitted from real stimulation. Panel b) shows a significant interaction between stimulation (off, real, and sham) and timepoint (early (green) and delayed (turquoise)), $F(2,46) = 5.54$, $p = 0.007$. Panel c) depicts valence effects, showing better memory performance for negative (green) compared to neutral (turquoise) events, $F(1,23) = 18.68$, $p < 0.001$. Panel d) presents the effects of stimulation, indicating significantly improved memory performance for real stimulation compared to off stimulation, and sham stimulation compared to off stimulation, $F(2,46) = 509$, $p < 0.001$. Panel e) demonstrates better memory performance during early (green) compared to delayed (turquoise) recognition tasks, $F(1,23) = 54.79$, $p < 0.001$. Each point represents an individual subject, and light grey lines connect the conditions for each subject. Significant differences or interaction effects are indicated by asterisks.

3.3.3 Faster RTs for Correct Responses during Short Bursts of Electrical Stimulation

In general, subjects showed longer RTs for new (M ± SD: 1.03 ± 0.34) compared to old (M ± SD: 0.96 ± 0.31) images (averaged across correct and incorrect responses), F (1,23) = 27.85, p < 0.001), which is in line with previous RTs during emotional memory task (Hämmerer et al., 2017). Additionally, subjects showed no difference in RTs between negative (M ± SD: 0.99 ± 0.33) and neutral (M ± SD: 0.99 ± 0.32) events, F (1,23) = 0.20, p = 0.65, and no RTs differences between early (M ± SD: 1.02 ± 0.34) and delayed (M ± SD: 0.96 ± 0.31) recognition, F (1,23) = 3.14, p = 0.09. However, there was a significant interaction between "old vs. new" images and valence, F (1,23) = 6.40, p = 0.02, indicating that RTs for negative events were generally longer for new images compared to old images (Supplementary Figure S18). There were no significant interactions between "old vs. new" images and timepoint, F (1,23) = 0.65, p = 0.43 and between valence and timepoint, F (1,23) = 2.21, p = 0.15

Hit RTs (averaged speed of correct responses to target image) revealed faster RTs during real (M ± SD: 0.87 ± 0.12) as compared to off (M ± SD: 0.93 ± 0.16) stimulation (off-real: β = 0.05 (SE = 0.01; t-value = 3.80, p = 0.002)) and during sham (M ± SD: 0.87 ± 0.11) as compared to off (M ± SD: 0.92 ± 0.16) stimulation (off-sham: β = 0.05 (SE = 0.01; t-value = 3.81, p = 0.002)); but RTs were not faster during real as compared to sham stimulation (real-sham: β = -0.003 (SE = 0.02; t-value = -0.15, p = 1)), F(2,46) = 6.95, p = 0.002 (Fig. 20b). Hit RTs were not different between negative (M ± SD: 0.89 ± 0.13) and neutral (M ± SD: 0.89 ± 0.13) events, F (1,23) = 0.01, p = 0.92 (Fig. 20a). Furthermore, there was a tendency for hit RTs during early recognition (M ± SD: 0.92 ± 0.1) to be slower compared to delayed recognition (M ± SD: 0.86 ± 0.12), F (1,23) = 3.54, p = 0.07 (Fig. 20c). There were no significant hit RTs difference neither between stimulation and valence, F (2,46) = 0.008, p = 0.99), stimulation and timepoint (F(2,46) = 0.49, p = 0.61), nor valence and timepoint, F (1,23) = 0.05, p = 0.82 (Supplementary Figure S19). For results on certainty ratings for hit RTs see Supplementary Results 4.7.

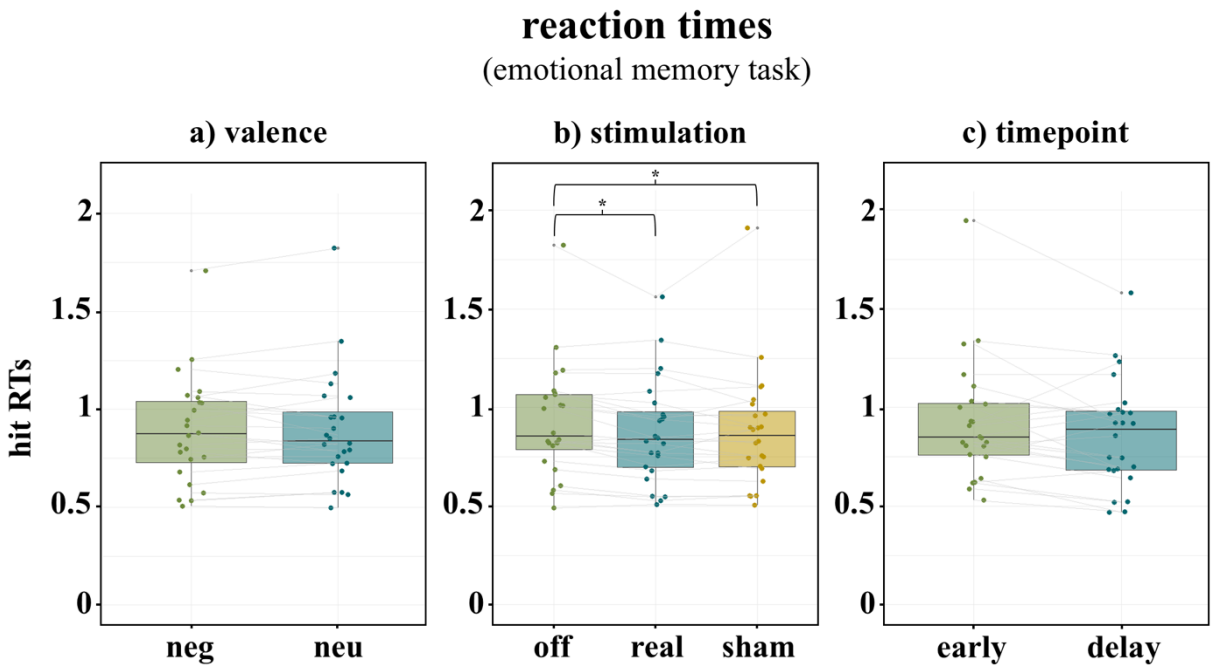

Figure 20. Reaction times during emotional memory task. Averaged speed of correct responses to target image (hit RTs) during emotional memory task is shown here aggregated at the subject level (N = 24) using boxplots. Panel a) depicts valence effects (negative (green) > neutral (turquoise)), $F(1,23) = 0.01$, $p = 0.92$, indicating no significant effects on RTs. Panel b) presents the effects of stimulation, indicating significant faster RTs for real stimulation compared to off stimulation and sham stimulation compared to off stimulation, $F(2,46) = 6.95$, $p = 0.002$. Panel **c)** shows timepoint effects (early (green) > delay (turquoise)), $F(1,23) = 3.54$, $p = 0.07$ indicating no significant effects on RTs. Each point represents an individual subject, and light grey lines connect the conditions for each subject. Significant differences are indicated by asterisks.

3.3.4 Pupillometry Results

3.3.4.1 Increased Pupil Dilation due to Short Bursts of Electrical Stimulation in the Emotional Memory Task

In accordance with increased pupil dilations observed during **emotionally salient events** (Hämmerer et al., 2018; Joshi et al., 2016), pupil dilation was increased during the presentation of negative (M ± SE: 0.44 ± 0.11) as compared to neutral (M ± SE: 0.34 ± 0.11) events ($\chi^2 = 5.65$, $p = 0.02$) (Fig. 21).

Regarding the influence of the **stimulation conditions** ($\chi^2 = 44.47$, $p < 0.001$), pupil dilation was increased during real (M ± SE: 0.49 ± 0.11) as compared to off (M ± SE: 0.19 ± 0.11) stimulation (off-real: $\beta = -0.31$ (SE = 0.05; t-value = -5.68, $p < 0.001$)) and during sham (M ± SE: 0.49 ± 0.11) as compared to off (M ± SE: 0.19 ± 0.11) stimulation (off-sham: $\beta = -0.31$ (SE = 0.05; t-value = -5.65, $p < 0.001$)); however pupil dilation was not increased during real as compared to sham stimulation (real-sham: $\beta = 0.006$ (SE = 0.06; t-value = 0.12, $p = 1$)) (Fig. 21; Supplementary Table S34). Furthermore, some of the variance in pupil dilation was significantly explained by perception of stimulation (**VAS rating**) ($\chi^2 = 4.45$, $p = 0.03$), although this did not imply that stimulation effects could no longer be explained in the emotional memory task, as was the case in the resting-state task (see section 3.3.4.2). There was no significant sensitivity difference in pupil dilation between subjects receiving 3 mA (M ± SE: 0.37 ± 0.18) compared to subjects receiving 5 mA (M ± SE: 0.41 ± 0.12), $\chi^2 = 0.03$, $p = 0.87$. Additionally, although the **order of stimulation** was counterbalanced in the experiment, subjects who received real (M ± SE: 0.68 ± 0.15) stimulation before sham (M ± SE: 0.10 ± 0.14) stimulation showed generally larger pupil dilations ($\chi^2 = 8.33$, $p = 0.004$).

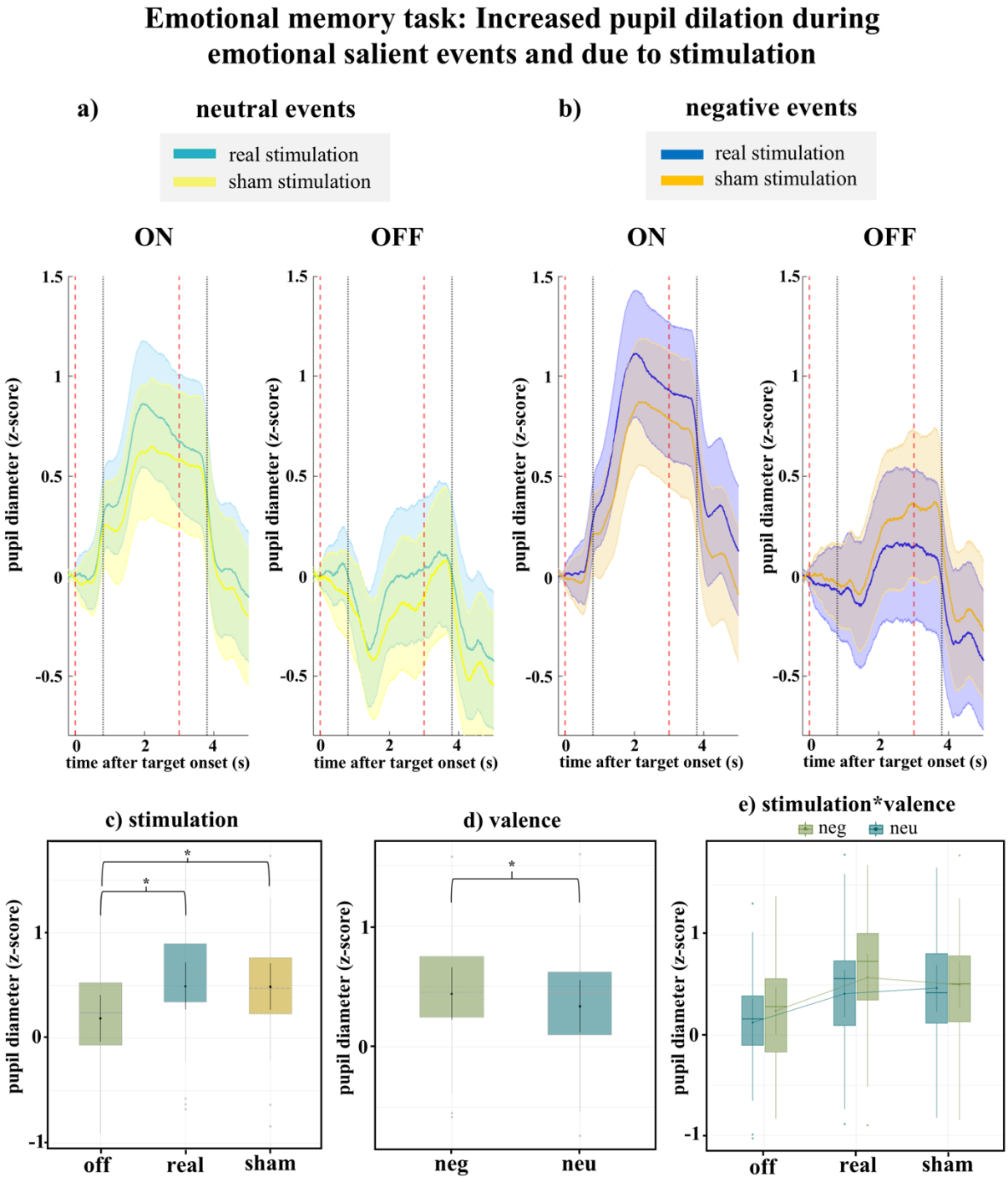

Figure 21. Changes in pupil dilation during the emotional memory task. Pupil diameters (z-scores) for the emotional memory task are shown for a) neutral events (left) under real stimulation (light blue) and sham stimulation (yellow), and b) negative events (right) under real stimulation (dark blue) and sham stimulation (orange), during both on (3 s) and off (15 s) periods of stimulation. The shaded areas represent the standard error across subjects (N = 24). Dashed red vertical lines indicate the time window when stimulation was applied, while dashed black vertical lines mark the analysis window between 0.8 and 3.8 seconds. In panel c) stimulation, boxplots show significantly increased pupil dilation for both real stimulation and sham compared to off stimulation ($\chi^2 = 44.47$, $p < 0.001$). In panel d) valence, boxplots significantly increased pupil dilation for negative compared to neutral events ($\chi^2 = 5.65$, $p = 0.02$). Panel e) shows the boxplot for the interaction between stimulation and valence, which was not significant ($\chi^2 = 1.44$, $p = 0.49$; model: pupil dilation ~ trials + stimulation × valence + VAS + sensitivity + real_first + (1|ID)). Significant differences or interaction effects are indicated by asterisks.

3.3.4.2 Increased Pupil Dilation due to Short Bursts of Electrical Stimulation and the Impact of Subjective Perception of Sensations in the Resting-State Task

In accordance with increased pupil dilation during short bursts of i/taVNS stimulation (D'Agostini et al., 2023; Mridha et al., 2021; Sharon et al., 2021), the **StimIntFreq-LMM** model suggested that pupil dilation was increased during real (M ± SE: 0.18 ± 0.03) as compared to sham (M ± SE: 0.1 ± 0.03) stimulation during **(I)** "on stimulation" ($\chi^2 = 18.98$, $p < 0.001$). Additionally, during the (**II**) "immediate response", immediately after stimulation was turned off, pupil dilation was still increased during real (M ± SE: 0.15 ± 0.04) as compared to sham (M ± SE: 0.04 ± 0.04) stimulation ($\chi^2 = 15.99$, $p < 0.001$), while there was no significant difference between real (M ± SE: - 0.04 ± 0.02) and sham (M ± SE: - 0.06 ± 0.02) stimulation ($\chi^2 = 0.61$, $p = 0.43$) for the (**III**) "delayed response", 3 s after stimulation was turned off (Fig. 22; Supplementary Table S35). However, the **StimIntFreq-VAS-LMM** model revealed that VAS rating explained significant proportion of pupil variance during **(I)** "on stimulation" ($\chi^2 = 38.79$, $p < 0.001$) and **(II)** "immediate response" ($\chi^2 = 30.82$, $p < 0.001$) ((III) "delayed response" ($\chi^2 = 3.37$, $p = 0.07$)). Therefore, the difference between real and sham stimulation was no longer statistically explainable (Supplementary Table S36 & Figure S21) during **(I)** "on stimulation" ($\chi^2 = 2.69$, $p = 0.1$) and the **(II)** "immediate response" ($\chi^2 = 2.42$, $p = 0.12$), after accounting for condition differences in VAS rating. This suggests that effects of real vs. sham stimulation and effects of different subjective perception of sensations of real vs. sham stimulation on pupil dilations cannot be distinguished statistically with the stimulation parameters employed here.

3.3.4.3 Did Higher Stimulation Parameters during the Resting-State Task lead to a more Dilated Pupil?

In line with iVNS approaches in animals showing increased pupil dilation during higher intensity stimulation (Collins et al., 2021; Hulsey et al., 2017), **StimIntFreq-LMM** suggested that pupil dilation was increased during higher (M ± SE: 0.23 ± 0.03) as compared to lower (M ± SE: 0.04 ± 0.03) intensity during (**I**) "on stimulation" ($\chi^2 = 103.40$, $p < 0.001$). During the **(II)** "immediate response", pupil dilation was still increased during higher (M ± SE: 0.21 ± 0.04) as compared to lower (M ± SE: - 0.03 ± 0.04) intensity ($\chi^2 = 76.79$, $p < 0.001$), and there was still a significant difference between higher (M ± SE: -0.01 ± 0.02) and lower (M ± SE: - 0.09 ± 0.02) intensity ($\chi^2 = 8.26$, $p = 0.004$) for the (**III**) "delayed response" (Fig. 22; Supplementary Table S35). When additionally controlling for VAS rating differences across stimulation conditions in the **StimIntFreq-VAS-LMM** model, pupil dilation was still increased during higher (M ± SE: (I) 0.20 ± 0.03; (II) 0.17 ± 0.04) as compared to lower (M ± SE: (I) 0.08 ± 0.03; (II) 0.02 ± 0.04) intensity during (**I**) "on stimulation" ($\chi^2 = 28.53$, $p < 0.001$), and during

the **(II)** “immediate response” (χ^2 = 20.10, p < 0.001), but not during **(III)** “delayed response” (χ^2 = 2.76, p = 0.1) (Supplementary Table S36). This suggests that stimulation intensity, especially higher intensity levels, and subjective perception of stimulation intensity may contribute to pupil dilation to varying degrees. Regarding frequency, the **StimIntFreq-LMM** suggested that pupil dilation was increased during higher (M ± SE: 0.17 ± 0.03) as compared to lower (M ± SE: 0.11 ± 0.03) frequency during (**I**) “on stimulation” (χ^2 = 10.88, p = 0.001). During the **(II)** “immediate response”, pupil dilation was statistically not increased during higher (M ± SE: 0.11 ± 0.04) as compared to lower (M ± SE: 0.07 ± 0.04) frequency (χ^2 = 2.92, p = 0.09), and there was also no significant difference between higher (M ± SE: -0.03 ± 0.02) and lower (M ± SE: -0.07 ± 0.02) frequency (χ^2 = 1.53, p = 0.22) anymore for the (**III**) “delayed response” (Fig. 22; Supplementary Table S35). These results would be in line with iVNS approaches in animals showing increased pupil dilation during higher frequency stimulation over a shorter period of time (Hulsey et al., 2017). However, after controlling for subjective perception of sensations in the **StimIntFreq-VAS-LMM** model, there was no effect of different stimulation frequencies observable neither for (**I**) “on stimulation” (χ^2 = 2.85, p = 0.1), nor for **(II)** “immediate response” (χ^2 = 0.09, p = 0.76) and **(III) “**delayed response” (χ^2 = 0.68, p = 0.41) (Supplementary Table S36).

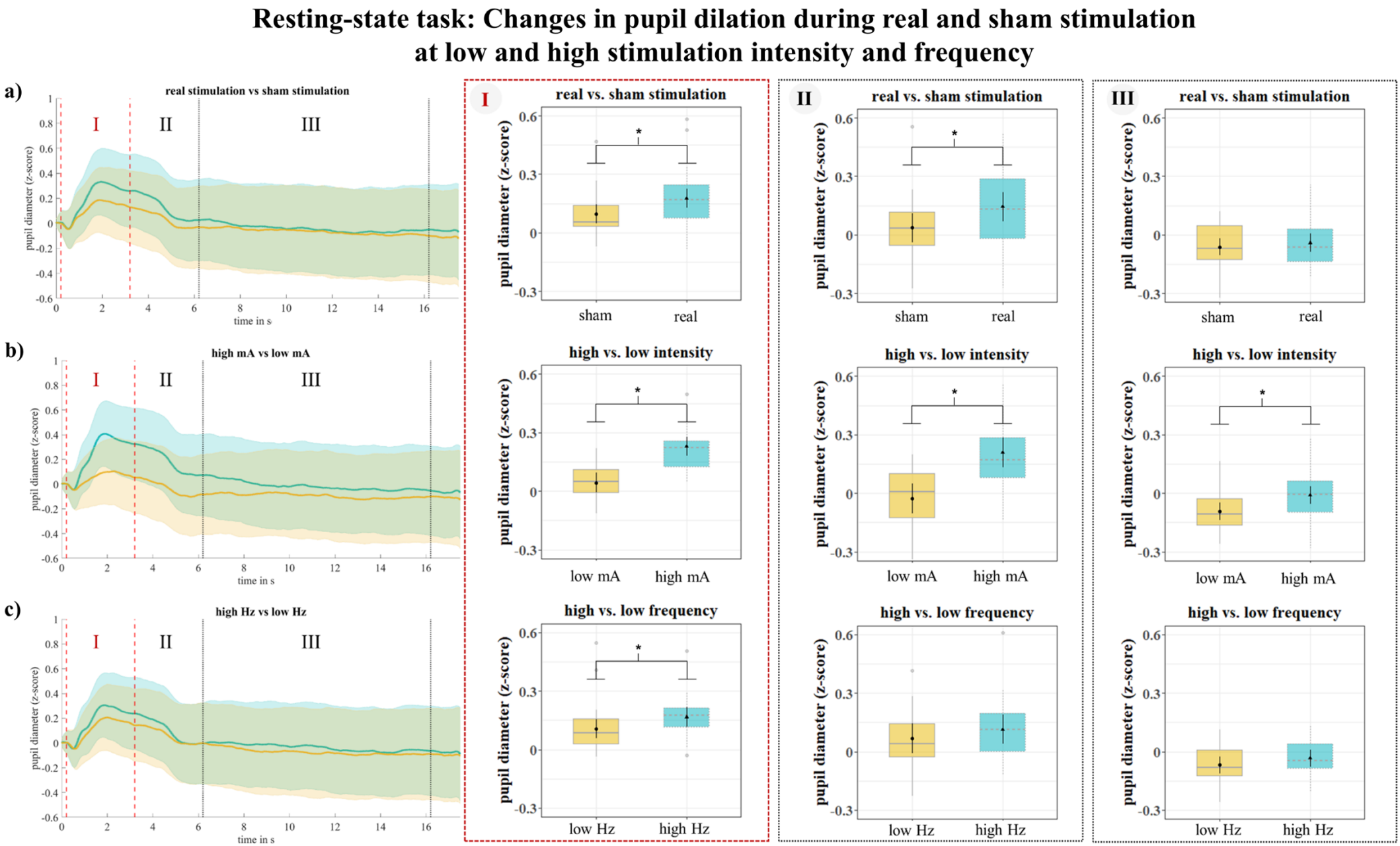

Figure 22. Changes in pupil dilation during the resting-state task. Pupil diameters (z-scores) during resting-state task for **a)** real (turquoise) and sham (ochre) stimulation, **b)** high (turquoise) and low (ochre) intensity and **c)** high (turquoise) and low (ochre) frequency. Shadowed lines represent the standard error across subjects (left panel). The dashed vertical red lines indicate the time window of (I) **"on stimulation"**, the (II) **"immediate response"** following to the first dashed vertical black line and the subsequent (III) **"delayed response"** to the second dashed vertical black line. The boxplots for the individual time windows are based on the ***StimIntFreq-LMM***, the asterisks indicate significant differences between conditions. The reader is encouraged to look at Supplementary Figure S21 to see the influence of VAS rating on stimulation and stimulation parameters in the **StimIntFreq-VAS-LMM** model.

3.3.4.4 Relationship between Subjective Perception of Sensations (VAS) of Stimulation and Pupil Dilation across Subjects

Since VAS rating was not kept constant due to systematically testing of different stimulation parameters during the resting-state task and given that LMM approach suggested including VAS rating as an explanatory variable for pupil dilation, it was necessary to evaluate the extent to which the subjectively experienced sensory effects are statistically associated with the stimulation parameters and changes in pupil dilation. VAS ratings after each stimulation session and corresponding pupil dilation (averaged per subject across all trials within a stimulation condition) were correlated to investigate further the potential effects of subjective perception of sensation on pupil dilation across subjects.

For the emotional memory task, there were no correlations between VAS rating and pupil dilation neither for real stimulation ($r = 0.21$, $p = 0.36$) nor for sham stimulation ($r = -0.1$, $0 = 0.70$) (Supplementary Figure S13). However, for the resting-state task (Supplementary Figure S14 & Table S25) correlations between VAS rating and pupil dilation considering outlier correction were found for **a)** real stimulation: low intensity & low frequency ($r = 0.43$, $p = 0.04$), **f)** sham stimulation: high intensity and low frequency ($r = 0.52$, $p = 0.01$) as well as **g)** sham stimulation: low intensity & high frequency ($r = - 0.45$, $p = 0.04$). However, there were no correlation between VAS rating and pupil dilation for **b)** real stimulation: high intensity & low frequency ($r = 0.01$, $p = 0.95$), **c)** real stimulation: low intensity & high frequency ($r = -0.11$, $p = 0.62$), **d)** real stimulation: high intensity & high frequency ($r = 0.31$, $p = 0.14$), **e)** sham stimulation: low intensity & low frequency ($r = 0.19$, $p = 0.37$), **h)** sham stimulation: high intensity & high frequency ($r = 0.27$, $p = 0.20$). Thus, while higher mean pupil dilation was not consistently associated with higher VAS ratings across all subjects, three instances of significant associations between pupil dilation and VAS ratings (two positive, one negative) were observed, suggesting that interindividual differences in subjective perceptions of stimulation also add variance to pupil dilation of stimulation effects.

3.3.4.5 Theory-Driven Analyses: Exploring the Impact of TaVNS with Stimulus Valence and Sensitivity on Pupil Dilation

The theory-driven analysis to a) assess the extent to which short bursts of electrical stimulation enhances the effect of stimulus valence on pupil dilation for the emotional memory task (model *pupil dilation ~ trials + stimulation × valence + VAS + sensitivity + real_first + (1|ID)*), revealed no significant interaction between stimulation and valence ($\chi^2 = 1.44$, $p = 0.49$) (Fig. 21e), while stimulation ($\chi^2 = 44.46$, $p < 0.01$), valence ($\chi^2 = 5.65$, $p = 0.02$), VAS ($\chi^2 = 4.42$, $p = 0.04$) and the order of stimulation ($\chi^2 = 8.33$, $p = 0.004$) were significant and sensitivity was

not significant ($\chi^2 = 0.03$, $p = 0.87$). The theory-driven analysis to b) assess how sensitivity influences the subjective perception of stimulation on pupil dilation (model *pupil dilation ~ trials + stimulation + valence + VAS × sensitivity + real_first + (1|ID)*), revealed a significant interaction between VAS rating and sensitivity ($\chi^2 = 7.13$, $p = 0.01$) (Fig. 23), indicating that higher sensitivity to stimulation (3 mA) led to more pronounced pupil dilation as the perceived intensity of the stimulation increased (higher VAS ratings), while subjects with lower sensitivity (5 mA) showed a more stable and moderate pupil dilation response across VAS ratings. Stimulation ($\chi^2 = 44.46$, $p < 0.01$), valence ($\chi^2 = 5.65$, $p = 0.02$), VAS rating ($\chi^2 = 4.67$, $p = 0.03$) and the order of stimulation ($\chi^2 = 5.75$, $p = 0.02$) were significant and while sensitivity was not significant ($\chi^2 = 0.03$, $p = 0.88$). Additionally, there were no correlation between pupil dilation and memory performance (Supplementary Results 4.10).

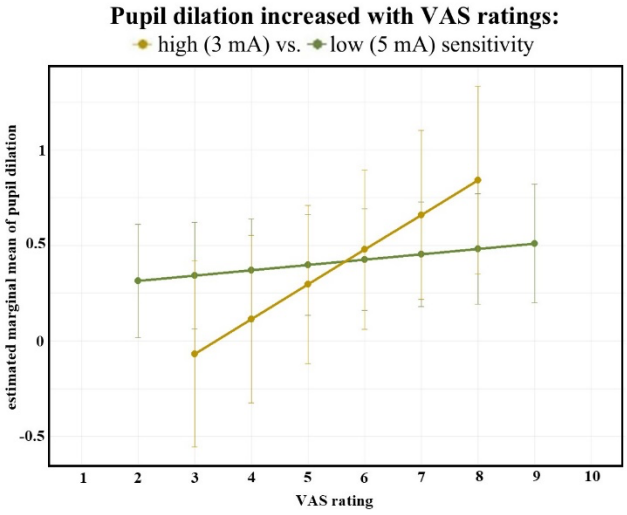

Figure 23. Interaction between VAS rating and sensitivity on pupil dilation for emotional memory task. Interaction between VAS rating and sensitivity on pupil dilation for emotional memory task. The model *pupil dilation ~ trials + stimulation + valence + VAS × sensitivity + real_first + (1|ID)* revealed a significant interaction between VAS rating and sensitivity ($\chi^2 = 7.13$, $p = 0.01$). The estimated marginal means (emmeans) of pupil dilation are presented across VAS ratings for both the low sensitivity group (5 mA, green (N = 17)) and the high sensitivity group (3 mA, ochre (N = 7)). **VAS 2**: In the low sensitivity group, the emmean is 0.314 (SE = 0.147, 95% CI [0.017, 0.611]). **VAS 3**: The emmean in the low sensitivity group is 0.342 (SE = 0.137, 95% CI [0.062, 0.622]), while in the high sensitivity group it is -0.069 (SE = 0.241, 95% CI [-0.555, 0.418]). **VAS 4**: The emmean is 0.370 (SE = 0.130, 95% CI [0.101, 0.639]) in the low sensitivity group and 0.114 (SE = 0.214, 95% CI [-0.326, 0.553]) in the high sensitivity group. **VAS 5**: The low sensitivity group has an emmean of 0.398 (SE = 0.127, 95% CI [0.134, 0.662]), while the high sensitivity group shows 0.296 (SE = 0.200, 95% CI [-0.119, 0.711]). **VAS 6**: The low sensitivity group emmean is 0.426 (SE = 0.128, 95% CI [0.160, 0.692]), and the high sensitivity group is 0.478 (SE = 0.200, 95% CI [0.062, 0.894]).**VAS 7**: The emmean for the low sensitivity group is 0.454 (SE = 0.133, 95% CI [0.179, 0.729]), while the high sensitivity group shows 0.660 (SE = 0.216, 95% CI [0.218, 1.103]).**VAS 8**: In the low sensitivity group, the emmean is 0.482 (SE = 0.142, 95% CI [0.192, 0.772]), while the high sensitivity group emmean is 0.842 (SE = 0.243, 95% CI [0.351, 1.334]). **VAS 9**: The low sensitivity group emmean is 0.510 (SE = 0.154, 95% CI [0.200, 0.820]). This illustrates that as VAS ratings increased, pupil dilation generally increased more in the high sensitivity group than in the low sensitivity group.

3.4 Interim Discussion

The efficacy of non-invasive taVNS in modulating the noradrenergic LC-NE system is increasingly discussed (D'Agostini et al., 2023; Jacobs et al., 2015; Sharon et al., 2021; Ventura-Bort et al., 2021; Vonck et al., 2014), but there is high heterogeneity in stimulation designs and a lack of appropriate outcome measurements (Ludwig et al., 2021). To investigate the impact of different stimulation parameters on pupil dilation and potential taVNS-induced effects on memory performance, I developed a taVNS setup that allows short bursts of event-related electrical stimulation (3 s) with time-synchronized pupil recording during an emotional memory task and resting-state task. The results provide evidence that short bursts of taVNS may modulate pupil dilation, a potential physiological indirect marker of LC-NE activity (Joshi et al., 2016), with higher stimulation intensities eliciting more pronounced pupil dilation than variations in stimulation frequency, which is in line with iVNS studies in animals (Hulsey et al., 2017; Mridha et al., 2021). However, there was an attenuation of taVNS-induced pupil dilation when differences in perception of sensations were considered. Specifically, pupil dilation during short bursts of taVNS increased with perceived stimulation intensity during the resting-state task. Regarding the emotional memory task, short bursts of taVNS applied during the encoding of negative events not only increased pupil dilation but also selectively improved memory performance for these events, particularly with real stimulation compared to sham or no stimulation. This observed effect is probably due to the attention-inducing sensory modulation of electrical stimulation since negative and neutral events were mixed within a stimulation session, and sensory perception was independent of valence. The results thus emphasize the importance of sensory perception in the stimulation process and the differentiation from a purely taVNS-induced change in pupil dilation and effects on memory performance, which I will discuss in more detail in the General Discussion. Moreover, the results demonstrate the importance of comparable stimulation sensations during systematic parameter testing to investigate the potential effects of short bursts of taVNS on pupil dilation and memory performance (Fig. 24). The taVNS design I established, which allows an event-related differentiation of the stimulation effects (real vs. sham) in comparison to no-stimulation condition, contributes to a more precise differentiation of the stimulation effects and could serve as a basis for further systematic taVNS research approaches.

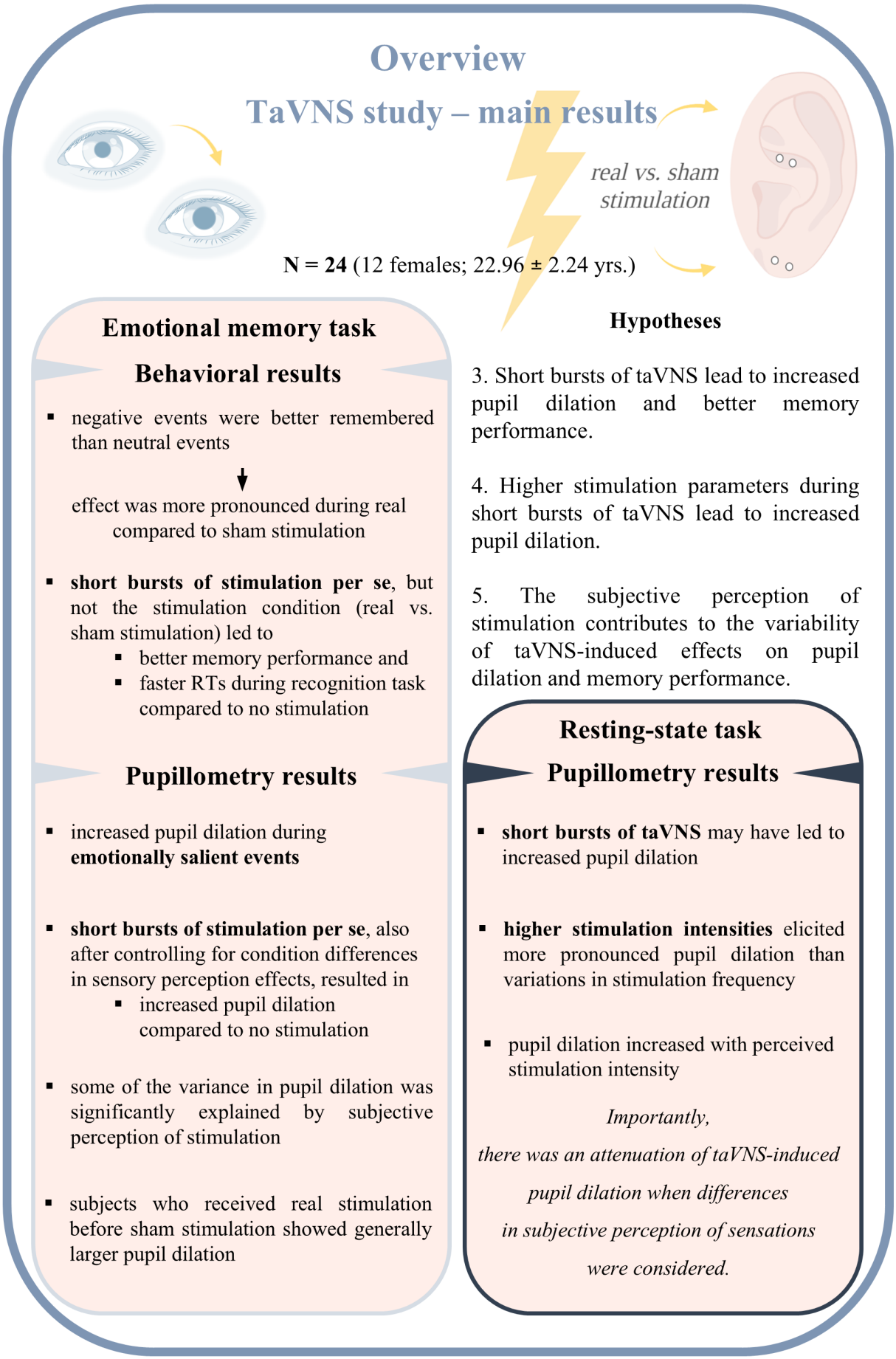

Figure 24. Overview highlighting main results of the taVNS study. The images were created with BioRender.com.

4 Chapter 4: General Discussion

The following discussion provides a comprehensive overview of the presented research findings regarding functional LC activation (fMRI) and short burst of taVNS, which is divided into five main parts: The first part presents a summary of the key findings from this dissertation, focusing on age-related differences in functional LC activation and indirect effects of short burst of taVNS on changes in pupil dilation and effects on memory performance in younger adults. The second part delves into a detailed discussion and interpretation of the integration of those findings, while in addition to increased LC activation in older adults, the different responses of the midbrain and brainstem to emotional and task-related salience are discussed. Furthermore, I will discuss the indirect effects of short bursts of taVNS and the effects of different stimulation parameters on pupil dilation, as well as effects on memory performance. Importantly, I will emphasize the importance of considering the subjective perception of sensation due to the stimulation when applying taVNS and when evaluating and interpreting taVNS effects. The third part outlines the limitations of the presented studies of this dissertation, addressing methodological constraints and how improvements could enhance future work. Based on that, the fourth part explores potential avenues for future research, e.g., combined taVNS-fMRI studies, highlighting the next steps to build on the findings of this dissertation. Finally, the fifth part concludes the discussion by synthesizing the insights gained and reflecting on their broader impact within the taVNS and LC research field.

4.1 Summary of Current Findings

In this dissertation, I presented age-related differences in functional LC activation (fMRI) and indirect effects of short bursts of taVNS on changes in pupil dilation and effects on memory performance in younger adults. In the **LC fMRI study,** I investigated age differences in functional activations of brainstem neuromodulatory nuclei during (1) emotional salience, (2) task-related salience, (3) memory performance, and (4) emotional memory performance. The **second** hypothesis could not be confirmed, as older and not younger adults showed increased LC activation, indicating a potential compensatory overactivation of the LC in older adults (Aron et al., 2022). However, consistent with the **first** hypothesis, LC activation was increased during emotionally negative and task-related salient events. This is consistent with both animal studies showing that LC integrity preferentially fires in response to negative events such as foot shocks (Bouret & Sara, 2004; Sara, 2009) and in vivo findings linking LC integrity with memory for negative events in older adults (Clewett et al., 2018; Hämmerer et al., 2018; Liu et al., 2020). In the **taVNS study**, I combined short bursts of event-related taVNS with an

emotional memory task with negative events involving the LC-NE system (Hämmerer et al., 2017, 2018) and a resting-state task in younger adults. I systematically investigated the effects of different stimulation parameters on changes in pupil dilation and to what extent real taVNS can enhance memory performance (immediate and delayed recognition task) and increase pupil dilation (encoding task) while varying the emotional content of the images. Importantly, I additionally investigated the influence of subjective perception of stimulation on taVNS-induced effects. Consistent with the **third** hypothesis, short bursts of taVNS led to increased pupil dilation and better memory performance. At the same time the **fourth** hypothesis was confirmed, indicating that higher compared to lower stimulation parameters, particularly increased stimulation intensities, led to more dilated pupil. These findings align with both animal and human studies on short bursts of i/taVNS, which have consistently demonstrated modulation of LC-NE activity (Collins et al., 2021; D'Agostini et al., 2023; Hulsey et al., 2017; Mridha et al., 2021; Sharon et al., 2021), whereas longer bursts of stimulation have yielded less consistent outcomes. However, as anticipated with hypothesis **five**, the subjective perception of stimulation attenuated taVNS-induced effects on pupil dilation, while memory performance was better with both real and sham stimulation, even after controlling for subjective perception of stimulation. This may indicate arousal and/or attentional-related processes involved during the stimulation process (Kahneman, 1973; Mather et al., 2016a; Miller et al., 2019).

4.2 Integration of Functional LC Activation and Short Bursts of TaVNS Findings

4.2.1 Increased LC Activation in Older Adults despite Age-Related Structural Decline

Both age groups showed better memory performance for stimuli associated with loss feedback, even if no age-related differences in memory were found, which is consistent with previous research showing better memory for negative events (Berridge & Waterhouse, 2003; Henson et al., 2016; Liu et al., 2020; Sara, 2009). This unexpected absence of age-related differences in memory performance may be attributed to floor effects that hinder the identification of interindividual differences in the challenging memory task, which involved greyscale stimuli in the recognition tests, potentially complicating the detection of older stimuli. Indeed, Hit-false alarm rates were rather low, and high false alarm rates, particularly in early recognition tests, could imply weaker memory representations and higher interference (Hämmerer et al., 2018). The absence of age differences in memory performance may also result from older individuals' stronger top-down focus on salient events, along with stronger top-down regulation of LC activity (Mather et al., 2016b; Sara & Bouret, 2012), which may compensate for their weaker memory representations during encoding. However, due to the inherently limited field of view in MRI acquisitions that excluded the prefrontal cortices, I

cannot validate this hypothesis in my imaging data, such as by analyzing age-related variations in frontal or parietal activations. It may be supported by concurrently acquired pupillometric data in the same data set, which revealed larger pupil diameters for loss and reversal stimuli in older adults compared to younger adults (Hämmerer et al., 2018). This might indicate that older adults had a stronger attentional focus on salient events. To validate this, however, future imaging research is required that systematically manipulates the attentional focus while encoding salient events. In contrast to previous findings indicating age-related structural decline in neuromodulatory structures, older adults showed increased activations in these brainstem structures relative to younger adults (Table 1). In aging research, larger functional activations in older adults are a recurring observation, generally signifying age-related differences in the prioritization of cognitive processes during fMRI studies, often associated with compensatory mechanisms for declining cognitive capacity (Aron et al., 2022; Reuter-Lorenz & Lustig, 2005; Spreng et al., 2010). Simultaneously, research indicates that in older adults, the functional connection of the LC with frontoparietal networks decreases, reducing the selectivity of their attention (Gallant et al., 2022; Lee et al., 2018b). Moreover, whereas older adults generally appear to have a bias for recalling positive stimuli (Charles et al., 2003; Mather & Carstensen, 2005), data suggests that older adults process negative stimuli with greater intricacy (Eppinger & Kray, 2011; Kensinger, 2009) and are more inclined to remember them when such stimuli offer performance feedback (Hämmerer & Eppinger, 2012). The increased LC engagement in older adults during this study's reversal reinforcement learning task may be attributed to **a) compensatory overactivation of the LC** or a structure targeting the LC in older adults. The aging brain engages attentional networks, cortical regions, and novel networks to compensate for deficits in other areas functionally (Aron et al., 2022). Therefore, increased activity of the LC and HPC in older adults may indicate such compensatory efforts. Despite the absence of memory performance differences between age groups, increased activations in older adults may suggest enhanced compensatory engagement. However, among older adults, there was no correlation between interindividual differences in LC activation and memory performance associated with either (1) emotional or (2) task-related salience (see Supplementary Figure S7-S8). Only higher MTG activation in older adults during (2) task-related salience was associated with better delayed memory performance (see Supplementary Fig. 8), indicating MTG's potential compensatory involvement in older adults' memory processes. Larger samples may be necessary to link behavioral correlates to functional activation in small brain regions like the LC. Alternatively, as there is evidence that the remaining neurons in a shrinking LC may increase firing rates in mice (Szot et al., 2016), b) **stronger functional LC responses** may be

linked to cell loss in the LC. More thorough research is necessary for reliable validation, as there is no link between LC integrity and its increased activation in older adults across conditions (see Supplementary Figure S7-S10). Moreover, it is plausible that **c) differences in task engagement between age groups** may contribute to differences in functional recruitment between age groups. The straightforward reinforcement learning task with deterministic feedback and few reversals (40 trials) may have led younger adults to exert less effort than older adults, aligning with reports of youth-like activations in high-performing older adults, especially during easy tasks (Nagel et al., 2009). However, the limited FoV hindered me from comparing task-focused activations in parietal and frontal regions across age groups, limiting the investigation into the extent of youth-like activation patterns. Furthermore, the LC is crucial for the preservation of vascular functioning. The individual diversity of the arteries supplying the LC, including distinct vascularization patterns such as dilatation and constriction, may subsequently affect cognition, perhaps elucidating differences within age groups (Bekar et al., 2012; Giorgi et al., 2020); however, this necessitates further investigation.

4.2.2 Distinct Midbrain and Brainstem Responses to Emotional and Task-Related Salience

Regarding the brainstem or midbrain's functional responses during (1) emotional salience and (2) task-related salience, the LC was more activated in processing loss rather than gain feedback, and feedback indicating a reversal in task conditions as compared to feedback indicating no reversal, respectively (Figures 2–4). The present study's increased LC responses to emotionally salient events are consistent with in vivo findings that relate LC integrity with memory for negative events in older adults (Clewett et al., 2018; Hämmerer et al., 2018; Liu et al., 2020), as well as animal studies that demonstrate its preferential firing to negative events such as foot shocks (Bouret & Sara, 2004; Sara, 2009). Additional converging evidence for the LC-NE systems' emphasis on emotional or salient events is supplied by pupil diameter measurements, which may reflect underlying phasic LC activity but are not solely linked to phasic LC responses (Aston-Jones & Cohen, 2005; Hämmerer et al., 2018; Joshi et al., 2016). Larger pupil diameters are generally observed in response to emotionally negative stimuli, such as adverse feedback (Braem et al., 2015; Hämmerer et al., 2017, 2019). Indeed, higher pupil dilations to negative feedback have also been observed in this study in both younger and older adults (Hämmerer et al., 2018). Despite negative feedback occurring less frequently (about 33% of trials) in this task, the LC's stronger responses to negative feedback were not attributable to differences in informativeness, as this non-probabilistic reversal reinforcement learning paradigm equitably balanced losing and gaining trials concerning reversal feedback. This

finding is supported by a recent pupillometry study showing that pupil dilations are higher during negative performance feedback in younger and older adults, accounting for informativeness and feedback frequency (Hämmerer et al., 2019). This would imply that the sheer negative value of an event is sufficient to provoke LC activation. Higher LC activations during loss feedback may be behaviorally related to a general reaction response invigoration, as I found that both younger and older adults responded more quickly following loss feedback but not gain feedback. This interpretation requires additional in vivo imaging investigations for validation; however, it aligns with animal research, indicating that phasic LC responses are especially associated with effortful response execution (Bouret & Richmond, 2009).

Regarding functional responses in the brainstem or midbrain to (2) task-related salience, increased activation of both the LC and SNr were observed in older adults during feedback indicating task reversals (Figures 9-11). As dopaminergic nuclei (VTA, SNc), GABAergic nucleus (SNr) (Tepper & Lee, 2007), and LC are reciprocally connected (Sara, 2009), a concurrent activation is both anatomically and functionally plausible. Concurrent electrical recordings in the ventral VTA and LC of mice indicated increased activity in both regions within a novel environment, with the LC exhibiting a more rapid decrease in response over time relative to the VTA (Takeuchi et al., 2016). Similarly, the SN has been reported to exhibit phasic activity in response to unexpected and unfamiliar stimuli, indicating coordinated responses by dopaminergic and noradrenergic structures (Schiemann et al., 2012; Schultz, 2007). In particular, animal research has demonstrated that (a) SNr neurons in rodents and (b) LC neurons in monkeys fire more frequently in response to task-relevant cues like (a) Go and Stop cues (Schmidt et al., 2013) or (b) infrequent deviant stimulus in so-called oddball tasks that call for particular behavioral responses (Aston-Jones & Cohen, 2005). Thus, higher LC and SNr activation during reversals aligns with animal studies, indicating that these regions are engaged in response to novel, unexpected, or deviant stimuli necessitating adaptive responses. In accordance with the necessity to modify stimulus category preferences following reversals in this task, younger and older adults responded slower on trials after reversals. Furthermore, midbrain and brainstem nuclei in older adults were more engaged in processing response feedback and subsequent memory effects during stimulus presentation. Specifically, they showed higher LC activations for (3) memory performance, especially for (4) emotional memory performance, during encoding compared to younger adults. The findings affirm the role of the LC in the encoding and remembering of emotional events, as the LC is known for facilitating long-term memory formation, particularly for negative events (Luo et al., 2015; Sara, 2015; Sterpenich et al., 2006; Veréb et al., 2023) by NE release in LC target regions such

as the amygdala and HPC, which are crucial for the encoding and retrieval of emotional events (Chen & Sara, 2007; Luo et al., 2015; Tully & Bolshakov, 2010). In line with this, previous studies indicate that older adults with higher rostral LC integrity exhibited better memory performance (Dahl et al., 2019), which aligns with the findings that rostral LC contrast in older adults is associated with the thickness of widespread cortical regions (Bachman et al., 2020) and that a loss of rostral LC is associated with poorer memory performance (Veréb et al., 2023). It is intriguing to speculate whether the overserved activation patterns of the LC, namely emotional salience predominantly activating large portions of the left LC and memory-related processes engaging the right LC (Fig. 9), may be associated with variations in the projection patterns of the LC. A study in older adults demonstrated a loss of rostral-like connectivity of the LC and differences in the spatial properties of the LC gradient associated with poorer emotional memory, with left rostral-like connectivity reduced compared to right connectivity in people with higher levels of anxiety and depression (Veréb et al., 2023). In animals, caudal portions of the LC preferentially project to the spinal cord and cerebellum, while rostral portions tend to project to the cerebral cortex and forebrain, including the amygdala and hippocampus (Loughlin et al., 1986; Samuels & Szabadi, 2008; Schwarz & Luo, 2015; Ungerstedt, 1971). If these projection patterns can be transferred to humans, the current observation in this study of right more rostral LC activations for memory-related processes would be consistent with these different projection patterns.

4.2.3 The Indirect Effects of Short Bursts of TaVNS on Pupil Dilation and the Influence of Subjective Stimulation Perception

Consistent with previous i/taVNS studies, short bursts of taVNS resulted in increased pupil dilation during real compared to sham stimulation, at higher compared to lower intensity and frequency stimulation during the resting-state task (D'Agostini et al., 2023; Ludwig et al., 2021). The impact of the electrical stimulation and stimulation parameters on changes in pupil dilation during the resting-state task were notably more pronounced during the (I) 3 s of short bursts of "on stimulation" compared to the (II) 3 seconds following stimulation ("immediate response") and in a subsequent (III) 10-second time-window ("delayed response"). The temporal progression of pupil dilation increases and peaks during the 3 s short bursts of real stimulation, followed by a subsequent decline. This aligns with the findings of the 3.4 s short bursts of real stimulation (Sharon et al., 2021) and a corresponding replication of these findings (Lloyd et al., 2023). Likewise, a recent study employing 5 s short bursts of stimulation demonstrated increased pupil dilation during taVNS, which diminished immediately after reaching the peak (D'Agostini et al., 2023). Another study also demonstrated that far shorter

bursts of taVNS (~ 600 ms) similarly led to increased pupil dilation, with canal stimulation leading to larger pupil dilation than conchae stimulation compared to sham stimulation (Urbin et al., 2021). The observed increase in pupil dilation by short bursts of taVNS may be consistent with previous findings from animal studies showing that phasic stimulation increased NE release and LC activation (Florin-Lechner et al., 1996; Hulsey et al., 2017). However, the perception of sensations due to stimulation during the resting-state task accounted for a substantial proportion of the stimulation effects on pupil dilation. The distinction between real and sham stimulation could no longer be statistically justified, and variations in stimulation frequencies and intensities were nearly entirely elucidated. This may imply that variations in the subjective perception of real versus sham stimulation may **solely account for the pupil differences** observed between these conditions, as well as between low and high intensity and frequency, or that the effects of stimulation and the **perception of stimulation overlap** to a statistically indistinguishable degree given the stimulation parameters employed in this study. The latter explanation is deemed more plausible, given that Sharon et al. (2021) demonstrated pupil dilatation resulting from short bursts of real compared to sham stimulation at a constant VAS rating.

Moreover, the event-related stimulation design of the emotional memory task enabled me to compare the effects of real or sham stimulation and no stimulation on pupil changes (and behavioral performance), specifically examining the effects of "stimulation on" and "stimulation off" across events during the encoding task. This indicated that short bursts of stimulation per se during the emotional memory task resulted in increased pupil dilation (and better memory performance) compared to no stimulation, even after accounting for variations in sensory perception, which contrasts with prior research demonstrating increased pupil dilation during real compared to sham stimulation in a resting-state task (D'Agostini et al., 2023; Lloyd et al., 2023; Sharon et al., 2021; Skora et al., 2024). Furthermore, the theory-driven pupillometry analysis revealed no interaction between stimulation and valence, indicating that pupil dilation was not differentially modulated by stimulus valence during either real or sham stimulation and that short bursts of stimulation per se led to increased pupil dilation. The absence of a difference between real and sham stimulation during the emotional memory task may be partially attributed to attentional factors. In the presence of subtle sensory differences between stimulation conditions, attentional resources may be allocated to assessing these differences, irrespective of the subjective perception of sensation due to stimulation. The simultaneous task (emotional memory task) may have utilized these attentional resources, hindering the distinction between the perceptual aspects of real and sham stimulation that might

otherwise be shown by pupil dilation. At present, these arguments are conjectural and necessitate evaluation in forthcoming investigations that either eliminate or meticulously regulate sensory disparities between real and sham stimulation conditions.

Finally, regardless of stimulation conditions, emotionally negative events led to increased pupil dilations compared to neutral events, confirming previous animal and human studies on pupil dilation during emotionally negative events (Hämmerer et al., 2017, 2018; Joshi et al., 2016). As changes in pupil dilation may be a proxy for LC-NE activity (Joshi et al., 2016), increased pupil dilation due to emotionally negative events may reflect stimulus-driven influences on the LC-NE system (Sara & Bouret, 2012).

4.2.4 Are Higher Stimulation Parameters Important for the Stimulation Process?

For the various stimulation parameters investigated during the resting-state task, varied effects were observed over time. While the differences in pupil dilation between real and sham stimulation persisted for another 3 seconds after the end of stimulation, differential effects of stimulation frequencies were no longer detectable after stimulation was turned off. In contrast, effects of stimulation intensity persisted in a time window of 6.2 to 16.2 s after stimulation was turned off. Thus, the results of the resting-state task might indicate that intensity, especially at higher levels, is pivotal for the stimulation process and may affect pupil dilation. Higher intensities (0 – 2.5 mA) and longer pulse widths (0 – 500 µs) during iVNS in rats did, in fact, alter LC activation (Hulsey et al., 2017), whereas increased pupil dilatation was caused by increased pulse widths (100, 200, 400, and 800 µs) during iVNS (Mridha et al., 2021). In line with this, a recent taVNS study in humans reported a more dilated pupil by increasing the pulse width (200 or 400 µs) with intensity (.2, .5, calibration intensity: 1.19 ± .65 mA (taVNS) and 1.49 ± .73 mA (sham)) (D'Agostini et al., 2023), which may suggest that pulse width appears to be an important contributing factor. A wider pulse width (500 µs) is thought to yield a more restricted spectrum of VNS intensities (Loerwald et al., 2018), which may elucidate why D'Agostini et al. (2023) were able to report increased pupil dilation at very low intensities combined with higher pulse width during short bursts of tAVNS. This may also account for the subjects' ability in this present study to tolerate stimulation up to 5 mA with a moderate pulse width of 250 µs during short bursts of 3 s stimulation. Furthermore, changes in pupil dilation appeared to be less affected by frequency during the resting-state task. Thus, iVNS studies revealed increased pupil dilation at 20 Hz compared to 5 Hz and 10 Hz (Mridha et al., 2021) and a greater increase in LC firing rate at higher frequencies (frequencies: 0, 7.5, 15, 30, 60, 120 Hz; 0.8 mA, 100 µs, 16 pulses) (Hulsey et al., 2017). However, higher frequencies did not alter the total amount of neuronal LC activity (Hulsey et al., 2017). Additionally, an elevated

LC firing rate is not invariably beneficial. Studies on cortical plasticity in rats with iVNS demonstrated that the effects of stimulation do not increase monotonically with intensity. Plasticity was maximized at low intensities (~ 0.8 mA), while elevated intensities (1.2 – 1.6 mA) impaired plasticity and associated behavioral advantages (Borland et al., 2016; Morrison et al., 2021; Souza et al., 2021). Nevertheless, given that the effects of stimulation intensity and frequency manifested without a discernible difference between real and sham stimulation (based on a low sample size of N = 24), it is challenging to conclude that the vagus nerve mediates these effects. An additional process influencing pupil dilation, such as attention-induced regulation of pupil size, may elucidate this phenomenon (Kahneman, 1973; Miller et al., 2019). The extent to which higher stimulation parameters are important for the stimulation process when modulating the LC-NE system, therefore, depends on the individual intervention group and goals and requires further in-depth research - especially in the field of taVNS in humans.

4.2.5 The Indirect Effects of Short Bursts of TaVNS on Memory Performance

The present study demonstrated that emotionally negative events were better remembered than neutral events, which is in line with previous studies on emotional memory performance (Hämmerer et al., 2017, 2018). Particularly, animal and human research suggest that the LC-NE system is a crucial part in the processing and encoding of emotionally negative events by releasing NE in LC target areas, including the amygdala and hippocampus (Chen & Sara, 2007; Hämmerer et al., 2018; Ludwig et al., 2024b; Luo et al., 2015; Sterpenich et al., 2006; Tully & Bolshakov, 2010). The impact of short bursts of taVNS on memory performance (hit-FA) and correct recognition (hit) showed no difference between real and sham stimulation; however, it was improved during any type of stimulation (real or sham) as compared to trials with no stimulation. Further analyses also indicated that this impact could not be attributed to the subjective sensory perception of the stimulation, which was higher for real compared to sham stimulation. Real or sham stimulation may thus facilitate the initial processing and storage of the images in memory, making them easier to recall in the recognition task, as evidenced by RTs, which showed that stimulation per se but not the stimulation condition resulted in a faster RT during the recognition task.

Importantly, while negative events were generally better remembered than neutral events, this effect was more pronounced for events encoded during real stimulation than sham or no stimulation. This indicates that beyond a general enhancement of encoding due to real or sham stimulation, real stimulation specifically further improved the encoding of negative events, which presumably depend more on the noradrenergic LC (Chen & Sara, 2007;

Hämmerer et al., 2018; Ludwig et al., 2024b; Manaye et al., 1995). These findings align with increased recollection-based memory performance for emotional images but not for neutral ones, using a tonic tAVNS paradigm (Ventura-Bort et al., 2021). As neutral and negative events were mixed within real stimulation sessions, and sensory perception was independent of valence rendering, this effect is unlikely to be driven by differences in subjective sensory perception related to the stimulation. Instead, a stronger LC engagement during real stimulation or a stronger overall arousal in the real stimulation condition, given higher ratings of subjective perception of sensations due to stimulation, may have further supported the encoding of emotionally negative events known to engage the noradrenergic system. Both notions would align with previous findings indicating that noradrenergic and glutamatergic processes interact to affect cognition via a combination of attentional focus and arousal, as proposed by the GANE model (Mather et al., 2016a). Likewise, as expected, the overall memory performance was better during the immediate recognition task compared to the delayed recognition task (24h), driven by both more frequent false alarms (FAs) and fewer correct recognitions (hits) in the delayed recognition. FAs were more frequent for emotional than neutral events during the delayed recognition task, while the hit rate tended to decrease less over time for emotional than neutral events. This may align with findings indicating that arousal impairs the retention of numerous representations at the same level in working memory (Mather et al., 2016b; Mather & Sutherland, 2011). Contrary to Hämmerer et al. (2018), I did not observe prolonged RTs for negative events during the encoding or recognition tasks; however, I replicated the effect of longer RTs for new images compared to old images during the recognition task (Hämmerer et al., 2018). This may be attributed to subjects focusing specifically on old images when classifying stimuli as old or new (Hämmerer et al., 2017; Kafkas & Montaldi, 2018).

4.2.6 The Influence of the Subjective Perception of Stimulation and Corresponding Implications

The subjective perception of stimulation appears to be a crucial factor in taVNS; therefore, it is essential to elucidate how this may have impacted the increased pupil dilation and better memory performance and how to address this in future taVNS studies. An effect of sham stimulation on the LC through the VN should be excluded because earlobe sham stimulation should not directly affect the VN (Peuker & Filler, 2002). Therefore, it can be assumed that attentional and/or arousal processes related to the sensory effects of stimulations may be responsible for increased pupil dilation and better memory encoding associated with real or simulated stimulation (as opposed to no stimulation). This would be consistent with earlier research demonstrating that arousal or attention can affect pupil size and encoding

performance (Kahneman, 1973; Lee et al., 2018b; Miller et al., 2019; Sara & Bouret, 2012). Indeed, real versus sham differences in stimulation sensations explained a significant portion of the explained variance in pupil dilation. Moreover, subjects receiving 3 mA (N = 7) exhibited a more pronounced pupil dilatation in response to increased perceived stimulation intensity. In contrast, those receiving 5 mA (N = 17) showed a more stable and moderate pupil dilation throughout VAS ratings. Nonetheless, considering the disparity between any type of sensory stimulation and the absence thereof, along with the fact that sensations were only acquired post-stimulation session, a remaining general effect on arousal or attention associated with the stimulation should be assumed. Unlike prior studies, the event-related design allowed for the trial-by-trial investigation of these cognitive and physiological effects associated with stimulation sensations, indicating assumably attentional or arousal-related changes on a timescale of seconds related to the sensory effects of stimulation. The effects of sensory stimulation were predominantly beneficial for memory encoding rather than distracting (Kong et al., 2005; Pleger & Villringer, 2013).

Notably, while a large proportion of the stimulation effects on pupil dilation could be explained in the same subjects while controlling for subjective perception of sensations in the resting-state task without a cognitive component, in the emotional memory task, both the behavioral and pupil effects of real versus sham stimulation could not be fully explained by the differences in the stimulation conditions in the subjective perception of sensations. This indicates that sensations of perception may not primarily influence the potentially arousal-related physiological and cognitive effects. For instance, compared to a resting-state task, attentional resources during an emotional memory might be additionally biased towards processing and storing emotional information, while the negative events themselves caused increased pupil dilations independent of stimulation sensations. This may have led to the observation that the variance of pupil dilation in the emotional memory task compared to the resting-state task was less explained by subjective sensory perceptions.

Therefore, I recommend that when employing pupillometry as an indirect outcome measure for taVNS studies, different levels of subjective perception of sensations between stimulation conditions should be considered as a potential confounding factor. More importantly, as the typical locations for real and sham stimulation showed a higher VAS rating for real stimulation at the cymba conchae for the same stimulation parameters, it is crucial to investigate to what extent alternative sham stimulation locations (e.g., earlobe, scapha) show a comparable level of stimulation-induced sensations to alternative real stimulation locations (e.g., cymba conchae, tragus). An often-applied approach is to keep the sensations for real and

sham stimulation constant (Burger et al., 2020; Farmer et al., 2021; Sharon et al., 2021). Observing potentially greater effects of real stimulation under these conditions enables a cautious evaluation of the advantages of real stimulation compared to sham stimulation. Investigating the effects of varying stimulation parameters while maintaining a constant stimulation sensation is a major challenge, which is crucial in human taVNS research.

An effort to fulfill this requirement was demonstrated, for instance, in a human taVNS study that controlled for subjective perception of stimulation and tested pairs of higher frequencies with lower amplitudes in addition to pairs of lower frequencies and higher amplitudes during respiratory auricular vagal afferent nerve stimulation (RAVANS) (Sclocco, 2020). RAVANS enables stimulation at the same location during inhalation and exhalation. Both 100 Hz and 2 Hz led to increased LC activation, while no stimulation was applied during sham stimulation (Sclocco, 2020). Considering that the LC is involved in attentional processes (Sara, 1985) and studies in monkeys have already shown that there is increased phasic LC activation during discriminative tasks (Aston-Jones et al., 1994), the question arises whether 2 and 100 Hz were more salient and could be discriminated, contributing to increased LC activation during RAVANS; potentially suggesting the influence of attention-induced modulation during taVNS.

Moreover, even if the subjective perception of sensations due to stimulation is kept constant, sensory characteristics that facilitate the difference of various stimulation parameters may affect pupillometric responses to taVNS. Individuals' capacity to discriminate between different stimulation parameter characteristics (e.g., increasing intensity with constant pulse width or vice versa) and if certain parameter combinations are more salient might be investigated. It is assumed that the stimulation activates A, B, and C fibers of the cVNS to varying degrees (Chang et al., 2020; Evans et al., 2004), while tAVNS may have been transmitted by thick afferent A-beta axons, as discussed by Safi et al. (2016). Similarly, the selective destruction of C-fibers with capsaicin in rats showed no effect on VNS-induced seizure suppression (Krahl et al., 2001). Consequently, an alternative approach may involve the application of an anesthetic cream (e.g., lidocaine) to the ear region designated for stimulation to inhibit sensory perception of the stimulation. However, exposure of the nerves to lidocaine has been shown to result in blockade of the A and B fibers (Brodin, 1985). Furthermore, the firing rate of the vagus nerve decreases when lidocaine is administered distally to the cervical vagus nerve (Zanos et al., 2018). Accordingly, with such anesthetic creams, it cannot be ruled out that nerve fiber connections could be blocked, which could be important for transmitting electrical impulses of tAVNS. Further experiments, including invasive fiber recordings, are

needed to determine optimal doses (probably the minimum most effective) of anesthetic creams during taVNS in humans. Interestingly, it may also be possible to modulate the effects of stimulation parameters and the sensations of stimulations separately, as increasing firing rates and frequencies have been shown to have different effects on LC activity, with increasing frequencies decaying much earlier than increasing intensities (Hulsey et al., 2017). As discussed in a review (Ludwig et al., 2021), it remains a central question which comparable real and sham stimulation locations and comparable stimulation sensations are best suited for different stimulation parameters.

5 Limitations

Regarding the LC fMRI study, limitations should be mentioned, as results observed in this study reflect activations in a partial volume of the brain (Fig. 5), which is a necessary limitation given the emphasis on high-resolution data acquisition. Therefore, other brain regions of interest, such as the insula, anterior cingulate cortex (ACC), or thalamus, which are known to be target areas for the LC and part of the salience network (Navratilova et al., 2014), could not be included in the joint area accessible for the second level analysis. Similarly, it was not possible to investigate compensatory interactions in supporting regions that input the LC, such as the frontal or parietal cortices (Jacobs et al., 2018; Lee et al., 2020). This should be investigated in future research employing greater magnetic field intensities. Furthermore, variations in the neurovascular coupling that underlies the BOLD response between age groups should be anticipated, given the growing understanding of age changes in neurovascular function, specifically regarding altered vasoreactivity and blood oxygen consumption (Tsvetanov et al., 2021). Although the various contributions to altered BOLD responses due to age and interindividual differences remain incompletely elucidated (Fesharaki et al., 2023; Huettel et al., 2001; Tsvetanov et al., 2021), baseline tasks expected to invoke comparable processes across age groups (e.g., finger tapping) typically yielded lower SNRs in older adults than younger adults (D'Esposito et al., 2003). Consequently, the reported age differences, pointing towards larger effects in older adults, might underestimate existing age differences somewhat. Regarding the taVNS study, limitations should be mentioned as further research is needed to systematically investigate possible carry-over effects of individual taVNS sessions of varying duration on pupil dilation and emotional memory. Another possibility as to why I found no differences between real and sham stimulation on a physiological and behavioral level could also be that the effects of real stimulation might have carried over into the following sham stimulation period. Although real and sham stimulation were balanced in our design across

subjects, both sessions took place directly after each other (wash-out approx. 5-10 min) and might have thus resulted in partial contamination through preceding stimulation effects. Additionally, it is currently unclear whether the duration of stimulation is related to the effects of taVNS on pupil dilation and memory performance and which wash-out period should be chosen between tasks. Since the subjects had already received real and sham stimulation in a counterbalanced order during the emotional memory task (approx. 44 min stimulation, see Fig. 14) before the resting-state task, followed by wash-out of approx. 45-60 min, it is challenging to assess to what extent the stimulation effects observed in the resting-state task are partly due to a prior "pre-stimulation effect". As there is currently no consensus regarding the presence and temporal extent of aftereffects of short bursts of event-related stimulation designs, these suggestions should be verified in future double-blinded studies investigating parallel interventions close in time and separated by a few days. Furthermore, an increased sample size might be advantageous for future research to achieve more reliable model estimates and enhance generalizability.

6 Future Research Avenues

Based on the functional LC findings presented in this dissertation, I advocate for future research endeavors to consider and further investigate fMRI LC activation as a biomarker for aging. In this context, I have demonstrated that using high-resolution fMRI, a structural LC sensitive scan, and suitable post-processing techniques tailored for the LC, it is feasible to visualize the small structure of the LC. Future research should build on these findings to explore the independent interplay between salience and compensatory processes, employing tasks that concurrently manipulate attentional focus and salience. Additionally, it is critical to determine whether changes in LC functional responses represent typical healthy aging or serve as potential biomarkers for MCI and AD (Clewett et al., 2016; Shibata et al., 2006). Future studies should incorporate CSF and/or blood-based biomarkers as pre-symptomatic indicators of dementia-related pathology (Engels-Domínguez et al., 2023; Murray et al., 2022) and evaluate the functional integrity of brainstem and midbrain nuclei to strengthen the connection between age-related and pathological decline.

Does taVNS reliably modulate the LC-NE system, and can it be used as a therapeutic intervention in a declining LC-NE system? This dissertation does not fully resolve it but marks an important milestone, paving the way for continued exploration of this ambitious research question. My research findings make a substantial contribution to this field, demonstrating that short bursts of taVNS at higher intensity and stimulation per se (whether real or sham

stimulation) led to increased pupil dilation and better memory performance, which aligns with prior i/taVNS research in animals and humans, respectively (Collins et al., 2021; D'Agostini et al., 2023; Hulsey et al., 2017; Mridha et al., 2021; Sharon et al., 2021). The findings of this dissertation should encourage researchers to persist in systematically investigating the effects of various stimulation parameters on different stimulation locations at the ear with appropriate outcome measurements. Above all, future taVNS studies should carefully control and evaluate not only the sensory effects of different stimulation conditions and locations but also potential cognitive enhancing effects related to the sensation of the stimulations per se. Furthermore, the temporal extent of the after-effects of short bursts of event-related stimulation designs and the long-term effects of taVNS require further investigations. My taVNS design, which facilitated event-related decorrelation of stimulation (real vs. sham) in comparison to a no-stimulation condition, may therefore encourage other researchers to incorporate no-stimulation trials to more effectively distinguish those effects of stimulation while considering sensory effects due to the stimulation.

To address the major challenge of sensory effects resulting from the stimulation, forthcoming taVNS investigations may utilize microneurography, which allows direct recording of nerve activity in awake humans. This methodological proposition is motivated by a study demonstrating the possibility of invasive microelectrode recordings from the cervical vagus nerve in awake humans associated with cardiac or respiratory cycles (Ottaviani et al., 2020). Specifically, microneurography can directly assess the function of the afferent sensory nerves and efferent sympathetic nerves leading to the muscle (MSNA) and skin (SSNA) (Vallbo, 2018). Due to the afferent and efferent nerve fiber connections of the VN, microneurography of the vagus nerve may allow measurements on visceral sensory neurons (e.g., NTS) as well as efferent motor neurons (nucleus ambiguus, DMV). In current animal studies, microneurography is used as a minimally invasive tool to assess target activity during neuromodulation to investigate optimal electrode placement and stimulation parameters to optimize the local nerve fiber engagement and mechanisms of action in the long term (Verma et al., 2021, 2023). To the best of my knowledge, at present, only one taVNS clinical trial study investigated taVNS-induced HRV changes combined with MSNA, reporting no differences between real and sham stimulation on HRV or MSNA indices (Gauthey et al., 2020). This again emphasizes the importance of further investigating the role of the active sham stimulation condition considering sensory perception and encourages further development of this new methodological approach of combined microneurography taVNS studies. However, the extent to which microneurography may be useful in taVNS-induced pupil dilation changes

has not yet been addressed. Overall, future studies combining microneurography and taVNS could map the objective neural responses from microneurography to the subjective reports of sensory perception regarding the stimulation. This could also enhance our understanding of the roles of different nerve fiber classes during VNS (Patros et al., 2024). Moreover, since personalized taVNS therapy is needed to avoid over- or under-stimulation, closed-loop aVNS systems seem to be another future avenue. A recent study developed a new aVNS hardware for closed-loop applications and demonstrated a promising methodological approach for flexible control of stimulation parameters using cardiorespiratory biosignals of the human body (Dabiri et al., 2022). However, combined microneurography taVNS and closed-loop aVNS present their own set of challenges and necessitate additional in-depth research to gain a comprehensive understanding of their potential and constraints for future taVNS studies.

As combined taVNS-fMRI studies have already shown promising functional activation of NTS in LC-NE projection areas such as the amygdala and hippocampus (Sclocco et al., 2019; Yakunina et al., 2017), taVNS MRI studies may be further implemented and refined in the near future. I advocate for future combined taVNS-fMRI investigations to include high-resolution fMRI and appropriate post-processing methods for small structures in the brainstem, which may aid in elucidating the processes of taVNS and clarifying potential contributions of the LC-NE system.

7 Conclusion

In my dissertation, I demonstrated the feasibility of investigating age-related differences in functional LC involvement during a cognitive task known to rely on noradrenergic function. Consistent with animal studies on LC function, I observed increased activation of the LC during emotionally and task-related salient events (Bouret & Sara, 2004; Joshi et al., 2016; Sara, 2009). Notably, I could show that a stronger LC engagement in response to emotionally and task-related salient events was associated with distinct reaction time effects: acceleration and deceleration, respectively. I highlighted that the LC and other salience-indicating structures might operate within a network of brain structures aiming to regulate context-specific adaptive responses. Despite the growing body of evidence showing a structural decline in LC with age, I showed that LC engagement was generally stronger in older adults. The comparable behavioral performance between younger and older adults could indicate a potential compensatory overactivation of the LC in older adults.

Furthermore, in my dissertation, I addressed a contribution to the open taVNS challenges by systematically investigating different stimulation parameters during short bursts

of stimulation, including an appropriate indirect outcome measure for the LC-NE system, specifically pupillometry. To achieve this, I established a taVNS setup that allows the individual setting of stimulation parameters and time-synchronized stimulation during an experimental task and pupillometry. Additionally, the taVNS design facilitated event-related decorrelation of stimulation (real vs. sham) compared to a no-stimulation condition, which may encourage other researchers to incorporate trials without stimulation to differentiate the effects of stimulation more effectively. I demonstrated that short bursts of real taVNS and higher intensity led to increased pupil dilation, which is consistent with short bursts of invasive VNS studies in animals (Collins et al., 2021; Hulsey et al., 2017; Mridha et al., 2021), offering valuable information for hypothesizing which transferable stimulation variants in taVNS studies may augment the effects on the NTS and LC. The findings of my dissertation also suggest that the influence of intensity on pupil dilation may be stronger than that of frequency. However, there was an attenuation of taVNS-induced pupil dilation when differences in perception of sensations were considered. Moreover, I observed that pupil dilation during short bursts of stimulation increased with perceived stimulation intensity. Therefore, I showed how important it is to consider the perception of sensations brought on by short bursts of taVNS, as many studies either control for VAS ratings or do not report systematically at all. Even if not all parameters can be systematically varied simultaneously and the sensations cannot be held perfectly constant for each individual, the pursuit of comparable sham stimulation sites and comparable sensations is important for future research. Additionally, I demonstrated that real or sham taVNS stimulation may enhance the encoding of events, while real stimulation, in particular, enhanced the encoding of negative as compared to neutral events, which is consistent with animal research showing an involvement of ascending vagal fibers in emotional memory (Clark et al., 1998; Hulsey et al., 2017; McIntyre et al., 2012; Williams & McGaugh, 1993) and suggests that taVNS represents a promising method to influence emotional memory processes. While the role of the LC in regulating arousal and attention, also in the context of emotionally negative events, is well known (Aston-Jones & Cohen, 2005; Bari et al., 2020; Berridge & Waterhouse, 2003; Clewett et al., 2016; Hämmerer et al., 2018; Jacobs et al., 2020; Lee et al., 2018b; Mather et al., 2016b; Samuels & Szabadi, 2008; Sara & Bouret, 2012), the broader network of cognitive and sensory processes leading to pupil dilation under these conditions is complex and not fully understood. Factors such as VN activity, attentional capture, and sensory perception may indirectly influence LC, but they might also affect pupil size and cognitive processes through additional pathways. Given the susceptibility of pupillometry to the sensations of taVNS, a more direct method could be functional fMRI during taVNS, which,

however, could also be affected by attention modulations and different sensations. Further research could build up on my findings, including combined high-resolution fMRI taVNS studies and appropriate post-processing methods for small structures in the brainstem, to elucidate the mechanisms of taVNS and clarify the specific contributions of the LC and other neuronal structures to pupil dilation. Additionally, changes in the effects of NE release during external modulation of NE via taVNS should be considered, particularly regarding the perception of sensations due to stimulation.

8 References

Akaike, T. (1982). Periodic bursting activities of locus coeruleus neurons in the rat. *Brain Research*, *239*(2), 629–633. https://doi.org/10.1016/0006-8993(82)90540-6

Andrés-Benito, P., Fernández-Dueñas, V., Carmona, M., Escobar, L. A., Torrejón-Escribano, B., Aso, E., Ciruela, F., & Ferrer, I. (2017). Locus coeruleus at asymptomatic early and middle Braak stages of neurofibrillary tangle pathology. *Neuropathology and Applied Neurobiology*, *43*(5), 373–392. https://doi.org/10.1111/nan.12386

Ardell, J. L., & Randall, W. C. (1986). Selective vagal innervation of sinoatrial and atrioventricular nodes in canine heart. *American Journal of Physiology-Heart and Circulatory Physiology*, *251*(4), H764–H773. https://doi.org/10.1152/ajpheart.1986.251.4.H764

Arnsten, A., & Goldman-Rakic, P. (1985). Alpha 2-adrenergic mechanisms in prefrontal cortex associated with cognitive decline in aged nonhuman primates. *Science*, *230*(4731), 1273–1276. https://doi.org/10.1126/science.2999977

Aron, L., Zullo, J., & Yankner, B. A. (2022). The adaptive aging brain. *Current Opinion in Neurobiology*, *72*, 91–100. https://doi.org/10.1016/j.conb.2021.09.009

Aston-Jones, G., & Bloom, F. E. (1981). Activity of norepinephrine-containing locus coeruleus neurons in behaving rats anticipates fluctuations in the sleep-waking cycle. *Journal of Neuroscience*, *1*(8), 876–886. https://doi.org/10.1523/JNEUROSCI.01-08-00876.1981

Aston-Jones, G., & Cohen, J. D. (2005). AN INTEGRATIVE THEORY OF LOCUS COERULEUS-NOREPINEPHRINE FUNCTION: Adaptive Gain and Optimal Performance. *Annual Review of Neuroscience*, *28*(1), 403–450. https://doi.org/10.1146/annurev.neuro.28.061604.135709

Aston-Jones, G., Rajkowski, J., & Kubiak, P. (1997). Conditioned responses of monkey locus coeruleus neurons anticipate acquisition of discriminative behavior in a vigilance task. *Neuroscience*, *80*(3), 697–715. https://doi.org/10.1016/s0306-4522(97)00060-2

Aston-Jones, G., Rajkowski, J., Kubiak, P., & Alexinsky, T. (1994). Locus coeruleus neurons in monkey are selectively activated by attended cues in a vigilance task. *The Journal of Neuroscience: The Official Journal of the Society for Neuroscience*, *14*(7), 4467–4480. https://doi.org/10.1523/JNEUROSCI.14-07-04467.1994

Aston-Jones, G., Shipley, M. T., Chouvet, G., Ennis, M., van Bockstaele, E., Pieribone, V., Shiekhattar, R., Akaoka, H., Drolet, G., & Astier, B. (1991). Afferent regulation of locus coeruleus neurons: Anatomy, physiology and pharmacology. *Progress in Brain Research*, *88*, 47–75. https://doi.org/10.1016/s0079-6123(08)63799-1

Bachman, S. L., Dahl, M. J., Werkle-Bergner, M., Düzel, S., Forlim, C. G., Lindenberger, U., Kühn, S., & Mather, M. (2020). *Locus coeruleus MRI contrast is associated with cortical thickness in older adults* [Preprint]. Neuroscience. https://doi.org/10.1101/2020.03.14.991596

Badran, B. W., Dowdle, L. T., Mithoefer, O. J., LaBate, N. T., Coatsworth, J., Brown, J. C., DeVries, W. H., Austelle, C. W., McTeague, L. M., & George, M. S. (2018). Neurophysiologic effects of transcutaneous auricular vagus nerve stimulation (taVNS) via electrical stimulation of the tragus: A concurrent taVNS/fMRI study and review. *Brain Stimulation*, *11*(3), 492–500. https://doi.org/10.1016/j.brs.2017.12.009

Baker, K. G., Törk, I., Hornung, J.-P., & Halasz, P. (1989). The human locus coeruleus complex: An immunohistochemical and three dimensional reconstruction study. *Experimental Brain Research*, *77*(2), 257–270. https://doi.org/10.1007/BF00274983

Bari, A., Xu, S., Pignatelli, M., Takeuchi, D., Feng, J., Li, Y., & Tonegawa, S. (2020). Differential attentional control mechanisms by two distinct noradrenergic coeruleo frontal cortical pathways. *Proceedings of the National Academy of Sciences*, *117*(46), 29080–29089. https://doi.org/10.1073/pnas.2015635117

Bates, D., Mächler, M., Bolker, B., & Walker, S. (2015). Fitting Linear Mixed-Effects Models

Using **lme4**. *Journal of Statistical Software*, *67*(1). https://doi.org/10.18637/jss.v067.i01

Bauer, S., Baier, H., Baumgartner, C., Bohlmann, K., Fauser, S., Graf, W., Hillenbrand, B., Hirsch, M., Last, C., Lerche, H., Mayer, T., Schulze-Bonhage, A., Steinhoff, B. J., Weber, Y., Hartlep, A., Rosenow, F., & Hamer, H. M. (2016). Transcutaneous Vagus Nerve Stimulation (tVNS) for Treatment of Drug-Resistant Epilepsy: A Randomized, Double-Blind Clinical Trial (cMPsE02). *Brain Stimulation*, *9*(3), 356–363. https://doi.org/10.1016/j.brs.2015.11.003

Beardmore, R., Hou, R., Darekar, A., Holmes, C., & Boche, D. (2021). The Locus Coeruleus in Aging and Alzheimer's Disease: A Postmortem and Brain Imaging Review. *Journal of Alzheimer's Disease*, *83*(1), 5–22. https://doi.org/10.3233/JAD-210191

Beas, B. S., Wright, B. J., Skirzewski, M., Leng, Y., Hyun, J. H., Koita, O., Ringelberg, N., Kwon, H.-B., Buonanno, A., & Penzo, M. A. (2018). The locus coeruleus drives disinhibition in the midline thalamus via a dopaminergic mechanism. *Nature Neuroscience*, *21*(7), 963–973. https://doi.org/10.1038/s41593-018-0167-4

Bekar, L. K., Wei, H. S., & Nedergaard, M. (2012). The Locus Coeruleus-Norepinephrine Network Optimizes Coupling of Cerebral Blood Volume with Oxygen Demand. *Journal of Cerebral Blood Flow & Metabolism*, *32*(12), 2135–2145. https://doi.org/10.1038/jcbfm.2012.115

Ben-Menachem, E., Hamberger, A., Hedner, T., Hammond, E. J., Uthman, B. M., Slater, J., Treig, T., Stefan, H., Ramsay, R. E., Wernicke, J. F., & Wilder, B. J. (1995). Effects of vagus nerve stimulation on amino acids and other metabolites in the CSF of patients with partial seizures. *Epilepsy Research*, *20*(3), 221–227. https://doi.org/10.1016/0920 1211(94)00083-9

Berger, A., Koshmanova, E., Beckers, E., Sharifpour, R., Paparella, I., Campbell, I., Mortazavi, N., Balda, F., Yi, Y.-J., Lamalle, L., Dricot, L., Phillips, C., Jacobs, H. I. L., Talwar, P., El Tahry, R., Sherif, S., & Vandewalle, G. (2023). Structural and functional characterization of the locus coeruleus in young and late middle-aged individuals. *Frontiers in Neuroimaging*, *2*. https://www.frontiersin.org/articles/10.3389/fnimg.2023.1207844

Bermejo, P., López, M., Larraya, I., Chamorro, J., Cobo, J. L., Ordóñez, S., & Vega, J. A. (2017). Innervation of the Human Cavum Conchae and Auditory Canal: Anatomical Basis for Transcutaneous Auricular Nerve Stimulation. *BioMed Research International*, *2017*, 1–10. https://doi.org/10.1155/2017/7830919

Bernard, R., Kerman, I. A., Thompson, R. C., Jones, E. G., Bunney, W. E., Barchas, J. D., Schatzberg, A. F., Myers, R. M., Akil, H., & Watson, S. J. (2011). Altered expression of glutamate signaling, growth factor and glia genes in the locus coeruleus of patients with major depression. *Molecular Psychiatry*, *16*(6), 634–646. https://doi.org/10.1038/mp.2010.44

Berridge, C. W., & Abercrombie, E. D. (1999). Relationship between locus coeruleus discharge rates and rates of norepinephrine release within neocortex as assessed by in vivo microdialysis. *Neuroscience*, *93*(4), 1263–1270. https://doi.org/10.1016/s0306 4522(99)00276-6

Berridge, C. W., & Waterhouse, B. D. (2003). The locus coeruleus–noradrenergic system: Modulation of behavioral state and state-dependent cognitive processes. *Brain Research Reviews*, *42*(1), 33–84. https://doi.org/10.1016/S0165-0173(03)00143-7

Berthoud, H. R., & Neuhuber, W. L. (2000). Functional and chemical anatomy of the afferent vagal system. *Autonomic Neuroscience: Basic & Clinical*, *85*(1–3), 1–17. https://doi.org/10.1016/S1566-0702(00)00215-0

Betts, M. J., Cardenas-Blanco, A., Kanowski, M., Jessen, F., & Düzel, E. (2017). In vivo MRI assessment of the human locus coeruleus along its rostrocaudal extent in young and

older adults. *NeuroImage*, *163*, 150–159. https://doi.org/10.1016/j.neuroimage.2017.09.042

Betts, M. J., Kirilina, E., Otaduy, M. C. G., Ivanov, D., Acosta-Cabronero, J., Callaghan, M. F., Lambert, C., Cardenas-Blanco, A., Pine, K., Passamonti, L., Loane, C., Keuken, M. C., Trujillo, P., Lüsebrink, F., Mattern, H., Liu, K. Y., Priovoulos, N., Fliessbach, K., Dahl, M. J., … Hämmerer, D. (2019). Locus coeruleus imaging as a biomarker for noradrenergic dysfunction in neurodegenerative diseases. *Brain*, *142*(9), 2558–2571. https://doi.org/10.1093/brain/awz193

Bianca, R., & Komisaruk, B. R. (2007). Pupil dilatation in response to vagal afferent electrical stimulation is mediated by inhibition of parasympathetic outflow in the rat. *Brain Research*, *1177*, 29–36. https://doi.org/10.1016/j.brainres.2007.06.104

Bonaz, B., Sinniger, V., & Pellissier, S. (2017). The Vagus Nerve in the Neuro-Immune Axis: Implications in the Pathology of the Gastrointestinal Tract. *Frontiers in Immunology*, *8*, 1452. https://doi.org/10.3389/fimmu.2017.01452

Bondareff, W., Mountjoy, C. Q., Roth, M., Rossor, M. N., Iversen, L. L., Reynolds, G. P., & Hauser, D. L. (1987). Neuronal degeneration in locus ceruleus and cortical correlates of Alzheimer disease. *Alzheimer Disease and Associated Disorders*, *1*(4), 256–262. https://doi.org/10.1097/00002093-198701040-00005

Borges, U., Laborde, S., & Raab, M. (2019). Influence of transcutaneous vagus nerve stimulation on cardiac vagal activity: Not different from sham stimulation and no effect of stimulation intensity. *PloS One*, *14*(10), e0223848. https://doi.org/10.1371/journal.pone.0223848

Borges, U., Pfannenstiel, M., Tsukahara, J., Laborde, S., Klatt, S., & Raab, M. (2021). Transcutaneous vagus nerve stimulation via tragus or cymba conchae: Are its psychophysiological effects dependent on the stimulation area? *International Journal of Psychophysiology*, *161*, 64–75. https://doi.org/10.1016/j.ijpsycho.2021.01.003

Borland, M. S., Vrana, W. A., Moreno, N. A., Fogarty, E. A., Buell, E. P., Sharma, P., Engineer, C. T., & Kilgard, M. P. (2016). Cortical Map Plasticity as a Function of Vagus Nerve Stimulation Intensity. *Brain Stimulation*, *9*(1), 117–123. https://doi.org/10.1016/j.brs.2015.08.018

Bouret, S., & Richmond, B. J. (2009). Relation of Locus Coeruleus Neurons in Monkeys to Pavlovian and Operant Behaviors. *Journal of Neurophysiology*, *101*(2), 898–911. https://doi.org/10.1152/jn.91048.2008

Bouret, S., & Sara, S. J. (2004). Reward expectation, orientation of attention and locus coeruleus-medial frontal cortex interplay during learning. *European Journal of Neuroscience*, *20*(3), 791–802. https://doi.org/10.1111/j.1460-9568.2004.03526.x

Bouret, S., & Sara, S. J. (2005). Network reset: A simplified overarching theory of locus coeruleus noradrenaline function. *Trends in Neurosciences*, *28*(11), 574–582. https://doi.org/10.1016/j.tins.2005.09.002

Braak, H., Thal, D. R., Ghebremedhin, E., & Del Tredici, K. (2011). Stages of the Pathologic Process in Alzheimer Disease: Age Categories From 1 to 100 Years. *Journal of Neuropathology & Experimental Neurology*, *70*(11), 960–969. https://doi.org/10.1097/NEN.0b013e318232a379

Braak, H., Tredici, K. D., Rüb, U., de Vos, R. A. I., Jansen Steur, E. N. H., & Braak, E. (2003). Staging of brain pathology related to sporadic Parkinson's disease. *Neurobiology of Aging*, *24*(2), 197–211. https://doi.org/10.1016/S0197-4580(02)00065-9

Braem, S., Coenen, E., Bombeke, K., van Bochove, M. E., & Notebaert, W. (2015). Open your eyes for prediction errors. *Cognitive, Affective, & Behavioral Neuroscience*, *15*(2), 374 380. https://doi.org/10.3758/s13415-014-0333-4

Breton-Provencher, V., Drummond, G. T., & Sur, M. (2021). Locus Coeruleus Norepinephrine in Learned Behavior: Anatomical Modularity and Spatiotemporal Integration in Targets.

Frontiers in Neural Circuits, *15*. https://www.frontiersin.org/articles/10.3389/fncir.2021.638007

Breton-Provencher, V., & Sur, M. (2019). Active control of arousal by a locus coeruleus GABAergic circuit. *Nature Neuroscience*, *22*(2), 218–228. https://doi.org/10.1038/s41593-018-0305-z

Bridelli, M. G., Tampellini, D., & Zecca, L. (1999). The structure of neuromelanin and its iron binding site studied by infrared spectroscopy. *FEBS Letters*, *457*(1), 18–22. https://doi.org/10.1016/s0014-5793(99)01001-7

Brodin, P. (1985). DIfferential inhibition of A, B and C fibres in the rat vagus nerve by lidocaine, eugenol and formaldehyde. *Archives of Oral Biology*, *30*(6), 477–480. https://doi.org/10.1016/0003-9969(85)90093-7

Brooks, J., Faull, O., Pattinson, K., & Jenkinson, M. (2013). Physiological Noise in Brainstem fMRI. *Frontiers in Human Neuroscience*, *7*, 623. https://doi.org/10.3389/fnhum.2013.00623

Burger, A. M., D'Agostini, M., Verkuil, B., & Van Diest, I. (2020). Moving beyond belief: A narrative review of potential biomarkers for transcutaneous vagus nerve stimulation. *Psychophysiology*, *57*(6), e13571. https://doi.org/10.1111/psyp.13571

Bush, W. D., Garguilo, J., Zucca, F. A., Albertini, A., Zecca, L., Edwards, G. S., Nemanich, R. J., & Simon, J. D. (2006). The surface oxidation potential of human neuromelanin reveals a spherical architecture with a pheomelanin core and a eumelanin surface. *Proceedings of the National Academy of Sciences of the United States of America*, *103*(40), 14785–14789. https://doi.org/10.1073/pnas.0604010103

Butt, M. F., Albusoda, A., Farmer, A. D., & Aziz, Q. (2020). The anatomical basis for transcutaneous auricular vagus nerve stimulation. *Journal of Anatomy*, *236*(4), 588–611. https://doi.org/10.1111/joa.13122

Cahill, L., Babinsky, R., Markowitsch, H. J., & McGaugh, J. L. (1995). The amygdala and emotional memory. *Nature*, *377*(6547), Article 6547. https://doi.org/10.1038/377295a0

Cakmak, Y. O. (2019). Concerning Auricular Vagal Nerve Stimulation: Occult Neural Networks. *Frontiers in Human Neuroscience*, *13*, 421. https://doi.org/10.3389/fnhum.2019.00421

Cakmak, Y. O., Cotofana, S., Jäger, C., Morawski, M., Sora, M.-C., Werner, M., & Hammer, N. (2018). Peri-arterial Autonomic Innervation of the Human Ear. *Scientific Reports*, *8*(1), 11469. https://doi.org/10.1038/s41598-018-29839-z

Campbell, H. L., Tivarus, M. E., Hillier, A., & Beversdorf, D. Q. (2008). Increased task difficulty results in greater impact of noradrenergic modulation of cognitive flexibility. *Pharmacology, Biochemistry, and Behavior*, *88*(3), 222–229. https://doi.org/10.1016/j.pbb.2007.08.003

Carpenter, L. L., Moreno, F. A., Kling, M. A., Anderson, G. M., Regenold, W. T., Labiner, D. M., & Price, L. H. (2004). Effect of vagus nerve stimulation on cerebrospinal fluid monoamine metabolites, norepinephrine, and gamma-aminobutyric acid concentrations in depressed patients. *Biological Psychiatry*, *56*(6), 418–426. https://doi.org/10.1016/j.biopsych.2004.06.025

Cazettes, F., Reato, D., Morais, J. P., Renart, A., & Mainen, Z. F. (2021). Phasic Activation of Dorsal Raphe Serotonergic Neurons Increases Pupil Size. *Current Biology*, *31*(1), 192 197.e4. https://doi.org/10.1016/j.cub.2020.09.090

Cedarbaum, J. M., & Aghajanian, G. K. (1978). Afferent projections to the rat locus coeruleus as determined by a retrograde tracing technique. *The Journal of Comparative Neurology*, *178*(1), 1–16. https://doi.org/10.1002/cne.901780102

Chamberlain, S. R., Müller, U., Blackwell, A. D., Robbins, T. W., & Sahakian, B. J. (2006). Noradrenergic modulation of working memory and emotional memory in humans. *Psychopharmacology*, *188*(4), 397–407. https://doi.org/10.1007/s00213-006-0391-6

Chamberlain, S. R., & Robbins, T. W. (2013). Noradrenergic modulation of cognition: Therapeutic implications. *Journal of Psychopharmacology (Oxford, England)*, *27*(8), 694–718. https://doi.org/10.1177/0269881113480988

Chang, Y.-C., Cracchiolo, M., Ahmed, U., Mughrabi, I., Gabalski, A., Daytz, A., Rieth, L., Becker, L., Datta-Chaudhuri, T., Al-Abed, Y., Zanos, T. P., & Zanos, S. (2020). Quantitative estimation of nerve fiber engagement by vagus nerve stimulation using physiological markers. *Brain Stimulation*, *13*(6), 1617–1630. https://doi.org/10.1016/j.brs.2020.09.002

Chan-Palay, V., & Asan, E. (1989). Quantitation of catecholamine neurons in the locus coeruleus in human brains of normal young and older adults and in depression. *The Journal of Comparative Neurology*, *287*(3), 357–372. https://doi.org/10.1002/cne.902870307

Charles, S. T., Mather, M., & Carstensen, L. L. (2003). Aging and emotional memory: The forgettable nature of negative images for older adults. *Journal of Experimental Psychology: General*, *132*(2), 310–324. https://doi.org/10.1037/0096-3445.132.2.310

Charney, D. S., Grillon, C., & Bremner, J. D. (1998). Review: The Neurobiological Basis of Anxiety and Fear: Circuits, Mechanisms, and Neurochemical Interactions (Part I. *The Neuroscientist*, *4*(1), 35–44. https://doi.org/10.1177/107385849800400111

Chen, F.-J., & Sara, S. J. (2007). Locus coeruleus activation by foot shock or electrical stimulation inhibits amygdala neurons. *Neuroscience*, *144*(2), 472–481. https://doi.org/10.1016/j.neuroscience.2006.09.037

Clark, K. B., Smith, D. C., Hassert, D. L., Browning, R. A., Naritoku, D. K., & Jensen, R. A. (1998). Posttraining Electrical Stimulation of Vagal Afferents with Concomitant Vagal Efferent Inactivation Enhances Memory Storage Processes in the Rat. *Neurobiology of Learning and Memory*, *70*(3), 364–373. https://doi.org/10.1006/nlme.1998.3863

Clayton, E. C., Rajkowski, J., Cohen, J. D., & Aston-Jones, G. (2004). Phasic activation of monkey locus ceruleus neurons by simple decisions in a forced-choice task. *The Journal of Neuroscience: The Official Journal of the Society for Neuroscience*, *24*(44), 9914 9920. https://doi.org/10.1523/JNEUROSCI.2446-04.2004

Clewett, D. V., Huang, R., Velasco, R., Lee, T.-H., & Mather, M. (2018). Locus Coeruleus Activity Strengthens Prioritized Memories Under Arousal. *The Journal of Neuroscience*, *38*(6), 1558–1574. https://doi.org/10.1523/JNEUROSCI.2097-17.2017

Clewett, D. V., Lee, T.-H., Greening, S., Ponzio, A., Margalit, E., & Mather, M. (2016). Neuromelanin marks the spot: Identifying a locus coeruleus biomarker of cognitive reserve in healthy aging. *Neurobiology of Aging*, *37*, 117–126. https://doi.org/10.1016/j.neurobiolaging.2015.09.019

Collins, L., Boddington, L., Steffan, P. J., & McCormick, D. (2021). Vagus nerve stimulation induces widespread cortical and behavioral activation. *Current Biology*, *31*(10), 2088 2098.e3. https://doi.org/10.1016/j.cub.2021.02.049

Colzato, L., & Beste, C. (2020). A literature review on the neurophysiological underpinnings and cognitive effects of transcutaneous vagus nerve stimulation: Challenges and future directions. *Journal of Neurophysiology*, *123*(5), 1739–1755. https://doi.org/10.1152/jn.00057.2020

Corbetta, M., Patel, G., & Shulman, G. L. (2008). The Reorienting System of the Human Brain: From Environment to Theory of Mind. *Neuron*, *58*(3), 306–324. https://doi.org/10.1016/j.neuron.2008.04.017

Coull, J. T., Middleton, H. C., Robbins, T. W., & Sahakian, B. J. (1995). Contrasting effects of clonidine and diazepam on tests of working memory and planning. *Psychopharmacology*, *120*(3), 311–321. https://doi.org/10.1007/BF02311179

Cowen, D. (1986). The melanoneurons of the human cerebellum (nucleus pigmentosus cerebellaris) and homologues in the monkey. *Journal of Neuropathology and*

Experimental Neurology, *45*(3), 205–221.
Cristancho, P., Cristancho, M. A., Baltuch, G. H., Thase, M. E., & O'Reardon, J. P. (2011). Effectiveness and safety of vagus nerve stimulation for severe treatment-resistant major depression in clinical practice after FDA approval: Outcomes at 1 year. *The Journal of Clinical Psychiatry*, *72*(10), 1376–1382. https://doi.org/10.4088/JCP.09m05888blu
Dabiri, B., Zeiner, K., Nativel, A., & Kaniusas, E. (2022). Auricular vagus nerve stimulator for closed-loop biofeedback-based operation. *Analog Integrated Circuits and Signal Processing*, *112*(2), 237–246. https://doi.org/10.1007/s10470-022-02037-8
D'Agostini, M., Burger, A. M., Franssen, M., Perkovic, A., Claes, S., von Leupoldt, A., Murphy, P. R., & Van Diest, I. (2023). Short bursts of transcutaneous auricular vagus nerve stimulation enhance evoked pupil dilation as a function of stimulation parameters. *Cortex*, *159*, 233–253. https://doi.org/10.1016/j.cortex.2022.11.012
Dahl, M. J., Mather, M., Düzel, S., Bodammer, N. C., Lindenberger, U., Kühn, S., & Werkle Bergner, M. (2019). Higher rostral locus coeruleus integrity is associated with better memory performance in older adults. *Nature Human Behaviour*, *3*(11), 1203–1214. https://doi.org/10.1038/s41562-019-0715-2
Dahl, M. J., Mather, M., Werkle-Bergner, M., Kennedy, B. L., Guzman, S., Hurth, K., Miller, C. A., Qiao, Y., Shi, Y., Chui, H. C., & Ringman, J. M. (2022). Locus coeruleus integrity is related to tau burden and memory loss in autosomal-dominant Alzheimer's disease. *Neurobiology of Aging*, *112*, 39–54. https://doi.org/10.1016/j.neurobiolaging.2021.11.006
Dan-Glauser, E. S., & Scherer, K. R. (2011). The Geneva Affective Picture Database (GAPED): A new 730-picture database focusing on valence and normative significance. *Behavior Research Methods*, *43*(2), 468–477. https://doi.org/10.3758/s13428-011-0064-1
Daubner, S. C., Le, T., & Wang, S. (2011). Tyrosine Hydroxylase and Regulation of Dopamine Synthesis. *Archives of Biochemistry and Biophysics*, *508*(1), 1–12. https://doi.org/10.1016/j.abb.2010.12.017
David, M. C. B., Del Giovane, M., Liu, K. Y., Gostick, B., Rowe, J. B., Oboh, I., Howard, R., & Malhotra, P. A. (2022). Cognitive and neuropsychiatric effects of noradrenergic treatment in Alzheimer's disease: Systematic review and meta-analysis. *Journal of Neurology, Neurosurgery, and Psychiatry*, *93*(10), 1080–1090. https://doi.org/10.1136/jnnp-2022-329136
Dayan, P., & Yu, A. J. (2005). *Norepinephrine and Neural Interrupts*.
De Couck, M., Cserjesi, R., Caers, R., Zijlstra, W. P., Widjaja, D., Wolf, N., Luminet, O., Ellrich, J., & Gidron, Y. (2017). Effects of short and prolonged transcutaneous vagus nerve stimulation on heart rate variability in healthy subjects. *Autonomic Neuroscience: Basic & Clinical*, *203*, 88–96. https://doi.org/10.1016/j.autneu.2016.11.003
de Gee, J. W., Colizoli, O., Kloosterman, N. A., Knapen, T., Nieuwenhuis, S., & Donner, T. H. (2017). Dynamic modulation of decision biases by brainstem arousal systems. *eLife*, *6*, e23232. https://doi.org/10.7554/eLife.23232
De Taeye, L., Vonck, K., van Bochove, M., Boon, P., Van Roost, D., Mollet, L., Meurs, A., De Herdt, V., Carrette, E., Dauwe, I., Gadeyne, S., van Mierlo, P., Verguts, T., & Raedt, R. (2014). The P3 event-related potential is a biomarker for the efficacy of vagus nerve stimulation in patients with epilepsy. *Neurotherapeutics: The Journal of the American Society for Experimental NeuroTherapeutics*, *11*(3), 612–622. https://doi.org/10.1007/s13311-014-0272-3
DeMattei, M., Levi, A. C., & Fariello, R. G. (1986). Neuromelanic pigment in substantia nigra neurons of rats and dogs. *Neuroscience Letters*, *72*(1), 37–42. https://doi.org/10.1016/0304-3940(86)90614-2
Desbeaumes Jodoin, V., Richer, F., Miron, J.-P., Fournier-Gosselin, M.-P., & Lespérance, P. (2018). Long-term Sustained Cognitive Benefits of Vagus Nerve Stimulation in

Refractory Depression. *The Journal of ECT*, *34*(4), 283–290. https://doi.org/10.1097/YCT.0000000000000502

D'Esposito, M., Deouell, L. Y., & Gazzaley, A. (2003). Alterations in the BOLD fMRI signal with ageing and disease: A challenge for neuroimaging. *Nature Reviews Neuroscience*, *4*(11), Article 11. https://doi.org/10.1038/nrn1246

Deutch, A. Y., Goldstein, M., & Roth, R. H. (1986). Activation of the locus coeruleus induced by selective stimulation of the ventral tegmental area. *Brain Research*, *363*(2), 307–314. https://doi.org/10.1016/0006-8993(86)91016-4

Devilbiss, D. M., & Waterhouse, B. D. (2011). Phasic and Tonic Patterns of Locus Coeruleus Output Differentially Modulate Sensory Network Function in the Awake Rat. *Journal of Neurophysiology*, *105*(1), 69–87. https://doi.org/10.1152/jn.00445.2010

Devoto, P., & Flore, G. (2006). On the Origin of Cortical Dopamine: Is it a Co-Transmitter in Noradrenergic Neurons? *Current Neuropharmacology*, *4*(2), 115–125.

Devoto, P., Flore, G., Pani, L., & Gessa, G. L. (2001). Evidence for co-release of noradrenaline and dopamine from noradrenergic neurons in the cerebral cortex. *Molecular Psychiatry*, *6*(6), 657–664. https://doi.org/10.1038/sj.mp.4000904

Devoto, P., Flore, G., Saba, P., Fà, M., & Gessa, G. L. (2005). Stimulation of the locus coeruleus elicits noradrenaline and dopamine release in the medial prefrontal and parietal cortex. *Journal of Neurochemistry*, *92*(2), 368–374. https://doi.org/10.1111/j.1471 4159.2004.02866.x

Dietrichs, E. (1988). Cerebellar cortical and nuclear afferents from the feline locus coeruleus complex. *Neuroscience*, *27*(1), 77–91. https://doi.org/10.1016/0306-4522(88)90220-5

Dorr, A. E., & Debonnel, G. (2006). Effect of Vagus Nerve Stimulation on Serotonergic and Noradrenergic Transmission. *Journal of Pharmacology and Experimental Therapeutics*, *318*(2), 890–898. https://doi.org/10.1124/jpet.106.104166

Duszkiewicz, A. J., McNamara, C. G., Takeuchi, T., & Genzel, L. (2019). Novelty and Dopaminergic Modulation of Memory Persistence: A Tale of Two Systems. *Trends in Neurosciences*, *42*(2), 102–114. https://doi.org/10.1016/j.tins.2018.10.002

Dutt, S., Bachman, S. L., Dahl, M. J., Li, Y., Yew, B., Jang, J. Y., Ho, J. K., Nashiro, K., Min, J., Yoo, H. J., Gaubert, A., Nguyen, A., Blanken, A. E., Sible, I. J., Marshall, A. J., Kapoor, A., Alitin, J. P. M., Hoang, K., Rouanet, J., … Nation, D. A. (2024). Locus coeruleus MRI contrast, cerebral perfusion, and plasma Alzheimer's disease biomarkers in older adults. *Neurobiology of Aging*, S0197458024002008. https://doi.org/10.1016/j.neurobiolaging.2024.11.008

Eckstein, M. K., Guerra-Carrillo, B., Miller Singley, A. T., & Bunge, S. A. (2017). Beyond eye gaze: What else can eyetracking reveal about cognition and cognitive development? *Developmental Cognitive Neuroscience*, *25*, 69–91. https://doi.org/10.1016/j.dcn.2016.11.001

Ehrenberg, A. J., Kelberman, M. A., Liu, K. Y., Dahl, M. J., Weinshenker, D., Falgàs, N., Dutt, S., Mather, M., Ludwig, M., Betts, M. J., Winer, J. R., Teipel, S., Weigand, A. J., Eschenko, O., Hämmerer, D., Leiman, M., Counts, S. E., Shine, J. M., Robertson, I. H., … Grinberg, L. T. (2023). Priorities for research on neuromodulatory subcortical systems in Alzheimer's disease: Position paper from the NSS PIA of ISTAART. *Alzheimer's & Dementia*, alz.12937. https://doi.org/10.1002/alz.12937

Eisenhofer, G., Kopin, I. J., & Goldstein, D. S. (2004). Catecholamine Metabolism: A Contemporary View with Implications for Physiology and Medicine. *Pharmacological Reviews*, *56*(3), 331–349. https://doi.org/10.1124/pr.56.3.1

Eldar, E., Cohen, J. D., & Niv, Y. (2013). The effects of neural gain on attention and learning. *Nature Neuroscience*, *16*(8), 1146–1153. https://doi.org/10.1038/nn.3428

Engels-Domínguez, N., Koops, E. A., Prokopiou, P. C., Van Egroo, M., Schneider, C., Riphagen, J. M., Singhal, T., & Jacobs, H. I. L. (2023). State-of-the-art imaging of

neuromodulatory subcortical systems in aging and Alzheimer's disease: Challenges and opportunities. *Neuroscience & Biobehavioral Reviews*, *144*, 104998. https://doi.org/10.1016/j.neubiorev.2022.104998

Engineer, N. D., Riley, J. R., Seale, J. D., Vrana, W. A., Shetake, J. A., Sudanagunta, S. P., Borland, M. S., & Kilgard, M. P. (2011). Reversing pathological neural activity using targeted plasticity. *Nature*, *470*(7332), 101–104. https://doi.org/10.1038/nature09656

Englot, D. J., Chang, E. F., & Auguste, K. I. (2011). Vagus nerve stimulation for epilepsy: A meta-analysis of efficacy and predictors of response. *Journal of Neurosurgery*, *115*(6), 1248–1255. https://doi.org/10.3171/2011.7.JNS11977

Enochs, W. S., Hyslop, W. B., Bennett, H. F., Brown, R. D., Koenig, S. H., & Swartz, H. M. (1989). Sources of the increased longitudinal relaxation rates observed in melanotic melanoma. An in vitro study of synthetic melanins. *Investigative Radiology*, *24*(10), 794–804. https://doi.org/10.1097/00004424-198910000-00014

Enochs, W. S., Petherick, P., Bogdanova, A., Mohr, U., & Weissleder, R. (1997). Paramagnetic metal scavenging by melanin: MR imaging. *Radiology*, *204*(2), 417–423. https://doi.org/10.1148/radiology.204.2.9240529

Eppinger, B., & Kray, J. (2011). To Choose or to Avoid: Age Differences in Learning from Positive and Negative Feedback. *Journal of Cognitive Neuroscience*, *23*(1), 41–52. https://doi.org/10.1162/jocn.2009.21364

Eschenko, O., Evrard, H. C., Neves, R. M., Beyerlein, M., Murayama, Y., & Logothetis, N. K. (2012). Tracing of noradrenergic projections using manganese-enhanced MRI. *NeuroImage*, *59*(4), 3252–3265. https://doi.org/10.1016/j.neuroimage.2011.11.031

Evans, M. S., Verma-Ahuja, S., Naritoku, D. K., & Espinosa, J. A. (2004). Intraoperative human vagus nerve compound action potentials. *Acta Neurologica Scandinavica*, *110*(4), 232–238. https://doi.org/10.1111/j.1600-0404.2004.00309.x

Farmer, A. D., Strzelczyk, A., Finisguerra, A., Gourine, A. V., Gharabaghi, A., Hasan, A., Burger, A. M., Jaramillo, A. M., Mertens, A., Majid, A., Verkuil, B., Badran, B. W., Ventura-Bort, C., Gaul, C., Beste, C., Warren, C. M., Quintana, D. S., Hämmerer, D., Freri, E., … Koenig, J. (2021). International Consensus Based Review and Recommendations for Minimum Reporting Standards in Research on Transcutaneous Vagus Nerve Stimulation (Version 2020). *Frontiers in Human Neuroscience*, *14*, 568051. https://doi.org/10.3389/fnhum.2020.568051

Fedorow, H., Halliday, G. M., Rickert, C. H., Gerlach, M., Riederer, P., & Double, K. L. (2006). Evidence for specific phases in the development of human neuromelanin. *Neurobiology of Aging*, *27*(3), 506–512. https://doi.org/10.1016/j.neurobiolaging.2005.02.015

Fedorow, H., Tribl, F., Halliday, G., Gerlach, M., Riederer, P., & Double, K. L. (2005). Neuromelanin in human dopamine neurons: Comparison with peripheral melanins and relevance to Parkinson's disease. *Progress in Neurobiology*, *75*(2), 109–124. https://doi.org/10.1016/j.pneurobio.2005.02.001

Feinstein, D. L., Heneka, M. T., Gavrilyuk, V., Russo, C. D., Weinberg, G., & Galea, E. (2002). Noradrenergic regulation of inflammatory gene expression in brain. *Neurochemistry International*, *41*(5), 357–365. https://doi.org/10.1016/S0197-0186(02)00049-9

Feinstein, D. L., Kalinin, S., & Braun, D. (2016). Causes, consequences, and cures for neuroinflammation mediated via the locus coeruleus: Noradrenergic signaling system. *Journal of Neurochemistry*, *139*(S2), 154–178. https://doi.org/10.1111/jnc.13447

Fernandes, P., Regala, J., Correia, F., & Gonçalves-Ferreira, A. J. (2012). The human locus coeruleus 3-D stereotactic anatomy. *Surgical and Radiologic Anatomy*, *34*(10), 879 885. https://doi.org/10.1007/s00276-012-0979-y

Ferstl, M., Teckentrup, V., Lin, W. M., Kräutlein, F., Klaus, J., Walter, M., & Kroemer, N. B. (2022). *Non-invasive vagus nerve stimulation boosts mood recovery after effort exertion*. 26.

Fesharaki, N. J., Taylor, A., Mosby, K., Kim, J. H., & Ress, D. (2023). Global effects of aging on the hemodynamic response function in the human brain. *Research Square*, rs.3.rs 3299293. https://doi.org/10.21203/rs.3.rs-3299293/v1

Florin-Lechner, S. M., Druhan, J. P., Aston-Jones, G., & Valentino, R. J. (1996). Enhanced norepinephrine release in prefrontal cortex with burst stimulation of the locus coeruleus. *Brain Research*, *742*(1–2), 89–97. https://doi.org/10.1016/S0006-8993(96)00967-5

Follesa, P., Biggio, F., Gorini, G., Caria, S., Talani, G., Dazzi, L., Puligheddu, M., Marrosu, F., & Biggio, G. (2007). Vagus nerve stimulation increases norepinephrine concentration and the gene expression of BDNF and bFGF in the rat brain. *Brain Research*, *1179*, 28 34. https://doi.org/10.1016/j.brainres.2007.08.045

Fonov, V., Evans, A. C., Botteron, K., Almli, C. R., McKinstry, R. C., & Collins, D. L. (2011). Unbiased average age-appropriate atlases for pediatric studies. *NeuroImage*, *54*(1), 313–327. https://doi.org/10.1016/j.neuroimage.2010.07.033

Foote, S. L., Aston-Jones, G., & Bloom, F. E. (1980). Impulse activity of locus coeruleus neurons in awake rats and monkeys is a function of sensory stimulation and arousal. *PNAS*, *77*(5), 3033–3037.

Fox, J., Weisberg, S., Price, B., Adler, D., Bates, D., Baud-Bovy, G., Bolker, B., Ellison, S., Firth, D., Friendly, M., Gorjanc, G., Graves, S., Heiberger, R., Krivitsky, P., Laboissiere, R., Maechler, M., Monette, G., Murdoch, D., Nilsson, H., … R-Core. (2023). *car: Companion to Applied Regression* (Version 3.1-2) [Computer software]. https://cran.r-project.org/web/packages/car/

Galgani, A., Lombardo, F., Della Latta, D., Martini, N., Bonuccelli, U., Fornai, F., & Giorgi, F. S. (2021). Locus Coeruleus Magnetic Resonance Imaging in Neurological Diseases. *Current Neurology and Neuroscience Reports*, *21*(1), 2. https://doi.org/10.1007/s11910 020-01087-7

Gallant, S. N., Kennedy, B. L., Bachman, S. L., Huang, R., Cho, C., Lee, T.-H., & Mather, M. (2022). Behavioral and fMRI evidence that arousal enhances bottom-up selectivity in young but not older adults. *Neurobiology of Aging*, *120*, 149–166. https://doi.org/10.1016/j.neurobiolaging.2022.08.006

Garcia, R. G., Lin, R. L., Lee, J., Kim, J., Barbieri, R., Sclocco, R., Wasan, A. D., Edwards, R. R., Rosen, B. R., Hadjikhani, N., & Napadow, V. (2017). Modulation of brainstem activity and connectivity by respiratory-gated auricular vagal afferent nerve stimulation (RAVANS) in migraine patients. *Pain*, *158*(8), 1461–1472. https://doi.org/10.1097/j.pain.0000000000000930

García-Lorenzo, D., Longo-Dos Santos, C., Ewenczyk, C., Leu-Semenescu, S., Gallea, C., Quattrocchi, G., Pita Lobo, P., Poupon, C., Benali, H., Arnulf, I., Vidailhet, M., & Lehericy, S. (2013). The coeruleus/subcoeruleus complex in rapid eye movement sleep behaviour disorders in Parkinson's disease. *Brain: A Journal of Neurology*, *136*(Pt 7), 2120–2129. https://doi.org/10.1093/brain/awt152

Gauthey, A., Morra, S., van de Borne, P., Deriaz, D., Maes, N., & le Polain de Waroux, J.-B. (2020). Sympathetic Effect of Auricular Transcutaneous Vagus Nerve Stimulation on Healthy Subjects: A Crossover Controlled Clinical Trial Comparing Vagally Mediated and Active Control Stimulation Using Microneurography. *Frontiers in Physiology*, *11*, 599896. https://doi.org/10.3389/fphys.2020.599896

German, D. C., Manaye, K. F., White, C. L., Woodward, D. J., McIntire, D. D., Smith, W. K., Kalaria, R. N., & Mann, D. M. (1992). Disease-specific patterns of locus coeruleus cell loss. *Annals of Neurology*, *32*(5), 667–676. https://doi.org/10.1002/ana.410320510

German, D. C., Manaye, K., Smith, W. K., Woodward, D. J., & Saper, C. B. (1989). Midbrain dopaminergic cell loss in parkinson's disease: Computer visualization. *Annals of Neurology*, *26*(4), 507–514. https://doi.org/10.1002/ana.410260403

German, D., Walker, B., Manaye, K., Smith, W., Woodward, D., & North, A. (1988). The

human locus coeruleus: Computer reconstruction of cellular distribution. *The Journal of Neuroscience*, *8*(5), 1776–1788. https://doi.org/10.1523/JNEUROSCI.08-05 01776.1988

Giguère, N., Burke Nanni, S., & Trudeau, L.-E. (2018). On Cell Loss and Selective Vulnerability of Neuronal Populations in Parkinson's Disease. *Frontiers in Neurology*, *9*, 455. https://doi.org/10.3389/fneur.2018.00455

Gilzenrat, M. S., Nieuwenhuis, S., Jepma, M., & Cohen, J. D. (2010). Pupil diameter tracks changes in control state predicted by the adaptive gain theory of locus coeruleus function. *Cognitive, Affective, & Behavioral Neuroscience*, *10*(2), 252–269. https://doi.org/10.3758/CABN.10.2.252

Giorgi, F. S., Galgani, A., Puglisi-Allegra, S., Limanaqi, F., Busceti, C. L., & Fornai, F. (2020). Locus Coeruleus and neurovascular unit: From its role in physiology to its potential role in Alzheimer's disease pathogenesis. *Journal of Neuroscience Research*, *98*(12), 2406 2434. https://doi.org/10.1002/jnr.24718

Goadsby, P. J., Grosberg, B. M., Mauskop, A., Cady, R., & Simmons, K. A. (2014). Effect of noninvasive vagus nerve stimulation on acute migraine: An open-label pilot study. *Cephalalgia: An International Journal of Headache*, *34*(12), 986–993. https://doi.org/10.1177/0333102414524494

Goldstein, D. S. (2021). The Catecholaldehyde Hypothesis for the Pathogenesis of Catecholaminergic Neurodegeneration: What We Know and What We Do Not Know. *International Journal of Molecular Sciences*, *22*(11), 5999. https://doi.org/10.3390/ijms22115999

Guiraud, D., Andreu, D., Bonnet, S., Carrault, G., Couderc, P., Hagège, A., Henry, C., Hernandez, A., Karam, N., Rolle, V. L., Mabo, P., Maciejasz, P., Malbert, C.-H., Marijon, E., Maubert, S., Picq, C., Rossel, O., & Bonnet, J.-L. (2016). Vagus nerve stimulation: State of the art of stimulation and recording strategies to address autonomic function neuromodulation. *Journal of Neural Engineering*, *13*(4), 041002. https://doi.org/10.1088/1741-2560/13/4/041002

Hall, C. A., & Chilcott, R. P. (2018). Eyeing up the Future of the Pupillary Light Reflex in Neurodiagnostics. *Diagnostics*, *8*(1), Article 1. https://doi.org/10.3390/diagnostics8010019

Hämmerer, D., Callaghan, M. F., Hopkins, A., Kosciessa, J., Betts, M., Cardenas-Blanco, A., Kanowski, M., Weiskopf, N., Dayan, P., & Dolan, R. J. (2018). Locus coeruleus integrity in old age is selectively related to memories linked with salient negative events. *Proceedings of the National Academy of Sciences*, *115*(9), 2228–2233.

Hämmerer, D., & Eppinger, B. (2012). Dopaminergic and prefrontal contributions to reward based learning and outcome monitoring during child development and aging. *Developmental Psychology*, *48*(3), 862–874. https://doi.org/10.1037/a0027342

Hämmerer, D., Hopkins, A., Betts, M. J., Maaß, A., Dolan, R. J., & Düzel, E. (2017). Emotional arousal and recognition memory are differentially reflected in pupil diameter responses during emotional memory for negative events in younger and older adults. *Neurobiology of Aging*, *58*, 129–139. https://doi.org/10.1016/j.neurobiolaging.2017.06.021

Hämmerer, D., Schwartenbeck, P., Gallagher, M., FitzGerald, T. H. B., Düzel, E., & Dolan, R. J. (2019). Older adults fail to form stable task representations during model-based reversal inference. *Neurobiology of Aging*, *74*, 90–100. https://doi.org/10.1016/j.neurobiolaging.2018.10.009

Han, W., Tellez, L. A., Perkins, M. H., Perez, I. O., Qu, T., Ferreira, J., Ferreira, T. L., Quinn, D., Liu, Z.-W., Gao, X.-B., Kaelberer, M. M., Bohórquez, D. V., Shammah-Lagnado, S. J., de Lartigue, G., & de Araujo, I. E. (2018). A Neural Circuit for Gut-Induced Reward. *Cell*, *175*(3), 665-678.e23. https://doi.org/10.1016/j.cell.2018.08.049

Hansen, N., & Manahan-Vaughan, D. (2015). Hippocampal long-term potentiation that is

elicited by perforant path stimulation or that occurs in conjunction with spatial learning is tightly controlled by beta-adrenoreceptors and the locus coeruleus. *Hippocampus*, *25*(11), 1285–1298. https://doi.org/10.1002/hipo.22436

Harrell, F. (2025). *Harrelfe/Hmisc* [R]. https://github.com/harrelfe/Hmisc (Original work published 2013)

Hassert, D. L., Miyashita, T., & Williams, C. L. (2004). The Effects of Peripheral Vagal Nerve Stimulation at a Memory-Modulating Intensity on Norepinephrine Output in the Basolateral Amygdala. *Behavioral Neuroscience*, *118*(1), 79–88. https://doi.org/10.1037/0735-7044.118.1.79

Helmers, S. L., Begnaud, J., Cowley, A., Corwin, H. M., Edwards, J. C., Holder, D. L., Kostov, H., Larsson, P. G., Levisohn, P. M., De Menezes, M. S., Stefan, H., & Labiner, D. M. (2012). Application of a computational model of vagus nerve stimulation. *Acta Neurologica Scandinavica*, *126*(5), 336–343. https://doi.org/10.1111/j.1600 0404.2012.01656.x

Heneka, M. T., Carson, M. J., El Khoury, J., Landreth, G. E., Brosseron, F., Feinstein, D. L., Jacobs, A. H., Wyss-Coray, T., Vitorica, J., Ransohoff, R. M., Herrup, K., Frautschy, S. A., Finsen, B., Brown, G. C., Verkhratsky, A., Yamanaka, K., Koistinaho, J., Latz, E., Halle, A., … Kummer, M. P. (2015). Neuroinflammation in Alzheimer's disease. *The Lancet. Neurology*, *14*(4), 388–405. https://doi.org/10.1016/S1474-4422(15)70016-5

Heneka, M. T., Nadrigny, F., Regen, T., Martinez-Hernandez, A., Dumitrescu-Ozimek, L., Terwel, D., Jardanhazi-Kurutz, D., Walter, J., Kirchhoff, F., Hanisch, U.-K., & Kummer, M. P. (2010). Locus ceruleus controls Alzheimer's disease pathology by modulating microglial functions through norepinephrine. *Proceedings of the National Academy of Sciences of the United States of America*, *107*(13), 6058–6063. https://doi.org/10.1073/pnas.0909586107

Henson, R. N., Campbell, K. L., Davis, S. W., Taylor, J. R., Emery, T., Erzinclioglu, S., & Kievit, R. A. (2016). Multiple determinants of lifespan memory differences. *Scientific Reports*, *6*(1), Article 1. https://doi.org/10.1038/srep32527

Hermann. (1992). The Journal of Neuropsychiatry and Clinical Neurosciences. *JAMA: The Journal of the American Medical Association*, *268*(11), 1473. https://doi.org/10.1001/jama.1992.03490110111047

Huang, R., & Clewett, D. (2024). The Locus Coeruleus: Where Cognitive and Emotional Processing Meet the Eye. In M. H. Papesh & S. D. Goldinger (Eds.), *Modern Pupillometry* (pp. 3–75). Springer International Publishing. https://doi.org/10.1007/978-3-031-54896-3_1

Huettel, S. A., Singerman, J. D., & McCarthy, G. (2001). The Effects of Aging upon the Hemodynamic Response Measured by Functional MRI. *NeuroImage*, *13*(1), 161–175. https://doi.org/10.1006/nimg.2000.0675

Hulsey, D. R. (2019). Norepinephrine and serotonin are required for vagus nerve stimulation directed cortical plasticity. *Experimental Neurology*, 8.

Hulsey, D. R., Riley, J. R., Loerwald, K. W., Rennaker, R. L., Kilgard, M. P., & Hays, S. A. (2017). Parametric characterization of neural activity in the locus coeruleus in response to vagus nerve stimulation. *Experimental Neurology*, *289*, 21–30. https://doi.org/10.1016/j.expneurol.2016.12.005

Iannitelli, A. F., & Weinshenker, D. (2023). Riddles in the dark: Decoding the relationship between neuromelanin and neurodegeneration in locus coeruleus neurons. *Neuroscience & Biobehavioral Reviews*, *152*, 105287. https://doi.org/10.1016/j.neubiorev.2023.105287

Iijima, K. (1989). An immunocytochemical study on the GABA-ergic and serotonin-ergic neurons in rat locus ceruleus with special reference to possible existence of the masked indoleamine cells. *Acta Histochemica*, *87*(1), 43–57. https://doi.org/10.1016/S0065

1281(89)80029-7
J, L. P. (1995). International Affective Picture System (IAPS): Technical Manual and Affective Ratings. *The Center for Research in Psychophysiology, University of Florida*. https://cir.nii.ac.jp/crid/1570291224896046464
Jacobs, H. I. L., Becker, J. A., Kwong, K., Engels-Domínguez, N., Prokopiou, P. C., Papp, K. V., Properzi, M., Hampton, O. L., d'Oleire Uquillas, F., Sanchez, J. S., Rentz, D. M., El Fakhri, G., Normandin, M. D., Price, J. C., Bennett, D. A., Sperling, R. A., & Johnson, K. A. (2021). In vivo and neuropathology data support locus coeruleus integrity as indicator of Alzheimer's disease pathology and cognitive decline. *Science Translational Medicine*, *13*(612), eabj2511. https://doi.org/10.1126/scitranslmed.abj2511
Jacobs, H. I. L., Becker, J. A., Kwong, K., Munera, D., Ramirez-Gomez, L., Engels Domínguez, N., Sanchez, J. S., Vila-Castelar, C., Baena, A., Sperling, R. A., Johnson, K. A., Lopera, F., & Quiroz, Y. T. (2023). Waning locus coeruleus integrity precedes cortical tau accrual in preclinical autosomal dominant Alzheimer's disease. *Alzheimer's & Dementia*, *19*(1), 169–180. https://doi.org/10.1002/alz.12656
Jacobs, H. I. L., Müller-Ehrenberg, L., Priovoulos, N., & Roebroeck, A. (2018). Curvilinear locus coeruleus functional connectivity trajectories over the adult lifespan: A 7T MRI study. *Neurobiology of Aging*, *69*, 167–176. https://doi.org/10.1016/j.neurobiolaging.2018.05.021
Jacobs, H. I. L., Riphagen, J. M., Razat, C. M., Wiese, S., & Sack, A. T. (2015). Transcutaneous vagus nerve stimulation boosts associative memory in older individuals. *Neurobiology of Aging*, *36*(5), 1860–1867. https://doi.org/10.1016/j.neurobiolaging.2015.02.023
Jacobs, H. I., Priovoulos, N., Poser, B. A., Pagen, L. H., Ivanov, D., Verhey, F. R., & Uludağ, K. (2020). Dynamic behavior of the locus coeruleus during arousal-related memory processing in a multi-modal 7T fMRI paradigm. *eLife*, *9*, e52059. https://doi.org/10.7554/eLife.52059
Jagust, W. J., & Mormino, E. C. (2011). Lifespan brain activity, β-amyloid, and Alzheimer's disease. *Trends in Cognitive Sciences*, *15*(11), 520–526. https://doi.org/10.1016/j.tics.2011.09.004
Jäkälä, P., Sirviö, J., Riekkinen, M., Koivisto, E., Kejonen, K., Vanhanen, M., & Riekkinen, P. (1999). Guanfacine and clonidine, alpha 2-agonists, improve paired associates learning, but not delayed matching to sample, in humans. *Neuropsychopharmacology: Official Publication of the American College of Neuropsychopharmacology*, *20*(2), 119–130. https://doi.org/10.1016/S0893-133X(98)00055-4
Jodo, E., & Aston-Jones, G. (1997). Activation of locus coeruleus by prefrontal cortex is mediated by excitatory amino acid inputs. *Brain Research*, *768*(1–2), 327–332. https://doi.org/10.1016/s0006-8993(97)00703-8
Jones, B. E., & Yang, T. Z. (1985). The efferent projections from the reticular formation and the locus coeruleus studied by anterograde and retrograde axonal transport in the rat. *The Journal of Comparative Neurology*, *242*(1), 56–92. https://doi.org/10.1002/cne.902420105
Joshi, S., & Gold, J. I. (2020). Pupil size as a window on neural substrates of cognition. *Trends in Cognitive Sciences*, *24*(6), 466–480. https://doi.org/10.1016/j.tics.2020.03.005
Joshi, S., Li, Y., Kalwani, R. M., & Gold, J. I. (2016). Relationships between Pupil Diameter and Neuronal Activity in the Locus Coeruleus, Colliculi, and Cingulate Cortex. *Neuron*, *89*(1), 221–234. https://doi.org/10.1016/j.neuron.2015.11.028
Kafkas, A., & Montaldi, D. (2018). How do memory systems detect and respond to novelty? *Neuroscience Letters*, *680*, 60–68. https://doi.org/10.1016/j.neulet.2018.01.053
Kahneman, D. (1973). *Attention and effort*. Prentice-Hall, Inc.
Kang, S. S., Liu, X., Ahn, E. H., Xiang, J., Manfredsson, F. P., Yang, X., Luo, H. R., Liles, L. C., Weinshenker, D., & Ye, K. (2020). Norepinephrine metabolite DOPEGAL activates

AEP and pathological Tau aggregation in locus coeruleus. *Journal of Clinical Investigation*, *130*(1), 422–437. https://doi.org/10.1172/JCI130513

Kaniusas, E., Kampusch, S., Tittgemeyer, M., Panetsos, F., Gines, R. F., Papa, M., Kiss, A., Podesser, B., Cassara, A. M., Tanghe, E., Samoudi, A. M., Tarnaud, T., Joseph, W., Marozas, V., Lukosevicius, A., Ištuk, N., Šarolić, A., Lechner, S., Klonowski, W., … Széles, J. C. (2019). Current Directions in the Auricular Vagus Nerve Stimulation I - A Physiological Perspective. *Frontiers in Neuroscience*, *13*, 854. https://doi.org/10.3389/fnins.2019.00854

Keller, T., & Kuhn, A. (2009). Skin properties and the influence on electrode design for transcutaneous (surface) electrical stimulation. In O. Dössel & W. C. Schlegel (Eds.), *World Congress on Medical Physics and Biomedical Engineering, September 7—12, 2009, Munich, Germany* (pp. 492–495). Springer. https://doi.org/10.1007/978-3-642 03889-1_131

Kempadoo, K. A., Mosharov, E. V., Choi, S. J., Sulzer, D., & Kandel, E. R. (2016). Dopamine release from the locus coeruleus to the dorsal hippocampus promotes spatial learning and memory. *Proceedings of the National Academy of Sciences*, *113*(51), 14835–14840. https://doi.org/10.1073/pnas.1616515114

Kensinger, E. A. (2009). Remembering the Details: Effects of Emotion. *Emotion Review*, *1*(2), 99–113. https://doi.org/10.1177/1754073908100432

Keren, N. I., Lozar, C. T., Harris, K. C., Morgan, P. S., & Eckert, M. A. (2009). In vivo mapping of the human locus coeruleus. *NeuroImage*, *47*(4), 1261–1267. https://doi.org/10.1016/j.neuroimage.2009.06.012

Keren, N. I., Taheri, S., Vazey, E. M., Morgan, P. S., Granholm, A.-C. E., Aston-Jones, G. S., & Eckert, M. A. (2015). Histologic validation of locus coeruleus MRI contrast in post mortem tissue. *NeuroImage*, *113*, 235–245. https://doi.org/10.1016/j.neuroimage.2015.03.020

Keute, M., Demirezen, M., Graf, A., Mueller, N. G., & Zaehle, T. (2019). No modulation of pupil size and event-related pupil response by transcutaneous auricular vagus nerve stimulation (taVNS). *Scientific Reports*, *9*(1), 11452. https://doi.org/10.1038/s41598 019-47961-4

Keute, M., Machetanz, K., Berelidze, L., Guggenberger, R., & Gharabaghi, A. (2021). Neuro cardiac coupling predicts transcutaneous auricular vagus nerve stimulation effects. *Brain Stimulation*, *14*(2), 209–216. https://doi.org/10.1016/j.brs.2021.01.001

Keute, M., Ruhnau, P., Heinze, H.-J., & Zaehle, T. (2018). Behavioral and electrophysiological evidence for GABAergic modulation through transcutaneous vagus nerve stimulation. *Clinical Neurophysiology*, *129*(9), 1789–1795. https://doi.org/10.1016/j.clinph.2018.05.026

Kiss, O., Sydó, N., Vargha, P., Vágó, H., Czimbalmos, C., Édes, E., Zima, E., Apponyi, G., Merkely, G., Sydó, T., Becker, D., Allison, T. G., & Merkely, B. (2016). Detailed heart rate variability analysis in athletes. *Clinical Autonomic Research*, *26*(4), 245–252. https://doi.org/10.1007/s10286-016-0360-z

Klavir, O., Prigge, M., Sarel, A., Paz, R., & Yizhar, O. (2017). Manipulating fear associations via optogenetic modulation of amygdala inputs to prefrontal cortex. *Nature Neuroscience*, *20*(6), 836–844. https://doi.org/10.1038/nn.4523 Klein, A., & Tourville, J. (2012). 101 Labeled Brain Images and a Consistent Human Cortical Labeling Protocol. *Frontiers in Neuroscience*, *6*. https://www.frontiersin.org/articles/10.3389/fnins.2012.00171

Kong, J., White, N. S., Kwong, K. K., Vangel, M. G., Rosman, I. S., Gracely, R. H., & Gollub, R. L. (2005). Using fMRI to dissociate sensory encoding from cognitive evaluation of heat pain intensity. *Human Brain Mapping*, *27*(9), 715–721. https://doi.org/10.1002/hbm.20213

Krahl, S. E., Senanayake, S. S., & Handforth, A. (2001). Destruction of Peripheral C-Fibers Does Not Alter Subsequent Vagus Nerve Stimulation-Induced Seizure Suppression in Rats. *Epilepsia*, *42*(5), 586–589. https://doi.org/10.1046/j.1528-1157.2001.09700.x

Krainc, T., Monje, M. H. G., Kinsinger, M., Bustos, B. I., & Lubbe, S. J. (2023). Melanin and Neuromelanin: Linking Skin Pigmentation and Parkinson's Disease. *Movement Disorders: Official Journal of the Movement Disorder Society*, *38*(2), 185–195. https://doi.org/10.1002/mds.29260

Kuznetsova, A., Brockhoff, P. B., & Christensen, R. H. B. (2017). **lmerTest** Package: Tests in Linear Mixed Effects Models. *Journal of Statistical Software*, *82*(13). https://doi.org/10.18637/jss.v082.i13

Langley, J., Hussain, S., Huddleston, D. E., Bennett, I. J., & Hu, X. P. (2022). Impact of Locus Coeruleus and Its Projections on Memory and Aging. *Brain Connectivity*, *12*(3), 223 233. https://doi.org/10.1089/brain.2020.0947

Lee, S. W., Anderson, A., Guzman, P. A., Nakano, A., Tolkacheva, E. G., & Wickman, K. (2018a). Atrial GIRK Channels Mediate the Effects of Vagus Nerve Stimulation on Heart Rate Dynamics and Arrhythmogenesis. *Frontiers in Physiology*, *9*. https://doi.org/10.3389/fphys.2018.00943

Lee, T.-H., Greening, S. G., Ueno, T., Clewett, D., Ponzio, A., Sakaki, M., & Mather, M. (2018b). Arousal increases neural gain via the locus coeruleus-norepinephrine system in younger adults but not in older adults. *Nature Human Behaviour*, *2*, 356–366. https://doi.org/10.1038/s41562-018-0344-1

Lee, T.-H., Kim, S. H., Katz, B., & Mather, M. (2020). The Decline in Intrinsic Connectivity Between the Salience Network and Locus Coeruleus in Older Adults: Implications for Distractibility. *Frontiers in Aging Neuroscience*, *12*. https://www.frontiersin.org/articles/10.3389/fnagi.2020.00002

Lemon, N., & Manahan-Vaughan, D. (2012). Dopamine D1/D5 receptors contribute to de novo hippocampal LTD mediated by novel spatial exploration or locus coeruleus activity. *Cerebral Cortex (New York, N.Y.: 1991)*, *22*(9), 2131–2138. https://doi.org/10.1093/cercor/bhr297

Lenth, R. V. (2023). *R package emmeans: Estimated marginal means* [R]. https://github.com/rvlenth/emmeans (Original work published 2017)

Levey, A. I., Qiu, D., Zhao, L., Hu, W. T., Duong, D. M., Higginbotham, L., Dammer, E. B., Seyfried, N. T., Wingo, T. S., Hales, C. M., Gámez Tansey, M., Goldstein, D. S., Abrol, A., Calhoun, V. D., Goldstein, F. C., Hajjar, I., Fagan, A. M., Galasko, D., Edland, S. D., … Weinshenker, D. (2022). A phase II study repurposing atomoxetine for neuroprotection in mild cognitive impairment. *Brain*, *145*(6), 1924–1938. https://doi.org/10.1093/brain/awab452

Li, S.-C., Lindenberger, U., Hommel, B., Aschersleben, G., Prinz, W., & Baltes, P. B. (2004). Transformations in the couplings among intellectual abilities and constituent cognitive processes across the life span. *Psychological Science*, *15*(3), 155–163. https://doi.org/10.1111/j.0956-7976.2004.01503003.x

Liebe, T., Kaufmann, J., Li, M., Skalej, M., Wagner, G., & Walter, M. (2020). In vivo anatomical mapping of human locus coeruleus functional connectivity at 3 T MRI. *Human Brain Mapping*, *41*(8), 2136–2151. https://doi.org/10.1002/hbm.24935

Liu, K. Y., Acosta-Cabronero, J., Cardenas-Blanco, A., Loane, C., Berry, A. J., Betts, M. J., Kievit, R. A., Henson, R. N., Düzel, E., Howard, R., & Hämmerer, D. (2019). In vivo visualization of age-related differences in the locus coeruleus. *Neurobiology of Aging*, *74*, 101–111. https://doi.org/10.1016/j.neurobiolaging.2018.10.014

Liu, K. Y., Kievit, R. A., Tsvetanov, K. A., Betts, M. J., Düzel, E., Rowe, J. B., Howard, R., & Hämmerer, D. (2020). Noradrenergic-dependent functions are associated with age related locus coeruleus signal intensity differences. *Nature Communications*, *11*(1),

Article 1. https://doi.org/10.1038/s41467-020-15410-w
Liu, K. Y., Marijatta, F., Hämmerer, D., Acosta-Cabronero, J., Düzel, E., & Howard, R. J. (2017a). Magnetic resonance imaging of the human locus coeruleus: A systematic review. *Neuroscience & Biobehavioral Reviews*, *83*, 325–355. https://doi.org/10.1016/j.neubiorev.2017.10.023
Liu, K. Y., Stringer, A. E., Reeves, S. J., & Howard, R. J. (2018). The neurochemistry of agitation in Alzheimer's disease: A systematic review. *Ageing Research Reviews*, *43*, 99–107. https://doi.org/10.1016/j.arr.2018.03.003
Liu, X., Ye, K., & Weinshenker, D. (2015). Norepinephrine Protects against Amyloid-β Toxicity via TrkB. *Journal of Alzheimer's Disease: JAD*, *44*(1), 251–260. https://doi.org/10.3233/JAD-141062
Liu, Y., Rodenkirch, C., Moskowitz, N., Schriver, B., & Wang, Q. (2017b). Dynamic Lateralization of Pupil Dilation Evoked by Locus Coeruleus Activation Results from Sympathetic, Not Parasympathetic, Contributions. *Cell Reports*, *20*(13), 3099–3112. https://doi.org/10.1016/j.celrep.2017.08.094
Llorca-Torralba, M., Suárez-Pereira, I., Bravo, L., Camarena-Delgado, C., Garcia-Partida, J. A., Mico, J. A., & Berrocoso, E. (2019). Chemogenetic Silencing of the Locus Coeruleus-Basolateral Amygdala Pathway Abolishes Pain-Induced Anxiety and Enhanced Aversive Learning in Rats. *Biological Psychiatry*, *85*(12), 1021–1035. https://doi.org/10.1016/j.biopsych.2019.02.018
Lloyd, B., Wurm, F., de Kleijn, R., & Nieuwenhuis, S. (2023). Short-term transcutaneous vagus nerve stimulation increases pupil size but does not affect EEG alpha power: A replication of Sharon et al. (2021, Journal of Neuroscience). *Brain Stimulation*, *16*(4), 1001–1008. https://doi.org/10.1016/j.brs.2023.06.010
Loerwald, K. W., Borland, M. S., Rennaker, R. L., Hays, S. A., & Kilgard, M. P. (2018). The interaction of pulse width and current intensity on the extent of cortical plasticity evoked by vagus nerve stimulation. *Brain Stimulation*, *11*(2), 271–277. https://doi.org/10.1016/j.brs.2017.11.007
Loughlin, S. E., Foote, S. L., & Bloom, F. E. (1986). Efferent projections of nucleus locus coeruleus: Topographic organization of cells of origin demonstrated by three dimensional reconstruction. *Neuroscience*, *18*(2), 291–306. https://doi.org/10.1016/0306-4522(86)90155-7
Lüdecke, D., Ben-Shachar, M., Patil, I., Waggoner, P., & Makowski, D. (2021). performance: An R Package for Assessment, Comparison and Testing of Statistical Models. *Journal of Open Source Software*, *6*(60), 3139. https://doi.org/10.21105/joss.03139
Ludwig, M., Betts, M. J., & Hämmerer, D. (2025). Stimulate to Remember? The Effects of Short Burst of Transcutaneous Vagus Nerve Stimulation (TAVNS) on Memory Performance and Pupil Dilation. *Psychophysiology*, *62*(1), e14753. https://doi.org/10.1111/psyp.14753
Ludwig, M., Pereira, C., Keute, M., Düzel, E., Betts, M. J., & Hämmerer, D. (2024a). Evaluating phasic transcutaneous vagus nerve stimulation (taVNS) with pupil dilation: The importance of stimulation intensity and sensory perception. *Scientific Reports*, *14*(1), 24391. https://doi.org/10.1038/s41598-024-72179-4
Ludwig, M., Wienke, C., Betts, M. J., Zaehle, T., & Hämmerer, D. (2021). Current challenges in reliably targeting the noradrenergic locus coeruleus using transcutaneous auricular vagus nerve stimulation (taVNS). *Autonomic Neuroscience*, *236*, 102900. https://doi.org/10.1016/j.autneu.2021.102900
Ludwig, M., Yi, Y.-J., Lüsebrink, F., Callaghan, M. F., Betts, M. J., Yakupov, R., Weiskopf, N., Dolan, R. J., Düzel, E., & Hämmerer, D. (2024b). Functional locus coeruleus imaging to investigate an ageing noradrenergic system. *Communications Biology*, *7*(1), 1–13. https://doi.org/10.1038/s42003-024-06446-5

Luo, Y., Zhou, J., Li, M.-X., Wu, P.-F., Hu, Z.-L., Ni, L., Jin, Y., Chen, J.-G., & Wang, F. (2015). Reversal of aging-related emotional memory deficits by norepinephrine via regulating the stability of surface AMPA receptors. *Aging Cell*, *14*(2), 170–179. https://doi.org/10.1111/acel.12282

Manaye, K. F., McIntire, D. D., Mann, D. M. A., & German, D. C. (1995). Locus coeruleus cell loss in the aging human brain: A non-random process. *Journal of Comparative Neurology*, *358*(1), 79–87. https://doi.org/10.1002/cne.903580105

Manera, A. L., Dadar, M., Fonov, V., & Collins, D. L. (2020). CerebrA, registration and manual label correction of Mindboggle-101 atlas for MNI-ICBM152 template. *Scientific Data*, *7*(1), Article 1. https://doi.org/10.1038/s41597-020-0557-9

Mann, D. M., Lincoln, J., Yates, P. O., Stamp, J. E., & Toper, S. (1980). Changes in the monoamine containing neurones of the human CNS in senile dementia. *The British Journal of Psychiatry: The Journal of Mental Science*, *136*, 533–541. https://doi.org/10.1192/bjp.136.6.533

Manta, S., Dong, J., Debonnel, G., & Blier, P. (2009). Enhancement of the function of rat serotonin and norepinephrine neurons by sustained vagus nerve stimulation. *J Psychiatry Neurosci*, 9.

Manta, S., El Mansari, M., Debonnel, G., & Blier, P. (2013). Electrophysiological and neurochemical effects of long-term vagus nerve stimulation on the rat monoaminergic systems. *International Journal of Neuropsychopharmacology*, *16*(2), 459–470. https://doi.org/10.1017/S1461145712000387

Marrosu, F., Serra, A., Maleci, A., Puligheddu, M., Biggio, G., & Piga, M. (2003). Correlation between GABA(A) receptor density and vagus nerve stimulation in individuals with drug-resistant partial epilepsy. *Epilepsy Research*, *55*(1–2), 59–70. https://doi.org/10.1016/s0920-1211(03)00107-4

Marsden, C. D. (1961). Pigmentation in the nucleus substantiae nigrae of mammals. *Journal of Anatomy*, *95*(Pt 2), 256–261.

Martin, J. L. R., & Martín-Sánchez, E. (2012). Systematic review and meta-analysis of vagus nerve stimulation in the treatment of depression: Variable results based on study designs. *European Psychiatry*, *27*(3), 147–155. https://doi.org/10.1016/j.eurpsy.2011.07.006

Martlé, V., Bavegems, V., Van Ham, L., Boon, P., Vonck, K., Raedt, R., Sys, S., & Bhatti, S. (2014). Evaluation of heart rate variability in dogs during standard and microburst vagus nerve stimulation: A pilot study. *Veterinary Journal (London, England: 1997)*, *202*(3), 651–653. https://doi.org/10.1016/j.tvjl.2014.09.009

Mather, M., & Carstensen, L. L. (2005). Aging and motivated cognition: The positivity effect in attention and memory. *Trends in Cognitive Sciences*, *9*(10), 496–502. https://doi.org/10.1016/j.tics.2005.08.005

Mather, M., Clewett, D., Sakaki, M., & Harley, C. W. (2016a). GANEing traction: The broad applicability of NE hotspots to diverse cognitive and arousal phenomena. *The Behavioral and Brain Sciences*, *39*, e228. https://doi.org/10.1017/S0140525X16000017

Mather, M., Clewett, D., Sakaki, M., & Harley, C. W. (2016b). Norepinephrine ignites local hotspots of neuronal excitation: How arousal amplifies selectivity in perception and memory. *Behavioral and Brain Sciences*, *39*, e200. https://doi.org/10.1017/S0140525X15000667

Mather, M., & Harley, C. W. (2016). The Locus Coeruleus: Essential for Maintaining Cognitive Function and the Aging Brain. *Trends in Cognitive Sciences*, *20*(3), 214–226. https://doi.org/10.1016/j.tics.2016.01.001

Mather, M., & Sutherland, M. R. (2011). Arousal-biased competition in perception and memory. *Perspectives on Psychological Science : A Journal of the Association for Psychological Science*, *6*(2), 114–133. https://doi.org/10.1177/1745691611400234

Mathôt, S. (2013). *A simple way to reconstruct pupil size during eye blinks*. 4.
Mathot, S. (2018). Pupillometry: Psychology, Physiology, and Function. *Journal of Cognition*, *1*(1). https://doi.org/10.5334/joc.18
Mathôt, S., & Vilotijević, A. (2022). Methods in cognitive pupillometry: Design, preprocessing, and statistical analysis. *Behavior Research Methods*, *55*(6), 3055–3077. https://doi.org/10.3758/s13428-022-01957-7
Matthews, K. L., Chen, C. P. L.-H., Esiri, M. M., Keene, J., Minger, S. L., & Francis, P. T. (2002). Noradrenergic changes, aggressive behavior, and cognition in patients with dementia. *Biological Psychiatry*, *51*(5), 407–416. https://doi.org/10.1016/s0006 3223(01)01235-5
McBurney-Lin, J., Lu, J., Zuo, Y., & Yang, H. (2019). Locus coeruleus-norepinephrine modulation of sensory processing and perception: A focused review. *Neuroscience and Biobehavioral Reviews*, *105*, 190–199. https://doi.org/10.1016/j.neubiorev.2019.06.009
McGaugh, J. L. (2004). THE AMYGDALA MODULATES THE CONSOLIDATION OF MEMORIES OF EMOTIONALLY AROUSING EXPERIENCES. *Annual Review of Neuroscience*, *27*(1), 1–28. https://doi.org/10.1146/annurev.neuro.27.070203.144157
McGaugh, J. L., Introini-Collison, I. B., Cahill, L. F., Castellano, C., Dalmaz, C., Parent, M. B., & Williams, C. L. (1993). Neuromodulatory systems and memory storage: Role of the amygdala. *Behavioural Brain Research*, *58*(1–2), 81–90. https://doi.org/10.1016/0166-4328(93)90092-5
McGraw, A. P., Larsen, J. T., Kahneman, D., & Schkade, D. (2010). Comparing Gains and Losses. *Psychological Science*, *21*(10), 1438–1445. https://doi.org/10.1177/0956797610381504
McIntyre, C. K., McGaugh, J. L., & Williams, C. L. (2012). Interacting Brain Systems Modulate Memory Consolidation. *Neuroscience and Biobehavioral Reviews*, *36*(7), 1750–1762. https://doi.org/10.1016/j.neubiorev.2011.11.001 Mejias-Aponte, C. A. (2016). Specificity and impact of adrenergic projections to the midbrain dopamine system. *Brain Research*, *1641*(Pt B), 258–273. https://doi.org/10.1016/j.brainres.2016.01.036
Mercan, D., & Heneka, M. T. (2022). The Contribution of the Locus Coeruleus–Noradrenaline System Degeneration during the Progression of Alzheimer's Disease. *Biology*, *11*(12), 1822. https://doi.org/10.3390/biology11121822
Miller, A. L., Gross, M. P., & Unsworth, N. (2019). Individual differences in working memory capacity and long-term memory: The influence of intensity of attention to items at encoding as measured by pupil dilation. *Journal of Memory and Language*, *104*, 25–42. https://doi.org/10.1016/j.jml.2018.09.005
Molinoff, P. B., & Axelrod, J. (1971). Biochemistry of catecholamines. *Annual Review of Biochemistry*, *40*, 465–500. https://doi.org/10.1146/annurev.bi.40.070171.002341
Monzani, E., Nicolis, S., Dell'Acqua, S., Capucciati, A., Bacchella, C., Zucca, F. A., Mosharov, E. V., Sulzer, D., Zecca, L., & Casella, L. (2019). Dopamine, Oxidative Stress and Protein-Quinone Modifications in Parkinson's and Other Neurodegenerative Diseases. *Angewandte Chemie (International Ed. in English)*, *58*(20), 6512–6527. https://doi.org/10.1002/anie.201811122
Morris, G. L., Gloss, D., Buchhalter, J., Mack, K. J., Nickels, K., & Harden, C. (2013). Evidence-based guideline update: Vagus nerve stimulation for the treatment of epilepsy: report of the Guideline Development Subcommittee of the American Academy of Neurology. *Neurology*, *81*(16), 1453–1459. https://doi.org/10.1212/WNL.0b013e3182a393d1
Morrison, R. A., Danaphongse, T. T., Abe, S. T., Stevens, M. E., Ezhil, V., Seyedahmadi, A., Adcock, K. S., Rennaker, R. L., Kilgard, M. P., & Hays, S. A. (2021). High intensity VNS disrupts VNS-mediated plasticity in motor cortex. *Brain Research*, *1756*, 147332.

https://doi.org/10.1016/j.brainres.2021.147332
Mouton, P. R., Pakkenberg, B., Gundersen, H. J., & Price, D. L. (1994). Absolute number and size of pigmented locus coeruleus neurons in young and aged individuals. *Journal of Chemical Neuroanatomy*, *7*(3), 185–190. https://doi.org/10.1016/0891-0618(94)900280
Mridha, Z., de Gee, J. W., Shi, Y., Alkashgari, R., Williams, J., Suminski, A., Ward, M. P., Zhang, W., & McGinley, M. J. (2021). Graded recruitment of pupil-linked neuromodulation by parametric stimulation of the vagus nerve. *Nature Communications*, *12*(1), 1539. https://doi.org/10.1038/s41467-021-21730-2
Müller, F. K., Teckentrup, V., Kühnel, A., Ferstl, M., & Kroemer, N. B. (2022). Acute vagus nerve stimulation does not affect liking or wanting ratings of food in healthy participants. *Appetite*, *169*, 105813. https://doi.org/10.1016/j.appet.2021.105813
Murphy, P. R., O'Connell, R. G., O'Sullivan, M., Robertson, I. H., & Balsters, J. H. (2014). Pupil diameter covaries with BOLD activity in human locus coeruleus. *Human Brain Mapping*, *35*(8), 4140–4154. https://doi.org/10.1002/hbm.22466
Murray, M. E., Moloney, C. M., Kouri, N., Syrjanen, J. A., Matchett, B. J., Rothberg, D. M., Tranovich, J. F., Sirmans, T. N. H., Wiste, H. J., Boon, B. D. C., Nguyen, A. T., Reichard, R. R., Dickson, D. W., Lowe, V. J., Dage, J. L., Petersen, R. C., Jack, C. R., Knopman, D. S., Vemuri, P., … Mielke, M. M. (2022). Global neuropathologic severity of Alzheimer's disease and locus coeruleus vulnerability influences plasma phosphorylated tau levels. *Molecular Neurodegeneration*, *17*(1), 85. https://doi.org/10.1186/s13024-022-00578-0
Nagatsu, T., Nakashima, A., Watanabe, H., Ito, S., Wakamatsu, K., Zucca, F. A., Zecca, L., Youdim, M., Wulf, M., Riederer, P., & Dijkstra, J. M. (2023). The role of tyrosine hydroxylase as a key player in neuromelanin synthesis and the association of neuromelanin with Parkinson's disease. *Journal of Neural Transmission*, *130*(5), 611625. https://doi.org/10.1007/s00702-023-02617-6
Nagel, I. E., Preuschhof, C., Li, S.-C., Nyberg, L., Bäckman, L., Lindenberger, U., & Heekeren, H. R. (2009). Performance level modulates adult age differences in brain activation during spatial working memory. *Proceedings of the National Academy of Sciences*, *106*(52), 22552–22557. https://doi.org/10.1073/pnas.0908238106
Nelson, P. T., Alafuzoff, I., Bigio, E. H., Bouras, C., Braak, H., Cairns, N. J., Castellani, R. J., Crain, B. J., Davies, P., Del Tredici, K., Duyckaerts, C., Frosch, M. P., Haroutunian, V., Hof, P. R., Hulette, C. M., Hyman, B. T., Iwatsubo, T., Jellinger, K. A., Jicha, G. A., … Beach, T. G. (2012). Correlation of Alzheimer disease neuropathologic changes with cognitive status: A review of the literature. *Journal of Neuropathology and Experimental Neurology*, *71*(5), 362–381. https://doi.org/10.1097/NEN.0b013e31825018f7
Nesbitt, A. D., Marin, J. C. A., Tompkins, E., Ruttledge, M. H., & Goadsby, P. J. (2015). Initial use of a novel noninvasive vagus nerve stimulator for cluster headache treatment. *Neurology*, *84*(12), 1249–1253. https://doi.org/10.1212/WNL.0000000000001394
Neuser, M. P., Teckentrup, V., Kühnel, A., Hallschmid, M., Walter, M., & Kroemer, N. B. (2020). Vagus nerve stimulation boosts the drive to work for rewards. *Nature Communications*, *11*(1), 3555. https://doi.org/10.1038/s41467-020-17344-9
Nichols, J. A., Nichols, A. R., Smirnakis, S. M., Engineer, N. D., Kilgard, M. P., & Atzori, M. (2011). Vagus nerve stimulation modulates cortical synchrony and excitability through the activation of muscarinic receptors. *Neuroscience*, *189*, 207–214. https://doi.org/10.1016/j.neuroscience.2011.05.024
Noller, C. M., Levine, Y. A., Urakov, T. M., Aronson, J. P., & Nash, M. S. (2019). Vagus Nerve Stimulation in Rodent Models: An Overview of Technical Considerations. *Frontiers in Neuroscience*, *13*, 911. https://doi.org/10.3389/fnins.2019.00911

Oei, N. Y. L., Tollenaar, M. S., Elzinga, B. M., & Spinhoven, P. (2010). Propranolol reduces emotional distraction in working memory: A partial mediating role of propranolol induced cortisol increases? *Neurobiology of Learning and Memory*, *93*(3), 388–395. https://doi.org/10.1016/j.nlm.2009.12.005

Ohm, T. G., Busch, C., & Bohl, J. (1997). Unbiased estimation of neuronal numbers in the human nucleus coeruleus during aging. *Neurobiology of Aging*, *18*(4), 393–399. https://doi.org/10.1016/s0197-4580(97)00034-1 Oldfield, R. C. (1971). The assessment and analysis of handedness: The Edinburgh inventory. *Neuropsychologia*, *9*(1), 97–113. https://doi.org/10.1016/0028-3932(71)90067-4

Olpe, H. R., & Steinmann, M. (1991). Responses of locus coeruleus neurons to neuropeptides. *Progress in Brain Research*, *88*, 241–248. https://doi.org/10.1016/s0079 6123(08)63813-3

Osorio-Forero, A., Cherrad, N., Banterle, L., Fernandez, L. M. J., & Lüthi, A. (2022). When the Locus Coeruleus Speaks Up in Sleep: Recent Insights, Emerging Perspectives. *International Journal of Molecular Sciences*, *23*(9), 5028. https://doi.org/10.3390/ijms23095028

Ottaviani, M. M., Wright, L., Dawood, T., & Macefield, V. G. (2020). *In vivo* recordings from the human vagus nerve using ultrasound-guided microneurography. *The Journal of Physiology*, *598*(17), 3569–3576. https://doi.org/10.1113/JP280077

Panebianco, M., Zavanone, C., Dupont, S., Restivo, D. A., & Pavone, A. (2016). Vagus nerve stimulation therapy in partial epilepsy: A review. *Acta Neurologica Belgica*, *116*(3), 241–248. https://doi.org/10.1007/s13760-016-0616-3

Patros, M., Farmer, D. G. S., Moneghetti, K., Ottaviani, M. M., Sivathamboo, S., Simpson, H. D., O'Brien, T. J., & Macefield, V. G. (2024). First-in-human microelectrode recordings from the vagus nerve during clinical vagus nerve stimulation. *Epilepsia Open*, *9*(6), 2522–2527. https://doi.org/10.1002/epi4.13083

Pauli, W. M., Nili, A. N., & Tyszka, J. M. (2018). A high-resolution probabilistic in vivo atlas of human subcortical brain nuclei. *Scientific Data*, *5*(1), 180063. https://doi.org/10.1038/sdata.2018.63

Penry, J. K., & Dean, J. C. (1990). Prevention of intractable partial seizures by intermittent vagal stimulation in humans: Preliminary results. *Epilepsia*, *31 Suppl 2*, S40-43. https://doi.org/10.1111/j.1528-1157.1990.tb05848.x

Pervaz, I., Thurn, L., Vezzani, C., Kaluza, L., Kühnel, A., & Kroemer, N. B. (2025). Does transcutaneous auricular vagus nerve stimulation alter pupil dilation? A living Bayesian meta-analysis. *Brain Stimulation*, *18*(2), 148–157. https://doi.org/10.1016/j.brs.2025.01.022

Peuker, E. T., & Filler, T. J. (2002). The nerve supply of the human auricle. *Clinical Anatomy*, *15*(1), 35–37. https://doi.org/10.1002/ca.1089

Pleger, B., & Villringer, A. (2013). The human somatosensory system: From perception to decision making. *Progress inNeurobiology*,*103*,76–97. https://doi.org/10.1016/j.pneurobio.2012.10.002

Poe, G. R., Foote, S., Eschenko, O., Johansen, J. P., Bouret, S., Aston-Jones, G., Harley, C. W., Manahan-Vaughan, D., Weinshenker, D., Valentino, R., Berridge, C., Chandler, D. J., Waterhouse, B., & Sara, S. J. (2020). Locus coeruleus: A new look at the blue spot. *Nature Reviews Neuroscience*, *21*(11), 644–659. https://doi.org/10.1038/s41583-020 0360-9

Priovoulos, N., Jacobs, H. I. L., Ivanov, D., Uludağ, K., Verhey, F. R. J., & Poser, B. A. (2018). High-resolution in vivo imaging of human locus coeruleus by magnetization transfer MRI at 3T and 7T. *NeuroImage*, *168*, 427–436. https://doi.org/10.1016/j.neuroimage.2017.07.045

Priovoulos, N., van Boxel, S. C. J., Jacobs, H. I. L., Poser, B. A., Uludag, K., Verhey, F. R. J.,

& Ivanov, D. (2020). Unraveling the contributions to the neuromelanin-MRI contrast. *Brain Structure and Function*, *225*(9), 2757–2774. https://doi.org/10.1007/s00429-020 02153-z

Raedt, R., Clinckers, R., Mollet, L., Vonck, K., El Tahry, R., Wyckhuys, T., De Herdt, V., Carrette, E., Wadman, W., Michotte, Y., Smolders, I., Boon, P., & Meurs, A. (2011). Increased hippocampal noradrenaline is a biomarker for efficacy of vagus nerve stimulation in a limbic seizure model. *Journal of Neurochemistry*, *117*(3), 461–469. https://doi.org/10.1111/j.1471-4159.2011.07214.x

Rajkowski, J., Kubiak, P., & Aston-Jones, G. (1994). Locus coeruleus activity in monkey: Phasic and tonic changes are associated with altered vigilance. *Brain Research Bulletin*, *35*(5–6), 607–616. https://doi.org/10.1016/0361-9230(94)90175-9

Rammsayer, T. H., Hennig, J., Haag, A., & Lange, N. (2001). Effects of noradrenergic activity on temporal information processing in humans. *The Quarterly Journal of Experimental Psychology. B, Comparative and Physiological Psychology*, *54*(3), 247–258. https://doi.org/10.1080/02724990143000036

Rangon, C.-M. (2018). Reconsidering Sham in Transcutaneous Vagus Nerve Stimulation studies. *Clinical Neurophysiology*, *129*(11), 2501–2502. https://doi.org/10.1016/j.clinph.2018.08.027

Raven, J. C., & Court, J. H. (1998). *Raven's Progressive Matrices and Vocabulary Scales*. Oxford Psychologists Press.

Reimer, J., McGinley, M. J., Liu, Y., Rodenkirch, C., Wang, Q., McCormick, D. A., & Tolias, A. S. (2016). Pupil fluctuations track rapid changes in adrenergic and cholinergic activity in cortex. *Nature Communications*, *7*(1), Article 1. https://doi.org/10.1038/ncomms13289

Rembado, I., Song, W., Su, D. K., Levari, A., Shupe, L. E., Perlmutter, S., Fetz, E., & Zanos, S. (2021). Cortical Responses to Vagus Nerve Stimulation Are Modulated by Brain State in Nonhuman Primates. *Cerebral Cortex (New York, N.Y.: 1991)*, *31*(12), 5289 5307. https://doi.org/10.1093/cercor/bhab158

Reuter-Lorenz, P. A., & Lustig, C. (2005). Brain aging: Reorganizing discoveries about the aging mind. *Current Opinion in Neurobiology*, *15*(2), 245–251. https://doi.org/10.1016/j.conb.2005.03.016

Revelle, W. (2023). *psych: Procedures for Psychological, Psychometric, and Personality Research* (Version 2.3.6) [Computer software]. https://cran.r project.org/web/packages/psych/

Rho, H.-J., Kim, J.-H., & Lee, S.-H. (2018). Function of Selective Neuromodulatory Projections in the Mammalian Cerebral Cortex: Comparison Between Cholinergic and Noradrenergic Systems. *Frontiers in Neural Circuits*, *12*. https://doi.org/10.3389/fncir.2018.00047

Robertson, H. A., & Leslie, R. A. (1985). Noradrenergic alpha 2 binding sites in vagal dorsal motor nucleus and nucleus tractus solitarius: Autoradiographic localization. *Canadian Journal of Physiology and Pharmacology*, *63*(9), 1190–1194. https://doi.org/10.1139/y85-195

Rodenkirch, C., Liu, Y., Schriver, B. J., & Wang, Q. (2019). Locus coeruleus activation enhances thalamic feature selectivity via norepinephrine regulation of intrathalamic circuit dynamics. *Nature Neuroscience*, *22*(1), 120–133. https://doi.org/10.1038/s41593-018-0283-1

Rommelfanger, K. S., & Weinshenker, D. (2007). Norepinephrine: The redheaded stepchild of Parkinson's disease. *Biochemical Pharmacology*, *74*(2), 177–190. https://doi.org/10.1016/j.bcp.2007.01.036

Roosevelt, R. W., Smith, D. C., Clough, R. W., Jensen, R. A., & Browning, R. A. (2006). Increased extracellular concentrations of norepinephrine in cortex and hippocampus

following vagus nerve stimulation in the rat. *Brain Research*, *1119*(1), 124–132. https://doi.org/10.1016/j.brainres.2006.08.048

Ruffoli, R., Giorgi, F. S., Pizzanelli, C., Murri, L., Paparelli, A., & Fornai, F. (2011). The chemical neuroanatomy of vagus nerve stimulation. *Journal of Chemical Neuroanatomy*, *42*(4), 288–296. https://doi.org/10.1016/j.jchemneu.2010.12.002

Safi, S., Ellrich, J., & Neuhuber, W. (2016). Myelinated Axons in the Auricular Branch of the Human Vagus Nerve: Auricular Vagus Nerve Branch. *The Anatomical Record*, *299*(9), 1184–1191. https://doi.org/10.1002/ar.23391

Sakaki, M., Ueno, T., Ponzio, A., Harley, C. W., & Mather, M. (2019). Emotional arousal amplifies competitions across goal-relevant representation: A neurocomputational framework. *Cognition*, *187*, 108–125. https://doi.org/10.1016/j.cognition.2019.02.011

Samniang, B., Shinlapawittayatorn, K., Chunchai, T., Pongkan, W., Kumfu, S., Chattipakorn, S. C., KenKnight, B. H., & Chattipakorn, N. (2016). Vagus Nerve Stimulation Improves Cardiac Function by Preventing Mitochondrial Dysfunction in Obese-Insulin Resistant Rats. *Scientific Reports*, *6*, 19749. https://doi.org/10.1038/srep19749

Samuels, E., & Szabadi, E. (2008). Functional Neuroanatomy of the Noradrenergic Locus Coeruleus: Its Roles in the Regulation of Arousal and Autonomic Function Part I: Principles of Functional Organisation. *Current Neuropharmacology*, *6*(3), 235–253. https://doi.org/10.2174/157015908785777229

Sanchez-Padilla, J., Guzman, J. N., Ilijic, E., Kondapalli, J., Galtieri, D. J., Yang, B., Schieber, S., Oertel, W., Wokosin, D., Schumacker, P. T., & Surmeier, D. J. (2014). Mitochondrial oxidant stress in locus coeruleus is regulated by activity and nitric oxide synthase. *Nature Neuroscience*, *17*(6), 832–840. https://doi.org/10.1038/nn.3717

Sara, S. J. (1985). Noradrenergic Modulation of Selective Attention: Its Role in Memory Retrieval. *Annals of the New York Academy of Sciences*, *444*(1), 178–193. https://doi.org/10.1111/j.1749-6632.1985.tb37588.x

Sara, S. J. (2009). The locus coeruleus and noradrenergic modulation of cognition. *Nature Reviews Neuroscience*, *10*(3), Article 3. https://doi.org/10.1038/nrn2573

Sara, S. J. (2015). Locus Coeruleus in time with the making of memories. *Current Opinion in Neurobiology*, *35*, 87–94. https://doi.org/10.1016/j.conb.2015.07.004

Sara, S. J., & Bouret, S. (2012). Orienting and Reorienting: The Locus Coeruleus Mediates Cognition through Arousal. *Neuron*, *76*(1), 130–141. https://doi.org/10.1016/j.neuron.2012.09.011

Sara, S. J., & Devauges, V. (1988). Priming stimulation of locus coeruleus facilitates memory retrieval in the rat. *Brain Research*, *438*(1–2), 299–303. https://doi.org/10.1016/0006 8993(88)91351-0

Sara, S. J., & Segal, M. (1991). Plasticity of sensory responses of locus coeruleus neurons in the behaving rat: Implications for cognition. In *Progress in Brain Research* (Vol. 88, pp. 571–585). Elsevier. https://doi.org/10.1016/S0079-6123(08)63835-2

Sasaki, M., Shibata, E., Tohyama, K., Takahashi, J., Otsuka, K., Tsuchiya, K., Takahashi, S., Ehara, S., Terayama, Y., & Sakai, A. (2006). Neuromelanin magnetic resonance imaging of locus ceruleus and substantia nigra in Parkinson's disease. *NeuroReport*, *17*(11), 1215–1218. https://doi.org/10.1097/01.wnr.0000227984.84927.a7

Schevernels, H., van Bochove, M. E., De Taeye, L., Bombeke, K., Vonck, K., Van Roost, D., De Herdt, V., Santens, P., Raedt, R., & Boehler, C. N. (2016). The effect of vagus nerve stimulation on response inhibition. *Epilepsy & Behavior*, *64*, 171–179. https://doi.org/10.1016/j.yebeh.2016.09.014

Schiemann, J., Schlaudraff, F., Klose, V., Bingmer, M., Seino, S., Magill, P. J., Zaghloul, K. A., Schneider, G., Liss, B., & Roeper, J. (2012). K-ATP channels in dopamine substantia nigra neurons control bursting and novelty-induced exploration. *Nature Neuroscience*, *15*(9), 1272–1280. https://doi.org/10.1038/nn.3185

Schmidt, R., Leventhal, D. K., Mallet, N., Chen, F., & Berke, J. D. (2013). Canceling actions involves a race between basal ganglia pathways. *Nature Neuroscience*, *16*(8), 1118 1124. https://doi.org/10.1038/nn.3456

Schultz, W. (2007). Multiple Dopamine Functions at Different Time Courses. *Annual Review of Neuroscience*, *30*(1), 259–288. https://doi.org/10.1146/annurev.neuro.28.061604.135722

Schwarz, L. A., & Luo, L. (2015). Organization of the Locus Coeruleus-Norepinephrine System. *Current Biology*, *25*(21), R1051–R1056. https://doi.org/10.1016/j.cub.2015.09.039

Schwarz, L. A., Miyamichi, K., Gao, X. J., Beier, K. T., Weissbourd, B., DeLoach, K. E., Ren, J., Ibanes, S., Malenka, R. C., Kremer, E. J., & Luo, L. (2015). Viral-genetic tracing of the input-output organization of a central noradrenaline circuit. *Nature*, *524*(7563), 88 92. https://doi.org/10.1038/nature14600

Sclocco, R. (2020). Stimulus frequency modulates brainstem response to respiratory-gated transcutaneous auricular vagus nerve stimulation. *Brain Stimulation*, 9.

Sclocco, R., Beissner, F., Bianciardi, M., Polimeni, J. R., & Napadow, V. (2018). Challenges and opportunities for brainstem neuroimaging with ultrahigh field MRI. *NeuroImage*, *168*, 412–426. https://doi.org/10.1016/j.neuroimage.2017.02.052

Sclocco, R., Garcia, R. G., Kettner, N. W., Isenburg, K., Fisher, H. P., Hubbard, C. S., Ay, I., Polimeni, J. R., Goldstein, J., Makris, N., Toschi, N., Barbieri, R., & Napadow, V. (2019). The influence of respiration on brainstem and cardiovagal response to auricular vagus nerve stimulation: A multimodal ultrahigh-field (7T) fMRI study. *Brain Stimulation*, *12*(4), 911–921. https://doi.org/10.1016/j.brs.2019.02.003

Sharma, Y., Xu, T., Graf, W. M., Fobbs, A., Sherwood, C. C., Hof, P. R., Allman, J. M., & Manaye, K. F. (2010). Comparative anatomy of the locus coeruleus in humans and nonhuman primates. *The Journal of Comparative Neurology*, *518*(7), 963–971. https://doi.org/10.1002/cne.22249

Sharon, O., Fahoum, F., & Nir, Y. (2021). Transcutaneous Vagus Nerve Stimulation in Humans Induces Pupil Dilation and Attenuates Alpha Oscillations. *The Journal of Neuroscience*, *41*(2), 320–330. https://doi.org/10.1523/JNEUROSCI.1361-20.2020

Shibata, E., Sasaki, M., Tohyama, K., Kanbara, Y., Otsuka, K., Ehara, S., & Sakai, A. (2006). Age-related Changes in Locus Ceruleus on Neuromelanin Magnetic Resonance Imaging at 3 Tesla. *Magnetic Resonance in Medical Sciences*, *5*(4), 197–200. https://doi.org/10.2463/mrms.5.197

Singmann, H., Bolker, B., Westfall, J., Aust, F., Ben-Shachar, M. S., Højsgaard, S., Fox, J., Lawrence, M. A., Mertens, U., Love, J., Lenth, R., & Christensen, R. H. B. (2023). *afex: Analysis of Factorial Experiments* (Version 1.3-0) [Computer software]. https://cran.r project.org/web/packages/afex/index.html

Skora, L., Marzecová, A., & Jocham, G. (2024). Tonic and phasic transcutaneous auricular vagus nerve stimulation (taVNS) both evoke rapid and transient pupil dilation. *Brain Stimulation*, *17*(2), 233–244. https://doi.org/10.1016/j.brs.2024.02.013

Smith, C. C., & Greene, R. W. (2012). CNS dopamine transmission mediated by noradrenergic innervation. *The Journal of Neuroscience: The Official Journal of the Society for Neuroscience*, *32*(18), 6072–6080. https://doi.org/10.1523/JNEUROSCI.6486-11.2012

Souza, R. R., Robertson, N. M., McIntyre, C. K., Rennaker, R. L., Hays, S. A., & Kilgard, M. P. (2021). Vagus nerve stimulation enhances fear extinction as an inverted-U function of stimulation intensity. *Experimental Neurology*, *341*, 113718. https://doi.org/10.1016/j.expneurol.2021.113718

Spreng, R. N., Wojtowicz, M., & Grady, C. L. (2010). Reliable differences in brain activity between young and old adults: A quantitative meta-analysis across multiple cognitive domains. *Neuroscience & Biobehavioral Reviews*, *34*(8), 1178–1194.

https://doi.org/10.1016/j.neubiorev.2010.01.009
Sterpenich, V., D'Argembeau, A., Desseilles, M., Balteau, E., Albouy, G., Vandewalle, G., Degueldre, C., Luxen, A., Collette, F., & Maquet, P. (2006). The Locus Ceruleus Is Involved in the Successful Retrieval of Emotional Memories in Humans. *The Journal of Neuroscience*, *26*(28), 7416–7423. https://doi.org/10.1523/JNEUROSCI.1001 06.2006
Sulzer, D., Bogulavsky, J., Larsen, K. E., Behr, G., Karatekin, E., Kleinman, M. H., Turro, N., Krantz, D., Edwards, R. H., Greene, L. A., & Zecca, L. (2000). Neuromelanin biosynthesis is driven by excess cytosolic catecholamines not accumulated by synaptic vesicles. *Proceedings of the National Academy of Sciences*, *97*(22), 11869–11874. https://doi.org/10.1073/pnas.97.22.11869
Szabadi, E. (2013). Functional neuroanatomy of the central noradrenergic system. *Journal of Psychopharmacology (Oxford, England)*, *27*(8), 659–693. https://doi.org/10.1177/0269881113490326
Szot, P., Franklin, A., Miguelez, C., Wang, Y., Vidaurrazaga, I., Ugedo, L., Sikkema, C., Wilkinson, C. W., & Raskind, M. A. (2016). Depressive-like behavior observed with a minimal loss of locus coeruleus (LC) neurons following administration of 6 hydroxydopamine is associated with electrophysiological changes and reversed with precursors of norepinephrine. *Neuropharmacology*, *101*, 76–86. https://doi.org/10.1016/j.neuropharm.2015.09.003
Szot, P., White, S. S., Greenup, J. L., Leverenz, J. B., Peskind, E. R., & Raskind, M. A. (2006). Compensatory Changes in the Noradrenergic Nervous System in the Locus Ceruleus and Hippocampus of Postmortem Subjects with Alzheimer's Disease and Dementia with Lewy Bodies. *Journal of Neuroscience*, *26*(2), 467–478. https://doi.org/10.1523/JNEUROSCI.4265-05.2006
Takahashi, J., Shibata, T., Sasaki, M., Kudo, M., Yanezawa, H., Obara, S., Kudo, K., Ito, K., Yamashita, F., & Terayama, Y. (2015). Detection of changes in the locus coeruleus in patients with mild cognitive impairment and Alzheimer's disease: High-resolution fast spin-echo T1-weighted imaging. *Geriatrics & Gerontology International*, *15*(3), 334 340. https://doi.org/10.1111/ggi.12280
Takeuchi, T., Duszkiewicz, A. J., Sonneborn, A., Spooner, P. A., Yamasaki, M., Watanabe, M., Smith, C. C., Fernández, G., Deisseroth, K., Greene, R. W., & Morris, R. G. M. (2016). Locus coeruleus and dopaminergic consolidation of everyday memory. *Nature*, *537*(7620), 357–362. https://doi.org/10.1038/nature19325
Tepper, J. M., & Lee, C. R. (2007). GABAergic control of substantia nigra dopaminergic neurons. In J. M. Tepper, E. D. Abercrombie, & J. P. Bolam (Eds.), *Progress in Brain Research* (Vol. 160, pp. 189–208). Elsevier. https://doi.org/10.1016/S0079 6123(06)60011-3
Ter Horst, G. J., Toes, G. J., & van Willigen, J. D. (1991). Locus coeruleus projections to the dorsal motor vagus nucleus in the rat. *Neuroscience*, *45*(1), 153–160. https://doi.org/10.1016/0306-4522(91)90111-Z
Theofilas, P., Ehrenberg, A. J., Dunlop, S., Alho, A. T. D. L., Nguy, A., Leite, R. E. P., Rodriguez, R. D., Mejia, M. B., Suemoto, C. K., Ferretti-Rebustini, R. E. D. L., Polichiso, L., Nascimento, C. F., Seeley, W. W., Nitrini, R., Pasqualucci, C. A., Filho, W. J., Rueb, U., Neuhaus, J., Heinsen, H., & Grinberg, L. T. (2017). Locus coeruleus volume and cell population changes during Alzheimer's disease progression: A stereological study in human postmortem brains with potential implication for early stage biomarker discovery. *Alzheimer's & Dementia*, *13*(3), 236–246. https://doi.org/10.1016/j.jalz.2016.06.2362
Tona, K.-D., Keuken, M. C., de Rover, M., Lakke, E., Forstmann, B. U., Nieuwenhuis, S., & van Osch, M. J. P. (2017). In vivo visualization of the locus coeruleus in humans:

Quantifying the test–retest reliability. *Brain Structure and Function*, *222*(9), 4203 4217. https://doi.org/10.1007/s00429-017-1464-5

Trujillo, P., Petersen, K. J., Cronin, M. J., Lin, Y.-C., Kang, H., Donahue, M. J., Smith, S. A., & Claassen, D. O. (2019). Quantitative magnetization transfer imaging of the human locus coeruleus. *NeuroImage*, *200*, 191–198. https://doi.org/10.1016/j.neuroimage.2019.06.049

Trujillo, P., Summers, P. E., Ferrari, E., Zucca, F. A., Sturini, M., Mainardi, L. T., Cerutti, S., Smith, A. K., Smith, S. A., Zecca, L., & Costa, A. (2017). Contrast mechanisms associated with neuromelanin-MRI. *Magnetic Resonance in Medicine*, *78*(5), 1790 1800.https://doi.org/10.1002/mrm.26584

Tsvetanov, K. A., Henson, R. N. A., & Rowe, J. B. (2021). Separating vascular and neuronal effects of age on fMRI BOLD signals. *Philosophical Transactions of the Royal Society of London. Series B, Biological Sciences*, *376*(1815), 20190631. https://doi.org/10.1098/rstb.2019.0631

Tully, K., & Bolshakov, V. Y. (2010). Emotional enhancement of memory: How norepinephrine enables synaptic plasticity. *Molecular Brain*, *3*(1), 15. https://doi.org/10.1186/1756-6606-3-15

Tustison, N. J., Avants, B. B., Cook, P. A., Zheng, Y., Egan, A., Yushkevich, P. A., & Gee, J. C. (2010). N4ITK: Improved N3 Bias Correction. *IEEE Transactions on Medical Imaging*, *29*(6), 1310–1320. https://doi.org/10.1109/TMI.2010.2046908

Uematsu, A., Tan, B. Z., & Johansen, J. P. (2015). Projection specificity in heterogeneous locus coeruleus cell populations: Implications for learning and memory. *Learning & Memory*, *22*(9), 444–451. https://doi.org/10.1101/lm.037283.114

Uematsu, A., Tan, B. Z., Ycu, E. A., Cuevas, J. S., Koivumaa, J., Junyent, F., Kremer, E. J., Witten, I. B., Deisseroth, K., & Johansen, J. P. (2017). Modular organization of the brainstem noradrenaline system coordinates opposing learning states. *Nature Neuroscience*, *20*(11), 1602–1611. https://doi.org/10.1038/nn.4642

Ungerstedt, U. (1971). Stereotaxic mapping of the monoamine pathways in the rat brain. *Acta Physiologica Scandinavica. Supplementum*, *367*, 1–48. https://doi.org/10.1111/j.1365 201x.1971.tb10998.x

Urbin, M. A., Lafe, C. W., Simpson, T. W., Wittenberg, G. F., Chandrasekaran, B., & Weber, D. J. (2021). Electrical stimulation of the external ear acutely activates noradrenergic mechanisms in humans. *Brain Stimulation*, *14*(4), 990–1001. https://doi.org/10.1016/j.brs.2021.06.002

Usher, M., Cohen, J. D., Servan-Schreiber, D., Rajkowski, J., & Aston-Jones, G. (1999). The Role of Locus Coeruleus in the Regulation of Cognitive Performance. *Science*, *283*(5401), 549–554. https://doi.org/10.1126/science.283.5401.549

Uthman, B. M., Wilder, B. J., Penry, J. K., Dean, C., Ramsay, R. E., Reid, S. A., Hammond, E. J., Tarver, W. B., & Wernicke, J. F. (1993). Treatment of epilepsy by stimulation of the vagus nerve. *Neurology*, *43*(7), 1338–1345. https://doi.org/10.1212/wnl.43.7.1338

Vallbo, Å. B. (2018). Microneurography: How it started and how it works. *Journal of Neurophysiology*, *120*(3), 1415–1427. https://doi.org/10.1152/jn.00933.2017

Van Bockstaele, E. J., Akaoka, H., & Aston-Jones, G. (1993). Brainstem afferents to the rostral (juxtafacial) nucleus paragigantocellularis: Integration of exteroceptive and interoceptive sensory inputs in the ventral tegmentum. *Brain Research*, *603*(1), 1–18. https://doi.org/10.1016/0006-8993(93)91293-2

Van Egroo, M., Riphagen, J. M., Ashton, N. J., Janelidze, S., Sperling, R. A., Johnson, K. A., Yang, H.-S., Bennett, D. A., Blennow, K., Hansson, O., Zetterberg, H., & Jacobs, H. I. L. (2023). Ultra-high field imaging, plasma markers and autopsy data uncover a specific rostral locus coeruleus vulnerability to hyperphosphorylated tau. *Molecular Psychiatry*. https://doi.org/10.1038/s41380-023-02041-y

Van Stegeren, A. H. (2008). The role of the noradrenergic system in emotional memory. *Acta Psychologica*, *127*(3), 532–541. https://doi.org/10.1016/j.actpsy.2007.10.004

Varazzani, C., San-Galli, A., Gilardeau, S., & Bouret, S. (2015). Noradrenaline and dopamine neurons in the reward/effort trade-off: A direct electrophysiological comparison in behaving monkeys. *The Journal of Neuroscience: The Official Journal of the Society for Neuroscience*, *35*(20), 7866–7877. https://doi.org/10.1523/JNEUROSCI.0454 15.2015

Vazey, E. M., Moorman, D. E., & Aston-Jones, G. (2018). Phasic locus coeruleus activity regulates cortical encoding of salience information. *Proceedings of the National Academy of Sciences*, *115*(40). https://doi.org/10.1073/pnas.1803716115

Ventura-Bort, C., Wirkner, J., Wendt, J., Hamm, A. O., & Weymar, M. (2021). Establishment of Emotional Memories Is Mediated by Vagal Nerve Activation: Evidence from Noninvasive taVNS. *The Journal of Neuroscience*, *41*(36), 7636–7648. https://doi.org/10.1523/JNEUROSCI.2329-20.2021

Ventureyra, E. C. G. (2000). Transcutaneous vagus nerve stimulation for partial onset seizure therapy. *Child's Nervous System*, *16*(2), 101–102. https://doi.org/10.1007/s003810050021

Veréb, D., Mijalkov, M., Canal-Garcia, A., Chang, Y.-W., Gomez-Ruiz, E., Gerboles, B. Z., Kivipelto, M., Svenningsson, P., Zetterberg, H., Volpe, G., Betts, M., Jacobs, H. I., & Pereira, J. B. (2023). Age-related differences in the functional topography of the locus coeruleus and their implications for cognitive and affective functions. *eLife*, *12*, RP87188. https://doi.org/10.7554/eLife.87188

Verma, N., Graham, R. D., Mudge, J., Trevathan, J. K., Franke, M., Shoffstall, A. J., Williams, J., Dalrymple, A. N., Fisher, L. E., Weber, D. J., Lempka, S. F., & Ludwig, K. A. (2021). Augmented Transcutaneous Stimulation Using an Injectable Electrode: A Computational Study. *Frontiers in Bioengineering and Biotechnology*, *9*, 796042. https://doi.org/10.3389/fbioe.2021.796042

Verma, N., Knudsen, B., Gholston, A., Skubal, A., Blanz, S., Settell, M., Frank, J., Trevathan, J., & Ludwig, K. (2023). Microneurography as a minimally invasive method to assess target engagement during neuromodulation. *Journal of Neural Engineering*, *20*(2), 026036. https://doi.org/10.1088/1741-2552/acc35c

Vicq-d'Azyr, F. (1786). *Traite d'Anatomie de Cerveau.*

Vila, M. (2019). Neuromelanin, aging, and neuronal vulnerability in Parkinson's disease. *Movement Disorders*, *34*(10), 1440–1451. https://doi.org/10.1002/mds.27776

Vonck, K., Raedt, R., Naulaerts, J., De Vogelaere, F., Thiery, E., Van Roost, D., Aldenkamp, B., Miatton, M., & Boon, P. (2014). Vagus nerve stimulation…25 years later! What do we know about the effects on cognition? *Neuroscience & Biobehavioral Reviews*, *45*, 63–71. https://doi.org/10.1016/j.neubiorev.2014.05.005

Vrieze, S. I. (2012). Model selection and psychological theory: A discussion of the differences between the Akaike Information Criterion (AIC) and the Bayesian Information Criterion (BIC). *Psychological Methods*, *17*(2), 228–243. https://doi.org/10.1037/a0027127

Wagatsuma, A., Okuyama, T., Sun, C., Smith, L. M., Abe, K., & Tonegawa, S. (2018). Locus coeruleus input to hippocampal CA3 drives single-trial learning of a novel context. *Proceedings of the National Academy of Sciences*, *115*(2), E310–E316. https://doi.org/10.1073/pnas.1714082115

Wakamatsu, K., Tabuchi, K., Ojika, M., Zucca, F. A., Zecca, L., & Ito, S. (2015). Norepinephrine and its metabolites are involved in the synthesis of neuromelanin derived from the locus coeruleus. *Journal of Neurochemistry*, *135*(4), 768–776. https://doi.org/10.1111/jnc.13237

Wanke, N., Müller, J. C., Wiedemann, K., & Schwabe, L. (2020). (Lack of) Effects of noradrenergic stimulation on human working memory performance.

Psychopharmacology, *237*(10), 3033–3046. https://doi.org/10.1007/s00213-020 05590-0

Watanabe, T., Tan, Z., Wang, X., Martinez-Hernandez, A., & Frahm, J. (2019). Magnetic resonance imaging of noradrenergic neurons. *Brain Structure & Function*, *224*(4), 1609–1625. https://doi.org/10.1007/s00429-019-01858-0

Watson, M., & McElligott, J. G. (1984). Cerebellar norepinephrine depletion and impaired acquisition of specific locomotor tasks in rats. *Brain Research*, *296*(1), 129–138. https://doi.org/10.1016/0006-8993(84)90518-3

Wei, T., & Simko, V. (2010). *corrplot: Visualization of a Correlation Matrix* (p. 0.95) [Dataset]. https://doi.org/10.32614/CRAN.package.corrplot

Weiskopf, N., Suckling, J., Williams, G., Correia, M. M., Inkster, B., Tait, R., Ooi, C., Bullmore, E. T., & Lutti, A. (2013). Quantitative multi-parameter mapping of R1, PD*, MT, and R2* at 3T: A multi-center validation. *Frontiers in Neuroscience*, *7*. https://doi.org/10.3389/fnins.2013.00095

Westlund, K. N., & Coulter, J. D. (1980). Descending projections of the locus coeruleus and subcoeruleus/medial parabrachial nuclei in monkey: Axonal transport studies and dopamine-beta-hydroxylase immunocytochemistry. *Brain Research*, *2*(3), 235–264. https://doi.org/10.1016/0165-0173(80)90009-0

Wickham, H., Chang, W., Henry, L., Pedersen, T. L., Takahashi, K., Wilke, C., Woo, K., Yutani, H., Dunnington, D., Posit, & PBC. (2023). *ggplot2: Create Elegant Data Visualisations Using the Grammar of Graphics* (Version 3.4.2) [Computer software]. https://cran.r-project.org/web/packages/ggplot2/

Williams, C. L., & McGaugh, J. L. (1993). Reversible lesions of the nucleus of the solitary tract attenuate the memory-modulating effects of posttraining epinephrine. *Behavioral Neuroscience*, *107*(6), 955–962.

Wilson, R. S., Nag, S., Boyle, P. A., Hizel, L. P., Yu, L., Buchman, A. S., Schneider, J. A., & Bennett, D. A. (2013). Neural reserve, neuronal density in the locus ceruleus, and cognitive decline. *Neurology*, *80*(13), 1202–1208. https://doi.org/10.1212/WNL.0b013e3182897103

Wittmann, B. C., Dolan, R. J., & Düzel, E. (2011). Behavioral specifications of reward associated long-term memory enhancement in humans. *Learning & Memory*, *18*(5), 296–300. https://doi.org/10.1101/lm.1996811

Yakunina, N., Kim, S. S., & Nam, E.-C. (2017). Optimization of Transcutaneous Vagus Nerve Stimulation Using Functional MRI: TRANSCUTANEOUS VNS OPTIMIZATION USING fMRI. *Neuromodulation: Technology at the Neural Interface*, *20*(3), 290–300. https://doi.org/10.1111/ner.12541

Yap, J. Y. Y., Keatch, C., Lambert, E., Woods, W., Stoddart, P. R., & Kameneva, T. (2020). Critical Review of Transcutaneous Vagus Nerve Stimulation: Challenges for Translation to Clinical Practice. *Frontiers in Neuroscience*, *14*, 284. https://doi.org/10.3389/fnins.2020.00284

Ye, R., Rua, C., O'Callaghan, C., Jones, P. S., Hezemans, F. H., Kaalund, S. S., Tsvetanov, K. A., Rodgers, C. T., Williams, G., Passamonti, L., & Rowe, J. B. (2021). An in vivo probabilistic atlas of the human locus coeruleus at ultra-high field. *NeuroImage*, *225*, 117487. https://doi.org/10.1016/j.neuroimage.2020.117487

Yeung, A. W. K., & Wong, N. S. M. (2019). The Historical Roots of Visual Analog Scale in Psychology as Revealed by Reference Publication Year Spectroscopy. *Frontiers in Human Neuroscience*, *13*, 86. https://doi.org/10.3389/fnhum.2019.00086

Yi, Y.-J., Lüsebrink, F., Ludwig, M., Maaß, A., Ziegler, G., Yakupov, R., Kreißl, M. C., Betts, M., Speck, O., Düzel, E., & Hämmerer, D. (2023). It is the locus coeruleus! Or… is it?: A proposition for analyses and reporting standards for structural and functional magnetic resonance imaging of the noradrenergic locus coeruleus. *Neurobiology of*

Aging, *129*, 137–148. https://doi.org/10.1016/j.neurobiolaging.2023.04.007

Yoshida, K., Saku, K., Kamada, K., Abe, K., Tanaka-Ishikawa, M., Tohyama, T., Nishikawa, T., Kishi, T., Sunagawa, K., & Tsutsui, H. (2018). Electrical Vagal Nerve Stimulation Ameliorates Pulmonary Vascular Remodeling and Improves Survival in Rats With Severe Pulmonary Arterial Hypertension. *JACC. Basic to Translational Science*, *3*(5), 657–671. https://doi.org/10.1016/j.jacbts.2018.07.007

Yu, A. J., & Dayan, P. (2005). Uncertainty, Neuromodulation, and Attention. *Neuron*, *46*(4), 681–692. https://doi.org/10.1016/j.neuron.2005.04.026

Yushkevich, P. A., Yang Gao, null, & Gerig, G. (2016). ITK-SNAP: An interactive tool for semi-automatic segmentation of multi-modality biomedical images. *Annual International Conference of the IEEE Engineering in Medicine and Biology Society. IEEE Engineering in Medicine and Biology Society. Annual International Conference*, *2016*, 3342–3345. https://doi.org/10.1109/EMBC.2016.7591443

Zabara, J. (1985). Time course of seizure control to brief, repetitive stimuli. *Epilepsia*, *26*, 518.

Zabara, J. (1992). Inhibition of Experimental Seizures in Canines by Repetitive Vagal Stimulation. *Epilepsia*, *33*(6), 1005–1012. https://doi.org/10.1111/j.1528 1157.1992.tb01751.x

Zanos, T. P., Silverman, H. A., Levy, T., Tsaava, T., Battinelli, E., Lorraine, P. W., Ashe, J. M., Chavan, S. S., Tracey, K. J., & Bouton, C. E. (2018). Identification of cytokine specific sensory neural signals by decoding murine vagus nerve activity. *Proceedings of the National Academy of Sciences*, *115*(21).https://doi.org/10.1073/pnas.1719083115

Zecca, L., Bellei, C., Costi, P., Albertini, A., Monzani, E., Casella, L., Gallorini, M., Bergamaschi, L., Moscatelli, A., Turro, N. J., Eisner, M., Crippa, P. R., Ito, S., Wakamatsu, K., Bush, W. D., Ward, W. C., Simon, J. D., & Zucca, F. A. (2008). New melanic pigments in the human brain that accumulate in aging and block environmental toxic metals. *Proceedings of the National Academy of Sciences of the United States of America*, *105*(45), 17567–17572. https://doi.org/10.1073/pnas.0808768105

Zecca, L., Stroppolo, A., Gatti, A., Tampellini, D., Toscani, M., Gallorini, M., Giaveri, G., Arosio, P., Santambrogio, P., Fariello, R. G., Karatekin, E., Kleinman, M. H., Turro, N., Hornykiewicz, O., & Zucca, F. A. (2004a). The role of iron and copper molecules in the neuronal vulnerability of locus coeruleus and substantia nigra during aging. *Proceedings of the National Academy of Sciences*, *101*(26), 9843–9848. https://doi.org/10.1073/pnas.0403495101

Zecca, L., Youdim, M. B. H., Riederer, P., Connor, J. R., & Crichton, R. R. (2004b). Iron, brain ageing and neurodegenerative disorders. *Nature Reviews Neuroscience*, *5*(11), 863–873. https://doi.org/10.1038/nrn1537

Zucca, F. A., Bellei, C., Giannelli, S., Terreni, M. R., Gallorini, M., Rizzio, E., Pezzoli, G., Albertini, A., & Zecca, L. (2006). Neuromelanin and iron in human locus coeruleus and substantia nigra during aging: Consequences for neuronal vulnerability. *Journal of Neural Transmission*, *113*(6), 757–767. https://doi.org/10.1007/s00702-006-0453-2

Zucca, F. A., Segura-Aguilar, J., Ferrari, E., Muñoz, P., Paris, I., Sulzer, D., Sarna, T., Casella, L., & Zecca, L. (2017). INTERACTIONS OF IRON, DOPAMINE AND NEUROMELANIN PATHWAYS IN BRAIN AGING AND PARKINSON'S DISEASE. *Progress in Neurobiology*, *155*, 96–119. https://doi.org/10.1016/j.pneurobio.2015.09.012

Zucca, F. A., Vanna, R., Cupaioli, F. A., Bellei, C., De Palma, A., Di Silvestre, D., Mauri, P., Grassi, S., Prinetti, A., Casella, L., Sulzer, D., & Zecca, L. (2018). Neuromelanin organelles are specialized autolysosomes that accumulate undegraded proteins and lipids in aging human brain and are likely involved in Parkinson's disease. *Npj Parkinson's Disease*, *4*(1), 1–23. https://doi.org/10.1038/s41531-018-0050-8

9 Appendix

Supplementary information

The supplementary information (SI) is part of peer-reviewed publications in Communication Biology (Ludwig et al., 2024b), Scientific Reports (Ludwig et al., 2024a), and Psychophysiology (Ludwig et al., 2025). Consistent with the structure of the dissertation, the SI focuses first on additional material related to the LC fMRI study and then on the taVNS study.

Supplementary Information to chapter 2

High resolutional functional Locus Coeruleus imaging study

1. Extended Methods

1.1 Subjects

Sample description

	older adults	younger adults
number of subjects	22	28
age (mean ± SD)	67.68 ± 5.68	23.14 ± 3.18
gender (F/M)	12 / 10	16 / 12
Raven´s matrices (mean ± SD)	14.09 ± 2.43	16.26 ± 1.37

Supplementary Table S1. Overview of sample description. A shortened version of Raven's matrices was used as a measure of fluid intelligence (older adults (N = 22); younger adults (N = 19). The values indicate the correct answers from a total of 18 matrices.

1.2 Age-related differences in 8 brainstem landmarks' mean functional images in MNI space

There were no age-related difference for the left 4th ventricle border (younger adults = 0.77, older adults = 0.73, t(1,48) = 0.52, p = 0.61), right 4th ventricle border (younger adults = 0.71, older adults = 0.68, t(1,48) = 0.37, p = 0.71), periaqueductal grey (younger adults = 0.68, older adults = 0.57, t(1,48) = 1.79, p = 0.08), perifastigial sulcus (younger adults = 0.54, older adults = 0.52, t(1,48) = 0.38, p = 0.71), left outline brainstem (younger adults = 0.38, older adults = 0.25, t(1,48) = 1.40, p = 0.17) as well as right outline brainstem (younger adults = 0.32, older adults = 0.27, t(1,48) = 0.53, p = 0.60). However, there were age-related difference for left nucleus ruber (younger adults = 0.79, older adults = 0.57, t(1,48) = 2.1, p = 0.04) and right nucleus ruber (younger adults = 0.82, older adults = 0.55, t(1,48) = 2.73, p = 0.01).

1.3 Anatomical masks

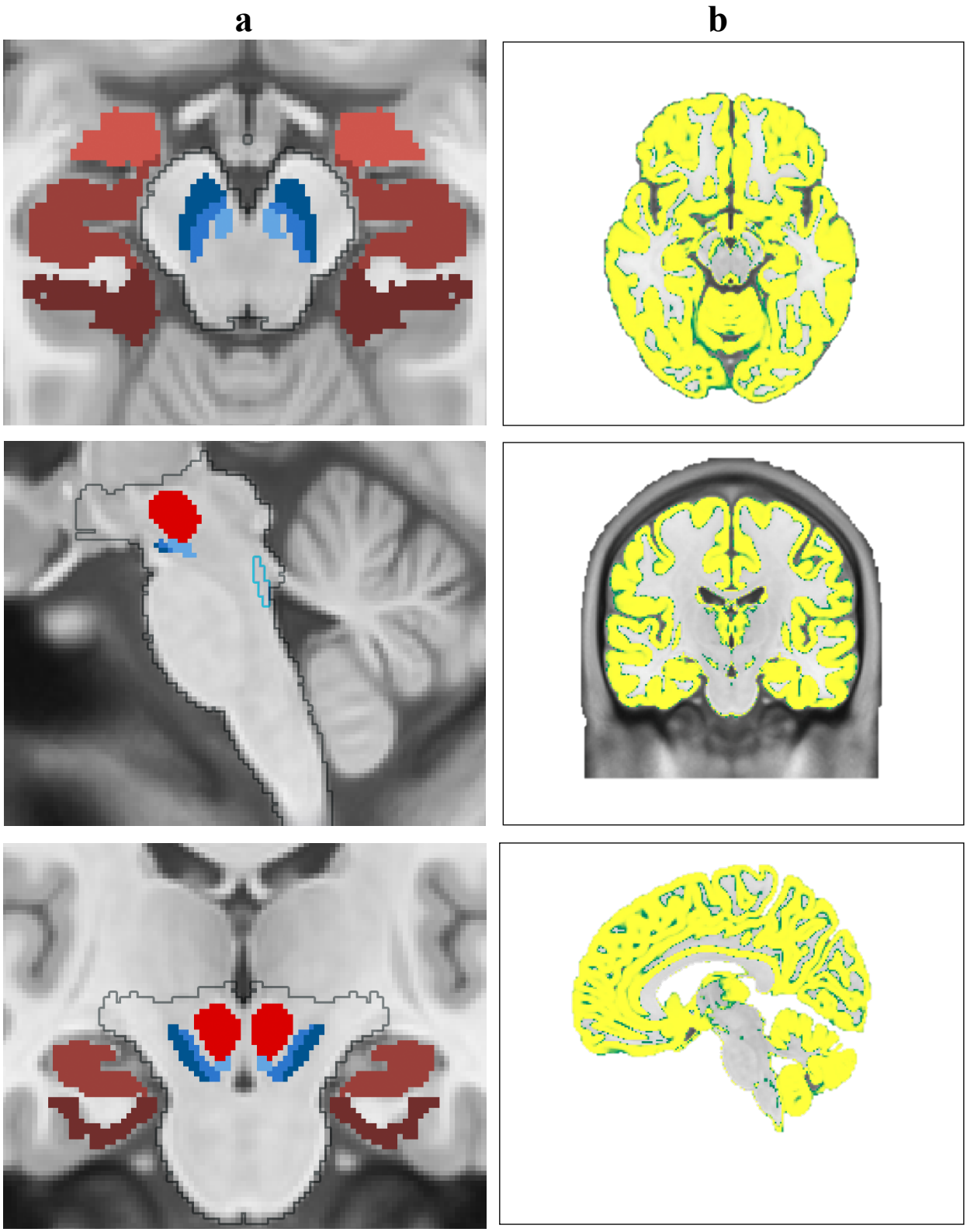

Supplementary Figure S1. Anatomical masks for second-level analyses for nuclei in the brainstem and midbrain (**a**): *substantia nigra pars reticulata (SNr,* dark blue*)*, *substantia nigra pars compacta (SNc,* middle blue*)*, *ventral tegmental area (VTA,* brighter blue*)*, *red nucleus* (red), amygdalae (rose), hippocampi (middle rose), para-hippocampi (dark rose) and locus coeruleus (turquoise outline) are shown within brainstem mask (grey outline). Additionally (**b**) grey matter mask (yellow-green) and **(b)** brainstem mask (grey outline) were used as an implicit mask in second-level analyses. Masks are presented in axial, coronal and sagittal view (row 1-3).

1.4 Types of event-related GLMs

Types of event-related GLMs	contrast of interest	fMRI results
(1) emotional salience	**loss feedback > gain feedback**	**younger adults** ▪ right **MTG** **older adults** ▪ left **LC** (Fig. 9a) ▪ bilateral **MTG** **older > younger** ▪ bilateral **LC** (Fig. 11a) ▪ bilateral **MTG** (Fig.12a-b) ▪ left **HPC** (Fig. 12c)
(2) task-related salience	**reversal feedback > no reversal feedback**	**younger adults** ▪ left **MTG** ▪ bilateral **STG** ▪ left **EC** **older adults** ▪ right **LC** (Fig. 9b) ▪ right **SNr** (Fig. 10) ▪ bilateral **MTG** ▪ right **PCUN** **older > younger** ▪ right **LC** (Fig. 11b) ▪ left **PCUN**
(3) memory performance	**remembered > not remembered**	**younger adults** / **older adults** ▪ right **LC** (Fig. 9c) **older > younger** ▪ right **LC** (Fig. 11c)
(4) emotional memory performance	**remembered before loss feedback > not remembered before loss feedback**	**younger adults** / **older adults** ▪ right **LC** (Fig. 9d) **older > younger** ▪ right **LC** (Fig. 11d)

Supplementary Table S2. Four types of event-related GLMs with corresponding contrasts of interest and overview of the main fMRI results of younger, older and the group comparison older > younger adults. Additional fMRI results (e.g., CAL, FuG, LiG) are mentioned in Supplementary Results 2.4.

1.5 Time course of the effect size

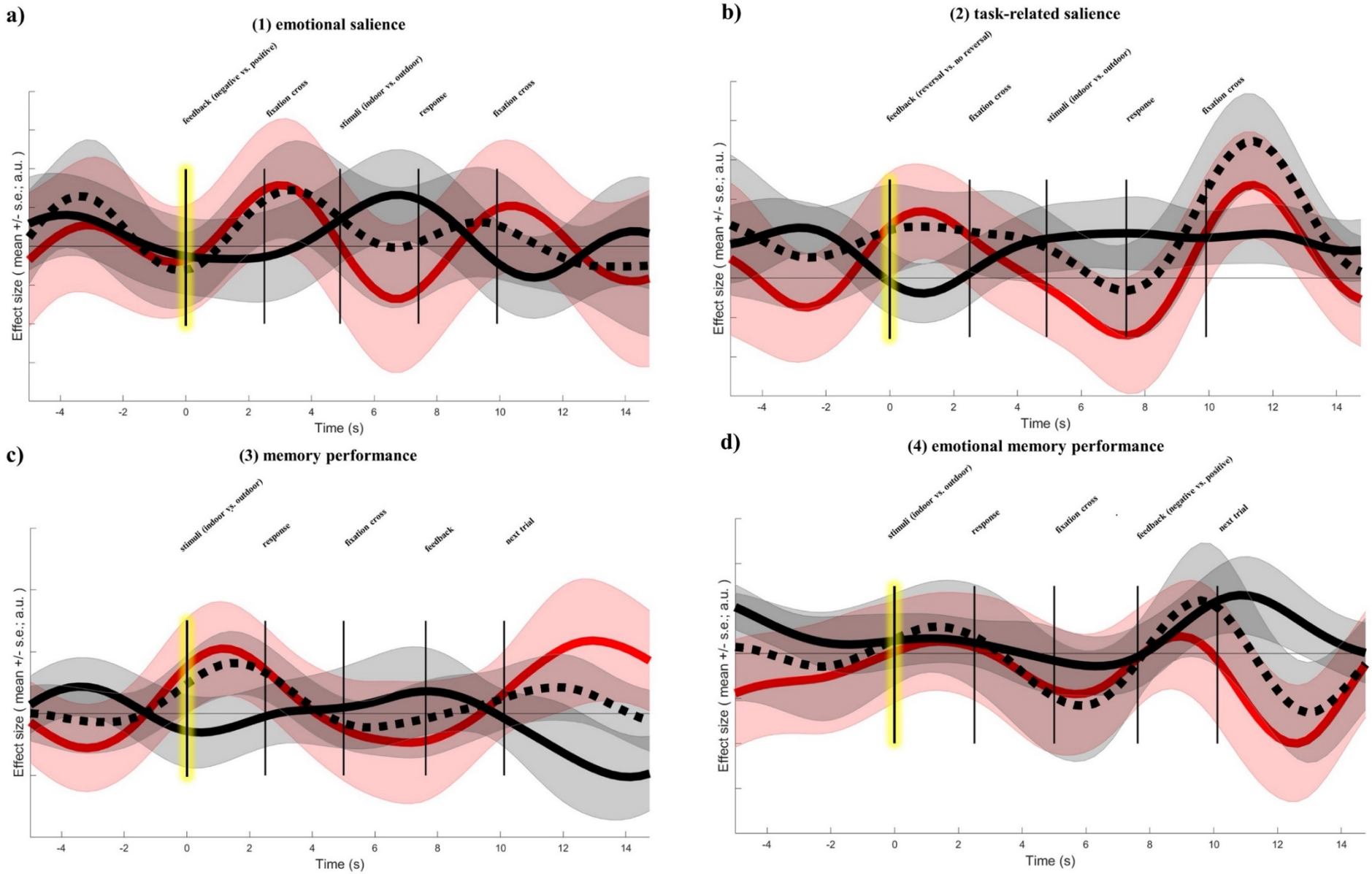

Supplementary Figure S2. Time course of the effect size for a) **(1)** emotional salience: loss > gain feedback, b) **(2)** task-related salience: reversal > no reversal feedback, c) **(3)** memory performance: remembered > not remembered and d) **(4)** emotional memory performance: remembered before loss feedback > not remembered before loss feedback for Locus Coeruleus (LC) activations (voxel cut-offs of $p < 0.005$). Beta values per contrast (a-d) for older adults (dotted black line) and younger adults (solid black line) and (a-d) the coefficient estimates for older adults > younger adults (solid red line) are plotted; shaded areas +/- 1 SE. Yellow lines indicate the onset of relevant task events.

2. Extended Results

2.1 Behavioral results

Regarding memory effects of **(1) emotional salience,** there was no or interaction between *loss vs. gain feedback* and *age group* ($F(1,48) = 0.013$, $p = 0.911$ [younger: loss feedback (M ± SD: 0.20 ± 0.02), gain feedback (M ± SD: 0.18 ± 0.02); older: loss feedback (M ± SD: 0.21 ± 0.02), gain feedback (M ± SD: 0.20 ± 0.02)]), as well as no interaction between *trials before vs. trials after feedback* and *age group* ($F(1,48) = 0.18$, $p = 0.693$ [younger: trials before (M ± SD: 0.19 ± 0.02), trials after (M ± SD: 0.19 ± 0.02); older: trials before (M ± SD: 0.20 ± 0.02), trials after (M ± SD: 0.20 ± 0.02)]).

2.2 Reaction times (RTs) for (1) emotional salience

Regarding RTs related to **(1) emotional salience**, RTs averaged across before and after trials were significantly slower related to gain feedback (M ± SD: 1.05 ± 0.02) as compared to loss feedback (M ± SD: 1.09 ± 0.02), $F(1,48) = 31.29$, $p < 0.0001$, partial $\eta^2 = .40$. There were significant interactions between *loss vs. gain feedback* and *age group* ($F(1,48) = 9.40$, $p = 0.04$, partial $\eta^2 = .164$, [younger: loss feedback (M ± SD: 0.99 ± 0.03), gain feedback (M ± SD: 0.98 ± 0.03), older: loss feedback (M ± SD: 1.18 ± 0.04), gain feedback (M ± SD: 1.12 ± 0.03) as well as between *number of stimuli* and *age group* ($F(1,48) = 5.34$, $p = 0.03$, partial $\eta^2 = .10$, [younger: single stimulus (M ± SD: 0.86 ± 0.03), double stimuli (M ± SD: 1.12 ± 0.04), older: single stimulus (M ± SD: 1.07 ± 0.03), double stimuli (M ± SD: 1.23 ± 0.04)]). RTs were slower during loss as compared to gain feedback. Older adults (M ± SD: 1.2 ± 0.4) showed a longer RTs as compared to younger adults (M ± SD: .98 ± 0.31), $F(1,48) = 12.94$, $p < 0.001$, partial $\eta^2 = .212$ during emotional salience. Likewise, RTs were slower on trials before the feedback (M ± SD: 1.07 ± 0.02) was presented as compared to after the feedback (M ± SD: 1.06 ± 0.02), $F(1,48) = 5.441$, $p = 0.024$, partial $\eta^2 = .10$, indicating that subjects have become faster over the task. RTs were also slower during the presentation of two stimuli (M ± SD: 1.17 ± 0.03) as compared to one stimuli (M ± SD: 0.97 ± 0.02), $F(1,48) = 140.30$, $p < 0.001$, partial $\eta^2 = .75$. Additionally, there was a significant interaction between the *single vs. double stimuli* and *loss vs. gain feedback*, $F(1,48) = 4.83$, $p = 0.03$, partial $\eta^2 = .09$: RTs were faster during single stimulus presentation and gain feedback [loss feedback: single stimulus (M ± SD: 0.98 ± 0.02), double stimuli (M ± SD: 1.19 ± 0.03), gain feedback: single stimulus (M ± SD: 0.95 ± 0.02), double stimuli (M ± SD: 1.15 ± 0.03). There was a significant three-way interaction between the *single vs. double stimuli*, *before loss vs. gain feedback* and *age group,* $F(1,48) = 5.87$, $p = 0.02$, partial $\eta^2 = .12$: Younger adults were generally faster, RTs were also faster during gain feedback and single stimulus presentation (younger: single stimulus loss feedback (M ± SD:

0.86 ± 0.03), single stimulus gain feedback (M ± SD: 0.86 ± 0.03), double stimulus loss feedback (M ± SD: 1.12 ± 0.04), double stimulus gain feedback (M ± SD: 1.09 ± 0.03); older: single stimulus loss feedback (M ± SD: 1.09 ± 0.04), single stimulus gain feedback (M ± SD: 1.04 ± 0.03), double stimulus loss feedback (M ± SD: 1.26 ± 0.04), double stimulus gain feedback (M ± SD: 1.21 ± 0.04). Another significant three-way interaction between the *single vs. double stimuli*, *before loss vs. gain feedback* and *before vs. after trials,* $F(1,48) = 12.28$, $p = 0.001$, partial $\eta^2 = .204$, indicated that, RTs were again faster during single stimulus presentation and gain feedback. However, for gain feedback, RTs were the same when presenting double stimuli both before and after trials (before: single stimulus loss feedback (M ± SD: 1 ± 0.03), single stimulus gain feedback (M ± SD: 0.93 ± 0.02), double stimulus loss feedback (M ± SD: 1.20 ± 0.03), double stimulus gain feedback (M ± SD: 1.15 ± 0.03); after: single stimulus loss feedback (M ± SD: 0.95 ± 0.03), single stimulus gain feedback (M ± SD: 0.98 ± 0.02), double stimulus loss feedback (M ± SD: 1.18 ± 0.03), double stimulus gain feedback (M ± SD: 1.15 ± 0.03). There was no significant interaction between *trials before vs. after* and the *age group* ($F(1,48) = .50$, $p = 0.49$, partial $\eta^2 = .01$, [younger: trials before (M ± SD: 0.97 ± 0.03), trials after (M ± SD: 0.98 ± 0.03), older: trials before (M ± SD: 1.16 ± 0.04), trials after (M ± SD: 1.15 ± 0.03)]). Regarding RTs related to **(2) task-related saliency,** older adults (M ± SD: 1.1 ± 0.4) showed a longer RTs as compared to younger adults (M ± SD: .94 ± 0.3), $F(1,48) = 18.20$, $p < 0.001$, partial $\eta^2 = .28$.

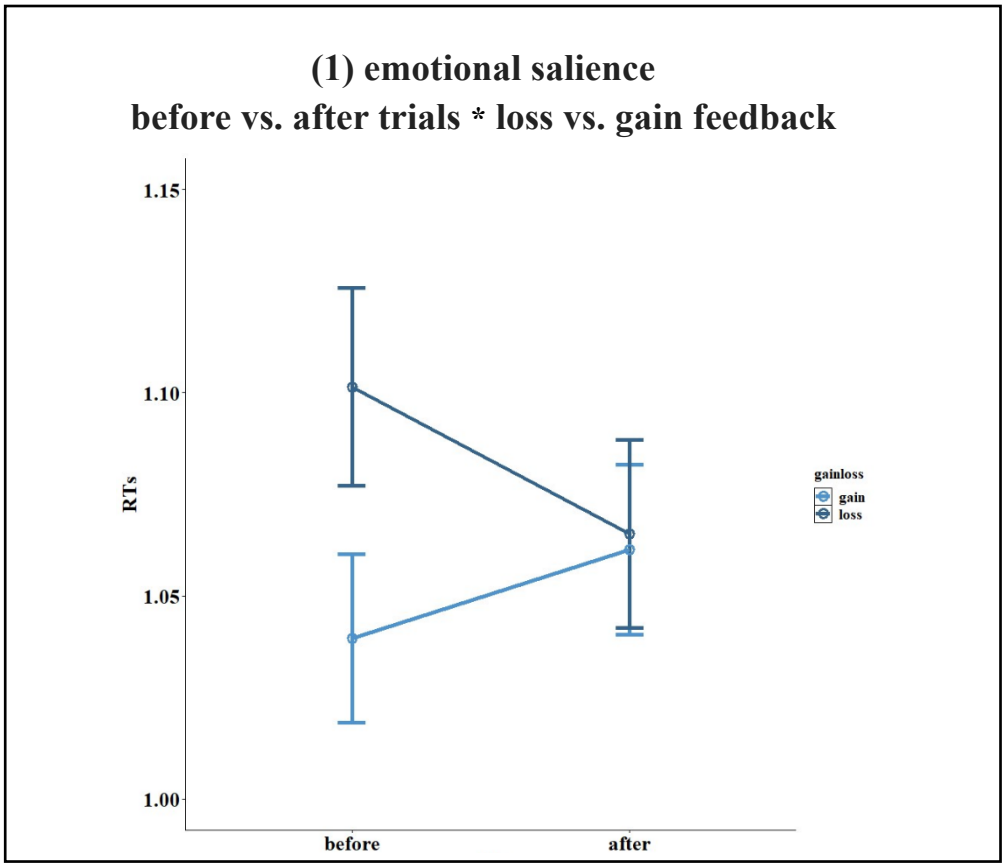

Supplementary Figure S3. Mean RTs for loss (dark blue) and gain (light blue) feedback after (x-axis, left) and before (x-axis, right) trials across age-groups for (1) emotional salience. RTs slowed down after gain feedback but sped up after loss feedback (loss feedback: before trials (M = 1.10, SD = 0.03), after trials (M = 1.07, SD = 0.02), gain feedback: before trials (M = 1.04, SD = 0.02), after trials (M = 1.06, SD = 0.02); $F(1,48) = 19.40$, $p < 0.001$, partial $\eta^2 = .29$).

2.3 fMRI results

The analysis procedure described in "fMRI results" resulted in no suprathreshold for a) **LC activation** in younger adults and younger > older adults for (**(1)** emotional salience, **(2)** task-related salience, **(3)** memory performance, **(4)** emotional memory performance)), b) for SNc, SNr, VTA and red nucleus activation in younger > older adults **(1)** emotional salience, **(2)** task-related salience**)** and older adults and older > younger adults **((3)** memory performance, **(4)** emotional memory performance**)**. Also, no suprathreshold clusters for **cortical areas** were found in younger and older adults (**(3)** memory performance, **(4)** emotional memory performance), younger > older adults (**(1)** emotional salience, **(2)** task-related salience, **(3)** memory performance) and older > younger adults (**(3)** memory performance). Finally, no suprathreshold clusters **for subcortical** areas were found in younger and older adults (**(1)** emotional salience, **(2)** task-related salience, **(3)** memory performance, **(4)** emotional memory performance), younger > older adults **(1)** emotional salience, **(2)** task-related salience, **(3)** memory performance, **(4)** emotional memory performance), as well as older > younger adults (**(2)** task-related salience, **(3)** memory performance, **(4)** emotional memory performance)).

2.4 Activation in cortical areas

During **(1) loss > gain feedback** (see Supplementary Figure S4 & Table S17-S19) higher left **CAL** [Younger adults: T = 6.93, pFDR < 0.01; Older adults: T = 4.60, pFDR < 0.01), and right **CAL** (Younger adults: T = 5.23, pFDR < 0.01) as well as right **FuG** (Older adults: T = 6.37, pFDR < 0.01) and right **LiG** (Older adults: T = 6.62, pFDR < 0.01) were observed. During **(2) reversal > no reversal feedback** (see Supplementary Figure S5; Table 20-22) older adults showed stronger engagement of left **CAL** (T = 4.74, pFDR < 0.01). Similarly, as compared to younger adults, older adults also showed higher activation of the left **LiG** during **(4) later remembered stimuli followed by loss** as compared to not remembered stimuli followed by loss feedback (see Supplementary Figure S6 & Table S23) (Older > Younger adults: T = 3.93, pFDR < 0.01). Additionally, for **(2)** task-related saliency in older adults, activation in MTG was significantly **correlated** with better memory performance for stimuli on trials immediately before a reversal in the delayed recognition (difference before and after trials), r (16) = .62, p < 0.009, indicating that stronger MTG activation is related to better memory performance before events of task-related salience (Supplementary Figure S8).

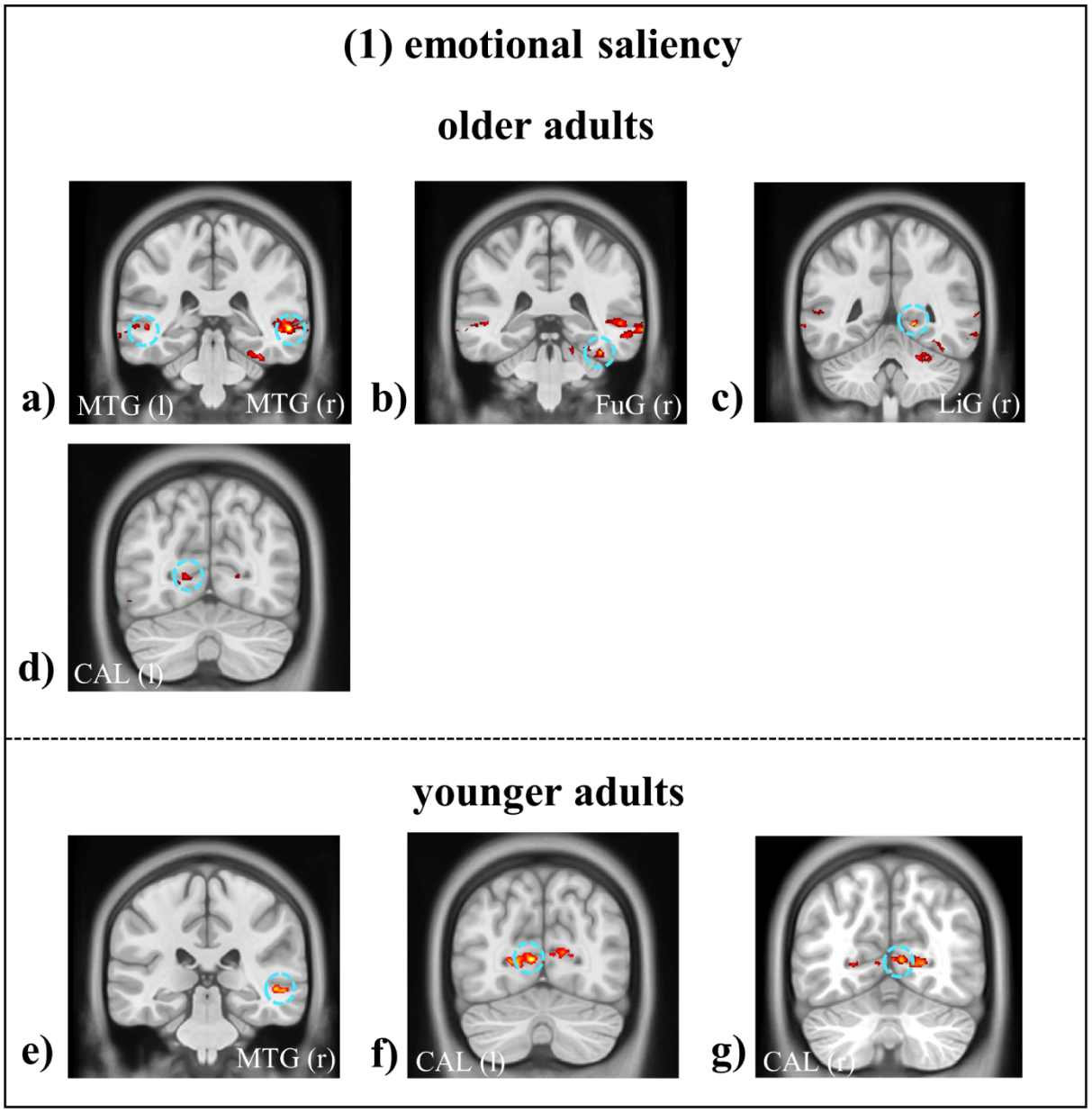

Supplementary Figure S4. Activations in cortical areas for **(1) emotional salience** (red-yellow) for (**a-d**) older adults and (**e-g**) younger adults. Turquoise circles highlight the corresponding significant activations, threshold of $p < 0.005$. Abbreviations: CAL calcarine cortex, FuG fusiform gyrus, l left, LiG lingual gyrus, MTG middle temporal gyrus, r right.

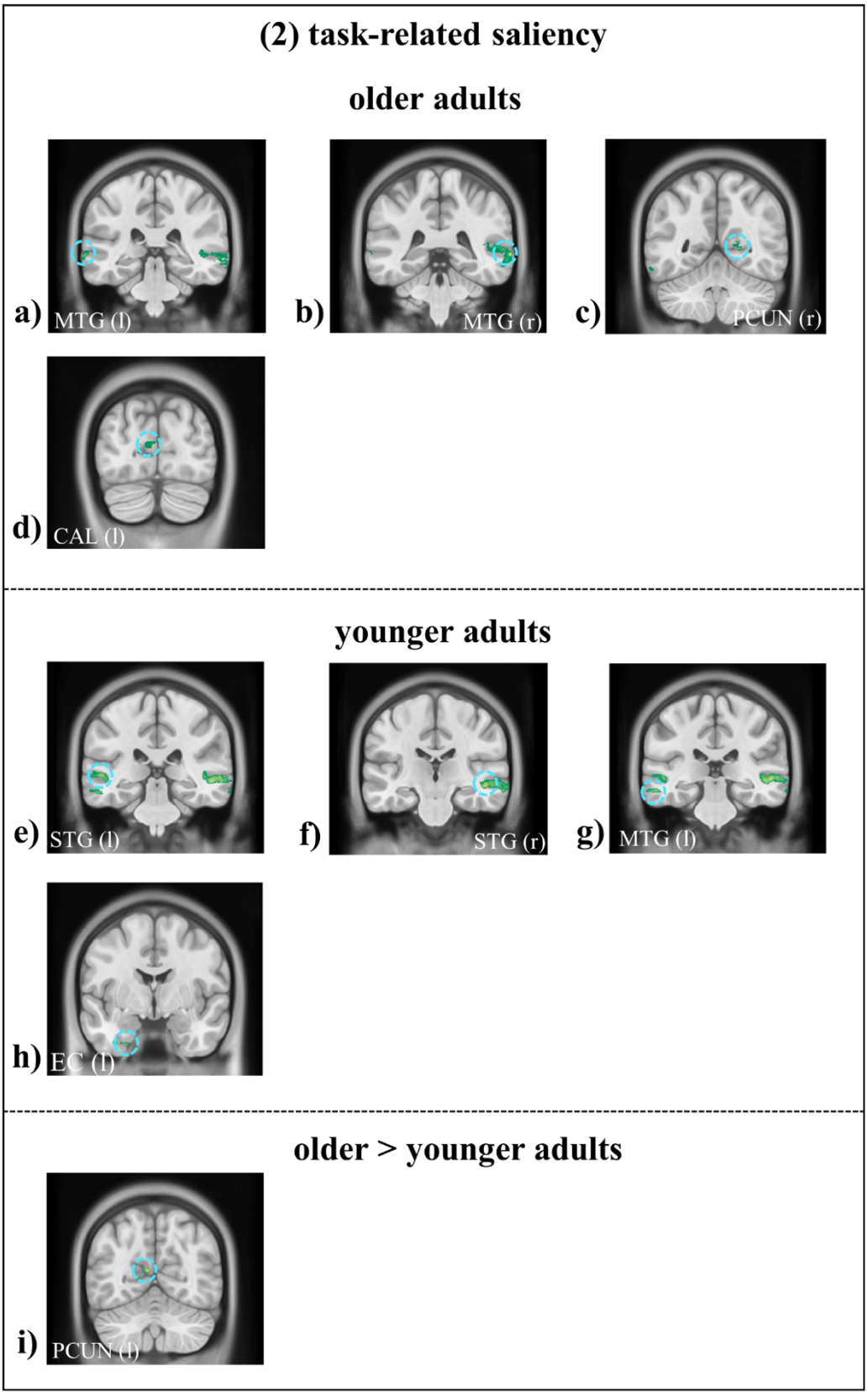

Supplementary Figure S5. Activations in cortical areas for **(2) task-related salience** (green-yellow) for (**a-d**) older adults (**e-h**) younger adults, (**i**) older > younger adults. Turquoise circles highlight the corresponding significant activations, threshold of $p < 0.005$. Abbreviations: CAL calcarine cortex, EC entorhinal cortex, l left, MTG middle temporal gyrus, PCUN precuneus, r right, STG superior temporal gyrus.

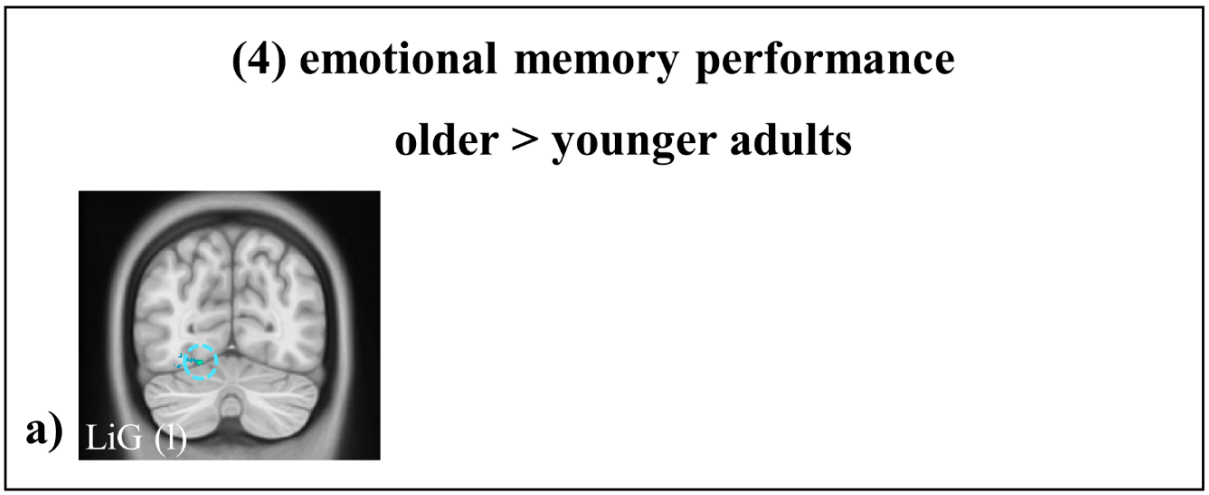

Supplementary Figure S6. Activation in cortical areas for **(4) emotional memory performance** (blue-green) for (**a**) older > younger adults. Turquoise circle highlights the corresponding significant activation, threshold of $p < 0.005$. Abbreviations: l left, LiG lingual gyrus.

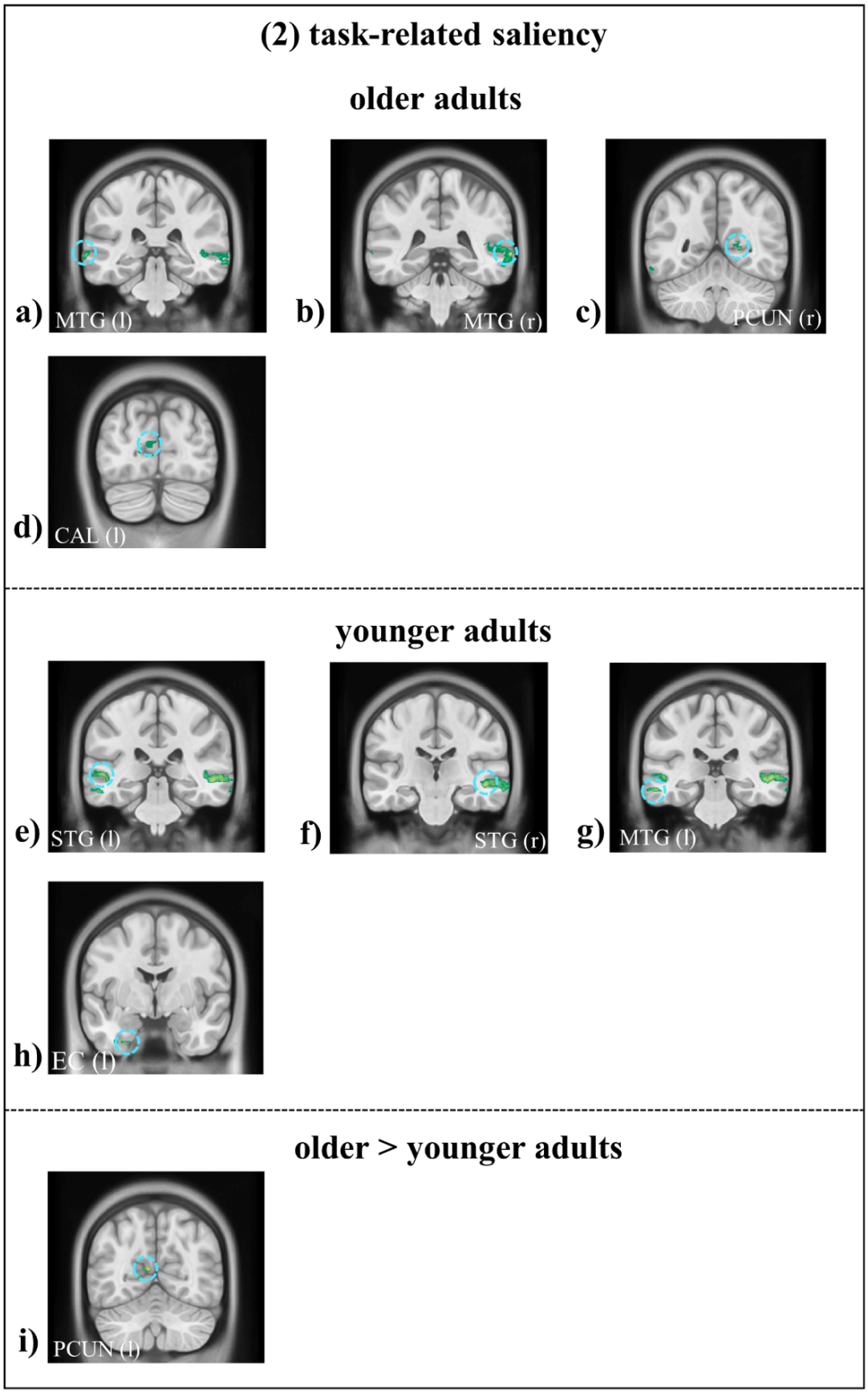

Supplementary Figure S5. Activations in cortical areas for **(2) task-related salience** (green-yellow) for (**a-d**) older adults (**e-h**) younger adults, (**i**) older > younger adults. Turquoise circles highlight the corresponding significant activations, threshold of $p < 0.005$. Abbreviations: CAL calcarine cortex, EC entorhinal cortex, l left, MTG middle temporal gyrus, PCUN precuneus, r right, STG superior temporal gyrus.

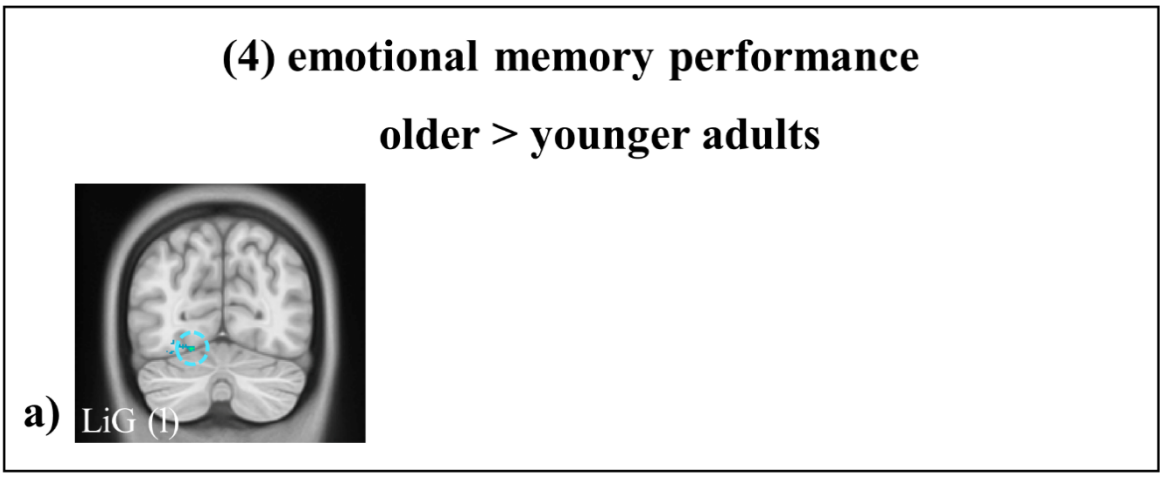

Supplementary Figure S6. Activation in cortical areas for **(4) emotional memory performance** (blue-green) for (**a**) older > younger adults. Turquoise circle highlights the corresponding significant activation, threshold of $p < 0.005$. Abbreviations: l left, LiG lingual gyrus.

The following **Supplementary Tables** report **(3-16) brainstem and midbrain activations** as well as **(17-23) cortical activations** for **(1)** emotional salience, **(2)** task-related salience, **(3)** memory performance and **(4)** emotional memory performance. Abbreviations: CAL *calcarine cortex*, CBM *cerebellum*, EC *entorhinal cortex*, FuG *fusiform gyrus*, HPC *hippocampus*, ITG *inferior temporal gyrus*, LC *locus coeruleus*, LiG *lingual gyrus*, MTG *middle temporal gyrus*, PCUN *precuneus*, red Ncl *red nucleus*, SNc *substantia nigra pars compacta*, SNr *substantia nigra pars reticulata*, VDC *ventral diencephalon*, VTA *ventral tegmental area*, WM *white matter.*

2.5 brainstem & midbrain activations

older adults **(1) emotional salience: loss feedback > gain feedback**

		cluster									peak				
	region	x (mm)	y (mm)	z (mm)	Z (max.)	C	p (FWE corr.)	p (FDR corr.)	K (equiv.)	p (unc.)	T	p (FWE corr.)	p (FDR corr.)	Z (equiv.)	p (unc.)
p < 0.005	**LC (l)**	-5	-38	-26	4.11	2	0.04	0.55	15	0.29	4.11	0.01	0.23	3.48	< 0.001
	LC (r)	4	-37	-22	3.05	2	0.07	0.55	5	0.55	3.05	0.08	0.88	2.75	0.003
	SNr (l)	-6	-18	-18	4.46	3	0.31	0.66	20	0.22	4.46	0.09	0.17	3.69	0.001
	VDC (r)	4	-19	-6	3.02	3	0.75	0.82	1	0.82	3.02	0.71	0.99	2.72	0.003
	VDC (l)	-10	-23	-16	2.84	3	0.75	0.82	1	0.82	2.84	0.81	0.99	2.59	0.004
p < 0.003	**LC (l)**	-5	-38	-26	4.11	1	0.02	0.29	12	0.29	4.11	0.01	0.12	3.48	< 0.001
	SNr (l)	-6	-18	-18	4.46	1	0.24	0.23	15	0.23	4.46	0.09	0.08	3.70	< 0.001

Supplementary Table S3. Activations in older subjects for emotional salience with applying a **"brainstem mask"** and small volume image of **"LC meta mask"** or **"SNredVTA mask"** cluster threshold p < 0.005 and p < 0.003 with no adjusted FDRc.

older adults > younger adults

		cluster									peak				
	region	x (mm)	y (mm)	z (mm)	Z (max.)	C	p (FWE corr.)	p (FDR corr.)	K (equiv.)	p (unc.)	T	p (FWE corr.)	p (FDR corr.)	Z (equiv.)	p (unc.)
p < 0.005	**LC (l)**	-5	-37	-25	3.40	2	0.06	0.69	6	0.55	3.40	0.02	0.34	3.20	< 0.001
	LC (r)	4	-37	-22	3.14	2	0.08	0.69	3	0.69	3.14	0.04	0.34	2.98	0.001
	VDC (r)	4	-19	-6	2.74	1	0.72	0.83	1	0.83	2.74	0.74	0.90	2.63	0.004
p < 0.003	**LC (l)**	-5	-37	-25	3.40	2	0.04	0.72	4	0.59	3.40	0.53	0.53	3.20	< 0.001
	LC (r)	4	-37	-22	3.14	2	0.05	0.72	2	0.72	3.14	0.53	0.53	2.98	0.001

Supplementary Table S4. Activations in older > younger subjects for emotional salience with applying a **"brainstem mask"** and small volume image of **"LCmeta mask"** or **"SNredVTA mask"** cluster threshold p < 0.005 and p < 0.003 with no adjusted FDRc.

(1) emotional salience: loss feedback > gain feedback

younger adults

		cluster									peak				
	region	x (mm)	y (mm)	z (mm)	Z (max.)	C	p (FWE corr.)	p (FDR corr.)	K (equiv.)	p (unc.)	T	p (FWE corr.)	p (FDR corr.)	Z (equiv.)	p (unc.)
p < 0.005	SNc (r)	10	-21	-11	4.35	5	0.41	0.75	14	0.34	4.35	0.06	0.16	3.75	< 0.001
	SNr (r)	9	-16	-17	4.33	5	0.52	0.75	8	0.48	4.33	0.07	0.16	3.74	< 0.001
	SNr (l)	-10	-14	-15	3.73	5	0.28	0.75	24	0.22	3.73	0.22	0.38	3.32	< 0.001
	SNr (r)	9	-13	-11	3.08	5	0.65	0.75	3	0.68	3.08	0.59	0.67	2.83	0.002
	SNc (r)	5	-20	-19	3.00	5	0.68	0.75	2	0.75	3.00	0.64	0.67	2.76	0.003
p < 0.003	SNc (r)	10	-21	-11	4.35	5	0.29	0.81	12	0.32	4.35	0.06	0.23	3.75	< 0.001
	SNr (r)	9	-16	-17	4.32	5	0.43	0.81	5	0.53	4.33	0.07	0.23	3.74	< 0.001
	SNr (l)	-10	-14	-15	3.72	5	0.24	0.81	16	0.25	3.73	0.22	0.55	3.31	< 0.001
	SNr (r)	9	-13	-11	3.08	5	0.57	0.81	1	0.81	3.08	0.59	0.96	2.83	0.002
	SNc (r)	5	-20	-19	3.00	5	0.57	0.81	1	0.81	3.00	0.64	0.96	2.76	0.003

Supplementary Table S5. Activations in younger subjects for emotional salience with applying a **"brainstem mask"** and small volume image of **"LC meta mask"** or **"SNredVTA mask"** cluster threshold $p < 0.005$ and $p < 0.003$ with no adjusted FDRc.

older adults

(2) task related salience: reversal > no reversal

		cluster									peak				
	region	x (mm)	y (mm)	z (mm)	Z (max.)	C	p (FWE corr.)	p (FDR corr.)	K (equiv.)	p (unc.)	T	p (FWE corr.)	p (FDR corr.)	Z (equiv.)	p (unc.)
p < 0.005	**LC (r)**	5	-37	-27	3.37	2	0.08	0.71	3	0.64	3.37	0.05	0.49	2.98	0.001
	LC (r)	3	-36	-19	3.37	2	0.09	0.71	2	0.71	3.37	0.05	0.49	2.98	0.001
	SNr (r)	13	-18	-9	4.77	5	0.02	0.07	89	0.01	4.77	0.05	0.37	3.88	< 0.001
	red Ncl (l)	-5	-17	-8	3.87	5	0.12	0.11	44	0.07	3.87	0.26	0.66	3.33	< 0.001
	red Ncl (r)	7	-22	-13	3.83	5	0.61	0.53	5	0.53	3.83	0.28	0.66	3.30	< 0.001
	red Ncl (r)	7	-18	-7	3.59	5	0.06	0.09	62	0.03	3.59	0.39	0.66	3.14	< 0.001
	SNr (l)	-12	-15	-13	3.47	5	0.29	0.24	21	0.19	3.47	0.46	0.66	3.05	0.001
p < 0.003	**LC (r)**	5	-37	-27	3.37	2	0.05	0.67	3	0.59	3.37	0.05	0.75	2.98	0.001
	LC (r)	3	-26	-19	3.37	2	0.06	0.67	2	0.67	3.37	0.05	0.75	2.98	0.001
	SNr (r)	13	-18	-9	4.77	9	0.02	0.12	70	0.01	4.77	0.05	0.49	4.77	< 0.001
	red Ncl (l)	-5	-17	-8	3.87	9	0.25	0.60	14	0.23	3.87	0.26	0.87	3.87	< 0.001
	red Ncl (r)	7	-22	-13	3.83	9	0.52	0.75	3	0.59	3.83	0.28	0.87	3.83	< 0.001
	red Ncl (r)	7	-18	-7	3.60	9	0.22	0.60	16	0.20	3.60	0.39	0.87	3.59	< 0.001
	SNr (l)	-12	-15	-13	3.47	9	0.32	0.60	10	0.31	3.47	0.46	0.87	3.47	0.001
	red Ncl (l)	-3	-21	-7	3.34	9	0.45	0.72	5	0.48	3.34	0.54	0.87	3.34	0.001
	red Ncl (r)	3	-18	-8	3.33	9	0.34	0.60	9	0.34	3.33	0.55	0.87	3.33	0.001

	red Ncl (l)	-9	-18	-7	3.19	9	0.57	0.75	2	0.67	3.19	0.63	0.88	3.19	0.002
	VDC (r)	2	-22	-8	3.10	9	0.62	0.78	1	0.78	3.10	0.69	0.93	3.10	0.003

Supplementary Table S6. Activations in older subjects for task-related salience with applying a **"brainstem mask"** and small volume image of **"LC meta mask"** or **"SNredVTA mask"** cluster threshold $p < 0.005$ and $p < 0.003$ with no adjusted FDRc.

(2) task related salience: reversal > no reversal

older adults > younger adults

		cluster									peak				
	region	x (mm)	y (mm)	z (mm)	Z (max.)	C	p (FWE corr.)	p (FDR corr.)	K (equiv.)	p (unc.)	T	p (FWE corr.)	p (FDR corr.)	Z (equiv.)	p (unc.)
$p < 0.005$	**LC** (r)	4	-38	-28	3.02	1	0.07	0.63	4	0.63	3.02	0.05	0.77	2.88	0.002
	red Ncl (l)	-3	-21	-7	3.18	3	0.68	0.74	2	0.74	3.18	0.43	0.55	3.01	0.001
	VDC (l)	-9	-18	-7	3.18	3	0.48	0.74	10	0.42	3.18	0.43	0.55	3.01	0.001
	red Ncl (r)	3	-21	-7	2.83	3	0.68	0.74	2	0.74	2.83	0.69	0.76	2.70	0.003
$p < 0.003$	**LC (r)**	4	-38	-28	3.02	1	0.06	0.81	1	0.81	2.88	0.05	0.71	2.88	0.001
	red Ncl (l)	-3	-21	-7	3.18	2	0.57	0.81	1	0.81	3.18	0.43	0.60	3.01	0.001
	VDC (l)	-9	-18	-7	3.18	2	0.41	0.81	6	0.49	3.18	0.43	0.60	3.01	0.001

Supplementary Table S7. Activations in older > younger subjects for task-related salience with applying a **"brainstem mask"** and small volume image of **"LC meta mask"** or **"SNredVTA mask"** cluster threshold $p < 0.005$ and $p < 0.003$ with no adjusted FDRc.

younger adults **(2) task related salience: reversal > no reversal**

						cluster					peak				
	region	x (mm)	y (mm)	z (mm)	Z (max.)	C	p (FWE corr.)	p (FDR corr.)	K (equiv.)	p (unc.)	T	p (FWE corr.)	p (FDR corr.)	Z (equiv.)	p (unc.)
p < 0.005	SNc (l)	-10	-24	-13	4.34	6	0.25	0.56	27	0.19	4.34	0.07	0.54	3.75	0.001
	SNr (r)	4	-17	-17	3.46	6	0.65	0.83	3	0.68	3.46	0.36	0.78	3.12	0.001
	red Ncl (r)	8	-19	-10	3.44	6	0.08	0.34	60	0.06	3.44	0.36	0.78	3.12	0.001
	VDC (r)	4	-14	-7	3.02	6	0.72	0.83	1	0.83	3.02	0.64	0.80	2.78	0.003
	red Ncl (r)	5	-16	-12	2.85	6	0.72	0.83	1	0.83	2.85	0.74	0.88	2.64	0.004
	SNc (l)	-10	-19	-13	2.85	6	0.65	0.83	3	0.68	2.85	0.74	0.88	2.64	0.004
p < 0.003	SNc (l)	-10	-24	-13	4.34	8	0.21	0.80	18	0.22	4.34	0.07	0.65	3.75	< 0.001
	SNr (r)	4	-17	-17	3.46	8	0.50	0.80	3	0.63	3.46	0.36	0.94	3.12	< 0.001
	red Ncl. (r)	8	-19	-10	3.44	8	0.32	0.80	10	0.36	3.44	0.36	0.94	3.11	< 0.001
	SNr (r)	10	-22	-12	3.43	8	0.32	0.80	10	0.36	3.43	0.37	0.94	3.10	< 0.001
	SNr (r)	9	-18	-12	3.31	8	0.38	0.80	7	0.45	3.32	0.44	0.94	3.01	0.001
	red Ncl. (r)	5	-18	-10	3.14	8	0.53	0.80	2	0.71	3.14	0.55	0.94	2.87	0.002
	VDC (r)	4	-14	-7	3.02	8	0.58	0.80	1	0.80	3.02	0.64	0.96	2.78	0.003
	SNr (r)	11	-16	-14	3.00	8	0.58	0.80	1	0.80	3.00	0.64	0.96	2.77	0.003

Supplementary Table S8. Activations in younger subjects for task-related salience with applying a **"brainstem mask"** and small volume image of **"LC meta mask"** or **"SNredVTA mask"** cluster threshold p < 0.005 and p < 0.003 with no adjusted FDRc.

(3) memory performance: remembered > not remembered

older adults

		cluster									peak				
	region	x (mm)	y (mm)	z (mm)	Z (max.)	C	p (FWE corr.)	p (FDR corr.)	K (equiv.)	p (unc.)	T	p (FWE corr.)	p (FDR corr.)	Z (equiv.)	p (unc.)
p < 0.005	**LC (r)**	5	-38	-25	3.64	1	0.07	0.53	5	0.53	3.64	0.03	0.21	3.17	< 0.001
p < 0.003	**LC (r)**	5	-38	-25	3.64	1	0.05	0.59	3	0.59	3.64	0.03	0.31	3.17	< 0.001

Supplementary Table S9. Activations in older subjects for memory performance with applying a **"brainstem mask"** and small volume image of **"LC meta mask"** cluster threshold p < 0.005 and p < 0.003 with no adjusted FDRc.

older > younger adults

		cluster									peak				
	region	x (mm)	y (mm)	z (mm)	Z (max.)	C	p (FWE corr.)	p (FDR corr.)	K (equiv.)	p (unc.)	T	p (FWE corr.)	p (FDR corr.)	Z (equiv.)	p (unc.)
p < 0.005	**LC (r)**	5	-38	-25	3.42	1	0.08	0.67	3	0.67	3.42	0.02	0.17	3.22	< 0.001
p < 0.003	**LC (r)**	5	-38	-25	3.42	1	0.05	0.70	2	0.70	3.42	0.02	0.26	3.22	< 0.001

Supplementary Table S10. Activations in older > younger subjects for memory performance with applying a **"brainstem mask"** and small volume image of **"LC meta mask"** cluster threshold p < 0.005 and p < 0.003 with no adjusted FDRc.

younger adults

(3) memory performance: remembered > not remembered

						cluster					peak				
	region	x (mm)	y (mm)	z (mm)	Z (max.)	C	p (FWE corr.)	p (FDR corr.)	K (equiv.)	p (unc.)	T	p (FWE corr.)	p (FDR corr.)	Z (equiv.)	p (unc.)
p < 0.005	SNr (l)	-11	-23	-17	3.23	2	0.74	0.82	1	0.82	3.23	0.51	0.66	2.95	0.002
	SNr (l)	-12	-24	-15	3.01	2	0.66	0.82	3	0.67	3.01	0.65	0.66	2.77	0.003
p < 0.003	SNr (l)	-11	-23	-17	3.23	2	0.59	0.80	1	0.80	3.23	0.51	0.95	2.95	0.002
	SNr (l)	-12	-24	-15	3.01	2	0.59	0.80	1	0.80	3.01	0.65	0.95	2.77	0.003

Supplementary Table S11. Activations in younger subjects for memory performance with applying a **"brainstem mask"** and small volume image of **"SNredVTA mask"** cluster threshold p < 0.005 and p < 0.003 with no adjusted FDRc.

younger > older adults

						cluster					peak				
	region	x (mm)	y (mm)	z (mm)	Z (max.)	C	p (FWE corr.)	p (FDR corr.)	K (equiv.)	p (unc.)	T	p (FWE corr.)	p (FDR corr.)	Z (equiv.)	p (unc.)
p < 0.005	SNc (r)	9	-26	-16	3.00	4	0.55	0.83	7	0.50	3.00	0.56	0.82	2.86	0.002
	red Ncl. (l)	-6	-24	-12	2.92	4	0.69	0.83	2	0.74	2.92	0.63	0.82	2.79	0.003
	VTA (l)	-3	-24	-19	2.90	4	0.73	0.83	1	0.83	2.90	0.64	0.82	2.77	0.003
	SNr (l)	-11	-23	-17	2.79	4	0.73	0.83	1	0.83	2.79	0.73	0.82	2.67	0.004
p < 0.003	SNc (r)	9	-26	-16	3.00	3	0.50	0.80	3	0.63	3.00	0.56	0.95	2.86	0.002
	red Ncl. (l)	-6	-24	-12	2.92	3	0.58	0.80	1	0.80	2.92	0.63	0.95	2.79	0.003
	VTA (l)	-3	-24	-19	2.90	3	0.58	0.80	1	0.80	2.90	0.64	0.95	2.77	0.003

Supplementary Table S12. Activations in younger > older subjects for memory performance with applying a **"brainstem mask"** and small volume image of **"LC meta mask"** or **"SNredVTA mask"** cluster threshold p < 0.005 and p < 0.003 with no adjusted FDRc.

older adults

(4) emotional memory performance: remembered before loss > not remembered before loss

		cluster									peak				
	region	x (mm)	y (mm)	z (mm)	Z (max.)	C	p (FWE corr.)	p (FDR corr.)	K (equiv.)	p (unc.)	T	p (FWE corr.)	p (FDR corr.)	Z (equiv.)	p (unc.)
p < 0.005	**LC (r)**	5	-38	-24	4.38	1	0.07	0.59	4	0.59	4.38	0.01	0.04	3.65	< 0.001
p < 0.003	**LC (r)**	5	-38	-24	4.38	1	0.06	0.67	2	0.67	4.38	0.01	0.07	3.65	< 0.001

Supplementary Table S13. Activations in older subjects for emotional memory performance with applying a **"brainstem mask"** and small volume image of **"LC meta mask"** cluster threshold p < 0.005 and p < 0.003 with no adjusted FDRc.

older > younger adults

		cluster									peak				
	region	x (mm)	y (mm)	z (mm)	Z (max.)	C	p (FWE corr.)	p (FDR corr.)	K (equiv.)	p (unc.)	T	p (FWE corr.)	p (FDR corr.)	Z (equiv.)	p (unc.)
p < 0.005	**LC (r)**	5	-38	-24	3.46	1	0.09	0.74	2	0.74	3.46	0.02	0.15	3.25	< 0.001
p < 0.003	**LC (r)**	5	-38	-24	3.46	1	0.05	0.70	2	0.70	3.46	0.02	0.23	3.25	< 0.001

Supplementary Table S14. Activations in older > younger subjects for emotional memory performance with applying a **"brainstem mask"** and small volume image **"LC meta mask"** cluster threshold p < 0.005 and p < 0.003 with no adjusted FDRc.

younger **(4) emotional memory performance: remembered before loss > not remembered before loss**

		cluster									peak				
	region	x (mm)	y (mm)	z (mm)	Z (max.)	C	p (FWE corr.)	p (FDR corr.)	K (equiv.)	p (unc.)	T	p (FWE corr.)	p (FDR corr.)	Z (equiv.)	p (unc.)
p < 0.005	SNr (l)	-7	-24	-11	3.86	6	0.53	0.73	8	0.45	3.86	0.19	0.54	3.42	< 0.001
	SNc (l)	-11	-23	-17	3.44	6	0.70	0.73	2	0.73	3.44	0.39	0.54	3.12	< 0.001
	VTA (l)	-4	-22	-16	3.28	6	0.67	0.73	3	0.66	3.28	0.49	0.54	2.98	0.001
	red Ncl. (r)	5	-20	-11	3.26	6	0.55	0.73	7	0.48	3.26	0.50	0.54	2.97	0.001
	SNc (r)	10	-25	-15	3.22	6	0.63	0.73	4	0.60	3.22	0.53	0.54	2.93	0.003
	red Ncl. (l)	-2	-21	-12	3.12	6	0.60	0.73	5	0.55	3.12	0.60	0.54	2.86	0.002
p < 0.003	SNr (l)	-7	-24	-11	3.86	6	0.44	0.79	5	0.50	3.86	0.19	0.78	3.42	< 0.001
	SNc (l)	-11	-23	-17	3.44	6	0.55	0.79	2	0.69	3.44	0.39	0.78	3.12	0.001
	VTA (l)	-4	-22	-16	3.28	6	0.55	0.79	2	0.69	3.28	0.49	0.78	2.98	0.001
	red Ncl. (r)	5	-20	-11	3.26	6	0.47	0.79	4	0.55	3.26	0.50	0.78	2.97	0.001
	SNc (r)	10	-25	-15	3.22	6	0.47	0.79	4	0.55	3.22	0.53	0.78	2.93	0.002
	red Ncl. (l)	-2	-21	-12	3.12	6	0.60	0.79	1	0.79	3.12	0.60	0.78	2.89	0.002

Supplementary Table S15. Activations in younger subjects for emotional memory performance with applying a **"brainstem mask"** and small volume image of **"LC meta mask"** or **"SNredVTA mask"** cluster threshold $p < 0.005$ and $p < 0.003$ with no adjusted FDRc.

(4) emotional memory performance: remembered before loss > not remembered before loss

younger > older adults

						cluster					peak				
	region	x (mm)	y (mm)	z (mm)	Z (max.)	C	p (FWE corr.)	p (FDR corr.)	K (equiv.)	p (unc.)	T	p (FWE corr.)	p (FDR corr.)	Z (equiv.)	p (unc.)
p < 0.005	red Ncl. (l)	-4	-24	-12	2.96	3	0.69	0.82	2	0.74	2.96	0.60	0.91	2.82	0.002
	VDC (l)	-11	-24	-17	2.81	3	0.73	0.82	1	0.82	2.81	0.72	0.91	2.69	0.004
	SNr (l)	-10	-23	-18	2.73	3	0.73	0.82	1	0.82	2.73	0.77	0.91	2.62	0.004
p < 0.003	red Ncl (l)	-4	-24	-12	2.96	1	0.59	0.80	1	0.80	2.96	0.60	0.84	2.82	0.002

Supplementary Table S16. Activations in younger > older subjects for emotional memory performance with applying a **"brainstem mask"** and small volume image **"LC meta mask"** or **"SNredVTA mask"** cluster threshold p < 0.005 and p < 0.003 with no adjusted FDRc.

2.6 cortical activations

older adults

(1) emotional salience: loss feedback > gain feedback

		cluster									peak				
	region	x (mm)	y (mm)	z (mm)	Z (max.)	C	p (FWE corr.)	p (FDR corr.)	K (equiv.)	p (unc.)	T	p (FWE corr.)	p (FDR corr.)	Z (equiv.)	p (unc.)
p < 0.005	**MTG (r)**	57	-35	-3	7.74	10	0	< 0.001	4935	< 0.001	7.74	0.03	0.19	5.27	< 0.001
	LiG (r)	17	-49	-2	6.62	10	< 0.001	< 0.001	481	< 0.001	6.62	0.28	0.23	4.81	< 0.001
	FuG (r)	39	-39	-23	6.37	10	< 0.001	< 0.001	2869	< 0.001	6.37	0.40	0.23	4.70	< 0.001
	WM	28	-62	-12	5.38	10	0.05	0.02	259	< 0.001	5.38	0.95	0.47	4.22	< 0.001
	CBM	-29	-62	-25	5.24	10	0.016	0.03	199	0.001	5.24	0.98	0.51	4.15	< 0.001
	ITG (l)	-43	-61	-5	5.08	10	0.19	0.04	199	0.001	5.08	0.99	0.59	4.06	< 0.001
	MTG (l)	-50	-34	-1	4.79	10	< 0.001	< 0.001	1451	< 0.001	4.79	0.99	0.64	3.90	< 0.001
	CAL (l)	-15	-70	5	4.60	10	0.01	0.004	325	< 0.001	4.60	0.99	0.65	3.78	< 0.001
	WM	11	-82	10	4.36	10	< 0.001	< 0.001	527	< 0.001	4.36	1	0.68	3.64	< 0.001
	CAL (l)	-7	-87	5	4.12	10	0.17	0.04	196	0.001	4.12	1	0.70	3.49	< 0.001

Supplementary Table S17. Activations in older subjects for emotional salience with applying a “grey matter mask”, cluster threshold p < 0.005 with adjusted FDRc = 173.

(1) emotional salience: loss feedback > gain feedback

older adults > younger adults

		cluster									peak				
	region	x (mm)	y (mm)	z (mm)	Z (max.)	C	p (FWE corr.)	p (FDR corr.)	K (equiv.)	p (unc.)	T	p (FWE corr.)	p (FDR corr.)	Z (equiv.)	p (unc.)
p < 0.005	CBM	20	-46	-25	4.99	3	0.07	0.04	272	< 0.001	4.99	0.51	0.92	4.46	< 0.001
	MTG (l)	-61	-42	-1	4.54	3	0.001	0.004	531	< 0.001	4.54	0.91	0.92	4.12	< 0.001
	MTG (r)	62	-12	-14	4.29	3	0.004	0.04	433	< 0.001	4.29	0.99	0.92	3.93	< 0.001
p < 0.05	**HPC (l)**	-30	-22	-17	3.94	31	0.008	0.007	1568	< 0.001	3.94	0.47	0.56	3.65	< 0.001

Supplementary Table S18. Activations in older > younger subjects for emotional salience with applying a "grey matter mask", cluster threshold p < 0.005 with adjusted FDRc = 253; with applying a "hippocampus amygdala mask", cluster threshold p < 0.05 no adjusted FDRc.

younger adults

		cluster									peak				
	region	x (mm)	y (mm)	z (mm)	Z (max.)	C	p (FWE corr.)	p (FDR corr.)	K (equiv.)	p (unc.)	T	p (FWE corr.)	p (FDR corr.)	Z (equiv.)	p (unc.)
p < 0.005	**CAL (l)**	-7	-71	8	6.93	3	< 0.001	< 0.001	1752	< 0.001	6.93	0.04	0.05	5.21	< 0.001
	MTG (r)	50	-31	-3	5.32	3	< 0.001	< 0.001	1271	< 0.001	5.32	0.76	0.27	4.36	< 0.001
	CAL (r)	7	-65	8	5.23	3	< 0.001	< 0.001	1311	< 0.001	5.23	0.82	0.27	4.31	< 0.001

Supplementary Table S19. Activations in younger subjects for emotional salience with applying a "grey matter mask", cluster threshold p < 0.005 with adjusted FDRc = 422.

(2) task related salience: reversal > no reversal

older adults

		cluster									peak				
	region	x (mm)	y (mm)	z (mm)	Z (max.)	C	p (FWE corr.)	p (FDR corr.)	K (equiv.)	p (unc.)	T	p (FWE corr.)	p (FDR corr.)	Z (equiv.)	p (unc.)
p < 0.005	**MTG (r)**	68	-39	0	8.14	5	0	< 0.001	3894	< 0.001	8.14	0.01	0.07	5.41	< 0.001
	PCUN (r)	21	-54	5	6.59	5	0.0002	< 0.001	512	0.31	6.59	0.31	0.32	4.80	< 0.001
	unknown	-61	-63	-10	5.85	5	0.07	0.04	222	0.75	5.85	0.75	0.70	4.56	< 0.001
	MTG (l)	-68	-35	-1	5.70	5	0.003	0.001	373	0.83	5.70	0.83	0.70	4.38	< 0.001
	CAL (l)	-9	-80	13	4.74	5	< 0.001	< 0.001	559	0.99	4.74	1	0.70	3.87	< 0.001

Supplementary Table S20. Activations in older subjects for task related salience with applying a "grey matter mask", cluster threshold p < 0.005 with adjusted FDRc = 181.

older adults > younger adults

		cluster									peak				
	region	x (mm)	y (mm)	z (mm)	Z (max.)	C	p (FWE corr.)	p (FDR corr.)	K (equiv.)	p (unc.)	T	p (FWE corr.)	p (FDR corr.)	Z (equiv.)	p (unc.)
p < 0.005	**PCUN (l)**	-7	-62	14	4.44	1	< 0.001	< 0.001	739	< 0.001	4.96	0.55	0.93	4.44	< 0.001

Supplementary Table S21. Activations in older > younger subjects for task related salience with applying a "grey matter mask", cluster threshold p < 0.005 with adjusted FDRc = 724.

(2) task related salience: reversal > no reversal

younger adults

		cluster									peak				
	region	x (mm)	y (mm)	z (mm)	Z (max.)	C	p (FWE corr.)	p (FDR corr.)	K (equiv.)	p (unc.)	T	p (FWE corr.)	p (FDR corr.)	Z (equiv.)	p (unc.)
p < 0.005	**STG (r)**	49	-22	-8	6.61	4	< 0.001	< 0.001	4252	< 0.001	6.61	0.09	0.13	5.05	< 0.001
	STG (l)	-53	-33	1	5.54	4	< 0.001	< 0.001	2073	< 0.001	5.54	0.60	0.20	4.50	< 0.001
	MTG (l)	-59	-30	-15	5.28	4	0.04	0.02	301	< 0.001	5.28	0.80	0.22	4.34	< 0.001
	EC (l)	-27	-3	-40	4.58	4	0.15	0.05	225	< 0.001	4.58	1	0.35	3.91	< 0.001

Supplementary Table S22. Activations in younger subjects for task related salience with applying a "grey matter mask", cluster threshold p < 0.005 with adjusted FDRc = 195.

(4) emotional memory performance: remembered before loss > not remembered before loss

older adults > younger adults

		cluster									peak				
	region	x (mm)	y (mm)	z (mm)	Z (max.)	C	p (FWE corr.)	p (FDR corr.)	K (equiv.)	p (unc.)	T	p (FWE corr.)	p (FDR corr.)	Z (equiv.)	p (unc.)
p < 0.005	**LiG (l)**	-20	-71	-14	3.93	1	0.009	0.01	358	< 0.001	3.93	0.99	0.92	3.64	< 0.001

Supplementary Table S23. Activations in older > younger subjects for emotional memory performance with applying a "grey matter mask", cluster threshold p < 0.005 with adjusted FDRc = 289.

2.7 Correlation matrices for (1) emotional salience, (2) task-related salience, (3) memory performance, (4) emotional memory performance

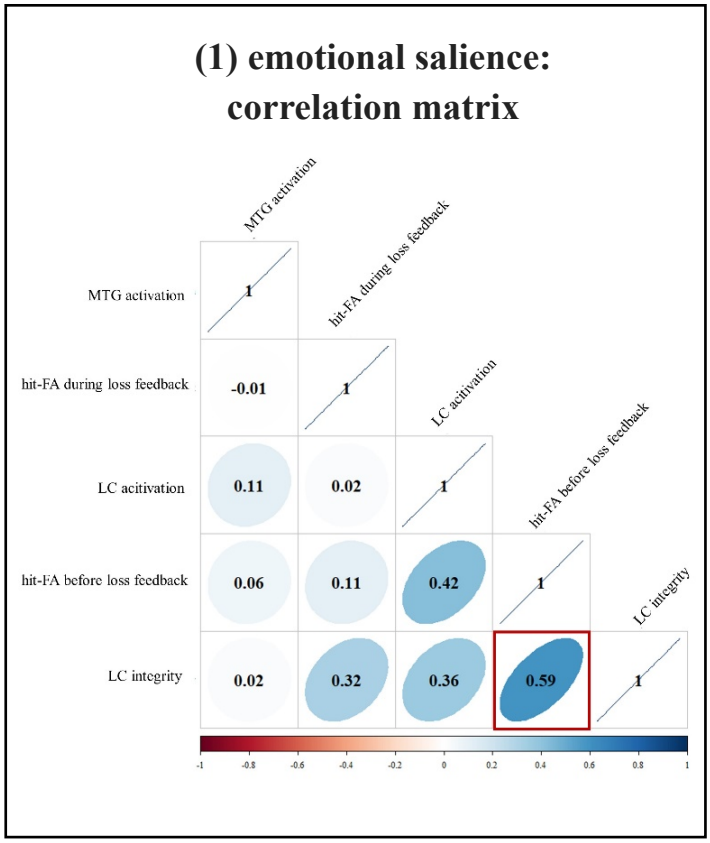

Supplementary Figure S7. Spearman´s rank correlation matrix for **emotional salience** in older adults displays the strength of the relationship (red to blue) of correlation coefficients for significant averaged LC activation with voxel-cut off of 0.005, averaged MTG activation, LC integrity and memory performance as hit-FA rate before loss feedback and the difference in hit-FA rate from loss feedback before vs. after trials. The *ellipsis* indicates the direction of the correlation, the *number* the strength of the correlation, and the *red rectangle* significant correlations. Correlations were outlier corrected (based on LC activation) and adjusted with Bonferroni corrections for multiple comparisons. Increased LC integrity led to better memory performance ($r(18) = 0.59$, $p = 0.004$). Removed outliers: ID 1 & 3.

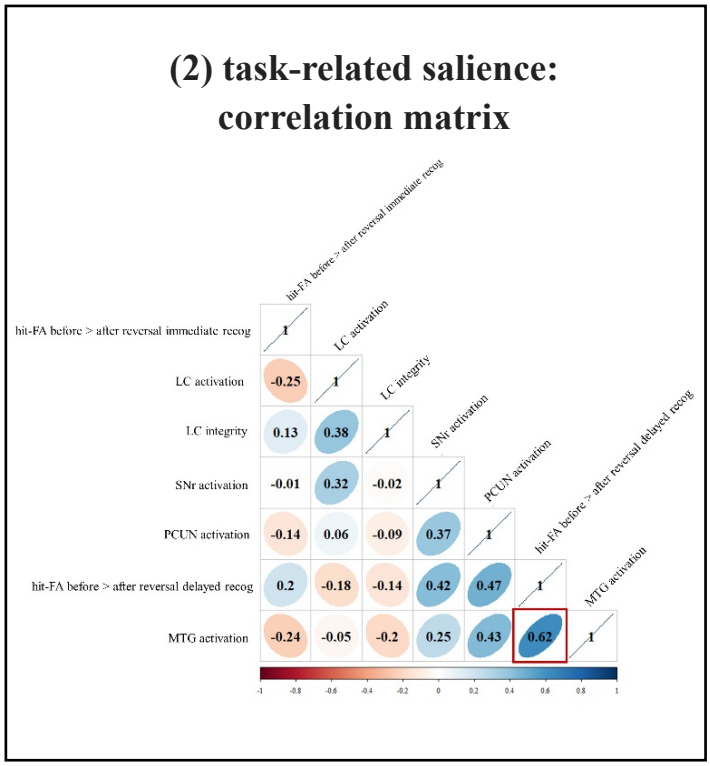

Supplementary Figure S8. Spearman´s rank correlation for **task-related salience** in older adults displays the strength of the relationship (red to blue) of correlation coefficients for significant averaged LC activation and SNr activation with voxel-cut off of 0.005, averaged MTG and PCUN activation, LC integrity and memory performance as the difference in hit-FA rate from reversals before vs. after three trials for immediate and delayed recognition. The *ellipsis* indicates the direction of the correlation, the *number* the strength of the correlation, and the *red rectangle* significant correlations. Correlations were outlier corrected (based on LC activation) and adjusted with Bonferroni corrections for multiple comparisons. Increased MTG activation led to better memory performance ($r(16) = 0.62$, $p = 0.009$). Removed outliers: ID 1, 3, 19, 21.

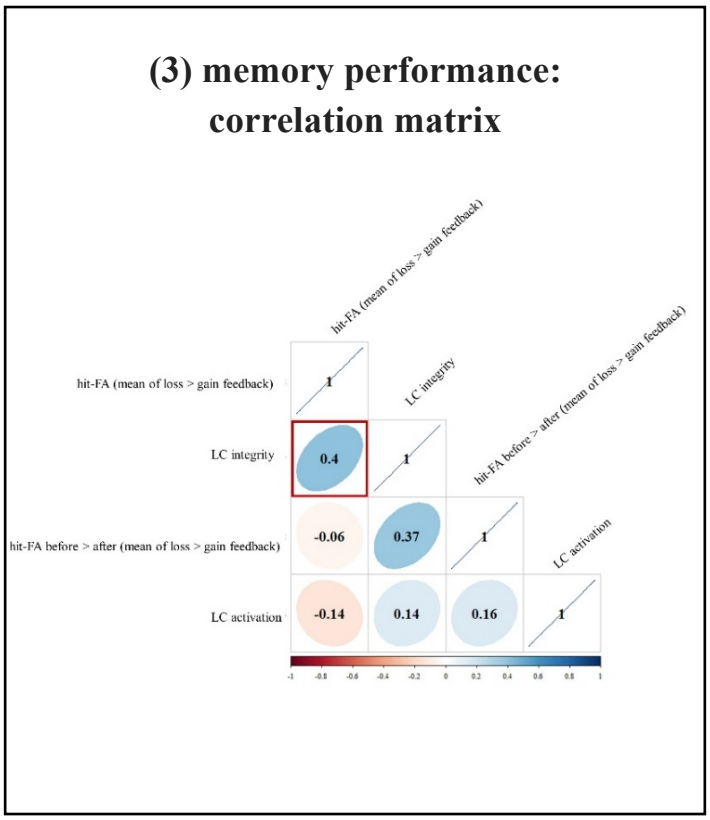

Supplementary Figure S9. Spearman´s rank correlation for **memory performance** in older adults displays the strength of the relationship (red to blue) of correlation coefficients for significant LC activation with voxel-cut off of 0.005, LC integrity and memory performance as hit-FA rate of mean of loss vs. gain feedback and the difference in hit-FA rate from loss vs gain feedback before vs. after trials. The *ellipsis* indicates the direction of the correlation, the *number* the strength of the correlation, and the *red rectangle* significant correlations. Correlations were outlier corrected (based on LC activation) and adjusted with Bonferroni corrections for multiple comparisons. Higher LC integrity was associated with better memory performance ($r(19) = 0.40$, $p = 0.03$). Removed outliers: ID 3.

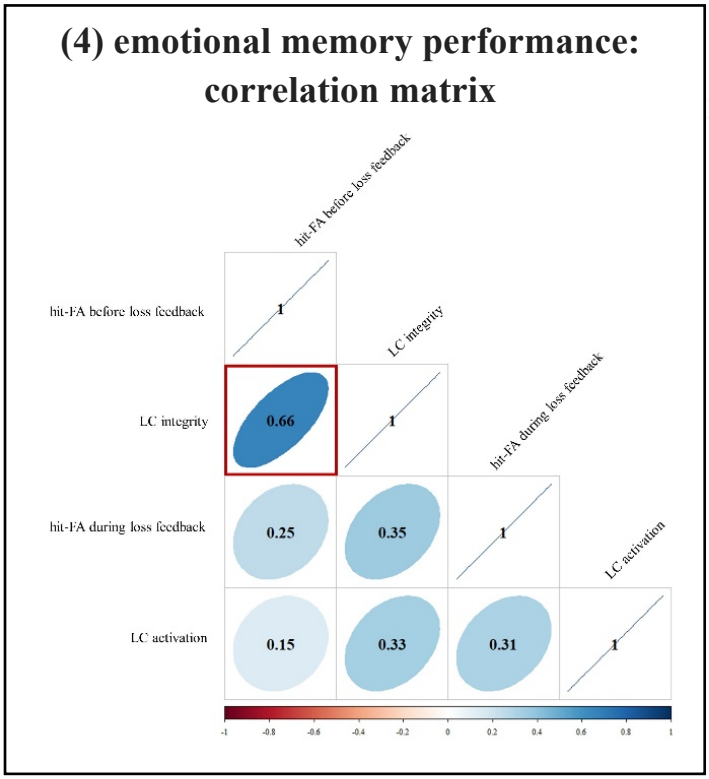

Supplementary Figure S10. Spearman´s rank correlation for **emotional memory performance** in older adults displays the strength of the relationship (red to blue) of correlation coefficients for significant LC activation with voxel-cut off of 0.005, LC integrity and memory performance as hit-FA rate after loss feedback and the difference in hit-FA rate from loss feedback before vs. after trials. The *ellipsis* indicates the direction of the correlation, the *number* the strength of the correlation, and the *red rectangle* significant correlations. Correlations were outlier corrected (based on LC activation) and adjusted with Bonferroni corrections for multiple comparisons. However, increased LC integrity and better memory performance based on the outlier correction of LC activation during emotional memory performance should not be interpreted in contrast to emotional salience, as outlier were corrected based on LC activation and not LC integrity. Removed outliers: ID 9 & 14.

Supplementary Information to chapter 3

Short bursts of transcutaneous auricular vagus nerve stimulation (taVNS) study

3. Extended Methods

3.1 Determination of sample size

A study with sixteen healthy younger adults were able to show combined behavioral and electrophy1siological evidence for GABAergic neuromodulation by taVNS with an effect size of η2 = 0.271; F(1,15) = 5.57, p =.032 (Keute et al., 2018). Based on our a-prior calculation in G*Power to determine the number of subjects, we used a medium effect size (0.25, based on Cohen´s guidelines) and set a conventional alpha level of 0.05 and power of 0.80 to ensure a high probability of detecting true effects, leading to a sample size of N = 24 subjects.

3.2 Number of Subjects

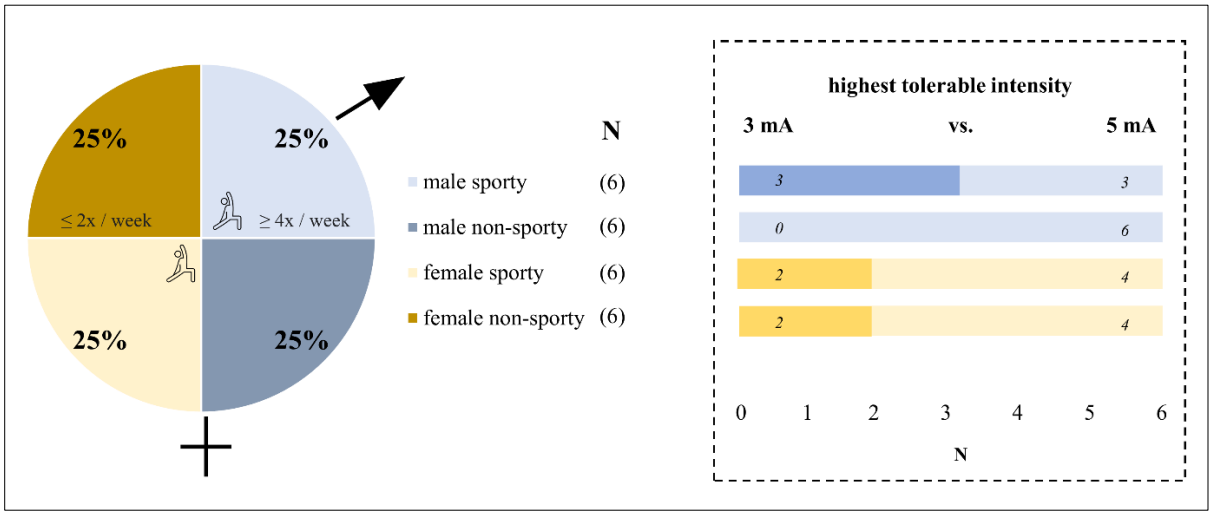

Supplementary Figure S11. Twenty-four subjects participated in the study, of which 50% female (ochre) and 50% male (blue) and of which 25% sporty vs. 25% non-sporty respectively, based on a prior established criterion (sporty = more than 3 times a week sport in the last 4 weeks; non-sporty = less than 2 times a week sport in the last 4 weeks). It was predetermined that subjects would receive 3 mA as the highest and 1.5 mA as the lowest intensity if they did not reach 5 mA as the highest intensity, which was the case for 7 of the 24 subjects.

3.3 Overview of number of stimuli for emotional memory task

Number of stimuli for the emotional memory task

		encoding real stim. on	**encoding** real stim. off	**encoding** sham stim. on	**encoding** sham stim. off	**recog. early**	**recog. delay**
neutral	**indoor (72)**	12	6	12	6	18	18
	outdoor (72)	12	6	12	6	18	18
negative	**indoor (72)**	12	6	12	6	18	18
	outdoor (72)	12	6	12	6	18	18

Supplementary Table S24. The stimuli for the emotional memory task consisted of 288 indoor and outdoor images representing emotionally negative or neutral events to allow for categorization of indoor and outdoor stimuli as a cover task while assessing effects of emotional stimulus materials (neutral indoor (72), neutral outdoor (72), emotional indoor (72), emotional outdoor (72)). Stimulus conditions were furthermore balanced with respect to stimulation conditions and early and delayed recognition.

3.4 Subjective higher perception of sensation (VAS) in response to stimulation during resting-state task

Perception of sensations (VAS) at low vs. high frequency and intensity for real and sham stimulation during resting-state task

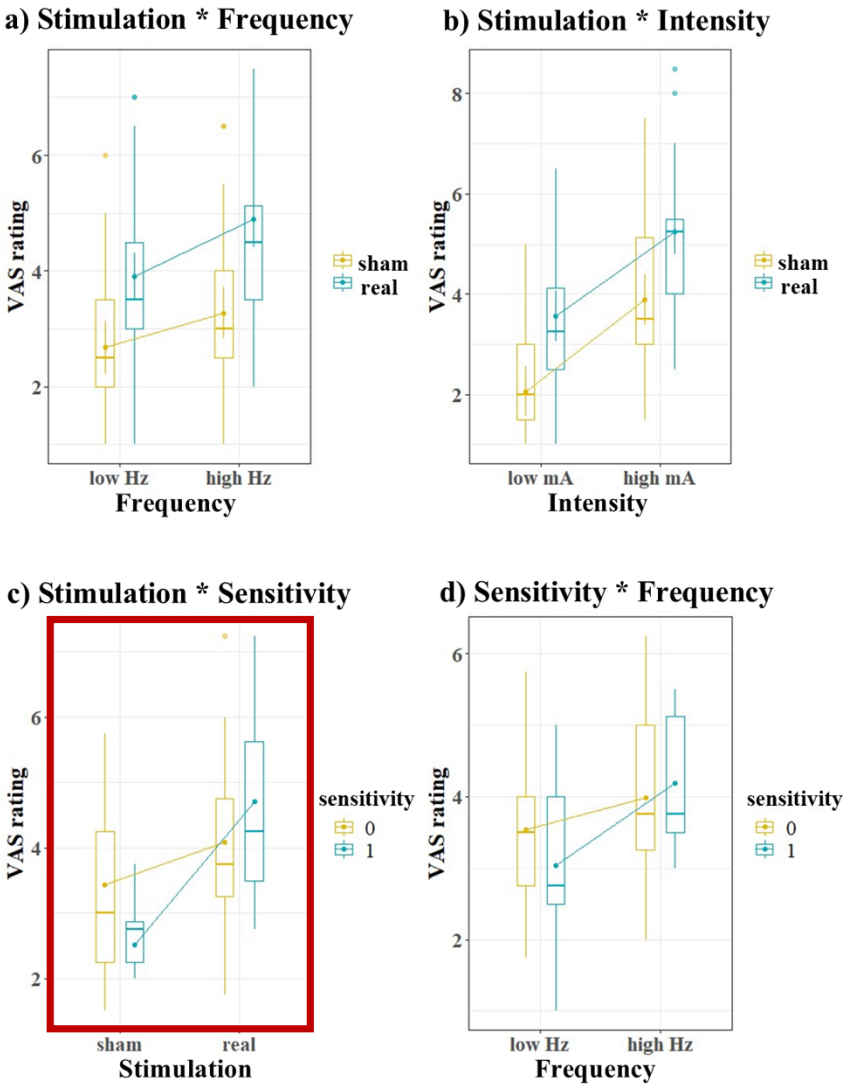

Supplementary Figure S12. Perception of sensations (VAS) (N =24) for a) Stimulation (real: turquoise; sham: ochre) × Frequency ($F(1,20) = 4.06$, $p = 0.06$), b) Stimulation (real: turquoise; sham: ochre) × Intensity ($F(1,20) = 0.20$, $p = 0.66$), c) Stimulation × Sensitivity (not sensitive (0): ochre; sensitive (1): turquoise) ($F(1,20) = 4.86$, $p = 0.04$) and d) Sensitivity (not sensitive (0): ochre; sensitive (1): turquoise) × Frequency ($F(1,20) = 3.61$, $p = 0.07$). The box outlined in red indicate significant interaction effect.

3.5 Relationship between subjective perception of sensations (VAS) of stimulation and pupil dilation across subjects for the emotional memory task and resting-state task

To further investigate the potential effects of VAS ratings on pupil dilation across subjects, VAS rating after each stimulation session and corresponding pupil dilation (averaged per subject across all trials within a stimulation condition) were correlated. For the emotional memory task, there were no correlations between VAS ratings and pupil dilation considering outlier correction neither for real stimulation (r = 0.21, p = 0.36), nor for sham stimulation (r = -0.1, 0 = 0.70).

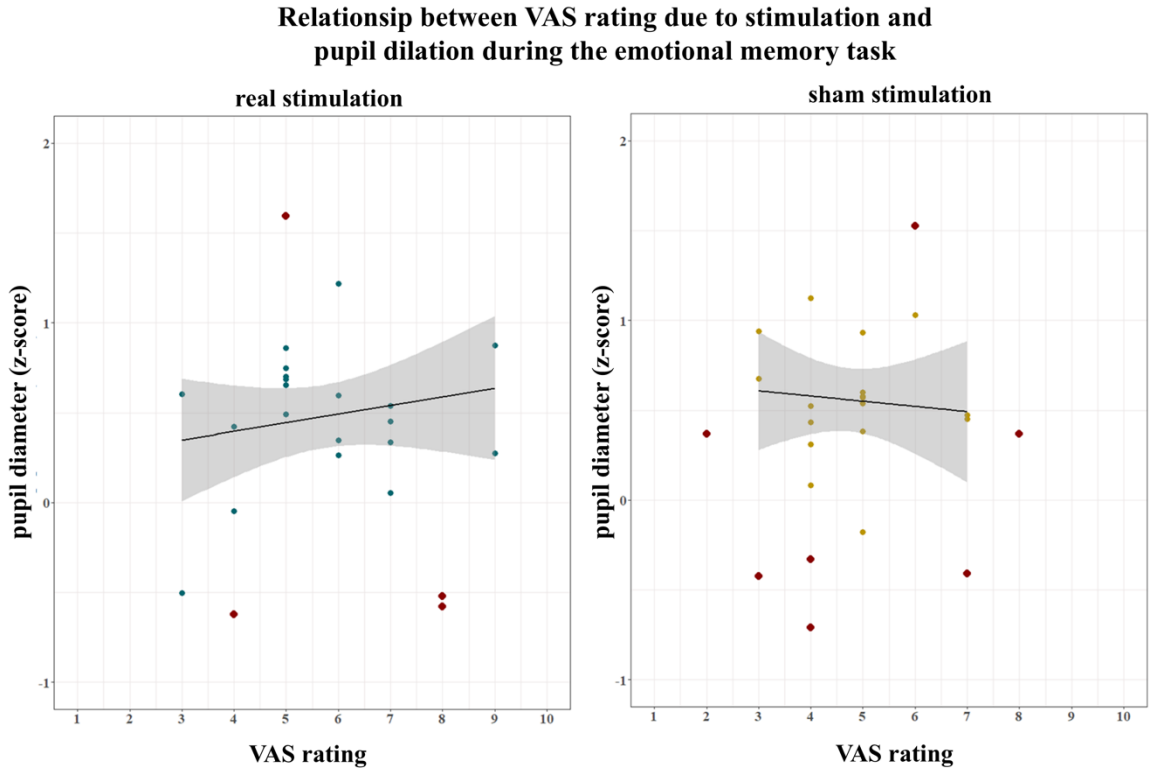

Supplementary Figure S13. Relationship between perception of sensations (VAS ratings) due to stimulation and pupil dilation during the emotional memory task for real stimulation (left: dark turquoise) and (right: sham stimulation (dark ochre). For each correlation (b), a regression line (black) and a confidence interval (shadowed area) are given. Additionally, outliers (thicker red dots) were identified based on interquartile range and a corresponding regression line (black). There were no correlations between VAS and pupil dilation neither for real stimulation (r = 0.21, p = 0.36), nor for sham stimulation (r = -0.1, 0 = 0.70).

For the resting-state task (see Supplementary Figure S14), correlations between VAS ratings and pupil dilation considering outlier correction (were found for **a)** real stimulation: low intensity & low frequency (r = 0.43, p = 0.04), **f)** sham stimulation: high intensity and low frequency (r = 0.52, p = 0.01) as well as **g)** sham stimulation: low intensity & high frequency (r = - 0.45, p = 0.04). However, there were no correlation between VAS and pupil dilation for **b)** real stimulation: high intensity & low frequency (r = 0.24, p = 0.27), **c)** real stimulation: low intensity & high frequency (r = -0.11, p = 0.62), **d)** real stimulation: high intensity & high frequency (r = 0.31, p = 0.14), **e)** sham stimulation: low

intensity & low frequency (r = 0.19, p = 0.37), **h)** sham stimulation: high intensity & high frequency (r = -0.45, p = 0.04). Thus, while higher mean pupil dilation was not consistently associated with higher VAS ratings across all subjects, three instances of significant associations between pupil dilation and VAS (two positive, one negative) were observed, suggesting that interindividual differences in subjective perceptions of stimulation also add variance to pupil dilation of stimulation effects.

Relationship between perception of sensations (VAS) due to stimulation and pupil dilation across subjects for resting-state task

		R	p-value	CI	
				lower	upper
Real (R)					
	a) R: low mA low Hz	**0.43**	**p = 0.04**	**0.03**	**0.71**
	b) R: high mA low Hz*	0.01	p = 0.95	- 0.41	0.43
	c) R: low mA high Hz*	- 0.11	p = 0.62	- 0.51	0.33
	d) R: high mA high Hz	0.31	p = 0.14	- 0.11	0.63
Sham (S)					
	e) S: low mA low Hz	0.19	p = 0.37	- 0.23	0.55
	f) S: high mA low Hz*	**0.52**	**p = 0.01**	**0.14**	**0.77**
	g) S: low mA high Hz*	**- 0.45**	**p = 0.04**	**- 0.74**	**- 0.02**
	h) S: high mA high Hz	0.27	p = 0.20	- 0.15	0.61

Supplementary Table S25. Overview of correlations between VAS rating after real (a-d) and sham stimulation (e-h). In addition to the significance (p-value), the confidence intervals (CI) are given for better evaluation and comparability of the different correlation effects. All correlations were adjusted for outliers (1.5 × IQR); however, this adjustment occurred only for correlations marked with an asterisk. Significant correlations are bold.

Relationship between perception of sensations (VAS rating) due to stimulation and pupil dilation during resting-state task

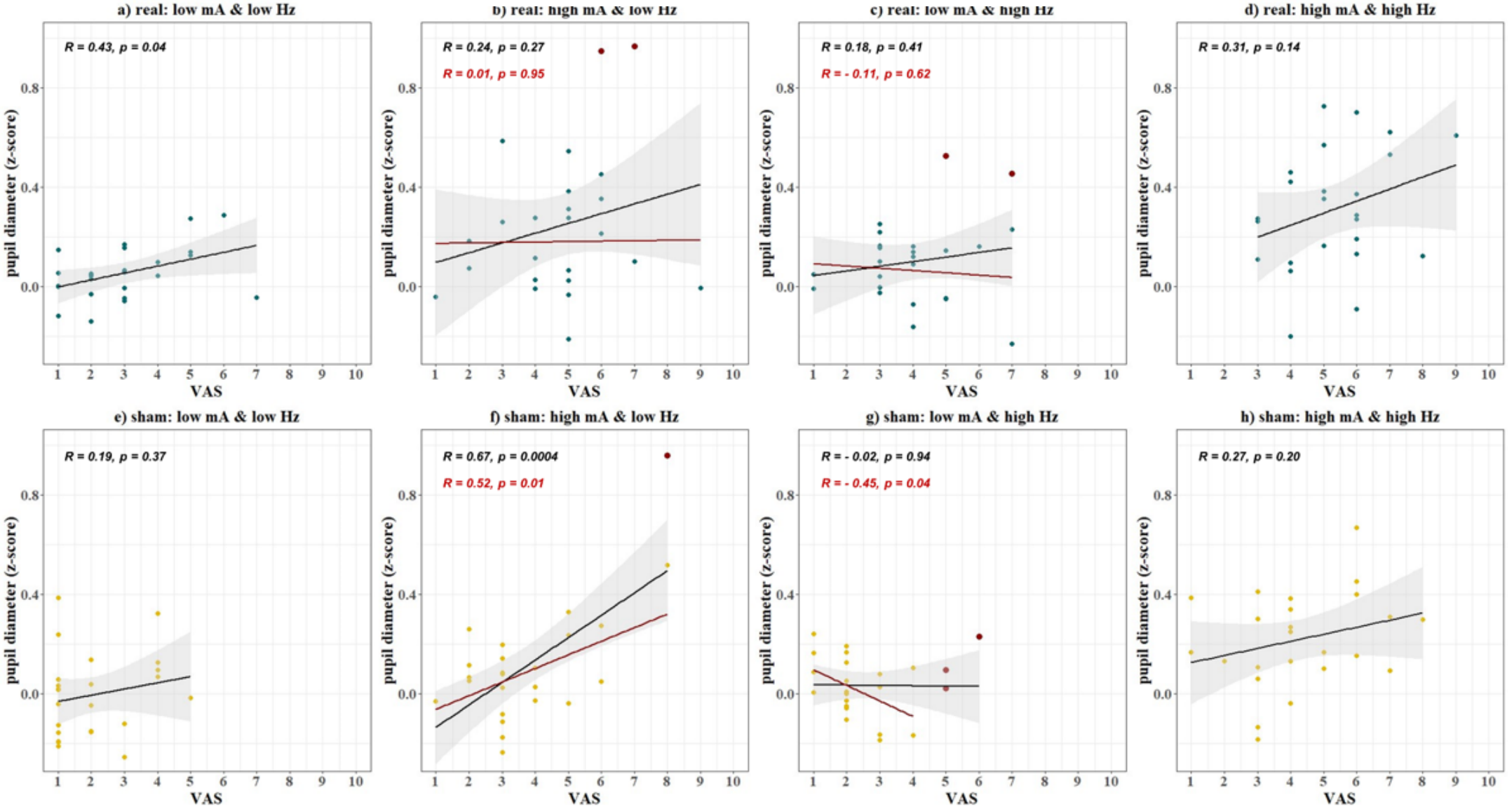

Supplementary Figure S14. Relationship between perception of sensations (VAS) due to stimulation and pupil dilation during resting-state task, for (a-d) real stimulation (dark turquoise) and (e-h) sham stimulation (ochre). After each of the following sessions, a) real: low intensity & low frequency, b) real: high intensity & low frequency, c) real: low intensity & high frequency, d) real: high intensity & high frequency, e) sham: low intensity & low frequency, f) sham: high intensity & low frequency, g) sham: low intensity & high frequency, h) sham: high intensity & high frequency, VAS scores were recorded. For each correlation (a-h), a regression line (black) and a confidence interval (shadowed area) are given. Additionally, outliers (thicker red dots) were identified based on interquartile range and a corresponding regression line (red).

3.6 State of health

The state of health queried in each case after stimulation to control for potential side effects are shown in Supplementary Table S26 & S27. The following items were asked: (1) headache, (2) nausea, (3) tiredness, (4) dizziness, (5) tingling sensation at the previously stimulated area, (6) feeling of heat at the previously stimulated area, (7) reddening of the skin at the previously stimulated area, (8) skin irritation at the previously stimulated site, (9) impaired concentration, (10) itching at the previously stimulated area. Subjects indicated on a 4-point scale (0: not at all – 3: strong) to what extent they perceived potential side effects.

Query of the state of health after the real and sham stimulation during emotional memory task

Item	Real Stimulation		Sham Stimulation	
	Mean	SD	Mean	SD
1	0.08	0.06	0.04	0.04
2	0.04	0.04	0	0
3	0.67	0.13	0.83	0.16
4	0.04	0.04	0.04	0.04
5	0.38	0.12	0.29	0.1
6	0.21	0.09	0.21	0.09
7	0	0	0	0
8	0	0	0	0
9	0.50	0.12	0.50	0.14
10	0.04	0.04	0	0

Supplementary Table S26. Query of the state of health (item 1-10) after real and sham stimulation. The mean value of the respective items (scale 0-3) across all subjects (N=24) for real and sham stimulation is shown. No side effects occurred and the reported sensations did not differ between real (M = 0.20, SD = 0.04) and sham (M = 0.19, SD = 0.04) stimulation, $F(1,9) = 0.06$, $p = 0.81$.

Query of the state of health after the real and sham stimulation during resting-state task

	Real Stimulation				Sham Stimulation			
	low Hz		high Hz		low Hz		high Hz	
Item	low mA	high mA	low mA	high mA	low mA	high mA	low mA	high mA
1	0.04 / 0.04	0.08 / 0.06	0 / 0	0 / 0	0 / 0	0 / 0	0 / 0	0 / 0
2	0.04 / 0.04	0 / 0	0 / 0	0 / 0	0 / 0	0 / 0	0 / 0	0 / 0
3	1.17 / 0.18	1.25 / 0.25	1.13 / 0.23	1.38 / 2.24	1 / 0.22	0.96 / 0.22	0.83 / 0.19	1.13 / 0.23
4	0 / 0	0 / 0	0 / 0	0 / 0	0 / 0	0.04 / 0.42	0 / 0	0 / 0
5	0.04 / 0.04	0.17 / 0.13	0.04 / 0.04	0.13 / 0.07	0 / 0	0.04 / 0.42	0 / 0	0.04 / 0.04
6	0 / 0	0.08 / 0.06	0.04 / 0.04	0.08 / 0.06	0 / 0	0.04 / 0.42	0 / 0	0.08 / 0.06
7	0 / 0	0 / 0	0 / 0	0 / 0	0 / 0	0 / 0	0 / 0	0 / 0
8	0 / 0	0 / 0	0 / 0	0 / 0	0 / 0	0 / 0	0 / 0	0 / 0
9	0.58 / 0.13	0.67 / 0.20	0.67 / 0.17	0.67 / 0.21	0.46 / 0.16	0.58 / 0.18	0.46 / 0.16	0.58 / 0.18
10	0 / 0	0 / 0	0 / 0	0 / 0	0.04 / 0.04	0.04 / 0.04	0 / 0	0 / 0

Supplementary Table S27. Query of the state of health (item 1-10) after real and sham stimulation. The mean value and standard deviation of the respective items (scale 0-3) across all subjects (N = 24) for low vs. high frequency at given low vs. high intensity for real and sham stimulation are shown. No side effects occurred and the slightly higher score on item 3 (tiredness) is not due to the stimulation itself, but to the total duration of the experiment (> 8h one day measurement).

3.7 No differences in pupil dilation in the off-stimulation condition for the emotional-memory task

To rule out any significant **differences in the off-stimulation condition**, a first model considered all levels of **"**stimulation" *[real on stimulation (1) vs. real off stimulation (2) vs. sham on stimulation (3) vs. sham off stimulation (4)]* and the differences in **"**valence" *[negative (1) vs. neutral (0)]:* pupil dilation ~ trials + stimulation + valence + (1|ID).

There was no significant difference between **real off stimulation** (M±SD: 0.23±0.12) and **sham off stimulation** (M±SD: 0.16±0.12); ß = 0.07 (SE = 0.07; t-value = 0.92, p = 1), while the model suggested that the pupil dilation was increased during real on stimulation (M±SD: 0.52±0.12) as compared to real off stimulation (M±SD: 0.23±0.12); ß = 0.30 (SE = 0.07; t-value = 4.5, p < 0.0001) and during sham on stimulation (M±SD: 0.47±0.12) as compared to sham off stimulation (M±SD: 0.16±0.12); ß = 0.31 (SE = 0.06; t-value = 4.91, p < 0.0001); **stimulation**: $\chi^2 = 46.21$, p < 0.001. Therefore, the off-stimulation conditions were combined for further analysis to investigate the effects of taVNS on pupil dilation.

3.8 Excluded trials for resting-state task

Variations in trial numbers per condition were observed following artifact correction. Specifically, sham stimulation (M ± SD: 58.5 ± 1.07) had more trials compared to real stimulation (M ± SD: 53.8 ± 1.91), F (1,23) = 15.89, p < 0.001; high frequency stimulation (M ± SD: 57.8 ± 1.27) had more trials than low frequency stimulation (M ± SD: 54.5 ± 1.65), F (1,23) = 24.33, p < 0.001 and high intensity stimulation (M ± SD: 57.2 ± 1.32) had more trials than low intensity stimulation (M ± SD: 55.0 ± 1.56), F (1,23) = 29.98, p < 0.001. Likewise, there was a significant interaction between stimulation condition and frequency (F (1,23) = 24.87, p < 0.001) (*high frequency during real stimulation (M ± SD: 56.8 ± 1.63) vs. low frequency during real stimulation (M ± SD: 50.8 ± 2.31), t(23) = 5.15, p = 0.0002; low frequency during real stimulation (M ± SD: 50.8 ± 2.31) vs. low frequency during sham stimulation (M ± SD: 58.2 ± 1.15), t(23) = - 4.74, p = 0.0005).* There was also a significant interaction between stimulation condition and intensity (F (1,23) = 31.13, p < 0.001) (*high intensity during real stimulation (M ± SD: 55.9 ± 1.67) vs. low intensity during real stimulation (M ± SD: 51.6 ± 2.19), t(23) = 5.54, p = 0.0001; low intensity during real stimulation (M ± SD: 51.6 ± 2.19) vs. low intensity during sham stimulation (M ± SD: 58.4 ± 1.08), t(23) = - 4.5, p = 0.0009).* Moreover there was a significant interaction between intensity and frequency (F (1,23) = 30, p < 0.001) *(low intensity and high frequency (M ± SD: 57.8 ± 1.27) vs. low intensity low frequency (M ± SD: 52.3 ± 1.94), t(23) = 5.19, p = 0.0002; high intensity and low frequency (M ± SD: 56.6 ± 1.40) vs. low intensity and low frequency (M ± SD: 52.3 ± 1.94), t(23) = 5.48, p = 0.0001).* Finally, there was a significant three-way-interaction between stimulation condition, frequency and intensity (F (1,23) = 31.13, p < 0.001).

3.9 Distinct models and Comparison of multiple statistical models of the emotional-memory task

Distinct models of the emotional memory task

Models:
m0: Pupil ~ (1 | ID)
m1: Pupil ~ trials + (1|ID)
m2: Pupil ~ trials + stimulation + (1|ID)
m3: Pupil ~ trials + stimulation + valence + (1|ID)
m4: Pupil ~ trials + stimulation × valence + (1|ID)
m3_1: Pupil ~ trials + stimulation + valence + vas + (1|ID)
m3_2: Pupil ~ trials + stimulation + valence + vas + sensitive + (1|ID)
m3_3: Pupil ~ trials + stimulation + valence + vas + sensitive + real_first + (1|ID)
m3_4: Pupil ~ trials + stimulation + valence + vas + sensitive + real_first + gender + (1|ID)
m3_5: Pupil ~ trials + stimulation + valence + vas + sensitive + real_first + gender + sporty + (1|ID)

Supplementary Table S28. Changes in pupil dilation were analyzed based on a fitted linear mixed-effects (LMM) model by using the {lme4} package (Bates et al., 2015), following a forward model selection approach. Thereby, a distinct model was using the same dummy coded variables *(**stimulation** [off (0) vs. real (1) vs. sham (2) stimulation], **valence** [negative (1) vs. neutral (0)], **sensitivity** [sensitive (1) vs. not sensitive (0)], **real_first** [counterbalanced: real (1) before sham (0) stimulation], **sporty** [sporty (1) vs. non-sport (0)], **gender** [female (1) vs. male (0)], **trial number** (trials) and **VAS**).*

Comparison of multiple statistical models of the emotional memory task

	npar	**AIC**	**BIC**	**logLik**	**deviance**	**Chisq**	**Df**	**Pr(>Chisq)**
m0	3	10904	10923	-5449.2	10898			
m1	4	10892	10916	-5442.0	10884	14.41	1	0.000147***
m2	6	10851	10888	-5419.5	10839	45.02	2	1.67e-10 ***
m3	7	10847	10890	-5416.6	10833	5.71	1	0.017 *
m3_1	8	10844	10892	-5413.8	10828	5.75	1	0.017 *
m3_2	9	10845	10900	-5413.7	10827	0.15	1	0.70
m3_3	10	10839	10900	-5409.7	10819	8.01	1	0.005 **
m3_4	11	10839	10906	-5408.6	10817	2.08	1	0.15
m3_5	12	10838	10911	-5406.9	10814	3.39	1	0.07
Signif. codes: 0 '***' 0.001 '**' 0.01 '*' 0.05 '.' 0.1 ' ' 1								

Supplementary Table S29. Comparison of multiple statistical models: The overview shows *npar*, which represents the number of parameters in each model, *AIC* (Akaike Information Criterion), *BIC* (Bayesian Information Criterion), *logLik* (Log-Likelihood), *deviance* which was used to assess the goodness of fit of a model, *Chisq* (Chi-Square),which represents the difference in deviance between the current model and the previous one, *Df* (Degrees of Freedom), which represents the degrees of freedom associated with the Chi-Square test and *Pr(>Chisq)* which represents p-values associated with the Chi-Square test. Model m3_3 (red) was the best fitting model.

3.10 Distinct models and Comparison of multiple statistical models of the resting-state task

Distinct models of the resting-state task

Models:
m0: Pupil ~ (1 | ID)
m1: Pupil ~ trials + (1|ID)
m2: Pupil ~ trials + stimulation + (1|ID)
m3: Pupil ~ trials + stimulation + freq + (1|ID)
m4: Pupil ~ trials + stimulation + freq + int + (1|ID)
m5: Pupil ~ trials + stimulation × freq + int + (1|ID)
m6: Pupil ~ trials + stimulation × freq + stimulation × int + (1|ID)
m7: Pupil ~ trials + stimulation × freq + stimulation × int + int × freq + (1|ID)
m4_1: Pupil ~ trials + stimulation + freq + int + vas + (1|ID)
m4_2: Pupil ~ trials + stimulation + freq + int + vas + sensitive + (1|ID)
m4_3: Pupil ~ trials + stimulation + freq + int + vas + sensitive + real_first + (1|ID)
m4_4: Pupil ~ trials + stimulation + freq + int + vas + sensitive + real_first + position + (1|ID)
m4_5: Pupil ~ trials + stimulation + freq + int + vas + sensitive + real_first + position + gender + (1|ID)
m4_6: Pupil ~ trials + stimulation + freq + int + vas + sensitive + real_first + position + gender + sporty + (1|ID)

Supplementary Table S30. Changes in pupil dilation were analyzed based on a fitted linear mixed-effects (LMM) model by using the {lme4} package (Bates et al., 2015), following a forward model selection approach. Thereby, a distinct model was fitted for each time window (**I-III**) using the same dummy coded variables *(**stimulation** [real (1) vs. sham (0)], **frequency** [high (1) vs. low (0)] (freq), **intensity** [high (1) vs. low (0)](int), **trial number** (trials), **sensitivity** [sensitive (1) vs. not sensitive (0)], **real_first** [counterbalanced: real (1) before sham (0) stimulation], **position** (four different stimulation combination possibilities), **sporty** [sporty (1) vs. non-sport (0)], **gender** [female (1) vs. male (0)] and **VAS).***

Comparison of multiple statistical models for (I) – 3 sec during on stimulation of the resting-state task

	npar	AIC	BIC	logLik	deviance	Chisq	Df	Pr(>Chisq)
m0	3	29526	29548	-14760	29520			
m1	4	29527	29556	-14759	29519	1.28	1	0.26
m2	5	29512	29549	-14751	29502	16.42	1	5.09e-05 ***
m3	6	29505	29548	-14746	29493	9.62	1	0.0019 **
m4	**7**	**29404**	**29455**	**-14695**	**29390**	**102.95**	**1**	**<2.2e-16 *****
m4_1	**8**	**29367**	**29425**	**-14675**	**29351**	**38.76**	**1**	**4.79e-10 *****
m5	8	29405	29464	-14695	29389	0	0	
m6	9	29407	29473	-14694	29389	0.39	1	0.53
m4_2	9	29369	29434	-14675	29351	38.31	0	
m7	10	29408	29481	-14694	29388	0	1	1
m4_3	10	29370	29443	-14675	29350	38.42	0	
m4_4	13	29373	29468	-14674	29347	2.64	3	0.45
m4_5	14	29375	29477	-14674	29347	0.06	1	0.81
m4_6	15	29377	29486	-14674	29347	0.04	1	0.84
Signif. codes: 0 '***' 0.001 '**' 0.01 '*' 0.05 '.' 0.1 ' ' 1								

Supplementary Table S31. Comparison of multiple statistical models for time window **(I) – 3 sec during on stimulation**. The overview shows *npar*, which represents the number of parameters in each model, *AIC* (Akaike Information Criterion), *BIC* (Bayesian Information Criterion), *logLik* (Log-Likelihood), *deviance* which was used to assess the goodness of fit of a model, *Chisq* (Chi-Square),which represents the difference in deviance between the current model and the previous one, *Df* (Degrees of Freedom), which represents the degrees of freedom associated with the Chi-Square test and *Pr(>Chisq)* which represents p-values associated with the Chi-Square test. Model m4 (red) was the best fitting model and m4_7 (red) was the second-best fitting model.

Comparison of multiple statistical models for (II) – immediate response of the resting-state task

	npar	AIC	BIC	logLik	deviance	Chisq	Df	Pr(>Chisq)
m0	3	37773	37795	-18884	37767			
m1	4	37775	37804	-18884	37767	0.2370	1	0.6263508
m2	5	37763	37799	-18876	37753	142.569	1	0.0002***
m3	6	37762	37806	-18875	37750	23.924	1	0.1219234
m4	**7**	**37688**	**37739**	**-18837**	**37674**	**765.394**	**1**	**< 2.2e-16*** **
m4_1	**8**	**37659**	**37717**	**-18822**	**37643**	**308.109**	**1**	**2.84e-08*** **
m5	8	37688	37746	-18836	37672	0.0000	0	
m6	9	37687	37752	-18834	37669	31.968	1	0.074
m4_2	9	37661	37727	-18822	37643	255.596	0	
m7	10	37688	37761	-18834	37668	0.0000	1	1
m4_3	10	37662	37735	-18821	37642	259.133	0	
m4_4	13	37660	37755	-18817	37634	84.556	3	0.04
m4_5	14	37662	37764	-18817	37634	0.0560	1	0.81
m4_6	15	37664	37773	-18817	37634	0.3817	1	0.54
Signif. codes: 0 '***' 0.001 '**' 0.01 '*' 0.05 '.' 0.1 ' ' 1								

Supplementary Table S32. Comparison of multiple statistical models for the **(II) – immediate response**. The overview shows *npar*, which represents the number of parameters in each model, *AIC* (Akaike Information Criterion), *BIC* (Bayesian Information Criterion), *logLik* (Log-Likelihood), *deviance* which was used to assess the goodness of fit of a model, *Chisq* (Chi-Square),which represents the difference in deviance between the current model and the previous one, *Df* (Degrees of Freedom), which represents the degrees of freedom associated with the Chi-Square test and *Pr(>Chisq)* which represents p-values associated with the Chi-Square test. Model m4 (red) was the best fitting model and m4_7 (red) was the second-best fitting model.

Comparison of multiple statistical models for (III) – delayed response of the resting-state task

	npar	AIC	BIC	logLik	deviance	Chisq	Df	Pr(>Chisq)
m0	3	39316	39338	-19655	39310			
m1	4	39309	39339	-19651	39301	8.42	1	0.004**
m2	5	39311	39347	-19650	39301	0.77	1	0.38
m3	6	39311	39355	-19650	39299	1.40	1	0.24
m4	**7**	**39305**	**39356**	**-19646**	**39291**	**8.27**	**1**	**0.004****
m4_1	**8**	**39304**	**39362**	**-19644**	**39288**	**3.32**	**1**	**0.07**
m5	8	39307	39365	-19646	39291	0	0	
m6	9	39304	39369	-19643	39286	5.45	1	0.02 *
m4_2	9	39306	39371	-19644	39288	0	0	
m7	10	39305	39378	-19643	39285	2.18	1	0.14
m4_3	10	39308	39381	-19644	39288	0	0	
m4_4	13	39308	39403	-19641	39282	5.76	3	0.12
m4_5	14	39309	39411	-19641	39281	0.70	1	0.40
m4_6	15	39310	39420	-19640	39280	0.75	1	0.39
Signif. codes: 0 '***' 0.001 '**' 0.01 '*' 0.05 '.' 0.1 ' ' 1								

Supplementary Table S33. Comparison of multiple statistical models for the **(III) – delayed response**. The overview shows *npar*, which represents the number of parameters in each model, *AIC* (Akaike Information Criterion), *BIC* (Bayesian Information Criterion), *logLik* (Log-Likelihood), *deviance* which was used to assess the goodness of fit of a model, *Chisq* (Chi-Square),which represents the difference in deviance between the current model and the previous one, *Df* (Degrees of Freedom), which represents the degrees of freedom associated with the Chi-Square test and *Pr(>Chisq)* which represents p-values associated with the Chi-Square test. Model m4 (red) was the best fitting model and m4_7 (red) was the second-best fitting model.

4. Extended Results

4.1 No differences in memory performance and HIT RTs in the off-stimulation condition

To rule out any significant **differences in the off-stimulation condition** for the behavioral data of the emotional memory task, a first analysis considered all levels of "stimulation" *[real on stimulation (1) vs. real off stimulation (2) vs. sham on stimulation (3) vs. sham off stimulation (4)]*. For memory performance (hit-FA), there was no significant difference between **real off stimulation** (M ± SD: 0.72 ± 0.23) and **sham off stimulation** (M ± SD: 0.75 ± 0.22), F(1,23) = 0.86, p = 0.36 (real off – sham off: ß = -0.03 (SE = 0.02; t-value = -1.34, p = 1). Likewise, for **HIT RTs** (averaged speed of correct responses to target image), there was no significant difference between **real off stimulation** (M ± SD: 0.93±0.32) and **sham off stimulation** (M ± SD: 0.94 ± 0.37), F(1,23) = 0.13, p = 0.73 (real off – sham off: ß = -0.01 (SE = 0.02; t-value = -0.64, p = 1). Therefore, the off-stimulation conditions were combined for further analyses to investigate the effects of taVNS on memory performance and RTs for the emotional memory task.

4.2 No interaction between timepoint and valence for memory performance (hit-FA (alarm) rate) For memory performance (hit-FA (false alarm) rate) there was no interaction between timepoint and valence, F(1,23) = 0.27, p = 0.61 (Supplementary Figure S15).

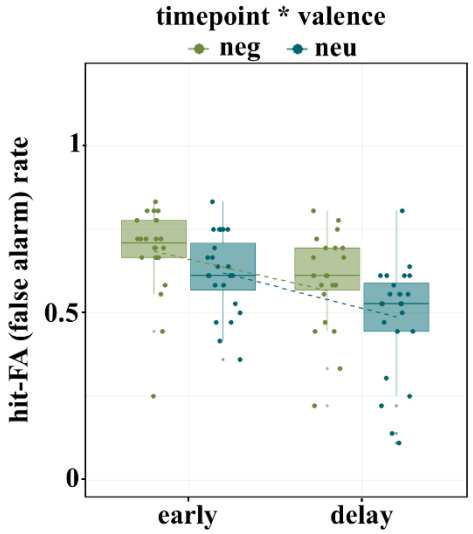

Supplementary Figure S15. Memory performance (hit-FA (false alarms)) is shown here aggregated at the subject level (N=24) using boxplots and each point represents an individual subject. There was no interaction between timepoint (early (left) and delay (right)) and valence (negative (green) and neutral (turquoise)), F(1,23) = 0.27, p = 0.61.

4.3 Better correct recognition (hit) for negative events and due to stimulation

Subjects showed higher number of hits for **negative events** (M ± SD: 0.73 ± 0.25) compared to neutral events (M ± SD: 0.66 ± 0.24), $F(1,23) = 25.67$, $p < 0.001$. Likewise, hits were fewer after delayed (M ± SD: 0.65 ± 0.24) as compared to early (M ± SD: 0.73 ± 0.25) recognition task, $F(1,23) = 39.12$, $p < 0.001$. There was a tendency for an interaction between timepoint and valence, $F(2,46) = 4.0$, $p = 0.06$ (Supplementary Figure S16).

Additionally, subjects showed higher number of hits during real (M ± SD: 0.83 ± 0.14) as compared to off (M ± SD: 0.41 ± 0.08) stimulation (off-real: β = -0.42 (SE = 0.01; t-value = -38.37, p < 0.001)) and during sham (M ± SD: 0.84 ± 0.11) as compared to off (M ± SD: 0.41 ± 0.08) stimulation (off-sham: β = -0.43 (SE = 0.02; t-value = -26.30, p < 0.001)); however number of hits were not higher during real as compared to sham stimulation (real-sham: β = -0.01 (SE = 0.02; t-value = -0.54, p = 1)), $F(2,46) = 509$, $p < 0.001$. There was a significant ordinal interaction between stimulation and valence, $F(2,46) = 6.46$, $p = 0.003$ (Supplementary Figure S16d). Specifically, during real stimulation the difference between negative and neutral events was more pronounced than during sham stimulation (emo-neu real-sham: β = 0.07 (SE = 0.03; t-value = 2.64, p = 0.01)) and during off stimulation (emo-neu off-real: β = -0.08 (SE = 0.02; t-value = -3.89, p = 0.007)). There was no interaction between valence and "off vs. sham" stimulation (emo-neu off-sham: β = -0.02 (SE = 0.03; t-value = -0.59, p = 0.56)). Additionally, there was a significant ordinal interaction between stimulation and timepoint, $F(2,46) = 5.54$, $p = 0.007$ (Supplementary Figure S16e), indicating that during off stimulation the difference in number of hits between early and delayed recognition was higher than during real stimulation (delay-early off-real: β = 0.1 (SE = 0.03; t-value = 3.77, p = 0.001)) and sham stimulation (delay-early off-sham: β = 0.07 (SE = 0.03; t-value = 2.25, p = 0.03)). However, there was no significant interaction between timepoint and "real vs. sham" stimulation (delay-early real-sham: β = -0.02 (SE = 0.03; t-value = -0.70, p = 0.49)). For results on certainty ratings for correctly identified images see Supplementary Results 4.6.

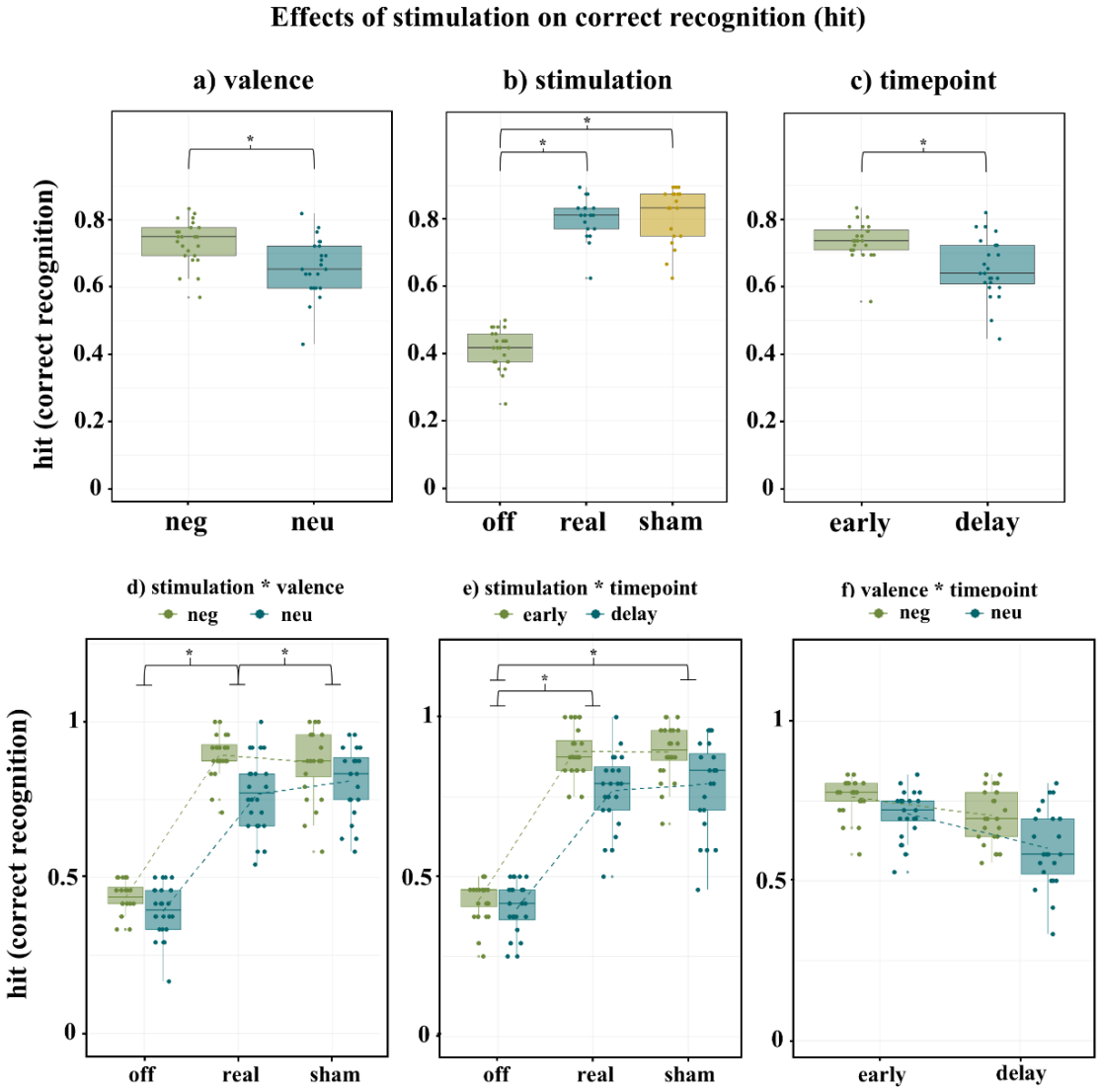

Supplementary Figure S16. Correct recognition (hit) is shown here aggregated at the subject level (N=24) using boxplots, while each point represents an individual subject. Panel a) presents valence effects, showing higher number of hits for negative (green) compared to neutral (turquoise) events, $F(1,23) = 25.67$, $p < 0.001$. Panel b) presents the effects of stimulation, indicating higher number of hits for real stimulation compared to off stimulation, and sham stimulation compared to off stimulation, $F(2,46) = 509$, $p < 0.001$. Panel c) demonstrates higher number of hits during early (green) compared to delayed (turquoise) recognition tasks, $F(1,23) = 39.12$, $p < 0.001$.Panel d) shows a significant interaction between stimulation (off, real, and sham) and valence (negative (green) and neutral (turquoise)), $F(2,46) = 6.46$, $p = 0.003$. Panel e) shows a significant interaction between stimulation (off, real, and sham) and timepoint (early (green) and delayed (turquoise)), $F(2,46) = 5.54$, $p = 0.007$. Panel f) shows a tendency for an interaction between valence (negative (green) and neutral (turquoise)) and timepoint (early (green) and delayed (turquoise)), $F(1,23) = 4.0$, $p = 0.06$. Significant differences are indicated by asterisks.

4.4 Less false alarms (FA) during early recognition task

Subjects showed fewer false alarms (FA) during early (M ± SD: 0.08 ± 0.02) as compared to delayed (M ± SD: 0.13 ± 0.04) recognition task, $F(1,23) = 10.44$, $p = 0.004$. There was no significant difference between negative (M ± SD: 0.11 ± 0.03) and neutral (M ± SD: 0.10 ± 0.03) events for FA, $F(1,23) = 0.07$, $p = 0.79$. However, there was a significant ordinal interaction between timepoint and valence, $F(1,23) = 4.18$, $p = 0.05$ (Supplementary Figure S17c), indicating in FA-rate that the negative events may be more strongly influenced by timing (delayed vs. early) compared to the neutral events (delay-early emo-neu: $\beta = 0.03$ (SE = 0.02; t-value = 2.04, $p = 0.05$)). For results on certainty ratings for incorrect identified images (FA) Supplementary Results 4.6 and for certainty ratings for FA RTs see Supplementary Results 4.7.

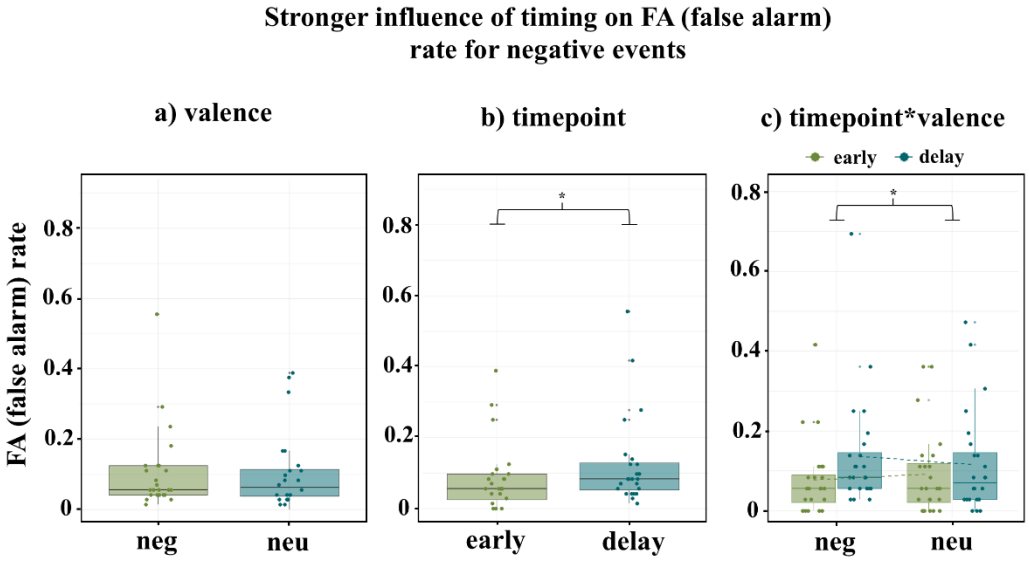

Supplementary Figure S17. False alarms (FA) are shown here aggregated at the subject level (N=24) using boxplots, while each point represents an individual subject. Panel a) shows no significant difference in FA-rate between negative (green) and neutral (turquoise) events, $F(1,23) = 25.67$, $p < 0.001$. Panel b) shows fewer false alarms (FA) during early (green) as compared to delayed (turquoise) recognition task, $F(1,23) = 10.44$, $p = 0.004$. Panel c) shows a significant ordinal interaction between valence (negative (left) and neutral (right)) and timepoint (early (green) and delayed (turquoise)), $F(1,23) = 4.18$, $p = 0.05$. Significant differences are indicated by asterisks.

4.5 RTs for negative events were generally longer for new images compared to old images

There was a significant interaction between "old vs. new" images and valence, F (1,23) = 6.40, p = 0.02, indicating that RTs for negative events were generally longer for new images compared to old images (Supplementary Figure S18).

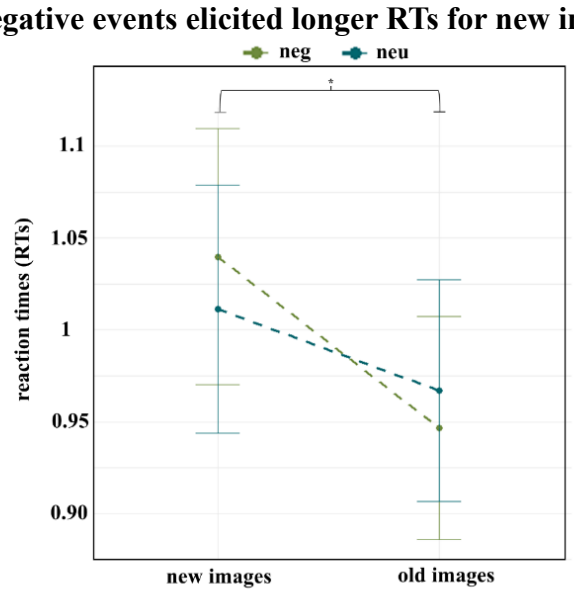

Supplementary Figure S18. Reaction times (RTs) for old and new images are shown here aggregated at the subject level (N=24). There was a significant interaction between new (left) vs. old (right) images and valence (negative (green) and neutral (turquoise), F (1,23) = 6.40, p = 0.02, indicating that RTs for negative events were generally longer for new images compared to old images. Significant differences are indicated by asterisks.

There were no significant hit RTs difference neither between stimulation and valence, F (2,46) = 0.008, p = 0.99), stimulation and timepoint (F(2,46) = 0.49, p = 0.61), nor valence and timepoint, F (1,23) = 0.05, p = 0.82 (Supplementary Figure S19).

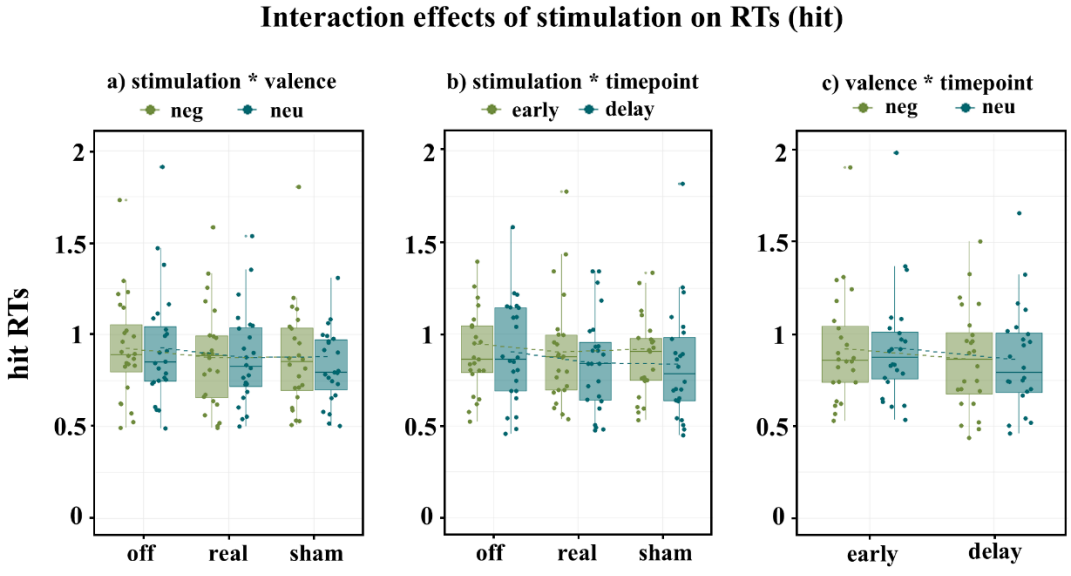

Supplementary Figure S19. Averaged speed of correct responses to target image (hit RTs) is shown here aggregated at the subject level (N = 24) using boxplots, while each point represents an individual subject. Panel a) shows no significant interaction between stimulation (off, real, and sham) and valence (negative (green) and neutral (turquoise)), F (2,46) = 0.008, p = 0.99. Panel b) shows no significant

interaction between stimulation (off, real, and sham) and timepoint (early (green) and delayed (turquoise)), $F(2,46) = 0.49$, $p = 0.61$. Panel c) shows no significant interaction between valence (negative (green) and neutral (turquoise)) and timepoint (early (green) and delayed (turquoise)), $F(1,23) = 0.05$, $p = 0.82$.

4.6 Results on correctly and incorrectly identified images with high and low degree of certainty

For the *correctly identified images (hit)*, for which the subjects indicated a **high degree of certainty**, correct recognition was better for negative (M ± SD: 0.66 ± 0.24) compared to neutral (M ± SD: 0.58 ± 0.25) events, $F(1,23) = 23.81$, $p < 0.001$. Additionally, correct recognition with high degree of certainty was better during early (M ± SD: 0.68 ± 0.24) as compared to delayed recognition (M ± SD: 0.56 ± 0.24), $F(1,23) = 45.32$, $p < 0.001$. Furthermore, there was better correct recognition with high degree of certainty for real (M ± SD: 0.74 ± 0.18) as compared to off (M ± SD: 0.37 ± 0.12) stimulation (off-real: $\beta = -0.37$ (SE = 0.01; t-value = -28, $p < 0.001$)) and for sham (M ± SD: 0.76 ± 0.19) as compared to off (M ± SD: 0.37 ± 0.12) stimulation (off-sham: $\beta = -0.39$ (SE = 0.02; t-value = -19.44, $p < 0.001$)); but not for real as compared to sham stimulating (real-sham: $\beta = -0.02$ (SE = 0.02; t-value = -1.29, $p = 0.62$)), $F(2,46) = 311.64$, $p < 0.001$. There was as significant interaction between stimulation and timepoint, $F(2,46) = 5.70$, $p = 0.006$, and a tendency for stimulation and valence, $F(2,46) = 3.06$, $p = 0.06$, but no interaction between timepoint and valence, $F(1,23) = 0.56$, $p = 0.46$. For the *correctly identified images (hit)*, for which the subjects indicated a **low degree of certainty**, correct recognition did not differ between negative (M ± SD: 0.07 ± 0.08) and neutral (M ± SD: 0.08 ± 0.08) stimuli, $F(1,23) = 0.59$, $p = 0.45$. Furthermore, correct recognition with low degree of certainty was more pronounced during delayed (M ± SD: 0.09 ± 0.09) as compared to early recognition (M ± SD: 0.05 ± 0.07), $F(1,23) = 15.92$, $p < 0.001$. There was better correct recognition with low degree of certainty for real (M ± SD: 0.09 ± 0.09) as compared to off (M ± SD: 0.04 ± 0.06) stimulation (off-real: $\beta = -0.06$ (SE = 0.01; t-value = -5.93, $p < 0.001$)) and for sham (M ± SD: 0.08 ± 0.09) as compared to off (M ± SD: 0.04 ± 0.06) stimulation (off-sham: $\beta = -0.03$ (SE = 0.01; t-value = -3.18, $p = 0.01$)); but not for real as compared to off stimulating (real-sham: $\beta = -0.02$ (SE = 0.01; t-value = 1.70, $p = 0.31$)), $F(2,46) = 13.55$, $p < 0.001$. There was no interaction between stimulation and timepoint, $F(2,46) = 1.15$, $p = 0.33$, stimulation and valence, $F(2,46) = 1.90$, $p = 0.16$, nor between timepoint and valence, $F(1,23) = 0.87$, $p = 0.36$.

For *incorrectly identified images (FA)*, for which the subjects indicated a **high degree of certainty**, there was no significant effect of valence, $F(1,23) = 0.05$, $p = 0.83$ (negative M ± SD: 0.04 ± 0.07; neutral M ± SD: 0.09 ± 0.07) nor timepoint, $F(1,23) = 1.53$, $p = 0.23$ (early M

± SD: 0.04 ± 0.06; delay M ± SD: 0.04 ± 0.08), nor any significant interaction between valence and timepoint, F(1,23) = 0.18, p = 0.68. For *incorrectly identified images (FA)*, for which the subjects indicated a **low degree of certainty,** there was also no significant effect of valence F(1,23) = 0.06, p = 0.82, (negative M ± SD: 0.07 ± 0.07; neutral M ± SD: 0.07 ± 0.06). However, FA with low degree of certainty was more pronounced during delayed (M ± SD: 0.08 ± 0.07) as compared to early recognition (M ± SD: 0.05 ± 0.05), F(1,23) = 14.32, p < 0.001 and there was a significant interaction between valence and timepoint, F(1,23) = 7.30, p = 0.01, that FA-rate with low degree of certainty for negative images was more strongly influenced by timing (delayed vs. early) compared to the neutral images (delay-early emo-neu: β = 0.04 (SE = 0.01; t-value = 2.07, p = 0.01)).

4.7 RT results on correctly and incorrectly identified images with high and low degree of certainty

For the RTs on correctly identified (hit) images, for which the subjects indicated a **high degree of certainty**, there was no effect of stimulation, F(2,46) = 2.44 p = 0.1 (real M ± SD: 0.82 ± 0.30; sham M ± SD: 0.81 ± 0.31; off M ± SD: 0.82 ± 0.30), valence, F(1,23) = 0.03, p = 0.86 (negative M ± SD: 0.83 ± 0.31; neutral M ± SD: 0.83 ± 0.33), nor timepoint, F(1,23) = 2.02 p = 0.17 (early M ± SD: 0.85 ± 0.33; delay M ± SD: 0.81 ± 0.31). There was a tendency for an interaction between stimulation and valence, F(2,46) = 2.90, p = 0.07. There was no interaction between stimulation and timepoint, F(2,46) = 1.12, p = 0.89 and no interaction between timepoint and valence, F(1,23) = 1.14, p = 0.30. For the RTs on correctly identified images, for which the test subjects indicated a **low degree of certainty**, RTs were only faster for images during real (M ± SD: 0.57 ± 0.54) as compared to off (M ± SD: 0.34 ± 0.51) stimulation but not as compared to sham (M ± SD: 0.51 ± 0.55) (off-real: β = -0.23 (SE = 0.05; t-value = -4.21, p = 0.001); sham (M±SD: 0.51±0.57): off-sham: β = -0.16 (SE = 0.07; t-value = -2.24, p = 0.1); real-sham: β = 0.06 (SE = 0.07; t-value = 0.83, p = 1)), F(2,46) = 6.04, p = 0.005. There were no RT effects of valence, F(1,23) = 0.02, p = 0.88 (negative M ± SD: 0.47 ± 0.54; neutral M ± SD: 0.48 ± 0.55), or timepoint, F(1,23) = 1.32, p = 0.26 (early M ± SD: 0.45 ± 0.58; delay M ± SD: 0.51 ± 0.51). However, there was an interaction between stimulation and valence, F(2,46) = 6.51, p = 0.003 (emo-neu off-real: β = -0.49 (SE = 0.14; t-value = -3.45, p = 0.002); emo-neu off-sham: β = -0.26 (SE = 0.15; t-value = -1.73, p = 0.1); emo-neu real-sham: β = 0.23 (SE = 0.12; t-value = 2.03, p = 0.05)). There was no interaction between stimulation and timepoint, F(2,46) = 0.01, p = 0.99 and no interaction between valence and timepoint (F(1,23) = 1.14, p = 0.24).

FA RTs (averaged speed of responses to nontarget images) revealed no faster RTs

neither for valence, F(1,23) = 2.50, p = 0.13 (negative M ± SD: 1.18 ± 0.67; neutral M ± SD: 1.02 ± 0.65), nor timepoint, F(1,23) = 0.02, p = 0.88 (early M ± SD: 1.09 ± 0.83; delay M ± SD: 1.11 ± 0.45), nor the interaction between valence and timepoint, F(1,23) = 0.75, p = 0.40. Likewise there were not faster RTs for incorrectly identified images, for which the subjects indicated a **high degree of certainty**, neither for valence, F(1,23) = 2.11, p = 0.16 (negative M ± SD: 0.56 ± 0.62; neutral M ± SD: 0.45 ± 0.60), nor timepoint, F(1,23) = 0.93, p = 0.34 (early M ± SD: 0.57 ± 0.66; delay M ± SD: 0.44 ± 0.56), nor the interaction between valence and timepoint, F(1,23) = 0.94, p = 0.34. However, for incorrectly identified images with **low degree of certainty**, subjects showed faster RTs during early (M ± SD: 0.62 ± 0.57) as compared to delayed (M ± SD: 0.84 ± 0.45) recognition, F(1,23) = 5.44, p = 0.03. There was no effect for valence, F(1,23) = 0.14, p = 0.71 (negative M ± SD: 0.74 ± 0.50; neutral M ± SD: 0.72 ± 0.55), nor the interaction between valence and timepoint, F(1,23) = 3.07, p = 0.1.

4.8 Exploratory analysis on pupillometry and memory performance

To explore potential effects of subjective sensory perception caused by stimulation on memory performance a comparable model for the behavioral data based the average memory performance (averaged per subject across trials) was set up. For the exploratory **memory performance** analysis, the model *memory performance (hit-FA) ~ stimulation × valence × timepoint + VAS + sensitivity + real_first + (1|ID)* revealed no significant impact of sensory perception (VAS) on memory performance (χ^2 = 1.08, p = 0.30). Stimulation (χ^2 = 933, p < 0.001), valence (χ^2 = 29.48, p < 0.001) and timepoint (χ^2 = 92.33, p < 0.001) as well es the interaction between stimulation and valence (χ^2 = 8.47, p = 0.01) and stimulation and timepoint (χ^2 = 10.20, p = 0.006) were still significant.

4.9 Exploratory analysis of memory performance: Investigating individual factors like sensitivity and gender in relation to taVNS

An additional exploratory analysis for memory performance was performed to investigate individual factors on taVNS such as sensitivity and gender of the subjects. There were no gender-specific (F(1,20) = 3.09, p = 0.09) or sensitivity differences (F(1,20) = 3.29, p = 0.08) in memory performance due to tAVNS. At the same time, the main effect of stimulation (F(2,40) = 395.95, p < 0.001), valence (F(1,20) = 12.15, p = 0.002), and timepoint (F(1,20) = 52.46, p < 0.001) as well as interactions between stimulation and valence (F(2,40) = 8.77, p < 0.001) and stimulation and timepoint (F(2,40) = 4.93, p = 0.01) were still significant.

4.10 Absence of correlations between pupil dilation, memory performance, VAS ratings, and RTs during encoding

There were no observed correlations between pupil dilation and memory performance, VAS rating and memory performance and no correlations between pupil dilation and RTs during encoding.

Overview correlations

4.10.1 Pupil dilation and reaction times (RTs) during real stimulation

a. pupil dilation x RTs during real encoding (total): r = 0.10, p = 0.70
b. pupil dilation x RTs during real encoding of negative images: r = 0.08 p = 0.76
c. pupil dilation x RTs during real encoding of neutral images: r = 0.07 p = 0.80

4.10.2 Pupil dilation and reaction times (RTs) during sham stimulation

a. pupil dilation x RTs during sham encoding (total): r = 0.16, p = 0.59
b. pupil dilation x RTs during sham encoding of negative images: r = 0.04, p = 0.88
c. pupil dilation x RTs during sham encoding of neutral images: r = 0.22, p = 0.44

4.10.3 Pupil dilation and hit-FA (early, delay) within stimulation (off, real, sham) and valence (negative, neutral) conditions

a. pupil dilation during off for neg x off early neg hit-FA: r = -0.14, p = 0.55
b. pupil dilation during off for neg x off delay neg hit-FA: r = -0.11, p = 0.63
c. pupil dilation during off for neu x off early neu hit-FA: r = 0.02, p = 0.94
d. pupil dilation during off for neu x off delay neu hit-FA: r = 0.04, p = 0.88

e. pupil dilation during real for neg x real early neg hit-FA: r = -0.3, p = 0.22
f. pupil dilation during real for neg x real delay neg hit-FA: r = -0.05, p = 0.82
g. pupil dilation during real for neu x real early neu hit-FA: r =-0.43, p = 0.05
h. pupil dilation during real for neu x real delay neu hit-FA: r = -0.21, p = 0.37

i. pupil dilation during sham for neg x sham early neg hit-FA: r = -0.18, p = 0.48
j. pupil dilation during sham for neg x sham delay neg hit-FA: r = -0.19, p = 0.45
k. pupil dilation during sham for neu x sham early neu hit-FA: r = -0.09, p = 0.70
l. pupil dilation during sham for neu x sham delay neu hit-FA: r = 0.03, p = 0.91

4.10.4 hit and hit-FA (early, delay) for real and sham stimulation and VAS rating

a. VAS rating real stimulation x real early hit: r = 0.34, p = 0.21
b. VAS rating real stimulation x real early neg hit: r = 0.62, p = 0.11
c. VAS rating real stimulation x real early neu hit: r = 0.55, p = 0.14

d. VAS rating real stimulation x real delay hit: r =- 0.01, p = 0.97

e. VAS rating real stimulation x real delay neg hit: r = 0.20, p = 0.35
f. VAS rating real stimulation x real delay neu hit: r = -0.14, p = 0.51

g. VAS rating real stimulation x real early hit-FA: r = 0.11, p = 0.63
h. VAS rating real stimulation x real early neg hit-FA: r = -0.04, p = 0.84
i. VAS rating real stimulation x real early neu hit-FA: r = 0.10, p = 0.65

j. VAS rating real stimulation x real delay hit-FA: r =- 0.07, p = 0.74
k. VAS rating real stimulation x real delay neg hit-FA: r = 0.01, p = 0.95
l. VAS rating real stimulation x real delay neu hit-FA: r = -0.17, p = 0.42

m. VAS rating sham stimulation x sham early hit: r = 0.01, p = 0.97
n. VAS rating sham stimulation x sham early neg hit: r = -0.01, p = 0.68
o. VAS rating sham stimulation x sham early neu hit: r = 0.09, p = 0.71

p. VAS rating sham stimulation x sham delay hit: r = 0.26 , p = 0.26
q. VAS rating sham stimulation x sham delay neg hit: r = 0.13, p = 0.55
r. VAS rating sham stimulation x sham delay neu hit: r = 0.02, p = 0.93

s. VAS rating sham stimulation x sham early hit-FA: r = -0.08, p = 0.72
t. VAS rating sham stimulation x sham early neg hit-FA: r = 0.10, p = 0.67
u. VAS rating sham stimulation x sham early neu hit-FA: r = 0.26, p = 0.25

v. VAS rating sham stimulation x sham delay hit-FA: r = 0.31, p = 0.18
w. VAS rating sham stimulation x sham delay neg hit-FA: r = 0.20, p = 0.40
x. VAS rating sham stimulation x sham delay neu hit-FA: r = 0.36, p = 0.11

4.11 Additional analysis including random slopes for stimulation intensity (resting-state task):

An additional analysis with random slopes in the model was added: ***pupil dilation* ~ trials + stimulation + intensity + frequency + VAS + (1+ intensity \|ID)***

pupil dilation during **(I) or **(II)** or **(III)***

During (**I**) "on stimulation" the model revealed that VAS explained significant proportion of pupil variance ($\chi^2 = 33.27$, $p < 0.001$). Therefore, there was no increase in pupil dilation during real (M ± SE: 0.16 ± 0.02) as compared to sham (M ± SE: 0.12 ± 0.03) stimulation ($\chi^2 = 3.09$, $p = 0.08$) and during low (M ± SE: 0.12 ± 0.03) as compared to high (M ± SE: 0.16 ± 0.02) frequency ($\chi^2 = 3.13$, $p = 0.08$) explainable. However, pupil dilation was still increased during high (M ± SE: 0.20 ± 0.03) as compared to low (M ± SE: 0.08 ± 0.02) intensity ($\chi^2 = 15.71$, $p < 0.001$). During (**II**) "immediate response" the model revealed that VAS explained significant proportion of pupil variance ($\chi^2 = 27.96$, $p < 0.001$). Therefore, there was no increase in pupil

dilation during real (M ± SE: 0.12 ± 0.04) as compared to sham (M ± SE: 0.07 ± 0.04) stimulation (χ^2 = 2.51, p = 0.11) and during low (M ± SE: 0.09 ± 0.04) as compared to high (M ± SE: 0.1 ± 0.04) frequency (χ^2 = 0.1, p = 0.75) explainable. However, pupil dilation was still increased during high (M ± SE: 0.16 ± 0.05) as compared to low (M ± SE: 0.02 ± 0.03) intensity (χ^2 = 6.33, p < 0.01). During (**III**) "delayed response" the model revealed that VAS did not explain significant proportion of pupil variance (χ^2 = 2.67, p = 0.10) anymore. There was also no increase in pupil dilation during real (M ± SE: - 0.05 ± 0.02) as compared to sham (M ± SE: - 0.05 ± 0.02) stimulation (χ^2 = 0.02, p = 0.89) and during low (M ± SE: - 0.06 ± 0.02) as compared to high (M ± SE: - 0.04 ± 0.02) frequency (χ^2 = 0.76, p = 0.38) explainable. Additionally, dilation was also not increased during high (M ± SE: - 0.02 ± 0.02) as compared to low (M ± SE: - 0.08 ± 0.02) intensity (χ^2 = 2.55, p = 0.11).

4.12 Theory-driven exploratory analysis of the interaction between VAS and stimulation and stimulation parameters (resting-state task).

For the resting-state task two theory-driven exploratory analyses were also conducted to a) better explain the potential influence of sensory perception (VAS) due to stimulation on pupil dilation controlled for sensitivity and to b) investigate how sensitivity affects the subjective perception of stimulation on pupil dilation

The additional exploratory analysis based on the model

- a) StimIntFreq*VAS-LMM

  $$pupil\ dilation^{*} \sim trials + stimulation \times VAS + intensity \times VAS + frequency \times VAS + sensitivity + (1|ID)$$

  *pupil dilation during **(I)** or **(II)** or **(III)***

(Supplementary Figure S20) showed for (**I**) "on stimulation", that by adding VAS as individual interactions, while VAS was significant (χ^2 = 38.74, p < 0.001), stimulation (χ^2 = 3.39, p = 0.07) and frequency (χ^2 = 3.38, p = 0.07) got marginal significant, while intensity (χ^2 = 28.40, p < 0.001) still explained large portions of variance. There was no significant effect for sensitivity (χ^2 = 0.12, p = 0.73). The model also revealed a significant interaction between VAS and intensity (χ^2 = 12.08, p = 0.0005). Specifically, during low intensity an increase in VAS was associated with a 0.024 increase in pupil dilation, while during high intensity the effect was significantly larger with 0.062 increase in pupil dilation compared to low intensity stimulation (low vs. high: estimate -0.04, SE: 0.01; t (10466) = - 3.47, p = 0.0005). There was no significant interaction between VAS and stimulation (χ^2 = 0.002, p = 0.1) nor VAS and frequency (χ^2 = 0.58, p = 0.44). The (**II**) "immediate response" time-window showed, that by adding VAS as individual interactions, while VAS was significant (χ^2 = 30.81, p < 0.001), intensity (χ^2 = 19.93,

$p < 0.001$) still explained large portions of variance, while stimulation ($\chi^2 = 3.06$, $p = 0.08$) and frequency ($\chi^2 = 0.27$, $p = 0.60$) were not or marginal significant. There was no significant effect for sensitivity ($\chi^2 = 0.02$, $p = 0.88$). The model also revealed a significant interaction between VAS and intensity ($\chi^2 = 18.63$, $p < 0.001$). Specifically, during low intensity an increase in VAS was associated with a 0.02 increase in pupil dilation, while during high intensity the effect was significantly larger with 0.1 increase in pupil dilation compared to low intensity stimulation (low vs. high: estimate -0.07, SE: 0.02; t (10535) = - 4.30, $p < 0.001$). There was no significant interaction between VAS and stimulation ($\chi^2 = 0.15$, $p = 0.70$) nor VAS and frequency ($\chi^2 = 0.04$, $p = 0.85$). The (**III**) "delayed response" time-window showed, that by adding VAS as individual interactions, neither VAS ($\chi^2 = 3.40$, $p = 0.07$), intensity ($\chi^2 = 2.88$, $p = 0.09$), stimulation ($\chi^2 = 0.08$, $p = 0.78$), frequency ($\chi^2 = 0.90$, $p = 0.34$) and sensitivity ($\chi^2 = 0.29$, $p = 0.60$) was significant. However, the model revealed a significant interaction between VAS and intensity ($\chi^2 = 7.49$, $p = 0.006$). Specifically, during low intensity an increase in VAS was associated with a -0.009 decrease in pupil dilation, while during high intensity the effect was significantly larger with 0.04 increase in pupil dilation compared to low intensity stimulation (low vs. high: estimate -0.05, SE: 0.02; t (7096) = - 2.73, $p = 0.006$). There was no significant interaction between VAS and stimulation ($\chi^2 = 1.95$, $p = 0.16$) nor VAS and frequency ($\chi^2 = 0.03$, $p = 0.87$).

The additional exploratory analysis based on the model**:**

- b) Sensitivity*VAS-LMM

  pupil dilation ~ trials + stimulation + intensity + frequency + VAS × sensitivity + (1|ID)*

  pupil dilation during (I**)*

revealed no significant interaction between VAS rating and sensitivity ($\chi^2 = 0.20$, $p = 0.65$). Intensity ($\chi^2 = 28.22$, $p < 0.001$) and VAS ($\chi^2 = 38.70$, $p < 0.001$) were significant, while stimulation ($\chi^2 = 2.78$, 0.09), frequency ($\chi^2 = 2.91$, $p = 0.09$) and sensitivity were not significant ($\chi^2 = 0.08$, $p = 0.78$).

Exploratory analysis of the interaction between VAS and stimulation and stimulation parameters (resting-state task)

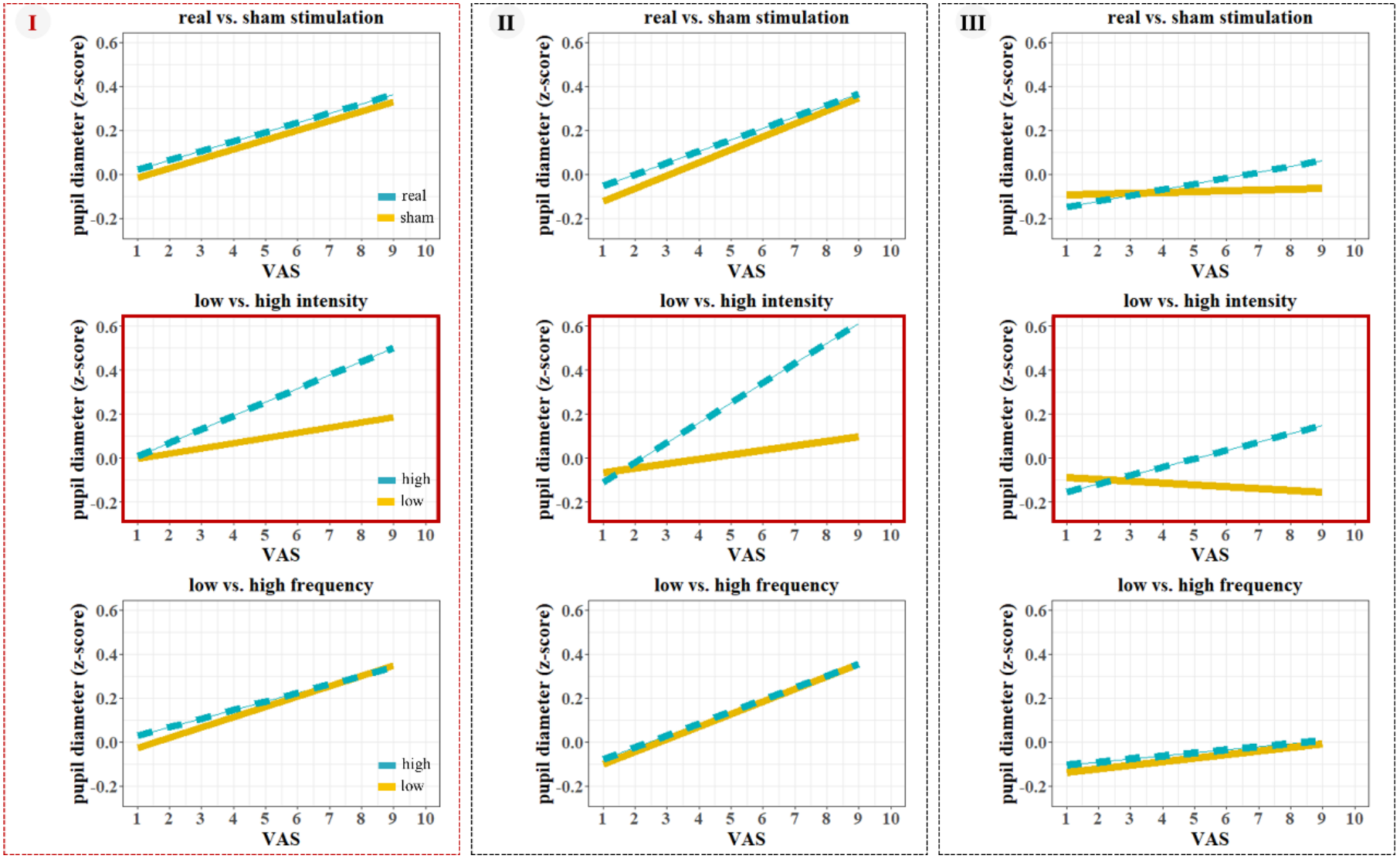

Supplementary Figure S20. Interaction plot between VAS and a) stimulation, b) intensity, and c) frequency for phasic (I) "on stimulation", (II) "immediate response", and (III) "delayed response" (from left to right). Shown are estimated marginal means for different levels of VAS. The boxes outlined in red indicate the significant difference from between high and low frequency at all time windows (I-III): higher intensities and higher VAS rating predict a more dilated pupil than lower intensities ((I): $\chi^2 = 12.08$, $p = 0.0005$; (II) $\chi^2 = 18.63$, $p < 0.001$; (III) $\chi^2 = 7.49$, $p = 0.006$).

Emotional memory task: Linear mixed models

model		Anova	β and t-value	mean ± se
m_3	Trial			
	real vs. sham vs. off	χ^2 = 45.39, p < 0.001	off-real: β = -0.33 (SE = 0.05; t-value = -6.24, p < 0.001) off-sham: β = -0.28 (SE = 0.05; t-value = -5.34, p < 0.001) real-sham: β = 0.05 (SE = 0.05; t-value = 0.98, p = 0.98)	off (0.19±0.12) vs. real (0.52±0.12) off (0.19±0.12) vs. sham (0.47±0.12) real (0.52±0.12) vs. sham (0.47±0.12)
	neg vs. neut	χ^2 = 5.71, p = 0.02	neut- neg: β = -0.10 (SE = 0.04; t-value = -2.39, p = 0.02)	neut (0.34±0.11) vs. neg (0.45±0.11)
	Mean			
	real vs. sham vs. off	χ^2 = 33.20, p < 0.001	off-real: β = -0.33 (SE = 0.06; t-value = -5.37, p < 0.001) off-sham: β = -0.28 (SE = 0.06; t-value = -4.50, p < 0.001) real-sham: β = 0.05 (SE = 0.06; t-value = 0.86, p = 1)	off (0.19±0.12) vs. real (0.52±0.12) off (0.19±0.12) vs. sham (0.47±0.12) real (0.52±0.12) vs. sham (0.47±0.12)
	neg vs. neut	χ^2 = 4.56, p = 0.03	neut- neg: β = -0.11 (SE = 0.05; t-value = -2.14, p = 0.03)	neut (0.34±0.11) vs. emo (0.45±0.11)
m_3_1	Trial			
	real vs. sham vs. off	χ^2 = 44.43, p < 0.001	off-real: β = -0.03 (SE = 0.05; t-value = -5.61, p < 0.001) off-sham: β = -0.03 (SE = 0.05; t-value = -5.70, p < 0.001) real-sham: β = 0.00006 (SE = 0.06; t-value = 0.001, p = 1)	off (0.19±0.12) vs. real (0.50±0.12) off (0.19±0.12) vs. sham (0.50±0.12) real (0.50±0.12) vs. sham (0.50±0.12)
	neg vs. neut	χ^2 = 5.64, p = 0.02	neut- neg: β = -0.10 (SE = 0.04; t-value = -2.38, p = 0.02)	neut (0.34±0.11) vs. neg (0.45±0.11)
	Mean			
	real vs. sham vs. off	χ^2 = 33.50, p < 0.001	off-real: β = -0.30 (SE = 0.06; t-value = -4.77, p < 0.001) off-sham: β = -0.31 (SE = 0.06; t-value = -4.93, p < 0.001) real-sham: β = -0.01 (SE = 0.07; t-value = -0.15, p = 1)	off (0.19±0.12) vs. real (0.49±0.12) off (0.19±0.12) vs. sham (0.50±0.12) real (0.49±0.12) vs. sham (0.50±0.12)
	neg vs. neut	χ^2 = 4.70, p = 0.04	neut- neg: β = -0.11 (SE = 0.05; t-value = -2.17, p = 0.03)	neut (0.34±0.12) vs. neg (0.45±0.12)
m_3_3	**Trial**			
	real vs. sham vs. off	χ^2 = 44.47, p < 0.001	off-real: β = -0.31 (SE = 0.05; t-value = -5.68, p < 0.001) off-sham: β = -0.31 (SE = 0.05; t-value = -5.65, p < 0.001) real-sham: β = 0.006 (SE = 0.06; t-value = 0.12, p = 1)	off (0.19±0.11) vs. real (0.49±0.11) off (0.19±0.11) vs. sham (0.48±0.11) real (0.49±0.11) vs. sham (0.48±0.11)
	neg vs. neut	χ^2 = 5.65, p = 0.02	neut-neg: β = -0.10 (SE = 0.04; t-value = -2.37, p = 0.02)	neut (0.34±0.11) vs. neg (0.44±0.11)
	rfirst vs. sfirst	χ^2 = 8.33, p = 0.004	sfirst-rfirst: β = -0.57 (SE = 0.2; t-value = -2.89, p = 0.009)	sfirst (0.10±0.14) vs. rfirst (0.68±0.15)
	Mean			
	real vs. sham vs. off	χ^2 = 44.47, p < 0.001	off-real: β = -0.31 (SE = 0.05; t-value = -5.68, p < 0.001) off-sham: β = -0.31 (SE = 0.05; t-value = -5.65, p < 0.001) real-sham: β = 0.006 (SE = 0.06; t-value = 0.12, p = 1)	off (0.19±0.11) vs. real (0.49±0.11) off (0.19±0.11) vs. sham (0.48±0.11) real (0.49±0.11) vs. sham (0.48±0.11)
	neg vs. neut	χ^2 = 5.65, p = 0.02	neut- neg: β = -0.10 (SE = 0.04; t-value = -2.37, p = 0.02)	neut (0.34±0.11) vs. neg (0.44±0.11)
	rfirst vs. sfirst	χ^2 = 8.33, p = 0.004	sfirst-rfirst: β = -0.57 (SE = 0.2; t-value = -2.89, p = 0.009)	sfirst (0.10±0.14) vs. rfirst (0.68±0.15)

Supplementary Table S34. Distinct LMM for emotional memory task (m_3: *pupil dilation ~ trials + stimulation + valence + (1|ID));* m_3_1: *pupil dilation ~ trials + stimulation + valence + VAS + (1|ID));* m_3_3: *pupil dilation ~ trials + stimulation + valence + VAS + sensitivity + real_first + (1|ID))* based on data at the level of individual trials (blue; Trial) or on the average pupil dilation per session (grey; Mean).

Resting-state task: Linear mixed models (model m4: *StimIntFreq-LMM*) for each time window (I-III):

	model		Anova	β and t-value	mean ± se
(I) ON	**Trial_m4**				
		real vs. sham	χ^2 = 18.97, p < 0.001	real-sham: β = 0.08 (SE = 0.02; t-value = 4.37, p < 0.001)	real (0.18±0.03) vs. sham (0.1±0.03)
		high vs. low Hz	χ^2 = 10.88, p = 0.001	high-low: β = 0.06 (SE = 0.02; t-value = 3.30, p = 0.001)	high (0.17±0.03) vs. low (0.11±0.03) Hz
		high vs. low mA	χ^2 = 103.40, p < 0.001	high-low: β = 0.2 (SE = 0.02; t-value = 10.17, p < 0.001)	high (0.23±0.03) vs. low (0.04±0.03) mA
	Mean_m4				
		real vs. sham	χ^2 = 11.29, p = 0.0007	real-sham: β = 0.09 (SE = 0.03; t-value = 3.36, p = 0.0009)	real (0.18±0.03) vs. sham (0.1±0.03)
		high vs. low Hz	χ^2 = 5.94, p = 0.01	high-low: β = 0.06 (SE = 0.03; t-value = 2.44, p = 0.02)	high (0.17±0.03) vs. low (0.10±0.03) Hz
		high vs. low mA	χ^2 = 46.92, p < 0.001	high-low: β = 0.18 (SE = 0.03; t-value = 6.85, p < 0.001)	high (0.22±0.03) vs. low (0.05±0.03) mA
(II) OFF	**Trial_m4**				
		real vs. sham	χ^2 = 15.99, p < 0.001	real-sham: β = 0.1 (SE = 0.03; t-value = 3.99, p < 0.001)	real (0.15±0.04) vs. sham (0.04±0.04)
		high vs. low Hz	χ^2 = 2.92, p = 0.09	high-low: β = 0.05 (SE = 0.03; t-value = 1.71, p = 0.09)	high (0.11±0.04) vs. low (0.07±0.04) Hz
		high vs. low mA	χ^2 = 76.79, p < 0.001	high-low: β = 0.2 (SE = 0.03; t-value = 8.76, p < 0.001)	high (0.21±0.04) vs. low (-0.03±0.04) mA
	Mean_m4				
		real vs. sham	χ^2 = 5.21, p = 0.02	real-sham: β = 0.1 (SE = 0.04; t-value = 2.30, p = 0.02)	real (0.15±0.04) vs. sham (0.05±0.04)
		high vs. low Hz	χ^2 = 0.75, p = 0.39	high-low: β = 0.04 (SE = 0.04; t-value = 0.86, p = 0.39)	high (0.12±0.04) vs. low (0.08±0.04) Hz
		high vs. low mA	χ^2 = 22.12, p < 0.001	high-low: β = 0.20 (SE = 0.04; t-value = 4.70, p < 0.001)	high (0.20±0.04) vs.low (-0.004±0.04) mA
(III) OFF	**Trial_m4**				
		real vs. sham	χ^2 = 0.61, p = 0.43	real-sham: β = 0.02 (SE = 0.03; t-value = 0.78, p = 0.43)	real (-0.04±0.02) vs. sham (-0.06±0.02)
		high vs. low Hz	χ^2 = 1.52, p = 0.22	high-low: β = 0.04 (SE = 0.03; t-value = 1.24, p = 0.22)	high (-0.03±0.02) vs. low (-0.07±0.02) Hz
		high vs. low mA	χ^2 = 8.26, p = 0.004	high-low: β = 0.08 (SE = 0.03; t-value = 2.88, p = 0.004)	high (-0.01±0.02) vs. low (-0.09±0.02) mA
	Mean_m4				
		real vs. sham	χ^2 = 0.57, p = 0.45	real-sham: β = 0.02 (SE = 0.03; t-value = 0.76, p = 0.45)	real (-0.04±0.02) vs. sham (-0.06±0.02)
		high vs. low Hz	χ^2 = 1.74, p = 0.19	high-low: β = 0.04 (SE = 0.03; t-value = 1.32, p = 0.19)	high (-0.03±0.02) vs. low (-0.07±0.02) Hz
		high vs. low mA	χ^2 = 9.19, p = 0.002	high-low: β = 0.08 (SE = 0.03; t-value = 3.03, p = 0.002)	high (-0.01±0.02) vs. low (-0.09±0.02) mA

Supplementary Table S35. Distinct LMM (*pupil dilation ~ trials + stimulation + intensity + frequency + (1|ID))* for each time window of the resting-state task (**(I)** the 3 sec during on stimulation, **(II)** the immediate response and **(III)** the delayed response) based on data at the level of individual trials (blue; Trial_m4) or on the average pupil dilation per session (grey; Mean_m4).

Resting-state task: Linear mixed models (model m4_1 *StimIntFreq-VAS-LMM*) for each time window (I-III)

	model		Anova	β and t-value	mean ± se
(I) ON	**Trial_m4_1**				
		real vs. sham	$\chi^2 = 2.69$, p = 0.1	real-sham: β = 0.03 (SE = 0.02; t-value = 1.64, p = 0.1)	real (0.16±0.03) vs. sham (0.12±0.03)
		high vs. low Hz	$\chi^2 = 2.85$, p = 0.1	high-low: β = 0.03 (SE = 0.02; t-value = 1.69, p = 0.1)	high (0.16±0.02) vs. low (0.12±0.03) Hz
		high vs. low mA	$\chi^2 = 28.79$, p < 0.001	high-low: β = 0.1 (SE = 0.02; t-value = 5.34, p < 0.001)	high (0.20±0.03) vs. low (0.08±0.03) mA
	Mean_m4_1				
		real vs. sham	$\chi^2 = 2.35$, p = 0.13	real-sham: β = 0.04 (SE = 0.03; t-value = 1.53, p = 0.13)	real (0.15±0.03) vs. sham (0.11±0.03)
		high vs. low Hz	$\chi^2 = 2.04$, p = 0.15	high-low: β = 0.04 (SE = 0.03; t-value = 1.43, p = 0.16)	high (0.15±0.03) vs. low (0.11±0.03) Hz
		high vs. low mA	$\chi^2 = 14.69$, p = 0.0001	high-low: β = 0.11 (SE = 0.03; t-value = 3.83, p < 0.0002)	high (0.19±0.03) vs. low (0.08±0.03) mA
(II) OFF	**Trial_m4_1**				
		real vs. sham	$\chi^2 = 2.42$, p = 0.12	real-sham: β = 0.04 (SE = 0.03; t-value = 1.56, p = 0.12)	real (0.12±0.04) vs. sham (0.07±0.04)
		high vs. low Hz	$\chi^2 = 0.09$, p = 0.76	high-low: β = 0.008 (SE = 0.03; t-value = 0.30, p = 0.76)	high (0.1±0.04) vs. low (0.09±0.04) Hz
		high vs. low mA	$\chi^2 = 20.10$, p < 0.001	high-low: β = 0.13 (SE = 0.03; t-value = 4.48, p < 0.001)	high (0.17±0.04) vs. low (0.03±0.04) mA
	Mean_m4_1				
		real vs. sham	$\chi^2 = 0.95$, p = 0.33	real-sham: β = 0.04 (SE = 0.04; t-value = 0.98, p = 0.38)	real (0.12±0.04) vs. sham (0.07±0.04)
		high vs. low Hz	$\chi^2 = 0.02$, p = 0.90	high-low: β = 0.006 (SE = 0.04; t-value = 0.13, p = 0.95)	high (0.1±0.04) vs. low (0.1±0.04) Hz
		high vs. low mA	$\chi^2 = 6.43$, p = 0.01	high-low: β = 0.12 (SE = 0.05; t-value = 2.54, p = 0.01)	high (0.16±0.04) vs. low (0.03±0.04) mA
(III) OFF	**Trial_m4_1**				
		real vs. sham	$\chi^2 = 0.009$, p = 0.92	real-sham: β = 0.003 (SE = 0.03; t-value = 0.09, p = 0.92)	real (-0.05±0.02) vs. sham (-0.05±0.02)
		high vs. low Hz	$\chi^2 = 0.68$, p = 0.41	high-low: β = 0.02 (SE = 0.03; t-value = 0.82, p = 0.41)	high (-0.04±0.02) vs. low (-0.06±0.02) Hz
		high vs. low mA	$\chi^2 = 2.76$, p = 0.1	high-low: β = 0.05 (SE = 0.03; t-value = 1.66, p = 0.1)	high (-0.02±0.02) vs. low (-0.08±0.02) mA
	Mean_m4_1				
		real vs. sham	$\chi^2 = 0.003$, p = 0.95	real-sham: β = 0.002 (SE = 0.03; t-value = 0.06, p = 0.95)	real (-0.05±0.02) vs. sham (-0.05±0.02)
		high vs. low Hz	$\chi^2 = 0.81$, p = 0.37	high-low: β = 0.02 (SE = 0.03; t-value = 0.90, p = 0.37)	high (-0.04±0.02) vs. low (-0.06±0.02) Hz
		high vs. low mA	$\chi^2 = 3.18$, p = 0.07	high-low: β = 0.05 (SE = 0.03; t-value = 1.78, p = 0.08)	high (-0.02±0.02) vs. low (-0.07±0.02) mA

Supplementary Table S36. Distinct LMM for each time window for resting-state task (**(I)** the 3 sec during on stimulation, **(II)** the immediate response and **(III)** the delayed response) based on data at the level of individual trials (blue; Trial_m4_1 (*pupil dilation ~ trials + stimulation + intensity + frequency + VAS + (1|ID)*) or on the average pupil dilation per session (grey; Mean_m4_1 (*pupil dilation ~ stimulation + intensity + frequency + VAS + (1|ID)*).

Changes in pupil dilation during real and sham stimulation for low and high stimulation intensity and frequency based on *StimIntFreq-LMM* and *StimIntFreq-VAS-LMM* (resting-state task)

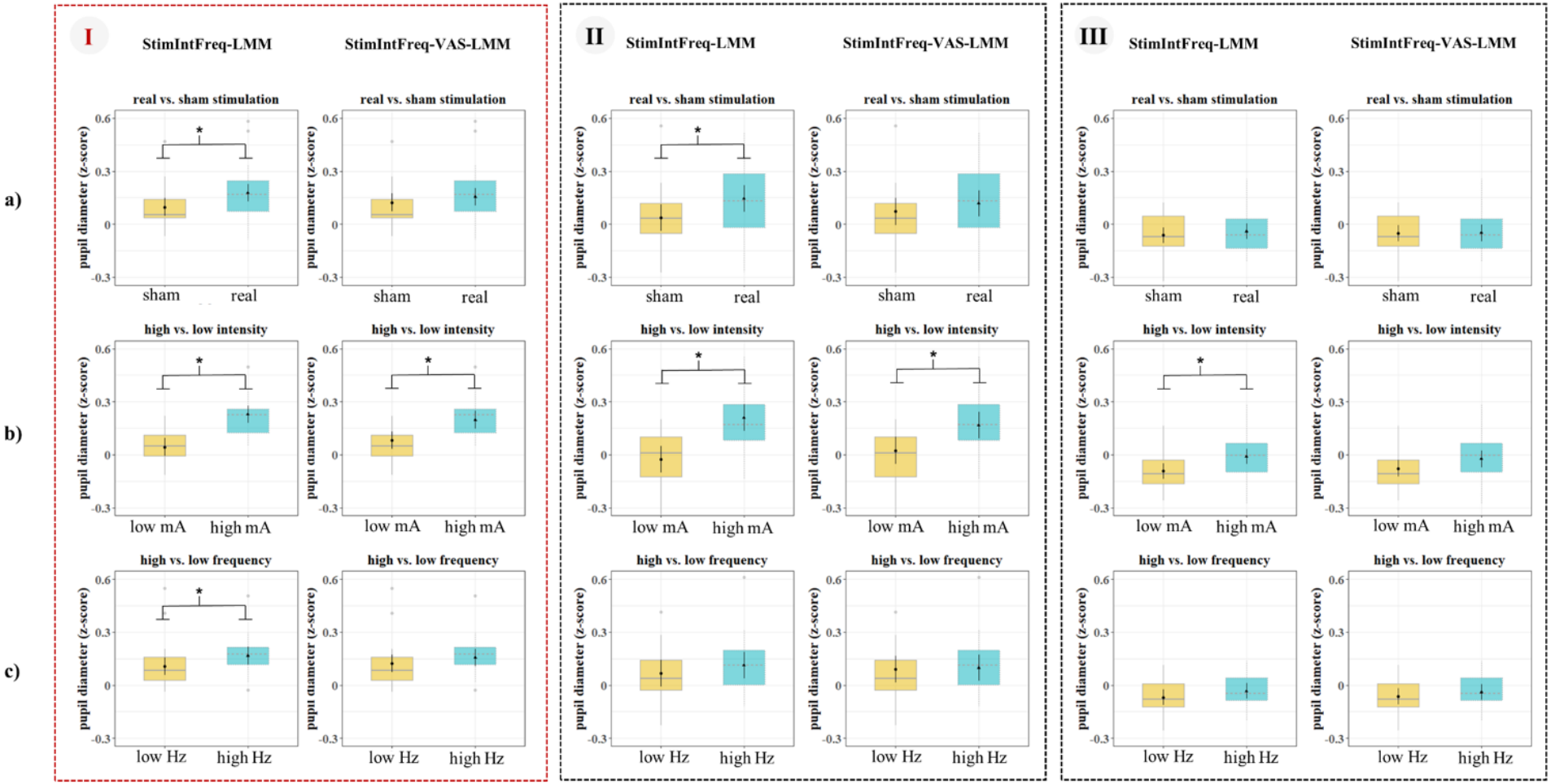

Supplementary Figure S21. Pupil diameters (z score) for **a)** real (turquoise) and sham (ochre) stimulation, **b)** high (turquoise) and low (ochre) intensity and **c)** high (turquoise) and low (ochre) frequency. The dashed vertical red lines indicate the time window when the **stimulation** was (I) **on**, the (II) **immediate response** following to the first dashed vertical black line and the subsequent (III) **delayed response** to the second dashed vertical black line. The boxplots for the individual time points are based on ***StimIntFreq-LMM and StimIntFreq-VAS-LMM***, the asterisks indicate significant differences between conditions.

10 Declaration of Honour

I hereby declare that I prepared this thesis without impermissible help of third parties and that none other than the indicated tools have been used; all sources of information are clearly marked, including my own publications.

In particular I have not consciously:

- Fabricated data or rejected undesired results,
- Misused statistical methods with the aim of drawing other conclusions than those warranted by the available data,
- Plagiarized external data or publications,
- Presented the results of other researchers in a distorted way.

I am aware that violations of copyright may lead to injunction and damage claims of the author and also to prosecution by the law enforcement authorities.

I hereby agree that the thesis may be reviewed for plagiarism by mean of electronic data processing.

This work has not yet been submitted as a doctoral thesis in the same or a similar form in Germany, nor in any other country. It has not yet been published as a whole

Hamburg, 17.02.2025

M.Sc. Mareike Ludwig